Universidad Autónoma de Madrid

Departamento de Bioquímica

Tesis Doctoral

Development of Technological Platforms for the Identification of Novel Cellular Modulators of FOXO Activity

Fábian Zanella de Sá

Madrid, Febrero de 2009

Departamento de Bioquímica

Facultad de Medicina

Universidad Autónoma de Madrid

Tesis Doctoral:

Development of Technological Platforms for the Identification of Novel Cellular Modulators of FOXO Activity.

Doctorando:
Fábian Zanella de Sá,
Licenciado en Biología
por la Facultad de Ciencias de la Universidad de Oporto - Portugal

Directores:
Wolfgang Link
Amancio Carnero Moya

Tutora:
Rosario Perona,
Profesora Honoraria del Departamento de Bioquímica de la UAM.

Trabajo experimental realizado en los laboratorios de la
Sección de Desarollo de Ensayos, Programa de Terapias Experimentales en el
Centro Nacional de Investigaciones Oncológicas (CNIO) - Madrid

Madrid, febrero de 2009

A la Comisión de doctorado de la UAM,

La finalidad de la presente carta es informar a la Comisión de doctorado de la Universidad Autónoma de Madrid sobre el doctorando Fábian Zanella de Sá, que actualmente se encuentra realizando sus estudios de doctorado en el CNIO bajo nuestra co-dirección. Fábian es un joven investigador que ha comenzado su trabajo en nuestro laboratorio en marzo de 2005, durante este tiempo ha llevado adelante el trabajo experimental de su tesis doctoral en responsable y existosa; ha planeado y llevado a cabo sus experimentos con gran motivación y eficiencia y también se ha destacado por la correcta interpretación y valoración de los resultados obtenidos. Debido a su buen conocimiento de la literatura científica relevante y dominio de la lengua inglesa, ha sido capaz de presentar y discutir exitosamente sus resultados tanto en reuniones grupales como en congresos internacionales.

En estos años de investigación científica dentro nuestro grupo, Fábian ha demostrado estar preparado para la lectura de su tesis doctoral.

Por otro lado, la solidez y relevancia de los resultados obtenidos a lo largo de su trabajo de tesis se evidencian en la publicación de los mismos. Estos resultados generados por el trabajo de Fábian son coherentes, la línea de trabajo realizada constituye un aporte relevante a la investigación científica y, fundamentalmente, es completa como para constituir una sólida tesis doctoral.

Por los motivos aquí expuestos y mediante la presente, autorizamos a Fábian a leer su tesis doctoral ante el Tribunal que ustedes consideren apropiado para optar al título de Doctor.

Sin más, saludamos a ustedes muy atentamente,

Wolfgang Link
Director de Tesis

Amancio Carnero Moya
Director de Tesis

Rosario Perona
Tutora y Profesora Honoraria del Depto. de Bioquímica

Acknowledgments

Four years have passed since I visited my lab for the first time. It is amazing to think of how my life changed since then. The decision to move to Madrid to do my PhD was hard but looking at my scientific and personal growth, it makes me happy to have taken this decision. I would like to thank the special people that followed me and helped me over this period.

First of all I would like to thank Wolfgang for choosing me for this project, for believing in me, for the methodic reviewing of everything, all along, for sharing his knowledge and for his infinite patience from the beginning until the very end of this thesis.

I would like to thank Amancio for his help and support, suggestions and insightful critics during the whole thesis.

I feel that I am extremely fortunate for having you both as directors. Thank you!

To the Assay Development Section I must dedicate a very special thank you. You all became another family of mine, since my first day in the CNIO and that made my stay here much easier. I wished all labs had the great environment combined with such competent people I found when I got there. I thank Wolf, Amancio, Arantxa, Valle, Estrella, Irene, Juanfe, Carmen, Oli, Fernando, Lidia, Belén and Vicky for the welcome and for the help in the first steps. I also thank the people who joined the group afterwards and kept adding to this great team: Maja, Mer and Sandra.

Thank you Valle and Estrella, for the help and for sharing many special moments in the beggining and until your final sprint. You did great and inspired me to keep on running after it. A very special thanks to Arantxa, for the collaboration from the initial steps of the projects until her departure. I must thank Fernando for his fundamental help with the setup of the automation of our screening procedures. I thank Bea for her great help since she joined the projects. A very special thanks to Irene for the help, ideas and “consulting” when it was my turn to carry on with “the experiments that everybody has to do to”. I thank Oliver for the great help with the mice in the last months and to Juanfe and Carmen for always being there with technical advice whenever I needed them. I also thank the three of you for the constant support with ideas and critics following the projects. I would also like to thank Sandra for her help with the very final experiments.

To my dearest “amiguitos” (you know who you are), there are not enough words describe so many amazing moments shared in the lab and in other places around the world. You are all very special to me.

I would like to thank Arantxa García, Diego Megías and Jorge Monsech from the Biotechnology Program for their technical support.

I also thank Thomas Horn and Neil Vincent from BD bisociences for their support in the setup of our high content systems.

I believe that what we are and what we do is far more than just our work. So I would like to mention some special friends I made during my stay, who became a fundamental aspect of my life here. I thank Filipe, Ricardo, Josue, Artur, Rick, Magda and Lina for being the best flatmates one can ever have. I also would like to mention some very special people who were present in many moments: Bibiana, Silvana, Lorena, Dani, Mer, Cristina, David, Azucena and Geno. I would keep adding names forever as I am glad to have made many friends through other friends, in many groups, so I thank all of you who sincerely supported me through this process.

Agradeço ao Mestre Veneno e a todos os meus amigos da Capoeira em Madrid por me ajudar a manter o equilíbrio e pelos ótimos momentos dentro e fora da roda.

Agradeço a todos os meus amigos de Portugal, especialmente aos membros do GASE, aos camaradas do Capoeira Interação e aos colegas da FCUP e do IPATIMUP por sempre mostrarem interesse e entusiasmo quanto ao desenlace desta etapa.

Agradeço à Aline pelo seu apoio incondicional durante este ultimo ano, por me ajudar a respirar fundo e me dar mais um motivo para sorrir e olhar para frente, todos os dias.

Obrigado a toda a minha famíla no Brasil, pelo carinho, pelo interesse demonstrado e pelo apoio constante durante toda esta época. Sinto umas saudades de todos vocês que não cabem em palavras.

Agradeço à Michele e ao Pedro pelo seu constante apoio, motivação e carinho. Não existem palavras suficientes para agradecer aos meus pais, que sempre souberam me aconselhar. Por vocês eu vim e graças a vocês cheguei até aqui.

I dedicate this work to my parents. Their love and support helped me to get this far, allowing my dream to come true.

Abstract

FOXO proteins are evolutionarily conserved transcription factors implicated in several fundamental cellular processes, functioning as end-point for transcriptional programs involved in apoptosis, stress response and longevity. Abrogation of FOXO function is very frequent in human cancer, therefore the mechanisms of regulation of the FOXO proteins are receiving increasing attention in cancer research. The FOXO proteins integrate regulatory inputs from a variety of upstream signaling pathways, most importantly in response to growth factor and stress signaling. Recently, FOXO factors have been established as tumor suppressors, promoting the transcription of pro-apoptotic molecules like FasL and Bim when the PI3K/Akt pathway is downregulated. In order to reveal novel modulators of FOXO activity we developed several technological platforms suitable for high throughput screenings that allow for the specific identification of repressors of FOXO proteins.

The U2foxRELOC system is based on U2-OS Osteosarcoma cells stably expressing a GFP-FOXO3A fusion protein that translocates to the cell nucleus upon FOXO activation. This High Content Screening (HCS) system was shown to be accurate for the detection of small compounds able to induce the translocation of the fusion protein between both cell compartments. The U2nesRELOC system allows for the detection of unspecific FOXO nuclear trapping via the inhibition of CRM-1/exportin, members of the nuclear export machinery. The 293foxREP system can be used to detect FOXO activation by monitoring FOXO-dependent luciferase expression. The high transfection efficiency of those cells makes them ideal for RNAi-based screenings. Finally, the U2transLuc system constitutes a breakthrough in the screening field, combining both fluorescence-based translocation analysis and luciferase light emissions in a single multiplexed assay, offering the advantages of both U2foxRELOC and 293foxREP in a single cell-based system.

In parallel, a pathway deconvolution system was also developed. The BaFiso system contains genetically engineered BaF/3 cells that can be used for pathway dissection, defining whether the effects triggered by a given agent occur via Akt-dependent signaling.

The five technological platforms which have been developed in the scope of this thesis can be used either for primary screenings or deconvolution, offering a wide choice of complementary readouts either for compound or RNAi screenings for novel FOXO modulators.

Finally, we developed a large-scale RNAi and a chemical genetics screen, from which several novel FOXO associations were found including Calmodulin and the *Drosophila* homolog tribbles. We further validated and characterized these novel FOXO modulators.

Resumen

Las proteínas FOXO son una familia de factores de transcripción constituida por FOXO1, FOXO3A y FOXO6, que se encuentran conservados y están implicados en varios procesos celulares fundamentales. Funcionan como efectores de programas transcripcionales involucrados en apoptosis, respuesta a estrés y longevidad. La función de FOXO está frecuentemente desregulada en cáncer, con lo que la investigación de los mecanismos que regulan dichos factores de transcripción ha ganado relevancia. Las proteínas FOXO integran estímulos regulatorios de vías de señalización, sobre todo en respuesta a factores de crecimiento y estrés. Recientemente FOXO se ha establecido como supresor tumoral, promoviendo la transcripción de genes pro-apoptoticos como FasL y Bim en respuesta a la inhibición de la vía de señalización PI3K/Akt. Esto es lo que ocurre durante privación de factores de crecimiento o de nutrientes. Con objetivo de identificar nuevos reguladores de la función de FOXO hemos desarrollado plataformas tecnológicas adaptadas para rastreos de alto rendimiento. El sistema U2foxRELOC se basa en células de osteosarcoma U2-OS que expresan establemente una proteína de fusión, GFP-FOXO3A, que se transloca al núcleo de las células cuando se produce la activación de FOXO. Este sistema de rastreo de alto contenido (HCS) se ha demostrado fiable para la detección de moléculas pequeñas capaces de inducir la translocación de FOXO entre ambos compartimentos celulares. El sistema U2nesRELOC permite la detección de la localización inespecífica de FOXO en el núcleo de las células como consecuencia de la inhibición de la maquinaria de exporte nuclear CRM1/exportina. El sistema 293foxREP puede ser utilizado para detectar la activación de FOXO a través de la monitorización de la expresión de luciferasa dependiente de transcripción inducida por FOXO. La alta eficiencia de transfección de estas células les hace ideal para rastreos basados en siRNA. Finalmente, el sistema U2transLuc combina el análisis de la translocación con luminiscencia dependiente de FOXO en un ensayo multiparamétrico, combinando las ventajas de cada uno de los sistemas U2foxRELOC y 293foxREP en un único sistema celular. Paralelamente hemos desarrollado un sistema de deconvolución, el sistema BaFiso, que contiene células BaF/3 modificadas genéticamente que pueden ser usadas para el análisis de vías de señalización específicas, definiendo si el efecto de un determinado agente ocurre a través de la señalización dependiente de Akt. Los cinco sistemas desarrollados pueden ser usados tanto para rastreos primarios como para deconvolución, y con ese amplio espectro de análisis hemos podido realizar rastreos de de genética química y de interferencia de RNA en los cuales hemos encontrado dos nuevos moduladores de la actividad de FOXO: Calmodulina y el homólogo de Drosophila tribbles, que han sido validadas y caracterizadas en el presente trabajo.

Index

Abbreviations

Akt	v-akt murine thymoma viral oncogene homolog
Bad	BCL2-associated agonist of cell death
Bcl-2	B-cell lymphoma protein 2
BCR-ABL	Breakpoint cluster region (BCR) and Abelson tyrosine kinase (ABL) fusion protein
BNIP3L	BCL2/adenovirus E1B 19kDa interacting protein 3-like
bp	Base pairs
BTG-1	B-cell translocation gene 1
CaM	Calmodulin
CBP	CREB binding protein
CD3	Cluster of Differentiation 3
cDNA	Complementary DNA
CG	Chemical Genetics
CK1	Casein kinase 1
CRM1	Exportin-1 (required for chromosome region maintenance)
DAF-16	Abnormal Dauer Formation
DBE	Daf-16 Binding Element
DDB1	Damage-specific DNA binding protein 1
DNA	Deoxyribonucleic acid
dsRNA	Double-stranded RNA
DYRK	Dual-specificity tyrosine-(Y)-phosphorylation regulated kinase 1A
EGF	Epidermal growth factor
EGFR	Epidermal growth factor receptor
eNOS	Nitric oxide synthase
Fas	TNF superfamily, member 6
FAT	transcription factor acetyl-transferase
FKH	Forkhead
FOXO	Forkhead box O
G6Pase	Glucose 6 phosphatase
GADD45	Growth arrest and DNA-damage-inducible
HAT	Histone Acetyl Transferase
HCS	High Content Screening
HDAC	Histone deacetylases
HIF1	Hypoxia inducible factor 1
HIF1A	Hypoxia inducible factor 1, alpha subunit
hTERT	Telomerase reverse transcriptase
HTS	High Throughput Screening
IGF-I	Insulin-like growth factor 1
IGFR1	Insulin-like growth factor 1 receptor
IKKβ	Inhibitor of nuclear factor kappa B kinase beta subunit
IL2	Interleukin 2
JNK	JUN N-terminal kinase
LKB1	Serine/threonine kinase 11
MDM2	Transformed 3T3 cell double minute 2
MDR1	Multidrug resistance protein 1
MMP	Matrix metalloproteinase
MnSOD	Mn superoxide dismutase
MST1	Mammalian sterile 20-like 1
MST2	Mammalian sterile 20-like 2
MYC	Avian myelocytomatosis viral oncogene homolog
NAD	Nicotinamide adenine dinucleotide
NES	Nuclear Export Signal
NFκB	Nuclear factor of kappa light polypeptide gene enhancer in B-cells
NLS	Nuclear Localization Signal
p130	Retinoblastoma-like 2

p21	Cyclin-dependent kinase inhibitor 1A
p27KIP	Cyclin-dependent kinase inhibitor 1B
p300	E1A binding protein p300
p53	p53 transformation suppressor
PA26	p53 regulated PA26 nuclear protein / sestrin 1
PCAF	p300/CBP-associated factor
PCR	Polymerase Chain Reaction
PDGF	Platelet-derived growth factor
PDK1	3-phosphoinositide dependent protein kinase-1,
PEPCK	Phosphoenolpyruvate carboxykinase
PH	Pleckstrin homology domain
PI3K	Phosphoinositide 3-kinase
PIK3CA	Phosphoinositide-3-kinase, catalytic, alpha polypeptide
PIP2	Phosphatidylinositol 4,5-bisphosphate
PIP3	Phosphatidylinositol (3,4,5)-trisphosphate
PMA	Phorbol 12-myristate 13-Acetate
Pml	Promyelocytic leukaemia bodies
PPH4.1	Protein phosphatase 4
PTEN	Phosphatase and tensin homolog
qRT-PCR	Quantitative Reverse Transcription Polymerase Chain Reaction
Ran	Ras-related nuclear protein
RNA	Ribonucleic acid
RNAi	RNA interference
ROS	Reactive Oxygen Species
Ser	Serine
SGK	Serum/glucocorticoid regulated kinase
shRNA	Short Hairpin RNA
siRNA	Small interfering RNA
SIRT1	Sirtuin 1
Skp2	S-phase kinase-associated protein 2
SMAD	Mothers against decapentaplegic homolog 4
SMK-1	Suppressor of mek1
TA	Transactivation
TCF	Transcription factor-14
TGFβ	Transforming growth factor, beta
Thr	Threonine
TRAIL	Tumor necrosis factor (ligand) superfamily, member 10
TRIB2	Tribbles homolog 2
TSC1	Tuberous sclerosis 1
TSC2	Tuberous sclerosis 2
USP7	Ubiquitin specific peptidase 7, HAUSP
UTR	Unstranslated region
VEGF	Vascular endothelial growth factor
WB	Western Blot
WIP1	Protein phosphatase 1D magnesium-dependent

1 Introduction

1.1 Cancer

Over the last decades immense amounts of information have been gathered, revealing cancer to be a genetic disease and leading to the discovery of many genes responsible for tumorigenesis. In spite of this breakthrough, cancer is still one of the diseases with the highest mortality rates in western societies. While an important reduction in the number of deaths caused by cardiac, cerebro-vascular and infectious diseases could be achieved over the last decade, cancer-related deaths did not follow the same pattern. Only particular types of cancer, namely testicular cancers and childhood leukemias show a satisfactory rate of remission and/or cure via classical chemotherapy, when detected at early stages. The reason for the slow translation of accumulated knowledge to the clinic is thought to be due to the inherent complexity of cancer. Nowadays cancer is considered as a set of diseases instead of a single one, originated from multi-step and progressive genetic alterations that confer diverse abilities to the malignant cells. Those enhanced features will allow them to survive and proliferate under adverse conditions, either through the activation of proto-oncogenes or via the silencing of tumor suppressor genes (55) .

It has bee proposed that cancer cells harbor fundamental alterations that enable their success. Those enounced “hallmarks of cancer” consist in self-sufficiency in growth signals, insensitivity to growth-inhibitory (antigrowth) signals, evasion of programmed cell death (apoptosis), limitless replicative potential, sustained angiogenesis and tissue invasion and metastasis (55).

1.2 The PI3K/Akt pathway

The dysregulation of PI3K/Akt signaling has been shown to be implicated in the alteration of all the aspects of cell physiology that comprise these hallmark features that drive the formation and development of tumors (20, 55, 63, 155) (Figure 1).

Physiological activation of PI3K is induced by growth factors and insulin targeting the catalytic subunit to the membrane where it is in close proximity with its substrate, mainly PIP2, which will be phosphorylated by PI3K and hence PIP3 is generated (153). The activity of PI3K is opposed by the action of the phosphatase and tensin homolog deleted on chromosome 10 (PTEN), which removes the 3' phosphate of PIP_3, thus regenerating PIP_2 and attenuating signaling downstream of activated PI3K. PDK1 is activated by binding PIP3 through its C-terminal pleckstrin homology (PH) domain. Activated PDK1 phosphorylates Akt at Thr308 activating its Ser/Thr kinase activity. Once phosphorylated in Thr308, further activation occurs by PDK2 (the complex rictor/mTOR) by phosphorylation at Ser473. Akt amino terminus also contains a PH domain that binds phospholipids, therefore Akt activity is regulated through PIP3 binding, permitting its activation by PDK1. Akt activation and consequent phosphorylation of its many physiological substrates (25, 35, 71, 139, 155) stimulates cell cycle progression, survival, metabolism, resistance to hypoxia and migration, while apoptosis induced by growth factor withdrawal, detachment of extracellular matrix, UV irradiation, cell cycle discordance and activation of FAS signaling is inhibited (35, 71, 120). Hence, the activation of the PI3K/Akt signaling cascade confers oncogenic properties to the neoplasic cells and is considered as one of the most frequently altered pathways in human cancer (63). PTEN activity is lost by mutations, deletions or promoter methylation at high frequency in many primary and metastatic human cancers. Germline mutations of PTEN are found in Cowden, Bannayan-Riley-Ruvalcaba and a Proteus –like syndromes, all of them familial cancer predisposition syndromes (92, 95, 111, 136). Many activating mutations have been described in the PI3KCA gene (coding for the p110α catalytic subunit of PI3K) to be present in human tumors (119, 133), which are able to constitutively activate Akt. These enhanced biochemical capabilities translate into enhanced oncogenic activity of the PI3K mutants (6, 167). Carpten et al. (21), reported a somatic mutation of Akt in human breast, colorectal and ovarian cancers, resulting in the activation of Akt by means of pathological localization to the plasma membrane, which stimulates downstream signaling, transforms cells and induces leukemia in mice. Hence, a direct role of Akt1 in human cancer is established, and adds to the known genetic alterations that promote oncogenesis through the PI3K/Akt pathway (21).

Activation of PI3K and Akt without mutations in their coding genes is reported to occur in breast (5, 19, 79), ovarian (19, 110, 159) pancreatic (4), oesophageal (117), thyroid cancer (44) and other cancers (11, 119).

Several other genes of the pathway act as tumor suppressors and are frequently inactivated in some cancers, which carrying germ line familial mutations. The frequent dysregulation of the PI3K/Akt pathway in human cancer has made components of this pathway attractive for therapeutic targeting.

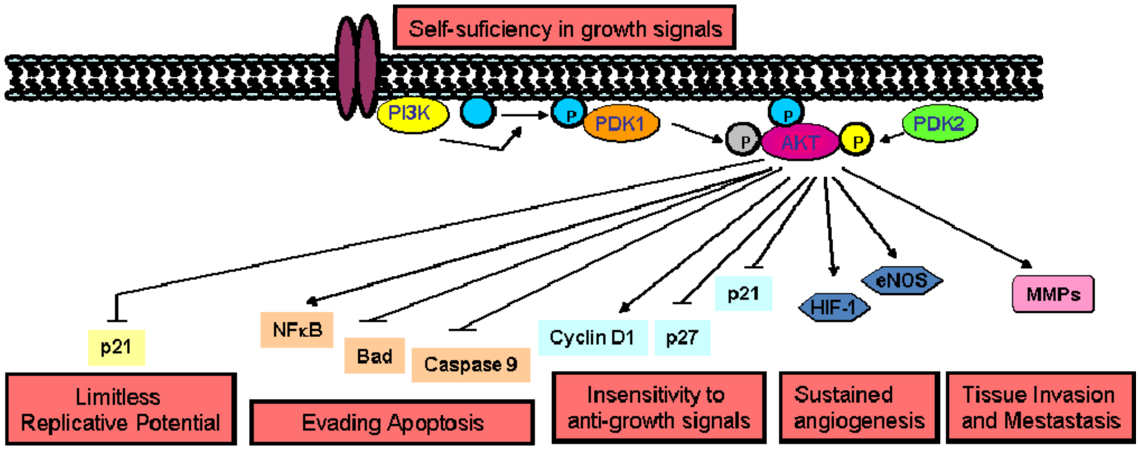

Figure 1. PI3K/Akt is a fundamental pathway in cancer. Its activation induces oncogenicity while tumor suppressor features are diminished, covering nearly all the established Hallmarks of Cancer (Boxes). Bad: BCL2-associated agonist of cell death; NFkB: nuclear factor of kappa light polypeptide gene enhancer in B-cells 1; HIF-1: hypoxia inducible factor 1; eNOS: nitric oxide synthase; MMPs: metalloproteinases. Adapted from (34).

1.3 FOXO proteins

One of the major signaling branches downstream of PI3K/Akt couples growth factor signaling to diverse transcriptional networks via the inactivation of FOXO transcription factors. The molecular link between FOXO factors and PI3K/Akt signaling is highly conserved among vertebrates and invertebrates. The mammalian members of FoxO subclass of forkhead transcription factors FOXO1, FOXO3A, FOXO4 and FOXO6 function as transcriptional regulators in the cell nucleus. They bind as monomers via the Forkhead box, a 110 amino acid region located in the central part of the molecule (Figure 2)(157) to their consensus DNA binding sequence TTGTTTAC, designated as DBE (DAF-16 binding element) (43).

The ever-growing list of target genes for these factors contains many elements that function in metabolism, apoptosis, resistance to oxidative stress, and cell-cycle inhibition, and includes glucose-6- phosphatase (108, 135, 163), phosphoenolpyruvate carboxykinase (122) FasL (13), Bim (32), MnSOD (84, 113), catalase (113), p27KIP1 (100), p130 (85), and cyclin G2 (42, 50).

Moreover, bioinformatic evidence indicates that a large number of genes contain conserved FOXO-binding sites (DBEs) in their promoters (160). When present in the nucleus and bound to DNA, FOXO proteins typically act as potent transcriptional activators (13, 83). The transactivation domain of FOXO proteins is located in the c-terminal region of the molecule. Gene array analyses have indicated that FOXO proteins can also act as transcriptional repressors (123). Thus, this family of transcription factors may activate or repress transcription, depending on the promoter context and extracellular conditions (50).

Figure 2. The general structure of FOXO transcription factors. FOXO proteins share a high structural similarity that comprises a forkhead domain (FKH), a nuclear localization signal (NLS), a nuclear export signal (NES) and a transactivation domain (TA).

FOXO transcription factors are considered *bona fide* tumor suppressors that are inactivated in the great majority of human cancers, due to overactivation of the PI3K/Akt pathway (13, 27, 50, 105). Akt-mediated phosphorylation of FOXO proteins induces their nuclear export and interrupts the transcription of their target genes.

Cellular stress or inhibition of the PI3K/Akt pathway promote the translocation of FOXO factors to the cell nucleus, where their transcriptional functions can be executed. Diverse cellular functions can be affected by the genes which are transcriptionally targeted by FOXO, ranging from metabolism to cell cycle, apoptosis and oxidative stress (50).

1.3.1 Regulation of FOXO factors

The activity of FOXO factors is regulated by a sophisticated signaling network that integrates information from PI3K/Akt and stress-induced signaling pathways resulting in a specific pattern of posttranscriptional modifications. The multiple post-transcriptional events include phosphorylation, acetylation and ubiquitylation at 3 different levels: subcellular localization, stability and transcriptional activity of FOXO proteins (Figure 3).

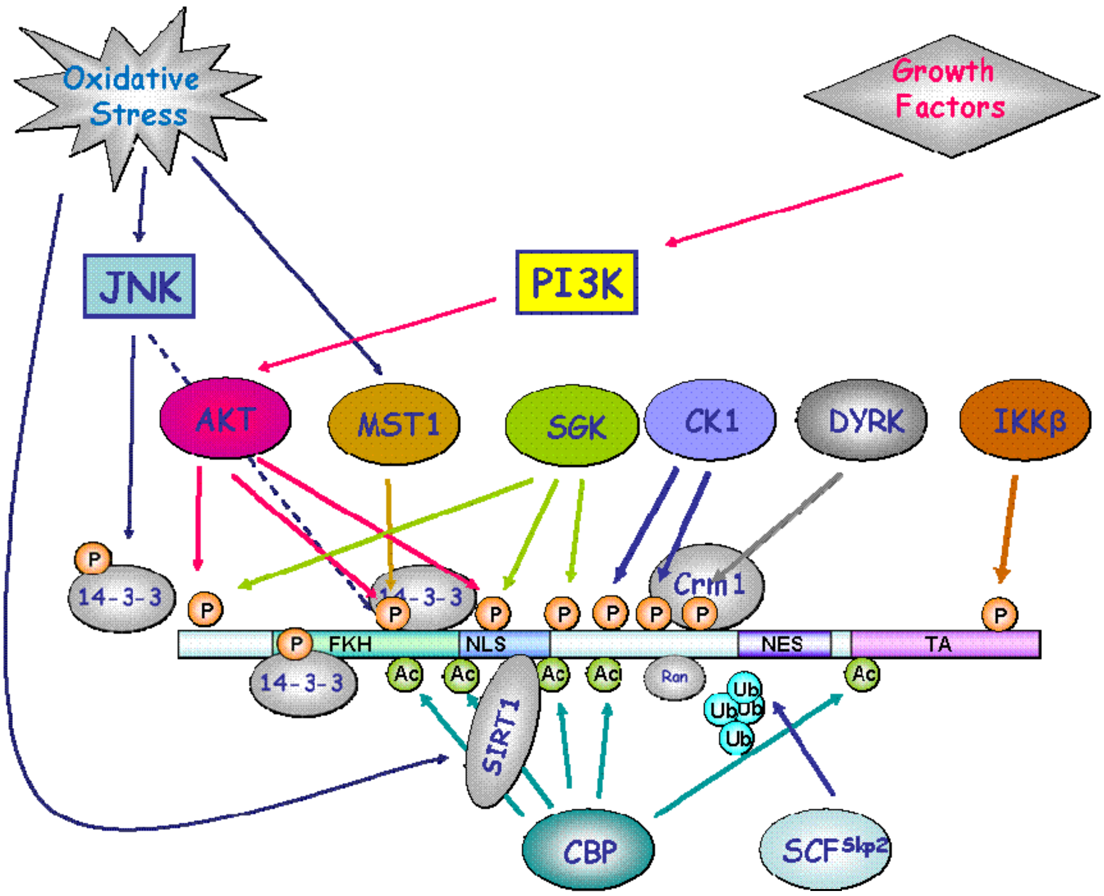

Figure 3 – The regulation of FOXO transcription factors occurs via phosphorylation, acetylation and ubiquitylation. The two phenomena that trigger FOXO translocation are growth factor signaling via the PI3K/Akt pathway and oxidative stress. Some of the main molecules known to influence the post-translational modifications of FOXO proteins are depicted in this figure. Akt: v-akt murine thymoma viral oncogene homolog; CBP: CREB binding protein; CK1: casein kinase 1; DYRK: dual tyrosine phosphorylated regulated kinase 1; IKKβ: I kappaB kinase β; JNK: c-Jun N-terminal kinase 1; MST1: mammalian Ste20-like kinase 1; PI3K: phosphoinositide-3-kinase; SIRT1: sirtuin; Skp2: S-phase kinase-associated protein 2.

1.3.1.1 Phosphorylation

Activation of PI3K and subsequent activation of the downstream families of kinases Akt and the related SGK has been shown to culminate in the phosphorylation and inactivation of FOXO (13). Biochemical studies in mammalian cells have shown that Akt directly phosphorylate FOXO transcription factors (8, 13, 83, 109, 127, 143). Phosphorylation of FOXO factors by Akt triggers the rapid relocalization of FOXO proteins from the nucleus to the cytoplasm. Akt phosphorylates FOXO3A at three key regulatory sites (Thr32, Ser253 and Ser315) that are conserved from *C. elegans* to mammals and are part of a perfect consensus sequence for Akt phosphorylation (2). SGK also phosphorylates FOXO factors, at a different combination of sites. While Akt preferentially phosphorylates Ser253, SGK favors the phosphorylation of Ser315.

Thr32 is phosphorylated by both kinases. The three regulatory sites are phosphorylated in response to a number of growth factors, including insulin growth factor I (IGF-I) (13), insulin (83), interleukin 3 (33), erythropoietin (72), epidermal growth factor (EGF) (68), and nerve growth factor (168). Hence, FOXO proteins integrate a broad range of external stimuli via phosphorylation of three conserved residues by Akt and SGK. The preferential phosphorylation of FOXO proteins by different protein kinases may allow FOXO to selectively respond to closely related but different stimuli, such as insulin and IGF-I (107).

The major consequence of the phosphorylation of FOXO transcription factors by Akt and SGK is a change in their subcellular localization (8, 13, 142). In the absence of growth factors, when Akt and SGK are inactive, FOXO localizes within the nucleus. Upon exposure to growth factors, the PI3K/Akt cascade is activated and triggers the export of FOXO factors to the cytoplasm. Mutation analyses revealed that one or two leucine-rich domains in the C-terminal region of FOXO proteins function as a nuclear export signal (NES) (8, 14). In addition, phosphorylated FOXO factors have been shown to specifically interact with 14-3-3 proteins, which serve as chaperone molecules to escort FOXO proteins out of the nucleus (13, 14). 14-3-3 binding to FOXO may actively promote the nuclear export of FOXO factors, perhaps by inducing a conformational change in FOXO molecules that would expose the NES and allow interaction with Exportin/CRM1 (14). 14-3-3 binding to FOXO may also prevent he nuclear re-import of these transcriptional factors by masking the FOXO proteins nuclear localization signal (NLS) (12, 128). Mutational analysis of the three regulatory Akt/SGK sites revealed that the phosphorylation of each site contributes to the nuclear exclusion of FOXO factors (15). One attractive possibility is that each site participates in different aspects of the mechanisms that ensure the localization of FOXO proteins to the cytoplasm. Thus, phosphorylation of FOXO factors may represent a way of modulating the extent of the relocalization of these transcription factors to the cytoplasm in different cell types in response to different combination of signals.

Insulin and growth factors also trigger the phosphorylation of several other sites of FOXO factors. Previous phosphorylation of Ser329 by the dual tyrosine phosphorylated regulated kinase 1 (DYRK1), a member of the MAP kinase family facilitates a further phosphorylation of Ser322 and Ser325 mediated by casein kinase 1 (CK1). The phosphorylation of FOXO factors at Ser322 and Ser325 appears to accelerate FOXO relocalization to the cytoplasm in response to growth factors by increasing the interaction between FOXO and the export machinery (Ran and exportin/CRM1) (129). These various mechanisms for regulating the translocation of FOXO transcription factors from the nucleus to the cytoplasm may serve as a fail-safe mechanism to ensure a complete sequestration of FOXO factors away from their target genes.

Another major input of FOXO regulation is cellular stress. In this context, JNK kinase is known to act upon FOXO, and contrarily to Akt JNK was shown to promote the activation of FOXO towards transcription. JNK has been shown to directly phosphorylate human FOXO1, FOXO3A and FOXO4 *in vitro*, as well as the worm homolog DAF-16, although the regulatory sites remain to be identified (50). Also, JNK has been shown to phosphorylate 14-3-3 proteins releasing FOXO into the cell nucleus (150). Therefore, stress-induced JNK will facilitate FOXO localization to the cell nucleus, either by direct phosphorylation or by lowering the ability of 14-3-3 to sequester FOXO proteins in the cell cytoplasm.

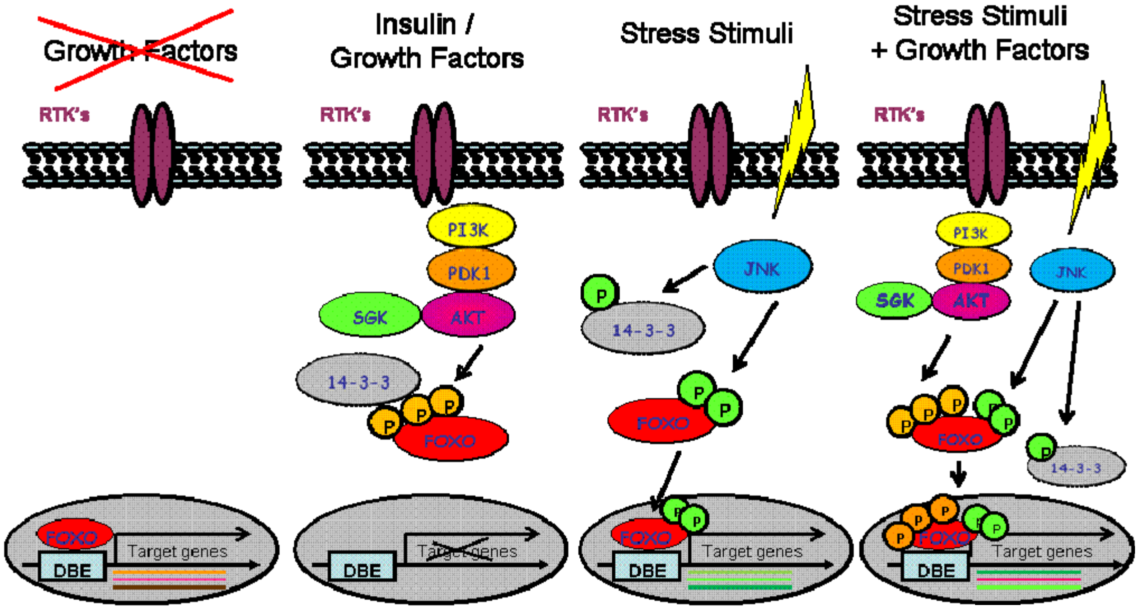

Figure 4. The regulation of FOXO factors by growth factors and stress stimuli. In response to growth factors the PI3K/Akt pathway inhibits FOXO-dependent transcription through phosphorylation and subsequent sequestration in the cytoplasm. Stress stimuli are sufficient to overcome the cytoplasmic localization of FOXO factors. In response to stress stimuli, JNK phosphorylates FOXO proteins, which causes their nuclear translocation. Although phosphorylation by JNK does not directly inhibit the binding of 14-3-3 proteins it induces the release of its substrates. JNK activity is sufficient to overcome Akt inhibition of FOXO factors and causes the transcription of genes involved in stress resistance. It has been proposed that a specific subset of genes is transcribed under each condition and the specific transcriptional programs may dictate whether cells undergo cell cycle arrest, stress resistance or apoptosis (Adapted from (50)).

Stress-mediated FOXO activation via JNK constitutes a powerful input that induces FOXO transcriptional activity even when the PI3K/Akt pathway is activated, which reflects a marked hierarchy of the signals that will culminate in FOXO modulation. When both inputs are present stress signaling overrides PI3K/Akt impairment of FOXO function, and the gene expression pattern that occur in this context resembles more the pattern observed in stress conditions alone (50).

The protein kinase Sterile 20 (Ste20) was reported to mediate hydrogen peroxide-induced cell death in S. cerevisiae (1). The mammalian Ste20-like kinases (MSTs), of which MST1 and MST2 share the highest degree of homology, and the *Drosophila* ortholog Hippo have important functions in apoptotic cell death (23, 49, 59, 115, 158). MST1 was found to phosphorylate the FOXO transcription factors at a site that is conserved within the forkhead domain of these proteins from mammals to *C. elegans* (90). In mammalian neurons, oxidative stress activates MST1, which in turn phosphorylates FOXO3A at Ser207. The MST1-induced phosphorylation of FOXO3A disrupts its interaction with 14-3-3 proteins, promotes FOXO3A translocation to the nucleus, and thereby induces neuronal cell death (90).

FOXO can also be phosphorylated by IKKβ, which was reported to promote tumorigenesis (66). IKKβ induces the phosphorylation of FOXO3A at Ser644, in the extreme C-terminal position of the molecule (Figure 2). This phosphorylation results in the ubiquitylation and subsequent degradation of FOXO3A (66).

Despite the abundant information concerning the phosphorylation events that regulate the subcellular localization of FOXO proteins very little is known about the phosphatases that dephosphorylate FOXO transcription factors. Protein phosphatase 2A was identified as a possible FOXO3A binding partner in a purified FOXO3A-containing protein complex, suggesting that protein phosphatase 2A may be one of the phosphatases that dephosphorylates FOXO (130). The subcellular localization of the FOXO phosphatases could provide another layer of spatial control of FOXO activity. In addition, the rate at which the phosphatases remove the phosphate group from each phosphorylated site of FOXO proteins may affect the kinetics of localization of these transcription factors.

Subcellular localization of FOXOs may also be deregulated independently of post-translational modifications. The Kaposi sarcoma-associated herpes virus can promote tumorigenesis through interaction of latent protein LANA2 with FOXO3A and 14-3-3 proteins, which are required for nuclear export of FOXO3A, resulting in a decrease in transcriptional activity.

1.3.1.2 Acetylation

Phosphorylation of FOXO proteins is a fundamental mode of regulating their activity. Still, other post-translational modifications such as acetylation also influence the activity of FOXO factors, adding another layer to this complex regulation network.

The nuclear proteins CBP and p300 and their associated proteins, such as p300- and CBP-associated factor (PCAF), possess intrinsic histone acetyl-transferase (HAT) activity. These proteins play essential roles promoting transcription by acetylating histones and integrating signaling from enhancer and promoter regions. They also directly acetylate transcription factors through FAT (transcription factor acetyl-transferase) activity (Li et al., 2002). CBP appears to play a dual role in FOXO-mediated gene transcription: it can facilitate FOXO-mediated transcription by acetylating chromosomal histones but also promotes acetylation and regulation of FoxO proteins themselves. Acetylation of FOXO proteins by acetylases such as CBP and p300 increases in response to oxidative stress (16, 41, 81). Acetyl-FOXO proteins accumulate in the nucleus and associate with Pml bodies, which hinders their activity (81).

Increased levels of FOXO acetylation in the nucleus suggests an additional layer of regulation by other pathways, such as those involving SIRT1, a nicotinamide adenine dinucleotide (NAD)- dependent histone deacetylase. SIRT1 is localized in the nucleus in cells stimulated with growth factors (88, 154). Upon stress stimuli, SIRT1 forms a complex with and deacetylates FOXO proteins in the nucleus (16, 81). Interestingly, expression of SIRT1 augments FOXO3A-induced cell cycle arrest by increasing expression of $p27^{KIP1}$ (16). This is consistent with the fact that acetylation of FoxO proteins by CBP inhibits their activity (26). By contrast, FOXO3A-induced expression of apoptotic genes such as Bim is further enhanced by inhibition of SIRT1 by the class III histone deacetylase (HDAC) inhibitor nicotinamide and the class I/II HDAC inhibitor trichostatin A (16). Moreover, expression of SIRT1 inhibits *Bim* promoter activity (104). Current evidence favors the hypothesis that association with SIRT1 differentially affects FOXO target genes, inducing cell cycle arrest, stress resistance and DNA repair rather than apoptosis (16, 86).

1.3.1.3 Ubiquitylation

FOXO proteins are also regulated by the ubiquitin-proteasome system. Steady-state levels of FOXO proteins are reduced in murine pro-B lymphocytes stably expressing Akt, and this effect is largely attenuated by treatment of cells with proteasome inhibitors (121). The levels of FOXO also decrease in HepG2 cells following insulin treatment (97). Similarly, treatment of chicken embryo fibroblasts with platelet-derived growth factor (PDGF) decreases levels of FOXO. This effect is inhibited by the proteasome inhibitor lactacystin or the PI3K inhibitor LY294002 (3), which suggests that proteasome-mediated degradation of FOXO depends on Akt signaling.

Moreover, phosphorylation by Akt is required for the polyubiquitylation of FOXO (97).

Ubiquitin-dependent degradation of FOXO requires its interaction with the F-box protein Skp2, the substrate-binding component of the Skp1/culin 1/F-box protein (SCFSkp2) E3 ligase complex (67), which targets various proteins, including $p27^{KIP1}$, for degradation in the nucleus (125). Skp2-dependent polyubiquitylation of FOXO requires phosphorylation by Akt (67). IKK-mediated phosphorylation of FOXO3A also leads to its ubiquitylation and degradation by the MDM2 E3 ubiquitin ligase (66, 162).

Whereas polyubiquitylation of FOXO proteins results in their degradation, monoubiquitylation leads to their nuclear localization and increases their transcriptional activity (152). Therefore, oxidative-stress-mediated monoubiquitylation provides another means for cells to regulate the subcellular localization and activity of FOXO.

Deubiquitylation of FOXO is known to be catalyzed by the deubiquitylating enzyme herpes virus-associated ubiquitin-specific protease (HAUSP/USP7) (152). USP7-mediated deubiquitylation of FOXO results in their relocalization from the nucleus to the cytoplasm.

1.3.2 Functions of FOXO proteins

FOXO factors are implicated in many fundamental cellular processes, through the transcriptional regulation of a wide array of target genes (Figure 5). The integration of diverse intracellular and extracellular stimuli translates in the post-translational modifications that occur on FOXO proteins generating a “FOXO code” that is read by protein partners and determines the level, intensity, duration and activity of FOXO transcription factors within cells (18).

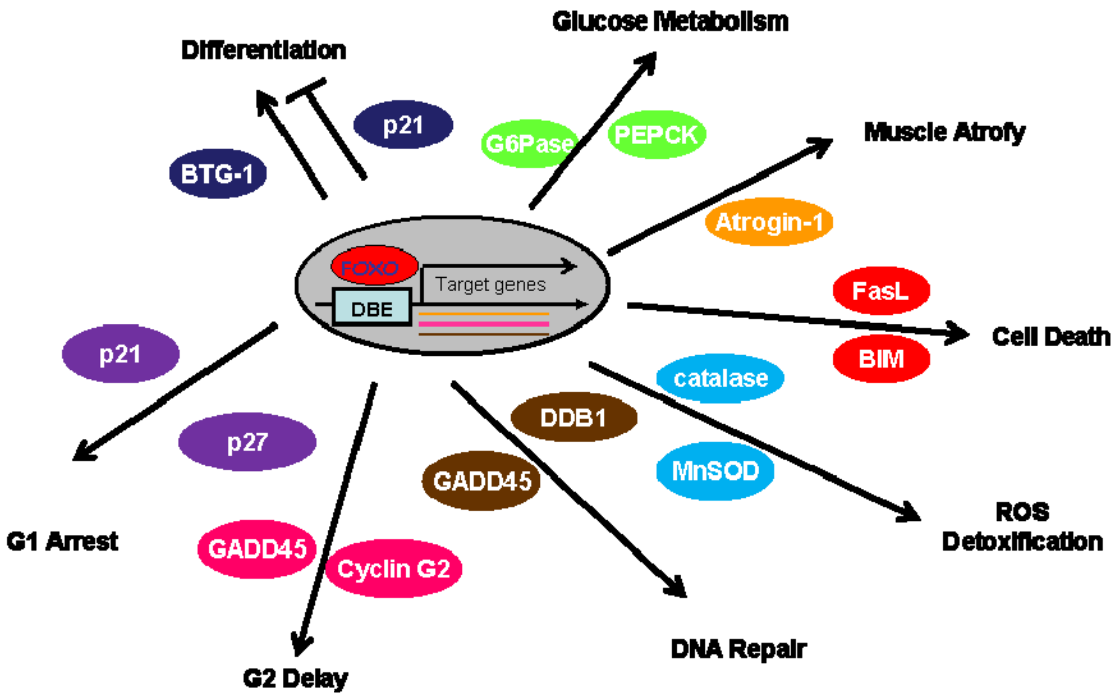

Figure 5 *A schematic representation of some FOXO target genes and cellular roles in which they are implicated. BTG-1: B-cell translocation gene 1; p21: cyclin-dependent kinase inhibitor 1A; p27: cyclin-dependent kinase inhibitor 1B; MnSOD: manganese superoxide dismutase; G6Pase: glucose-6-phosphatase; PEPCK: phosphoenolpyruvate carboxykinase; FasL: Fas ligand; GADD45: growth arrest and DNA damage-inducible protein 45; DDB1: damage-specific DNA-binding protein 1; FBE, FOXO binding element (Adapted from (50)).*

1.3.2.1 FOXO and apoptosis

The expression of constitutively nuclear forms of FOXO proteins has been shown to trigger cell death, particularly in neurons and lymphocytes (13, 31, 46, 169). One way by which Akt promotes cell survival is by sequestering FOXO factors away from the promoters of apoptotic genes. FOXO target genes that mediate apoptosis include Bim, a proapoptotic Bcl-2 family member (33). Apoptosis induced by the inactivation of the PI3K/Akt pathway is reduced in lymphocytes from Bim-deficient mice, indicating that Bim is an important target gene of FOXO factors to induce cell death. FOXO-induced apoptosis also appears to be dependent on the induction of death cytokines, including Fas ligand and TRAIL (13, 102). Fas ligand, TRAIL and other death cytokines may amplify the ability of FOXO proteins to induce apoptosis by triggering death pathways in neighboring cells.

1.3.2.2 FOXO and cell cycle arrest

The expression of active forms of FOXO proteins in dividing cells was shown to promote cell cycle arrest at the G1/S boundary (100). The target genes that mediate FOXO-induced cell cycle arrest are the Cdk inhibitor p27^{KIP1} (100), and the Rb family member p130 (85). The ability of FOXO factors to induce G1 arrest is diminished in p27/p130-deficient fibroblasts (85), suggesting that p27 and p130 are both critical to mediate FOXO-dependent G1 arrest. In the presence of TGFβ, FOXO proteins also bind to the promoter of the cell cycle inhibitor p21 and induce cell cycle arrest at G1/S transition (137). FOXO factors can also promote cell cycle arrest by repressing the expression of cyclin D1 and D2 (123, 134). Thus, FOXO proteins play a major role in G1 arrest by both upregulating cell cycle inhibitors (p21 and p27) and by repressing cell cycle activators (cyclins D1 and D2).

FOXO factors are also involved in other cell cycle checkpoints. Cells in which FOXO3A is activated in the S phase display a delay in their progression through the G2 phase of the cell cycle (148). Microarray analysis led to the identification of several FOXO3A target genes that may mediate the effect of FOXO proteins at the G2/M boundary, such as cyclin D2 and growth arrest and DNA damage-inducible protein 45 (GADD45) (42, 148). Hence, FOXO factors mediate cell cycle arrest at the G1/S and G2/M transitions, two checkpoints that are critical in the cellular response to stress. FOXO-induced cell cycle arrest may allow time for repair of damaged DNA and for detoxification of cells (50).

1.3.2.3 FOXO in stress resistance, DNA repair and detoxification

Consistent with the role of FOXO factors in promoting cell cycle arrest at the G1/S and G2/M boundaries, the expression of active forms of FOXO proteins upregulates several genes involved in DNA repair such as DBB1 and GADD45. (123, 148). In addition, FOXO proteins have been reported to allow detoxification of reactive oxygen species (ROS) by upregulating free radical scavenging enzymes, including Mn superoxide dismutase (MnSOD) and catalase (85, 113, 123, 148). Thus, FOXO transcription factors control two aspects of cellular resistance to stress: repair of damages caused by ROS and detoxification of ROS (50).

Recent work has shown that FOXO factors can stimulate the expression of multidrug transporter MDR1 (P- glycoprotein) that may promote increased resistance of tumor cells to the toxicity generated as a consequence of chemotherapy (54).

A recent cDNA microarray study identified IGFR1 and PIK3CA as target genes of FOXO3A in a colon carcinoma cell line (29). This negative feedback could be considered as another stress resistance mechanism regulated by FOXO proteins, as the transcription of both genes will increase the activation of the PI3K/Akt pathway which is known to contribute in resistance to stress stimuli.

1.3.2.4 FOXO in metabolism

FOXO transcription factors also play an important role in upregulating genes that control glucose metabolism (50). FOXO factors elicit gluconeogenesis by upregulating glucose 6 phosphatase (G6Pase), which is responsible for converting glucose-6-phosphate to glucose, and phosphoenolpyruvate carboxykinase (PEPCK), which converts oxaloacetate to phosphoenolpyruvate (108, 122, 135, 163). Thus, insulin effects on glucose metabolism are mediated in part through the repression of FOXO factors by the PI3K/Akt pathway.

1.3.2.5 FOXO proteins in ageing and lifespan

One of the most intriguing functions of FOXO transcription factors is their conserved ability to increase longevity (75). In worms, mutations in the insulin receptor or PI3K result in an extended longevity by up to threefold (69, 76, 78, 103). This lifespan extension is reverted when the worm FOXO ortholog (DAF-16) is mutated (93, 116). Thus, the FOXO ortholog DAF-16 plays a crucial role downstream of the insulin-signaling pathway to regulate longevity.

The target genes that mediate the ability of DAF-16 to increase longevity include MnSOD (SOD3 in worms) (65), MST1 (90), heat-shock proteins and antimicrobial agents (89, 99). DAF-16 appears to induce a program of genes that coordinately regulate longevity by promoting resistance to oxidative stress, protection of protein structure, and resistance to pathogens. Consistent with the notion that stress resistance is correlated with longevity, all the long-lived worm mutants that lead to the activation of DAF-16 also display resistance to oxidative stress, heat shock and UV radiations (62). Similarly, as for mammals, it has been shown that mice that are deficient for either the insulin or the IGF-1 receptor are long lived and resistant to oxidant stress stimuli (10, 64). In addition, FOXO proteins induce stress resistance in mammalian cells and some FOXO target genes involved in stress resistance, like MnSOD, are conserved between mammals and worms, raising the possibility that FOXO factors may also regulate the lifespan in mammals.

1.3.3 FOXO and cancer

In mammals, the antiproliferative and proapoptotic effects of FOXO proteins strongly suggested their functions as tumor suppressors (50).

Several lines of evidence indicate that FOXO factors are likely to play a significant role in cancer regulation. FOXO3A has been shown to be dysregulated in breast cancer. The presence of cytoplasmatic FOXO3A in breast cancer cells highly correlates with poor patient survival. A strong correlation has also been observed between the expression of IKKβ and the cytoplasmatic localization of FOXO3a in those tumors (27).

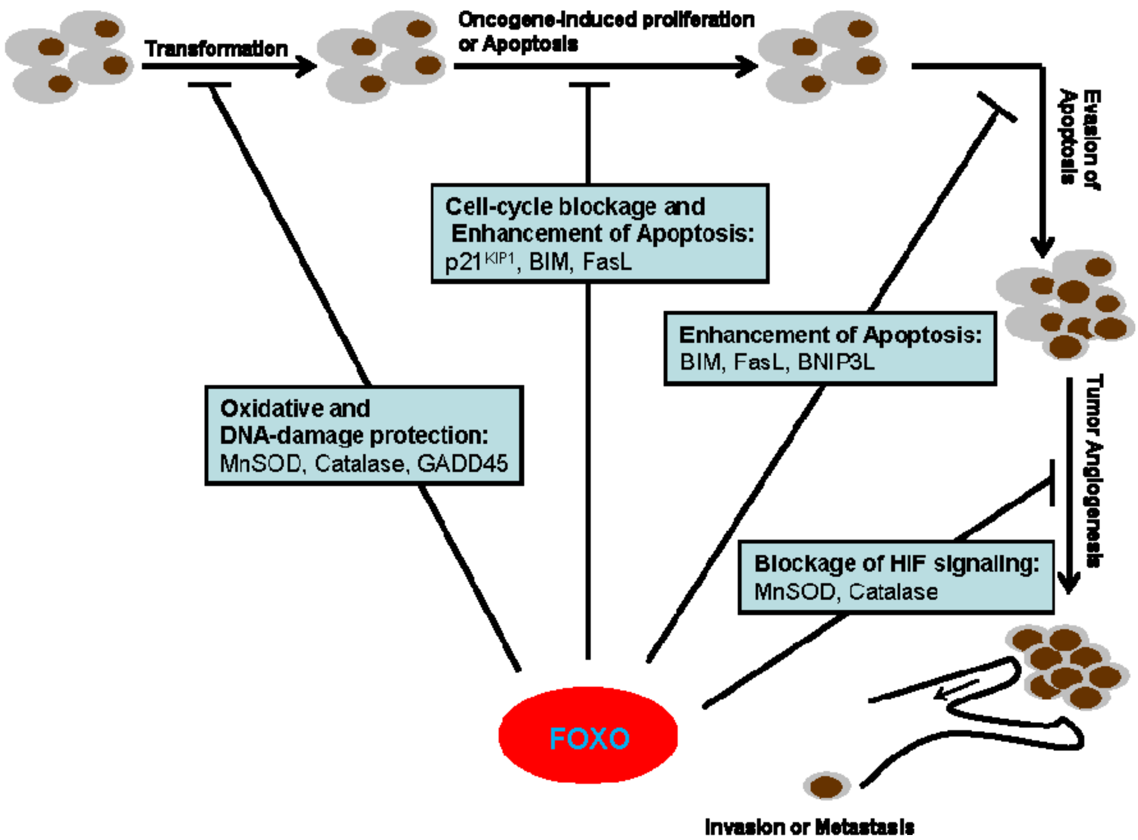

Figure 6 – The tumor-suppressive functions of FOXO proteins could operate to block tumor development at multiple stages. FOXO-induced oxidative stress scavenging and DNA-damage repair prevents the induction and propagation of mutations required for oncogenic transformation. Because the progression from each stage of tumorigenesis to the next is probably driven by mutations, this FOXO function might be tumor suppressive at multiple stages. A tumor can only form if the balance of proliferation and apoptosis is shifted towards proliferation. FOXO proteins block the cell cycle and induce the expression of pro-apoptotic genes, which could re-balance tissue homeostasis. This function of FOXO proteins could also be tumor suppressive at different stages of tumorigenesis. Finally, for a malignant tumor to form angiogenesis has to occur. FOXOs repress HIF signaling, which is required for tumor angiogenesis. Taken together, the FOXO proteins function as tumor suppressors throughout the formation, expansion and spreading of the tumor (Adapted from (27)).

FOXO proteins were shown to interact physically or functionally with tumor suppressors or oncogenes. In response to stress stimuli or to nutrient deprivation, FOXO3A has been found to interact with the tumor suppressor p53 in the nucleus (16, 112). The observation that FOXO and p53 interact, combined with reports that p53 and FOXO share similar target genes (p21, GADD45, WIP1, PA26), suggests that these two proteins may coordinate tumor suppression. Also, FOXO forms a complex with SMAD transcription factors (137), that act as tumor suppressor through the mediation of the cytostatic effect of transforming growth factor β (TGF-β). The interaction between FOXO factors and SMADs occurs at the p21 promoter in response to TGF-β stimulation. The FOXO/SMAD complex elicits the upregulation of p21 and subsequent G1 arrest (50). Finally, the proto-oncogene β-catenin has been shown to bind to FOXO proteins (39), enhancing their ability to inhibit cell-cycle progression. Since β-catenin has been implicated in cancer progression, in particular in colon cancer, it is possible that FOXO factors could counteract tumor progression by sequestering β-catenin thereby inhibiting cell cycle progression (50).

The expression of altered forms of FOXO proteins reduces tumorigenicity in several models. Cell proliferation and tumorigenicity in mice induced by IKKβ expression can be overridden by the expression of an active form of FOXO3A (66). In *Drosophila* it was shown that FOXO affects MYC-induced protein translation by interfering with ribosome biogenesis (144). Others have shown that expression of triple mutant FOXO1 or FOXO3A in which the three phosphorylation sites targeted by Akt have been altered to prevent FOXO inactivation efficiently induces apoptosis in melanoma cells (48).

1.3.3.1 FOXO transcription factors are bona fide tumor suppressors

The formal establishment of FOXO proteins as tumor suppressor came from a triple FOXO-knockout mouse model in which simultaneous loss of FoxO1, FoxO3a and FoxO4 induces spontaneous tumor formation, mainly aggressive lymphoblastic thymic lymphomas, with spread to spleen, liver, and lymph nodes. The knockdown of two FOXO genes does not produce such a marked phenotype, suggesting a strong redundancy of the three FOXO family members. The triple FOXO-knockout mice also displayed aberrant and widespread vasculature growth, indicating that FOXO has a major role in the regulation of vasculature homeostasis. All the mice developed a striking age-progressive hamartomatous phenotype in the endothelial cell lineage, and in a relative number of animals the condition progressed to lethal angiosarcomas.

The thymocytes of the triple knockout mice exhibited enhanced response to growth stimulation and conversely a greater resistance to death stimuli (118).

1.3.4 Reactivation of FOXO as a therapeutic strategy.

Due to mounting evidence of the inactivation of FOXO transcription factors in human tumors, the restoration of FOXO functions has been suggested as a promising strategy for anti-cancer therapy.

Unlike other tumor suppressors whose functions are lost due to mutations, the abrogation of FOXO function occurs mainly via post-translational modifications induced by growth and survival pathways. Thus, although FOXO proteins are inactivated in tumors, the gene – and thus the protein – is still present and possibly reactivatable, whereas genetic loss as it is often the case for p53 is irreversible. Therefore, therapies aimed at reactivating FOXO could prove effective (27).

Interestingly, several agents that are used in anti-cancer chemotherapy have been shown to reactivate FOXO proteins. FOXO3A was reported to be an indirect target of the chemotherapeutic drugs paclitaxel, a tubulin depolymerizing agent, and KP372-1, a multiple kinase inhibitor in breast carcinoma cells (140, 141) and in acute myeloid leukemia cells (166), respectively and both activate FOXO3A by reducing Akt activity. Paclitaxel also activates JNK, which has a double effect in the activating and stabilizing phosphorylation of FOXOs *per se*, and in the inhibition of 14-3-3 binding to FOXOs, preventing their nuclear exclusion.

FOXO3A is also important for imatinib (Glivec)-induced apoptosis in chronic myeloid leukemia cell lines that express the BCR-ABL oncoprotein (38). FOXO3A is constituvely phosphorylated in BCR-ABL-positive cell lines and the inhibition of BCR-ABL by imatinib induces FOXO3A transcriptional activity leading to Bim-dependent apoptosis (105). Blockade of epidermal growth factor receptors (EGFR) by antibodies (such as trustuzumab or cetuximab) or small molecules (such as lapatimib and gefitinib) represents a valuable therapeutic strategy against breast, prostate, kidney, ovarian, and NSCLC, and either single agent or combinational therapies have been put in clinical trials (126). The PI3K pathway is a major target of the EGFR pathway and EGFR blockade by the antibodies induces FOXO3A and transcriptional activation of the BNIP3L gene (124). Interestingly, FOXO3A is a crucial target of small molecule EGFR inhibitors, therefore the reintroduction of active FOXO3A may sensitize resistant cells to agents such as gefitinib (105).

Activation of FOXO3A may also be effective in combination with other agents to overcome resistance or increase tumor killing. FOXO3A-induced upregulation of Bim has been reported in p53-null osteosarcoma cell lines following exposure to ionizing radiation (161), suggesting that FOXO3A may be an important effector of radiation-inducing apoptosis, and chemotherapies targeting FOXO3A may also sensitize cells to radiotherapy.

However, the reactivation of FOXO has also been associated with resistance to chemotherapy, through the mechanisms that allows FOXO to protect the cells from stress.

Therefore, it is fundamental to identify and characterize all the molecular components that influence FOXO activation comprehensively. A complete knowledge on how to program the FOXO code will enable the tailoring of more efficient anti-cancer therapies that will take advantage of the tumor suppressor features of FOXO proteins and at the same time avoid the development of resistance.

1.4 The Search for Novel FOXO modulators

Traditionally, systematic genetic screenings in mammalian cell systems were hampered by the lack of reliable tools (70, 138).

However, recent technological advances have enriched the approaches available for the identification of components of complex signaling networks in cultured human cells.

RNAi is an evolutionarily conserved, sequence-specific gene-silencing mechanism that is induced by double-stranded RNA (dsRNA) (22). Long dsRNAs are processed into 21–25 base pairs (bp) dsRNAs called small interfering RNAs (siRNAs) (51, 52, 164) by Dicer, a ribonuclease III family (RNAse III). The resulting small RNAs enter the RNA-induced silencing complex (RISC), which uses a single-stranded version of the small RNA as a guide to substrate selection (52, 53, 151, 164).

Perfect complementarity between the substrate and the small RNA leads to target-RNA cleavage (22). RNAi can result in the knockdown of single or multiple genes, providing a quick and convenient method of analyzing gene function (36). RNAi libraries have been developed as a useful screening tool for assessing functional consequences of inhibiting members of signaling pathways (30, 96).

Chemical genetics is the study of gene-product function in a cellular or organismal context using exogenous ligands. In this approach, small molecules that bind directly to proteins are used to alter protein function, enabling a kinetic analysis of the *in vivo* consequences of these changes. Recent advances have strongly enhanced the power of exogenous ligands such that they can resemble genetic mutations in terms of their general applicability and target specificity. The growing sophistication of this approach raises the possibility of its application to any biological process (138).

The adaptation of the RNAi technology to mammalian cells, together with the expansion of chemical genetics enabled systematic loss-of-function studies capable of revealing protein functions implicated in many human disease processes. However, the lack of powerful technologies capable of detecting the changes induced upon interference in a cell basis and in a high throughput fashion constituted a technological gap that did not permit the implementation of large-scale RNAi and chemical genetic screenings.

This technological gap was filled with the implementation of image acquisition using robotic fluorescent microscopy and automated image analysis, generally referred to as High Content Screening (HCS). This technology has become an essential tool in early drug discovery programs. High content cellular imaging has increasingly met the challenges of high throughput needs and facilitates the integration of disease-relevant screens at early stages of the drug discovery process (56, 87, 165).

The combined use of RNAi, chemical genetics and HCS simultaneously constitutes a powerful methodology that allowed us to perform unbiased studies independent of preconceived notions on the network implicated in FOXO regulation. The identification and characterization of novel molecules implicated in FOXO modulation may provide new insights on how to re-activate FOXO, aiming for a better outcome of cancer treatment.

1 Introducción

1.1 Cáncer

En las últimas décadas se ha generado una gran cantidad de información revelando que el cáncer es una enfermedad genética. Esto ha llevado al descubrimiento de numerosos genes responsables del proceso de tumorigenesis. No obstante, el cáncer sigue siendo una de las enfermedades que presenta las tasas de mortalidad más elevadas en las sociedades occidentales. Mientras que se ha observado una importante reducción en el número de muertes causadas por enfermedades cardiacas, cerebro-vasculares e infecciosas en la última década, las muertes causadas por cáncer no han seguido ese patrón. Apenas algunos tipos particulares de cáncer, principalmente cánceres testiculares y leucemias infantiles, presentan una tasa satisfactoria de remisión y/o cura a través de la quimioterapia clásica, siempre y cuando sean detectados en estadios iniciales. La razón por la cual hay una transición lenta del conocimiento a la clínica se relaciona con la complejidad inherente del cáncer. Hoy en día el cáncer es considerado como un conjunto de enfermedades que se originan a partir de mutaciones progresivas a diversos niveles. Estas mutaciones confieren a las células neoplásicas las diversas capacidades que requieren para sobrevivir y proliferar en condiciones adversas, sea a través de la activación de proto-oncogenes o a través del silenciamiento de genes supresores tumorales (55).

Se ha propuesto que las células tumorales presentan alteraciones fundamentales que garantizan su éxito. Esas alteraciones, designadas *"características fundamentales del cáncer"* (55) consisten en autosuficiencia en factores de de crecimiento, insensibilidad a señales inhibidores del crecimiento, fuga a la muerte celular programada (apoptosis), capacidad de división ilimitada, mantenimiento de angiogénesis, y invasión tisular y metástasis (55).

1.2 La vía de señalización PI3K/Akt

Alteraciones de la vía de señalización PI3K/Akt modifican todos los aspectos de la fisiología celular que constituyen las características fundamentales del cáncer y que llevan a la formación y desarrollo de los tumores (20, 55, 63, 155) (Figura 1).

La activación fisiológica de PI3K se induce por factores de crecimiento e insulina a través de la aproximación de su subunidad catalítica a la membrana, en donde se encuentra su sustrato, PIP2, que será fosforilado por la PI3K formando PIP3 (153). La actividad de la PI3K es contrarrestada por la actividad de la fosfatasa PTEN, que elimina el fosfato de la posición 3' del PIP3, regenerando PIP2 y atenuando la señalización que ocurre gracias a PI3K. PDK1 se activa a través de la unión con PIP3 a través de su dominio de homología con plecstrina (dominio PH). Cuando está activada, PDK1 fosforila a Akt en la Thr308, activando así su función de kinasa de

Ser/Thr. Una vez fosforilada en la Thr308, se da un incremento de la activación a través de PDK2 (el complejo rictor/mTOR), a través de la fosforilación de la Ser473. La activación de Akt y la consecuente fosforilación de sus diversos sustratos (25, 35, 71, 139, 155) estimula la progresión del ciclo celular, la supervivencia, el metabolismo, la resistencia a hipoxia y la migración. Así mismo, inhibe la apoptosis inducida por la privación de factores de crecimiento, ausencia de contacto con la matriz extracelular, radiaciones ultravioleta, alteraciones en el ciclo celular y activación de la señalización mediada por Fas(35, 71, 120). Así, la activación de la cascada de señalización PI3K/Akt confiere características oncogénicas a las células y como tal es considerada una de las dianas que más frecuentemente se altera en el desarrollo del cáncer humano (63). La actividad de PTEN se pierde por mutaciones, deleciones o metilación del promotor. La inactivación de PTEN ocurre con una frecuencia elevada en muchos tumores primarios y metastáticos. Se encuentran mutaciones germinales de PTEN en los síndromes de Cowden, Bannayan-Riley-Ruvalcaba y en síndromes similares al síndrome de Proteus, siendo todos síndromes familiares con predisposición al cáncer (92, 95, 111, 136). Se han descrito varias mutaciones en el gen PIK3CA (que codifican p110α, la subunidad de PI3K) en tumores humanos (119, 133). Estas mutaciones son capaces de activar a Akt de forma constitutiva. La consecuente mejoría de las capacidades bioquímicas se traduce en un aumento de la actividad oncogénica de los mutantes de la PI3K (6, 167).

Carpten y colaboradores (21) han descrito una mutación de Akt en cánceres humanos de mama, colo-rectales, y de ovario, cuya consecuencia es la activación de Akt a través de su localización constitutiva en la membrana plasmática, que estimula la señalización de la vía de Akt , lleva a la transformación de las células e induce leucemia en ratones. De esta forma se establece un papel fundamental de Akt en el cáncer, que se suma a las alteraciones genéticas ya conocidas y que promueven el proceso oncogénico a través de la diana de la PI3K/Akt (21).

La activación de la PI3K y de Akt en ausencia de mutaciones en sus genes se ha descrito en cánceres de mama (5, 19, 79), de ovario (19, 110, 159), de páncreas (4), esófago (117), tiróide (44) y otros (11, 119).

También se ha demostrado que otros genes de esa vía de señalización funcionan como supresores tumorales, tales como TSC1, TSC2 o LKB1 encontrándose frecuentemente inactivados en algunos cánceres. La alteración frecuente de la diana de la PI3K/Akt ha hecho que varios componentes de esa ruta de señalización se conviertan en objetivos atractivos para el desarrollo de nuevos fármacos contra el cáncer.

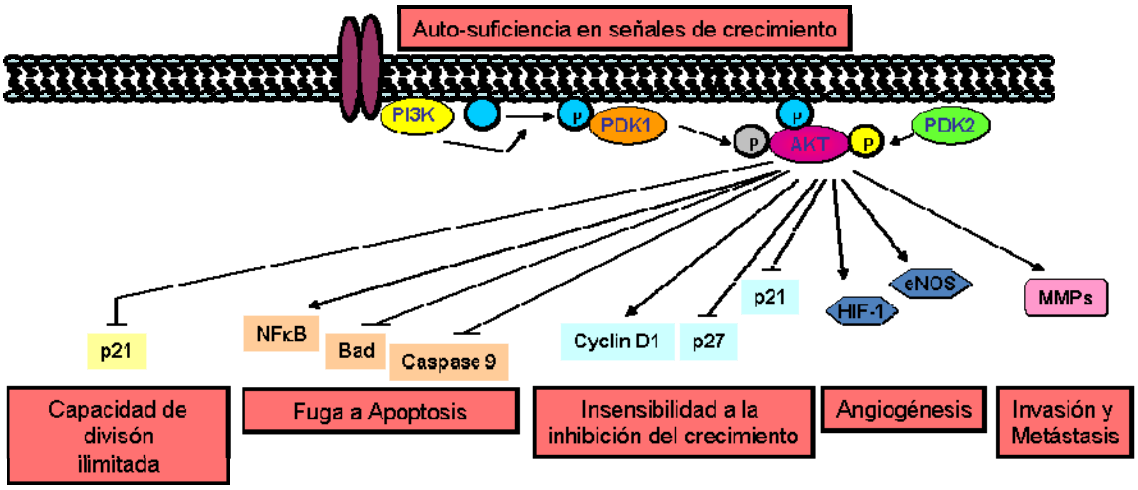

Figura 1. La diana PI3K/Akt es fundamental en cáncer. Su activación induce oncogenidad mientras disminuye la supresión tumoral, cubriendo casi todas las "características del cáncer" (cajas). Bad: BCL2-associated agonist of cell death ; NFkB: nuclear factor of kappa light polypeptide gene enhancer in B-cells 1; HIF-1: hypoxia inducible factor 1; eNOS: nitric oxide synthase; MMPs: metalloproteinases. Adaptado de (34).

1.3 Proteínas FOXO

Un importante nodo de señalización en la ruta de PI3K/Akt conecta la señalización desencadenada por factores de crecimiento con diversas redes transcripcionales a través de la inactivación de los factores de transcripción FOXO. La conexión molecular entre los factores FOXO y la señalización por PI3K/Akt está altamente conservada entre vertebrados e invertebrados. Los miembros de la subclase de factores de FOXO son FOXO1, FOXO3A, FOXO4 y FOXO6 actuando como reguladores de la transcripción en el núcleo.

Las proteínas FOXO actúan como monómeros, y a través de su dominio *forkhead*, una región de 110 aminoácidos situada en la zona central de la molécula (Figura 2) (157), se unen a su secuencia consenso de unión al DNA, TTGTTTAC, designada DBE (elemento de unión a DAF-16) (43).

La lista de genes cuyos promotores contienen sitios de unión para estos factores de transcripción está en expansión y contiene genes involucrados en apoptosis, resistencia a estrés oxidativo e inhibición del ciclo celular. Incluye genes como la glucosa-6-fosfatasa (108, 135, 163), la fosfoenolpiruvato carboxilasa (122), FasL (13), Bim (32), MnSOD (84, 113), catalasa (113), $p27^{KIP1}$ (100), p130 (85), y ciclina G2 (42, 50).

Cuando se localizan en el núcleo y ligados al DNA, las proteínas FOXO actúan típicamente como potentes activadores transcripcionales (13, 83). El dominio de transactivación de FOXO se localiza en el extremo carboxilo de la molécula. Análisis hechos en matrices de genes indican que las proteínas FOXO pueden también actuar como represores transcripcionales (123). De este modo, esta familia de factores de transcripción puede activar o reprimir la transcripción, dependiendo del contexto del promotor y de las condiciones extracelulares (50).

Figura 2. Estructura general de los factores de transcripción FOXO. Las proteínas FOXO comparten una gran similiaridad estructural, que incluye un dominio forkhead (FKH)*, una señal de localización nuclear (nuclear localization signal - NLS), una señal de exporte nuclear (nuclear export signal - NES) y un dominio de transactivación (transactivation domain - TA*).

Los factores de transcripción FOXO son considerados supresores tumorales *bona fide* que son inactivados en la mayoría de cánceres humanos, debido a la sobre-activación de la diana PI3K/Akt (13, 27, 50, 105). La fosforilación de las proteínas FOXO mediada por Akt induce su exporte nuclear y así interrumpe la transcripción de sus genes diana. El estrés celular, o bien, la inactivación de la vía PI3K/Akt, promueven la translocación de los FOXO al núcleo en donde pueden ejecutar su función transcripcional. Varias funciones celulares pueden ser afectadas por genes que son activados transcripcionalmente por FOXO, implicados en funciones que van desde metabolismo hasta ciclo celular, apoptosis y estrés oxidativo (50).

1.3.1 Regulación de los FOXO

La actividad de los factores FOXO es regulada por una sofisticada red de señalización que integra la información proveniente de la vía PI3K/Akt y dianas de señalización de estrés, lo que resulta en un patrón específico de modificaciones post-traducionales. Las modificaciones post-traducionales que los FOXO pueden sufrir incluyen fosforilación, acetilación y ubiquitinación, que afectan a las proteínas FOXO a tres diferentes niveles: localización subcelular, estabilidad y actividad transcripcional (Figura 3).

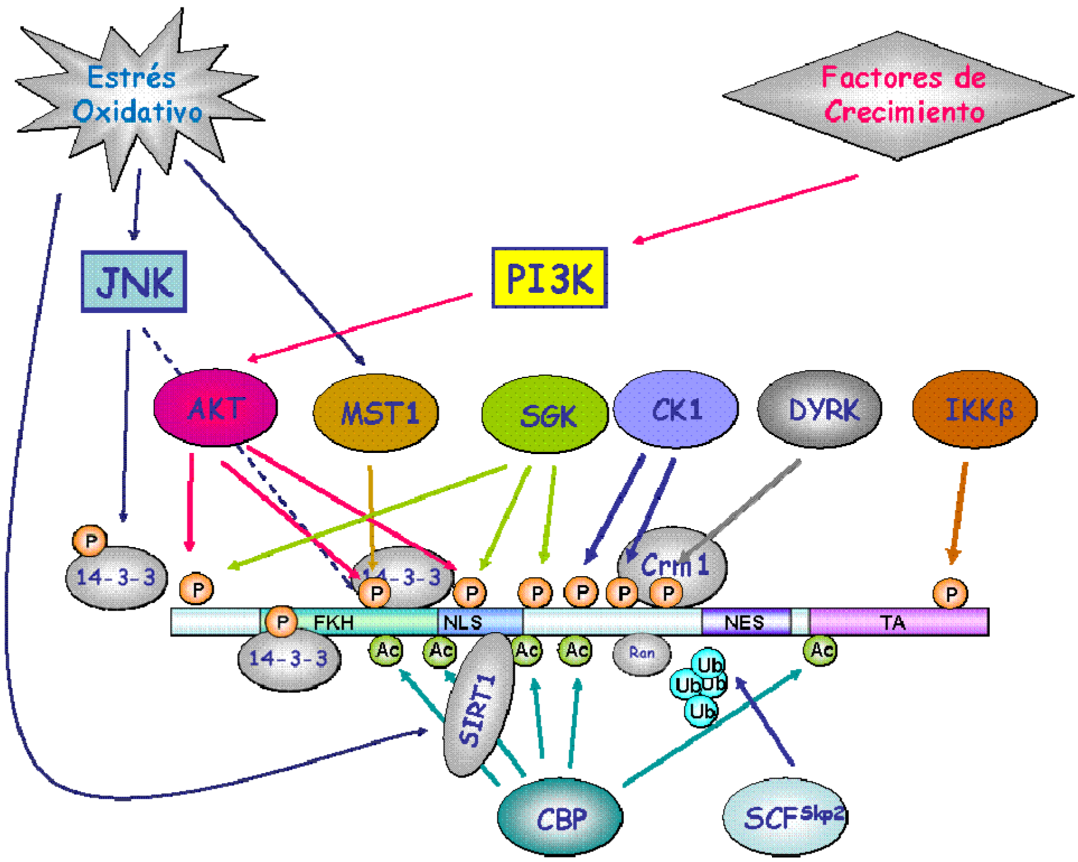

Figura 3 – La regulación de las proteínas FOXO ocurre a través de fosforilación, acetilación, y ubiquitinación. Los dos estímulos que desencadenan cambios en la localización subcelular de las proteínas FOXO son la señalización desencadenada por factores de crecimiento a través de PI3K/Akt y estrés oxidativo. Algunas de las principales moléculas capaces de inducir modificaciones post-traducionales en los FOXO se encuentran representadas en esta figura. Akt: v-akt murine thymoma viral oncogene homolog; CBP: CREB binding protein; CK1: casein kinase 1; DYRK: dual tyrosine phosphorylated regulated kinase 1; IKKβ: I kappaB kinase β; JNK: c-Jun N-terminal kinase 1; MST1: mammalian Ste20-like kinase 1; PI3K: phosphoinositide-3-kinase; SIRT1: sirtuin; Skp2: S-phase kinase-associated protein 2.

1.3.1.1 Fosforilación

La activación de PI3K y subsecuente activación de las familias de kinasas Akt y SGK culmina en la fosforilación e inactivación de los FOXO (13). Estudios bioquímicos realizados en células de mamíferos han demostrado que Akt fosforila a FOXO directamente (8, 13, 83, 109, 127, 143), llevando a la rápida relocalización de las proteínas FOXO desde el núcleo hasta el citoplasma. Akt fosforila FOXO3A en tres sitos regulatorios clave (Thr32, Ser253 y Ser315). SGK también fosforila los factores FOXO, pero en una combinación de sitios ligeramente distinta. Mientras Akt fosforila preferiblemente la Ser253, SGK favorece la fosforilación de la Ser315. La Thr32 es fosforilada por las dos kinasas. Los tres sitios regulatorios son fosforilados como respuesta a determinados factores de crecimiento, incluyendo IGF-I (13), insulina (83), interleukina 3 (33), eritropoyetina (72), factor de crecimiento epidermal (EGF) (68) y factor de crecimiento neuronal (NGF) (168). Así, las proteínas FOXO integran un largo rango de estímulos a través de la fosforilación por Akt y SGK de tres residuos conservados. La fosforilación preferencial de las proteínas FOXO por diferentes kinasas de proteínas puede permitir que los FOXO respondan de manera selectiva a estímulos muy similares, tales como insulina e IGF-I (107).

La consecuencia más evidente de la fosforilación de FOXO por Akt y SGK es el cambio en su localización subcelular (8, 13, 142). En ausencia de factores de crecimiento, contexto en el que Akt y SGK están inactivas, FOXO se localiza en el núcleo. Cuando las células son expuestas a factores de crecimiento, la cascada PI3K/Akt se activa y lleva a la exportación de FOXO al citoplasma. Estudios de análisis mutacional revelaron que uno o dos dominios ricos en leucina en la zona carboxílica de FOXO funcionan como señal de exporte nuclear (NES) (8, 14). Además, se ha demostrado que cuando las proteínas FOXO están fosforiladas interaccionan específicamente con las proteínas 14-3-3, que sirven de chaperones para escoltar las proteínas FOXO hacia fuera del núcleo (13, 14). La unión de 14-3-3 a FOXO puede activar el exporte nuclear de los factores FOXO, quizás induciendo un cambio conformacional en las moléculas FOXO que exponga su dominio NES y permita la interacción con la Exportina/CRM1 (14). Al unirse a FOXO, las proteínas 14-3-3 pueden también prevenir la re-importación de esos factores de transcripción, a través de la ocultación de su señal de localización nuclear (NLS) (12, 128). Análisis mutacionales de los tres sitios regulatorios de Akt y SGK han revelado que la fosforilación de cada sitio contribuye para la exclusión nuclear de los factores FOXO (15). Una posibilidad atractiva es que cada sitio participa en diferentes aspectos de los mecanismos que aseguran la localización de los FOXO en el citoplasma. Así, la fosforilación de los factores FOXO puede representar una manera de modular la extensión de la relocalización de esos factores de transcripción en diferentes tipos celulares en respuesta a diferentes combinaciones de señales.

Insulina y factores de crecimiento también desencadenan la fosforilación de otros residuos de FOXO. Una fosforilación previa por la kinasa DYRK1 (<u>d</u>ual t<u>y</u>rosine phosphorylated <u>r</u>egulated <u>k</u>inase 1), miembro de la familia de las MAP kinasas, facilita la fosforilación posterior de la Ser322 y la Ser325 mediadas por CK1 (casein kinase 1). La fosforilación de los FOXO en esos dos residuos parece acelerar la localización de FOXO en el citoplasma como respuesta a factores de crecimiento presumiblemente a través del aumento de la interacción entre los FOXO y la maquinaría de exporte (Ran y exportina/CRM1) (129). Puede que los diversos mecanismos de regulación de los factores de transcripción FOXO del núcleo hacia el citoplasma funcionen como un sistema de seguridad para asegurar el distanciamiento de los FOXO de los promotores de sus genes diana.

El otro elemento fundamental de la regulación de FOXO es el estrés celular. En ese contexto, se sabe que la kinasa JNK también actúa sobre FOXO y, al contrario de Akt, se ha demostrado que JNK promueve la activación de FOXO hacia su actividad transcripcional. Se ha demostrado que JNK fosforila directamente a FOXO1, FOXO3A y FOXO4 *in vitro* (50). Se ha demostrado también que JNK fosforila a las proteínas 14-3-3, liberando FOXO hacia el núcleo (150). Así, la inducción de JNK por estrés facilita la localización nuclear de FOXO, bien por la fosforilación directa de los FOXO o bien por reducir la capacidad de 14-3-3 para mantener a las proteínas FOXO en el citoplasma.

La activación de FOXO por JNK constituye un potente inductor de la actividad transcripcional de FOXO aunque la vía PI3K/Akt se encuentre activada, lo que refleja una jerarquía bien marcada de los señales que modulan a FOXO (Figura 4). Cuando ambos elementos están presentes, la señalización de estrés se solapa a la interrupción de la función de FOXO mediada por PI3K/Akt y el patrón de genes que se expresa en ese contexto se asemeja más al patrón de genes que se expresa cuando sólo se verifica estrés (50).

Se ha descrito que la kinasa de proteínas Ste20 participa en la muerte celular inducida por peróxido de hidrógeno en *S. cerevisae* (1). Las kinasas homólogas a Ste20 en mamíferos (MSTs), de entre las cuales MST1 y MST2 comparten el grado de homología más elevado, tienen funciones importantes en la muerte celular por apoptosis (23, 49, 59, 115, 158). Se ha descubierto que MST1 fosforila los factores de transcripción FOXO en un sitio conservado del dominio *forkhead* (90). En neuronas de mamíferos, el estrés oxidativo activa a MST1, que a su vez fosforila FOXO3A en Ser207. La fosforilación de FOXO3A inducida por MST1 rompe la interacción con 14-3-3, promueve la translocación de FOXO hacia el núcleo induciendo la muerte celular en neuronas.

FOXO también puede ser fosforilado por IKKβ, promoviendo tumorigenesis (66). IKKβ induce la fosforilación de FOXO3A en Ser644, en el extremo carboxílico de la molécula (Figura 2). Esa fosforilación lleva a la poli-ubiquitinación y posterior degradación de FOXO3A (66).

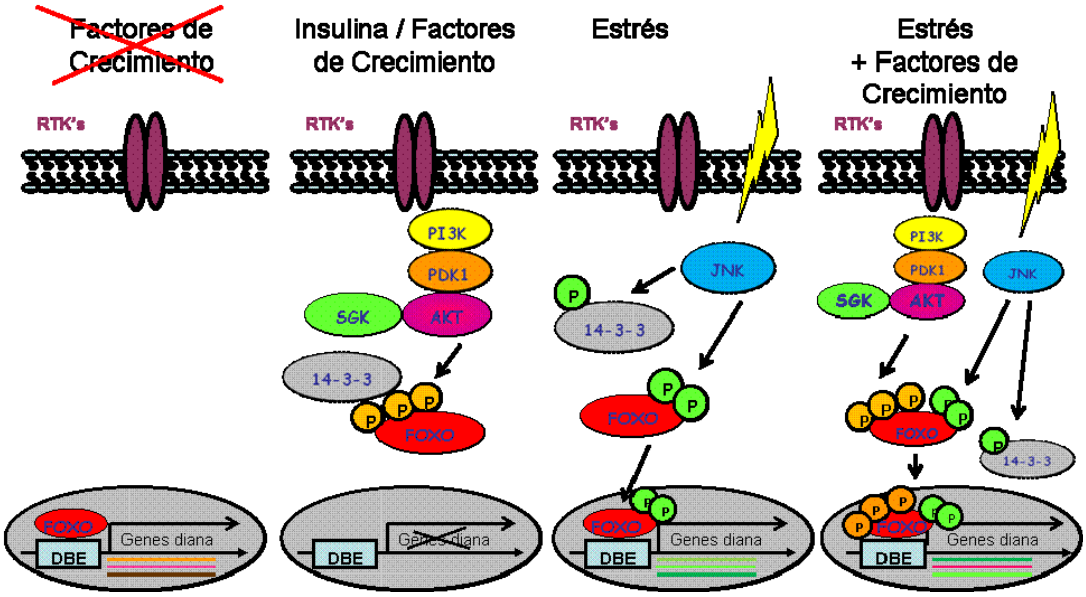

Figura 4. Regulación de FOXO por factores de crecimiento y estrés. La activación de PI3K/Akt inhibe a FOXO como respuesta a factores de crecimiento, a través de fosforilación y retención en el citoplasma. El estrés celular es suficiente para solapar la localización citoplasmática de los FOXO. JNK fosforila las proteínas FOXO como respuesta al estrés, lo que conlleva a su translocación nuclear. Aunque la fosforilación mediada por JNK no inhiba directamente la unión de 14-3-3 a las proteínas FOXO, induce la liberación de sus sustratos. La actividad de JNK es suficiente para solapar la inhibición de FOXO mediada por Akt y causa la transcripción de genes involucrados en resistencia a estrés. Se ha propuesto que en cada una de las condiciones se transcribe un conjunto específico de genes y los programas transcripcionales pueden determinar si se induce parada del ciclo celular, resistencia al estrés o apoptosis. (Adaptada de (50)).

A pesar de haber mucha información respecto a los eventos que regulan la localización subcelular de las proteínas FOXO, hay relativamente poco conocimiento en cuanto a las fosfatasas responsables de su desfosforilación. La proteína fosfatasa 2A ha sido identificada como un compañero de unión a FOXO en un complejo de proteínas purificadas que contenía FOXO3A, lo que sugiere que la proteína fosfatasa 2 puede ser una de las fosfatasas que defosforila a FOXO (130). La localización subcelular de las fosfatasas de FOXO podría aportar otro nivel de control de la actividad de FOXO. Además, la rapidez con que esas fosfatasas eliminan el grupo fosfato de cada sitio fosforilado de las proteínas FOXO puede afectar la cinética de la localización de estos factores de transcripción.

La localización subcelular de las proteínas FOXO puede también ser regulada independientemente de modificaciones post-traducionales. El virus de herpes asociado al sarcoma de Kaposi puede promover tumorigenesis a través de la proteína latente LANA2 con FOXO3A y 14-3-3, resultando en una disminución de la actividad transcripcional.

1.3.1.2 Acetilación

La fosforilación de las proteínas FOXO es un modo esencial de regular su actividad transcripcional. No obstante, otras modificaciones post-traducionales, tales como acetilación también influencian la actividad transcripcional de FOXO, añadiendo otra capa a esta compleja red de regulación.

Las proteínas nucleares CBP y p300 y sus proteínas asociadas, tales como el factor PCAF presentan una actividad intrínseca de acetil-transferasas de histonas (HAT). Esas proteínas tienen un papel esencial en la indución de transcripción a través de la acetilación de histonas y de la integración de señales de elementos de las regiones de *enhancers* y promotores. Esas proteínas también presentan actividad directa de acetil transferasas de factores de transcripción (FAT) (91). Se cree que CBP tiene un doble papel en la transcripción de genes mediada por FOXO: por un lado puede facilitar la transcripción a través de la acetilación de las histonas de los cromosomas, y por otro promueve la acetilación de las mismas proteínas FOXO. La acetilación de las proteínas FOXO por acetilasas como CBP y p300 aumenta en respuesta a estrés oxidativo (16, 41, 81). Las proteínas FOXO acetiladas se acumulan en el núcleo y se asocian con cuerpos Pml, lo que disminuye la actividad de FOXO (81).

Los niveles elevados de acetilación de FOXO en el núcleo sugieren otra capa regulatoria formada por otras dianas como SIRT1, una deacetilasa dependiente de nicotinamida adenina (NAD), que se localiza en el núcleo de células estimuladas con factores de crecimiento (88, 154). En condiciones de estrés SIRT1 forma un complejo con las proteínas FOXO promoviendo su deacetilación en el núcleo (16, 81). La expression de SIRT1 aumenta la parada del ciclo celular inducida por FOXO3A a través del aumento de la expresión de $p27^{KIP1}$ (16), lo que es consistente con el hecho de que la acetilación de las proteínas FOXO por CBP inhibe su actividad (26). En contraste, la expresión inducida por FOXO de genes implicados en apoptosis tales como Bim se ve aumentada con la inhibición de SIRT1 por los inhibidores de deacetilasas de histonas (HDAC) de clase III como nicotinamida y de los inhibidores de HDAC de la clase I y II como tricostatina A (16). Además, la expresión de SIRT1 inhibe a la actividad del promotor de Bim (104). Actualmente se favorece la hipótesis de que la asociación con SIRT1 afecta a la transcripción de los genes diana de FOXO de manera diferencial, induciendo parada de ciclo celular, resistencia a estrés y reparación del DNA (16, 86).

1.3.1.3 Ubiquitinación

Las proteínas FOXO también están reguladas por el sistema ubiquitina-proteasoma. Los niveles basales de proteínas FOXO en linfocitos pre-B murinos que expresan Akt establemente son bajos, aumentando significativamente con el tratamiento con inhibidores del proteasoma (121). Los niveles de FOXO también disminuyen en células HepG2 tras tratamiento con insulina (97). De igual manera, el tratamiento de fibroblastos embrionarios de pollo con el factor de crecimiento derivado de plaquetas (PDGF) disminuye los niveles de FOXO. Ese efecto se bloquea con inhibidores de proteasoma o de PI3K (3), lo que sugiere que la degradación de FOXO mediada por el proteasoma depende de la señalización por Akt. Además, la fosforilación causada por Akt es un requisito para la poliubiquitinación de FOXO (97). La degradación de FOXO dependiente de ubiquitina requiere la interacción con la proteína F-box Skp2, el componente de unión al sustrato del complejo Skp1/culin 1/proteína F-box (SCFSkp2) E3 ligase (67). La fosforilación de FOXO mediada por IKK también lleva a su poliubiquitinación y degradación, mediada por la ubiquitina ligasa E3 MDM2 (66, 162). Mientras que la poliubiquitinación de FOXO lleva a su degradación, la monubiquitinación, también mediada por MDM2, aumenta en respuesta a estrés oxidativo, llevando a translocación nuclear y aumento en actividad transcripcional (152). Por ultimo, se ha descrito que la desubiqutinación de FOXO es catalizada por HAUSP/USP7 (152). La desubiquitinación de FOXO mediada por USP-7 lleva a su relocalización celular en el citoplasma. Por tanto, la monoubiquitinación mediada por estrés oxidativo constituye un medio adicional de regulación de la localización subcelular y actividad de FOXO.

1.3.2 Funciones de las proteínas FOXO

Los factores de transcripción FOXO están implicados en muchos procesos celulares fundamentales, a través de la regulación de un amplio conjunto de genes diana (Figura 5). La integración de diversos estímulos extracelulares e intracelulares se refleja en modificaciones post-traducionales que ocurren en las proteínas FOXO, dando origen a un “código FOXO” que puede ser interpretado por otras proteínas, determinando el nivel, intensidad, duración y actividad de los factores de transcripción FOXO en las células (18).

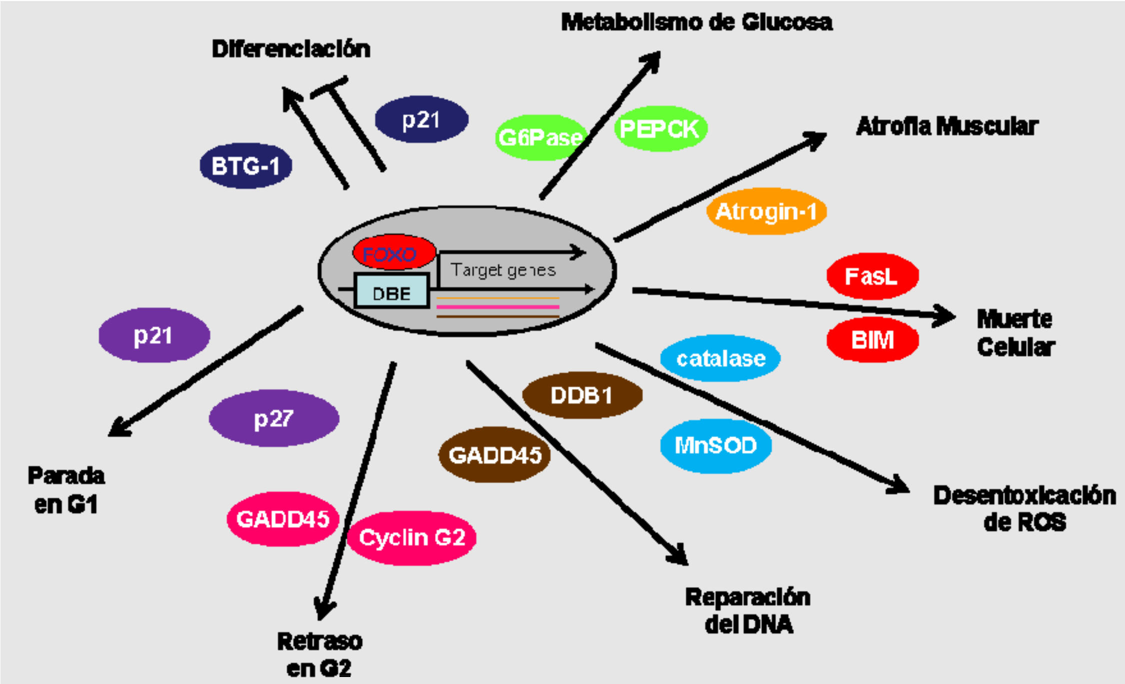

***Figura 5** Una representación esquemática de algunos de los genes diana de FOXO y los procesos celulares en los que están implicados. BTG-1: B-cell translocation gene 1; p21: cyclin-dependent kinase inhibitor 1A; p27^{KIP1}: cyclin-dependent kinase inhibitor 1B; MnSOD: manganese superoxide dismutase; G6Pase: glucose-6-phosphatase; PEPCK: phosphoenolpyruvate carboxykinase; FasL: Fas ligand; GADD45: growth arrest and DNA damage-inducible protein 45; DDB1: damage-specific DNA-binding protein 1; FBE, FOXO binding element (Adaptada de (50)).*

1.3.2.1 FOXO y apoptosis

Se ha demostrado que la expresión de mutantes nucleares de FOXO activan la muerte celular, particularmente en neuronas y linfocitos (13, 31, 46, 169). Una de las maneras por las cuales Akt promueve la supervivencia celular es a través del alejamiento de FOXO de los promotores de genes involucrados en apoptosis, como Bim (33). La apoptosis inducida por FOXO también parece ser dependiente de la inducción de citokinas relacionadas con muerte celular, en las que se incluyen el ligando de Fas y TRAIL (13, 102), que juntamente con otras citokinas pueden amplificar la capacidad de los factores FOXO en inducir apoptosis a través de la activación de dianas de muerte celular en células vecinas.

1.3.2.2 FOXO y ciclo celular

La expresión de formas constitutivamente activas de FOXO induce la parada del ciclo celular en el umbral G1/S (100). Los genes diana que median la parada del ciclo celular inducida por FOXO parecen ser el inhibidor de Cdk's p27^{KIP1} (100) y p130, miembro de la familia Rb (85). La capacidad de FOXO en inducir parada en G1 se ve reducida en fibroblastos deficientes en p27^{KIP1} y p130 (85), lo que sugiere que p27^{KIP1} y p130 son ambos fundamentales para mediar la parada en G1 inducida por FOXO. En presencia de TGFβ, los factores FOXO se unen al promotor de p21, que a su vez induce parada del ciclo celular en la transición G1/S(137). FOXO puede también promover la parada del ciclo celular a través de la represión de la expresión de las ciclinas D1 y D2(123, 134). Por tanto, las proteínas FOXO desempeñan un papel fundamental en la parada en G1 tanto por la sobre-expresión de inhibidores (p21 y $p27^{KIP1}$) como por la represión de activadores del ciclo celular (ciclinas D1 y D2).

Los factores FOXO también tienen un papel fundamental en otros puntos de control del ciclo celular. Las células en las que FOXO3A se encuentra inactivado en la fase S presentan un retraso en la progresión a la fase G2 del ciclo celular (148). A través de análisis genómico se identificaron diversos genes diana de FOXO que pueden mediar el efecto de FOXO en la transición G2/M, tales como la proteína GADD45 (42, 148). Por tanto, los factores FOXO median la parada del ciclo celular en las transiciones G1/S y G2/M, ambos puntos de control cruciales en la respuesta celular a estrés. La parada de ciclo celular inducida por FOXO podría permitir más tiempo para reparar el DNA dañado y para promover la desintoxicación de las células (50).

1.3.2.3 FOXO en resistencia a estrés, reparación del DNA y desintoxicación

Consistentemente con el papel de FOXO en la parada del ciclo celular en las transiciones G1/S y G2/M, la expresión de formas activas de FOXO lleva a la sobre-expresión de diversos genes involucrados en reparación del DNA tales como DBB1 y GADD45 (123, 148). Además, se ha descrito que las proteínas FOXO promueven la desintoxicación de especies reactivas de oxígeno (ROS) a través de la sobre-expresión de enzimas captadoras de radicales libres, tales como la súper-óxido dismutasa de Mn (MnSOD) y catalasa (85, 113, 123, 148). Así, los factores de transcripción FOXO controlan dos aspectos fundamentales de la resistencia celular al estrés: reparación de los daños al DNA causados por ROS y desintoxicación de ROS (50).

Se ha demostrado recientemente que los factores FOXO pueden estimular la expresión del transportador de drogas MDR1 (glicoproteína P), que puede inducir un aumento de la tolerancia de las células tumorales a la toxicidad generada por la quimioterapia (54).

A través de un estudios genómicos de expresión de mRNA se han identificado IGFR1 y PIK3CA como genes diana de FOXO3A en una línea de carcinoma del colon (29). Este mecanismo de retroalimentación negativa puede ser considerado un mecanismo añadido de tolerancia al estrés mediado por las proteínas FOXO, una vez que la transcripción de ambos genes contribuye a la activación de la diana PI3K/Akt, que está implicada en la resistencia al estrés.

1.3.2.4 FOXO en metabolismo

Los factores de transcripción FOXO también desempeñan un papel importante en la sobre-expresión de genes que controlan el metabolismo de glucosa (50). Los factores FOXO desencadenan la gluconeogénesis a través de la sobre-expresión de la glucosa 6 fosfatasa (G6Pase), que es responsable de la conversión de glucosa-6-fosfato en glucosa; y de la fosfoenolpiruvato carboxilasa (PEPCK), que convierte oxaloacetato en fosfoenolpiruvato (108, 122, 135, 163). De este modo, los efectos de la insulina en el metabolismo de glucosa son mediados parcialmente a través de la represión de FOXO por la diana PI3K/Akt.

1.3.2.5 FOXO en envejecimiento y longevidad

Una de las funciones más interesantes de FOXO es su capacidad de aumentar la longevidad (75). En nemátodos se ha demostrado que mutaciones inactivantes en el receptor de insulina o en PI3K llevan a un aumento de longevidad de hasta tres veces (69, 76, 78, 103). Esa extensión de la longevidad se revierte cuando se produce la mutación del ortólogo de FOXO en nemátodos DAF-16, demostrando que DAF-16 tiene un papel crucial en la señalización por debajo de la diana de insulina en la regulación de la longevidad.

Los genes que median la capacidad de DAF-16 de aumentar la longevidad incluyen la MnSOD (SOD3 en nemátodos) (65), MST1 (90), proteínas de choque térmico y agentes antimicrobianos (89, 99). DAF-16 parece inducir un programa de genes que coordinadamente regulan la longevidad promoviendo la resistencia a estrés oxidativo, protección de la estructura de las proteínas y resistencia a patógenos. Así, la resistencia a estrés se correlaciona con la longevidad, ya que todos los nematodos mutantes que presentan una activación de DAF-16 también presentan resistencia a estrés oxidativo, choque térmico y radiaciones UV (62). En mamíferos se ha demostrado que ratones que son deficientes para los receptores de insulina o de IGF-1 tienen una mayor esperanza de vida y son resistentes a estímulos desencadenados por estrés oxidativo (10, 64). Además, se sabe que las proteínas FOXO son capaces de inducir resistencia a estrés en células de mamíferos y algunos de los genes diana de FOXO involucrados en resistencia a estrés, como la MnSOD, están conservados entre mamíferos y nematodos, lo que sugiere que FOXO podría también regular la longevidad en mamíferos.

1.3.3 FOXO y cáncer

Los efectos anti-proliferativos y pro-apoptóticos de las proteínas FOXO en mamíferos han sugerido que estas podrían funcionar como supresores tumorales. En ausencia de FOXO, las células anormales que normalmente morirían pueden llegar a sobrevivir, lo que puede contribuir a la formación de tumores (Figura 6) (50).

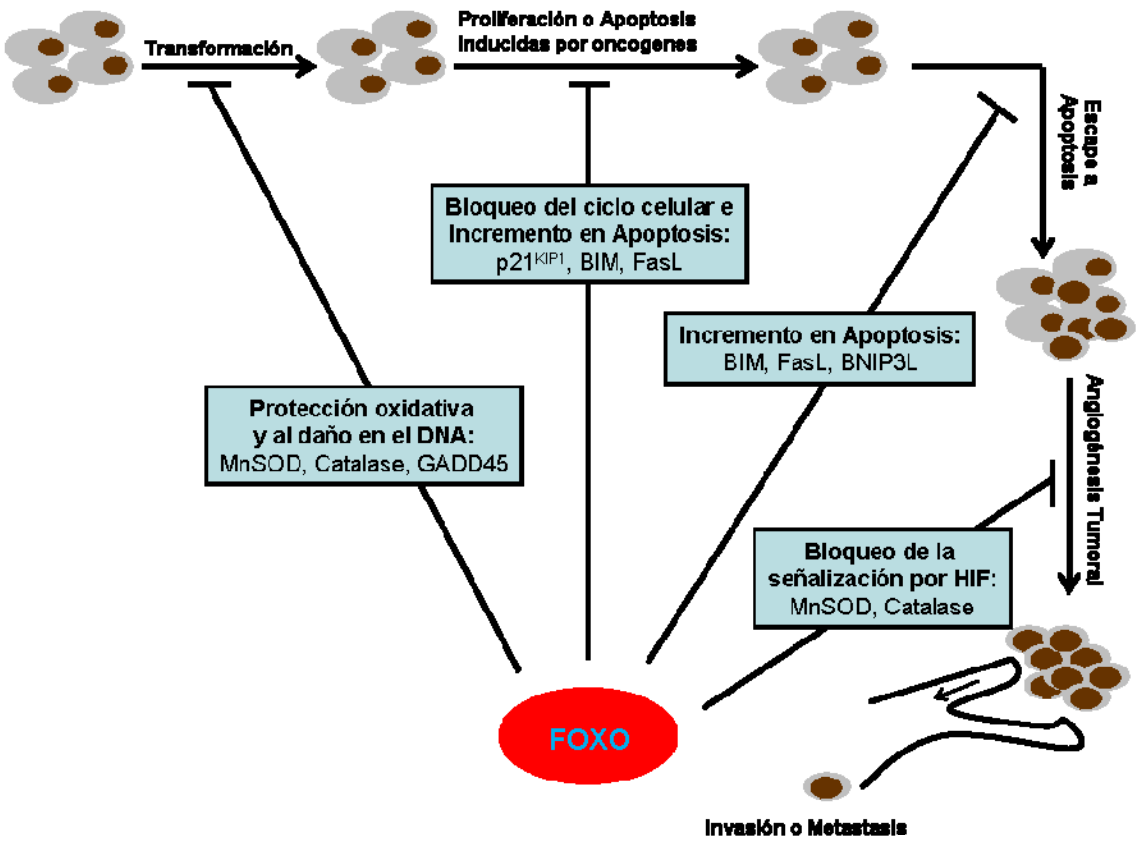

Figura 6 – Las funciones de supresor tumoral de FOXO pueden bloquear el desarrollo de tumores en diversos estadios. La reducción de estrés oxidativo y reparación del DNA inducidas por FOXO previenen la inducción y propagación de mutaciones requeridas a la transformación oncogénica. Como la progresión entre estadios de tumorigenesis probablemente ocurre a través de mutaciones, los FOXO pueden ser supresores en diversos estadios. Un tumor puede formarse si el balance entre proliferación y apoptosis se altera hacia la proliferación. Las proteínas FOXO bloquean el ciclo celular e inducen la expresión de genes pro-apoptóticos, que pueden re-balancear la homeostasis tisular. Finalmente, para que se pueda formar un tumor maligno, es necesario que ocurra angiogénesis. FOXO reprime la señalización de HIF, que es necesaria para la angiogénesis en los tumores. En suma, los FOXO funcionan como supresores tumorales al largo de todo el proceso de formación, expansión y diseminación del tumor (Adaptado de (27)).

Numerosas evidencias, por tanto, indican que los factores FOXO pueden tener un papel importante en cáncer. FOXO3A se encuentra desregulado en cáncer de mama. La localización citoplasmática de FOXO3A en células de cáncer de mama muestra una importante correlación con la reducción de la supervivencia. Se ha observado también una correlación entre la expresión de IKKβ y la localización citoplasmática de FOXO en esos tumores (27).

Las proteínas FOXO interaccionan física o funcionalmente con supresores tumorales y oncogenes. En respuesta a estrés o deprivación de nutrientes se ha visto que FOXO interacciona en el núcleo con el supresor tumoral p53 (16, 112). Esta observación junto con el hecho de que p53 y FOXO comparten genes dianas similares (p21, GADD45, WIP1, PA26), sugiere que esas dos proteínas pueden coordinar la supresión tumoral. Además, las proteínas FOXO forman complejos con los factores de transcripción SMAD (137), que funcionan como supresores tumorales mediando el efecto citoestático de TGF-β. La interacción entre FOXO y SMAD ocurre en el promotor de p21 como respuesta a la estimulación por TGF-β. El complejo FOXO/SMAD provocaría la sobre-expresión de p21 y la consecuente parada de ciclo celular (50). Finalmente, se ha demostrado que el proto-oncogen β-catenina se une a proteínas FOXO (39) aumentando su capacidad para forzar la progresión en el ciclo celular. Una vez que la β-catenina ha sido implicada en la progresión del cáncer, en particular en cáncer de colon, es posible que los factores FOXO puedan contrarrestar la progresión de los tumores inhibiendo a la β-catenina (50).

La expresión de mutantes activos de FOXO reduce la tumorigenesis en varios modelos. La proliferación celular y tumorigenicidad inducidas por IKKβ puede ser inhibida en ratones por la expresión de una forma activa de FOXO3A (66). Se ha demostrado en *Drosophila* que FOXO afecta a la traducción proteica de MYC, interfiriendo con la biogénesis de los ribosomas (144). Otros autores han demostrado que la expresión de mutantes de FOXO no fosforilables por Akt previne la inactivación de FOXO e induce apoptosis eficientemente en células de melanoma (48).

1.3.3.1 Los factores de transcripción FOXO son "*bona fide*" supresores tumorales.

En modelos de ratones genéticamente modificados, la eliminación simultanea de FoxO1, FoxO3a y FoxO4, produce la formación espontánea de tumores, principalmente linfomas tímicos linfoblásticos, diseminados por el bazo, hígado y nódulos linfáticos. La eliminación de 2 de ellos no produce un fenotipo tan evidente, sugiriendo una fuerte redundancia de los 3 factores FOXO (118).

El triple *knockout* también presenta un crecimiento aberrante y diseminado de la vasculatura, confirmando que FOXO tiene un papel fundamental en la homeostasis de la vasculatura (118). Todos los ratones desarrollan un fenotipo harmatomatoso progresivo con la edad en el tejido endotelial, con amplia diseminación de hemangiomas, resultando en muerte prematura. En un número relativo de animales la condición progresa a angiosarcomas letales.

Los timócitos de los triple *knockout* presentan una respuesta aumentada a estímulos de crecimiento y concordantemente una disminución de la muerte inducida por estímulos pró-apoptóticos.

1.3.4 La reactivación de FOXO como estrategia terapéutica.

Debido a la gran cantidad de evidencias de que los factores de transcripción FOXO son inactivados en los tumores humanos, se ha propuesto que la re-activación de FOXO puede ser una estrategia prometedora en la terapia contra el cáncer.

A diferencia de otros supresores tumorales cuyas funciones se pierden a través de mutaciones, la perdida de las funciones de FOXO ocurre sobre todo por alteraciones post-traducionales inducidas por dianas moleculares implicadas en crecimiento y supervivencia. De este modo, a pesar de que las proteínas FOXO están inactivadas en tumores, el gen y por tanto la proteína se encuentran todavía presentes y son fácilmente re-activables. Por tanto, puede que las terapias que buscan a la reactivación de FOXO sean efectivas (27). Además, se ha demostrado que la reactivación indirecta de FOXO es beneficiosa para el tratamiento del cáncer. Se ha descrito que FOXO3A es una indiana indirecta de taxol y del pan-inhibidor de kinasas KP372-1 (140, 141) en células de cáncer de mama y de leucemia mieloide aguda (166) respectivamente, y ambos activan a FOXO3A a través de la reducción de la actividad de Akt. Taxol también activa a JNK, lo que tiene un efecto doble en la fosforilación de FOXO *per se* y en la inhibición de la unión de 14-3-3 a FOXO, evitando su exclusión del núcleo.

FOXO3A también es importante en la apoptosis inducida por imatinib (Glivec) en líneas celulares de leucemia mieloide crónica que expresan la oncoproteína BCR-ABL (38). En las células que son positivas para BCR-ABL, FOXO3A está constitutivamente fosforilado y la inhibición de BCR-ABL causada por imatinib induce la actividad transcripcional de FOXO3A, lo que lleva a la apoptosis mediada por Bim (105). El bloqueo de los receptores de factores de crecimiento epidermales (EGFR) por anticuerpos (como trastuzumab o cetuximab) o moléculas pequeñas (como lapatinib y gefitinib) representa una valiosa estrategia terapéutica contra cánceres de mama, próstata, riñón, ovario y carcinomas pulmonares no microcíticos, y se han puesto en ensayos clínicos estos agentes individualmente o en combinaciones entre ellos (126).

La cascada de señalización de PI3K es diana de la cascada de EGFR y el bloqueo de EGFR con anticuerpos induce la activación transcripcional de FOXO, llevando a la activación del gen pro-apoptótico BNIP3L (124). FOXO es una diana crucial de pequeñas moléculas inhibidoras de EGFR, por tanto es posible que la re-introducción de FOXO3A activo sensibilice las células resistentes a agentes como gefitinib (105). La activación de FOXO3A puede también ser efectiva en combinación con otros agentes, para inhibir la resistencia o aumentar la muerte celular en el tumor. Se ha descrito una sobre-expresión de Bim inducida por FOXO3A como consecuencia de la exposición de de células de osteosarcoma mutantes para p53 a radiaciones ionizantes (161), lo que sugiere que FOXO3A es un importante efector de la apoptosis inducida por radiaciones. De este modo, puede que las quimioterapias que activan a FOXO3A también sensibilicen las células a radioterapia.

La reactivación de FOXO también ha sido asociada a resistencia a la quimioterapia, a través de los mecanismos que permiten que FOXO proteja las células de estrés. Por tanto, es fundamental identificar y caracterizar todas las moléculas que tienen influencia sobre la activación de FOXO, así como las modificaciones post-traducionales inducidas. El conocimiento completo de cómo programar el código FOXO permitirá el desarrollo de terapias más eficientes contra el cáncer, que aprovecharán las características supresoras de tumores de FOXO y al mismo tiempo evitarán el desarrollo de resistencia.

1.4 Búsqueda de nuevos moduladores de FOXO.

Tradicionalmente los estudios de perdida de función genética apenas podían ser llevados a cabo en sistemas biológicos simples, tales como *S. cerevisae* (58), *C. elegans* (101), y *Drosophila* (114). Se consideraba imposible la aplicación de este tipo de abordaje a mamíferos por su lenta tasa de reproducción, gran tamaño físico y genoma diploide (70, 138). No obstante, algunos avances tecnológicos recientes han enriquecido los abordajes disponibles para la identificación de componentes de redes de señalización complejas en células humanas en cultivo.

La interferencia de RNA (RNAi) es un mecanismo de silenciamiento de genes dependiente de la especificidad de las secuencias y que se induce por RNAs de doble cadena (dsRNA) (22). Cada dsRNA silenciador es procesado en elementos de 21-25 pares de bases (bp) designados “RNAs de interferencia pequeños” (siRNAs) (51, 52, 164) por Dicer, una ribonucleasa de la familia III (RNAse III). Los siRNAs resultantes entran en el complejo RISC, que utiliza una versión de cadena simples del siRNA como guía para la selección de sustrato (52, 53, 151, 164). Una perfecta complementariedad entre el sustrato y el siRNA lleva a la rotura del RNA diana (22). siRNA puede resultar en el *knockdown* de uno o varios genes, propiciando un método rápido y conveniente para el análisis de la función génica (36). Las librerías de siRNA se han desarrollado como un método útil para la identificación funcional de la inhibición de distintos miembros de cascadas de señalización (30, 96).

La genética química (*chemical genetics* – CG) consiste en el estudio del producto de un gen en un contexto celular o en un organismo utilizando moléculas químicas de bajo peso molecular. En este abordaje se utilizan moléculas pequeñas que se unen directamente a proteínas para alterar su función, lo que permite un análisis cinético de la consecuencia de esos cambios *in vivo*. Avances recientes han aumentado considerablemente el poder de estas moléculas, de forma que estas se asemejen a mutaciones genéticas, en cuanto a su aplicabilidad y especificidad para una diana. La sofisticación creciente de este abordaje lanza la posibilidad de que pueda ser aplicado a cualquier proceso biológico (138).

La adaptación de iRNA a células de mamíferos, junto con la expansión de la CG ha hecho posible los estudios sistemáticos de perdida de función capaces de revelar interacciones entre proteínas implicadas en muchas enfermedades humanas. No obstante, la falta de tecnología robusta, capaz de detectar los cambios producidos a consecuencia de las interferencias con un alto rendimiento constituía una laguna tecnológica que no permitía la implementación de rastreos por iRNA y CG a gran escala.

Esa laguna ha sido rellenada con la implementación de la adquisición de imágenes utilizando microscopía de fluorescencia robotizada y análisis de imágenes automatizado, a la que normalmente se refiere como rastreo de alto contenido (*High Content Screening* – HCS). Esa tecnología se ha convertido en una herramienta esencial en fases iniciales de programas de desarrollo de nuevos fármacos (56, 87, 165). La obtención de imágenes con alto contenido (de información) ha podido dar respuesta progresivamente a los retos crecientes que suponen la implementación de ensayos a larga escala y facilita la integración de rastreos dirigidos al tratamiento de enfermedades en estadios iniciales del desarrollo de fármacos.

El uso combinado de iRNA, CM y HCS simultáneamente constituye una metodología poderosa que nos ha permitido realizar estudios imparciales independientes de nociones pré-existentes a cerca de la red de señalización implicada en la regulación de FOXO. La identificación y caracterización de nuevas moléculas implicadas en la regulación de FOXO puede aportar información a cerca de cómo re-activar FOXO, con el objetivo de mejorar el tratamiento del cáncer.

2 Objectives

Given the importance of FOXO in many fundamental processes and its relevance in cancer, the aims of this work are:

1. Generation, validation and characterization of cellular systems suitable to perform large scale screenings to identify molecules implicated in FOXO regulation:

    - Generation of an image-based cellular system suitable to measure FOXO nuclear translocation.
    - Generation of a luciferase-based assay to measure FOXO transcriptional activity.
    - Generation of a multiplex cellular system in which FOXO nuclear translocation and transcriptional activity can be measured in a single assay.
    - Generation of an image-based cellular system able to measure unspecific nuclear trapping via CRM-1.
    - Generation of an image-based cellular system to identify Akt-mediated survival.

2. Realization of large-scale screenings to identify novel targets that can be exploited pharmacologically for the reactivation of FOXO:

    - Realization of a Chemical Genetic screening.
    - Realization of a large-scale loss-of-function RNAi screening.

3 Results

Following the objectives that have been proposed in the scope of this thesis we developed five technological platforms that allowed us to perform a chemical genetics screening and a large-scale RNAi screening. Undescribed interactions with FOXO were identified and a further characterization was carried out.

The following projects resulted in the publications that reflect the results obtained in each part of this work.

3.1 Development of technological platforms for the identification of new targets implicated in FOXO activity.

3.1.1 First Project: The U2nesRELOC system

Summary

FOXO transcription factors are excluded from the cell nucleus in a 14-3-3 and CRM1/exportin-dependent fashion. Therefore, the need for a complementary screening system in which the inhibition of this nuclear export machinery could be detected was evident. Based on a GFP fusion protein that contains a NES which is not regulated by Akt, but that relies on 14-3-3 and CRM1/exportin for nuclear exclusion, the U2nesRELOC system was generated by transfecting U2-OS cells stably with a plasmid containing the HIV virus Rev protein fused with a GFP reporter. This assay was upscaled to a high throughput format and a high content analysis of compounds known to influence CRM-1 -dependent nuclear export showed that this system can be used for the detection of nuclear trapping induced by those compounds. Thus, this system is a valuable tool for the deconvolution of the hits obtained in FOXO-based systems as the unspecific nuclear sequestration of FOXO can be distinguished from real activation that triggers nuclear translocation and consequent transcriptional activity. The specificity of the U2nesRELOC system was tested comparing the behavior of hose cells with U2-OS cells stably transfected with a FOXO-GFP fusion protein, generating the U2foxRELOC system. The U2foxRELOC cells were shown to accurately respond to PI3K/Akt inhibition, as seen by the shift in the localization of the fusion protein upon treatment with LY294002. Importantly, treatment with nuclear export inhibitor leptomycin B induced nuclear trapping of the reporter in both systems, while LY294002 only triggered nuclear accumulation of the reporter in the U2foxRELOC cells. Thus, the combined use of the U2nesRELOC with the U2foxRELOC system allows for the distinction between PI3K/Akt inhibitors and nuclear export inhibitors. Furthermore, the U2nesRELOC assay has also been shown to be suitable as a primary screening system for the identification of novel, nuclear export inhibitors which have been suggested to have therapeutic potential for several human diseases, including cancer. Therefore, the U2nesRELOC system represents a versatile technology platform well suited for primary high throughput screening and as a counter-screening system for deconvolution procedures.

Personal Contribution

I generated the cell-based system and performed the experiments required for its validation and adaptation to the high-throughput format. Once established, I performed the experiments carried with the compounds mentioned with the assistance of Aránzazu Rosado and helped in the data analysis and interpretation.

Publication:

Zanella F, Rosado A, Blanco F, Henderson BR, Carnero A, and Link W, **A HTS approach to screen for antagonists of the nuclear export machinery using high content cell based assays.** *ASSAY and Drug Development Technologies*. 2007 Jun; 5(3): 333-41.

ASSAY and Drug Development Technologies
Volume 5, Number 3, 2007
© Mary Ann Liebert, Inc.
DOI: 10.1089/adt.2007.058

An HTS Approach to Screen for Antagonists of the Nuclear Export Machinery Using High Content Cell-Based Assays

Fabian Zanella,[1] Aranzazú Rosado,[1] Fernando Blanco,[1] Beric R. Henderson,[2]
Amancio Carnero,[1] and Wolfgang Link[1]

Abstract: Intracellular localization is essential for the regulated activity of many signaling molecules associated with disease-relevant pathways. High content screening is a powerful technology to monitor the impact of small molecules or interfering RNAs on translocation of proteins within intact cells. Several assays have been developed to measure the nucleocytoplasmic shuttling of proteins like nuclear factor κB, FoxO, or nuclear factor of activated T-cells involved in distinct signaling networks. However, since all these proteins bear a leucine-rich nuclear export signal (NES), modulators of the NES-dependent export machinery can lead to misinterpretation of the assay readout. Here we report the generation of U2nesRELOC, a cell-based system for the identification of nuclear export inhibitors and specific silencers of the nuclear export machinery, and its adaptation to high throughput screening. The assay is based on mammalian cells stably expressing green fluorescent protein (GFP)-labeled Rev protein, which contains a strong heterologous NES. The fluorescent signal of untreated U2nesRELOC cells localizes exclusively to the cytoplasm. Upon treatment with the nuclear export inhibitor leptomycin B the GFP-labeled reporter protein accumulates rapidly in the cell nucleus. The assay has been adapted to 96-multiwell format and fully automated. Pilot experiments with a panel of 50 test compounds using three different concentrations per compound resulted in very consistent data sets with excellent reproducibility and an average Z' value of 0.76. In summary, U2nesRELOC is a cell-based nuclear export assay suitable for high throughput screening, providing counterscreens for pathway deconvolution.

Introduction

IMAGE ACQUISITION using robotic fluorescent microscopy and automated image analysis, generally referred to as HCS, has become an essential tool in early drug discovery programs. High content cellular imaging has increasingly met the challenges of high throughput needs and facilitates the integration of disease-relevant screens at early stages of the drug discovery process.[1,2] This effort aims to produce high-quality leads and decrease the current drug attrition rate by means of large-scale analysis of biologically relevant cellular events. Aberrant localization of proteins is known to be associated with many diseases, including cancer, inflammation, and cardiovascular diseases.[3–5] Consequently, monitoring the subcellular localization of proteins can yield important information about the impact of compounds on disease-relevant pathways in a cellular context. Several high content translocation assays using genetically tagged proteins or fluorescent-labeled antibodies to detect proteins that shuttle between cell nucleus and the cytoplasm have been published. Reporter proteins including nuclear

[1]Experimental Therapeutics Program, Centro Nacional de Investigaciones Oncologicas, Madrid, Spain.
[2]Westmead Millennium Institute, University of Sydney at Westmead Hospital, Sydney, NSW, Australia.

ABBREVIATIONS: DAPI, 4′,6-diamidino-2-phenylindole; DMSO, dimethyl sulfoxide; EGFP, enhanced green fluorescent protein; FACS, fluorescence-activated cell sorting; GFP, green fluorescent protein; IC_{50}, 50% inhibitory concentration; MAPK, mitogen-activated protein kinase; MAPKK (or MEK), mitogen-activated protein kinase kinase; NES, nuclear export signal; NF-κB, nuclear factor κB; PBS, phosphate-buffered saline; PI3K, phosphoinositide 3-kinase.

factor κB (NF-κB), FoxO, mitogen-activated protein kinase (MAPK)-activated protein kinase 2, and ERF1 were used to monitor the activity of the corresponding signaling pathways.[6–9] These proteins contain a leucine-rich nuclear export signal (NES) known to bind to the nuclear exportin receptor CRM-1, which mediates nucleocytoplasmic translocation through the nuclear pore.[10,11] CRM1 has a conserved Ran binding domain, and it binds Ran-GTP in the nucleus together with the NES cargo to form a tripartite complex.[12] Several compounds have been described that specifically inhibit CRM1-mediated nuclear export. The best-studied nuclear export inhibitor is leptomycin B, a fungal metabolite that binds covalently to a cysteine residue in the active center of CRM-1, preventing the efflux of NES-containing proteins.[13] Consequently, compounds that interfere with the general export machinery and in turn accumulate NES-containing proteins in the cell nucleus are likely to score in translocation assays for pathway analysis using NES-reporter proteins. In order to deselect hit wells treated with pathway-unrelated nuclear export inhibitors several counterscreens have been developed.[6,9] The basic strategy is to monitor a different NES-containing reporter protein whose cellular localization is regulated by a pathway-independent signaling pathway. In the present work we established an NES-dependent nuclear export assay in HTS format. Assay robustness and reproducibility are reflected in excellent Z'-factor values. Specificity of the system has been confirmed using test compounds with known mechanism of action.

Materials and Methods

Compounds and recombinant proteins

All chemicals were purchased from commercial sources except UCN01, which was kindly provided by the National Cancer Institute (Bethesda, MD), cisplatin, which was provided by C. Navarro (U.A.M., Madrid, Spain), minerval, which was generously provided by P. Escriba (University of the Balearic Islands, Palma de Mallorca, Spain), and gemcitabine, which was a gift from Eli Lilly Pharmaceuticals (Indianapolis, IN). Akt inhibitor, Akt inhibitor VIII, Akt inhibitor X, Bay11-7082, cisplatin, ionomycin, LY294002, NL71-101, PD98059, PP1, Raf1 kinase inhibitor, ratjadone A, SB203580, W-13 HCl, W-7 HCl, and wortmannin were purchased from Calbiochem (San Diego, CA). Brefeldin, cyclosporin A, forskolin, genistein, H-89, leptomycin B, rapamycin, roscovitine, thapsigargin, tyrphostatin AG 1478, tyrphostatin SU1498, and U0126 were purchased from LC Laboratories (Woburn, MA). D609, LY83583, manumycin A, pifithrin-α cyclic, rifampicin, tyrphostin AG 82, and tyrphostin AG 1433 were purchased from Alexis Biochemicals (San Diego). Caffeine, calmidazolium chloride, etoposide, staurosporine, and 12-*O*-tetradecanoylphorbol 13-acetate were purchased from Sigma-Aldrich (St. Louis, MO). Lithium chloride was purchased from Merck (Darmstadt, Germany). D000 was purchased from Labotest (Niederschoena, Germany). Epidermal growth factor and platelet-derived growth factor were purchased from RELIATech A.S. (Braunschweig, Germany). Human insulin-like growth factor-I and human insulin were purchased from Roche Diagnostics (Mannheim, Germany). Stock solutions of the test compounds were deposited in three different concentrations onto 96-well mother plates, transferred to multiple replicate plates, and frozen at -80°C.

Plasmids

The U2nesRELOC assay uses the reporter construct pRev$_{\mathrm{MAPKKnes}}$GFP, which has been described earlier.[14] pRev$_{\mathrm{MAPKKnes}}$GFP carries the NES from MAPK kinase (MAPKK) (or MEK) cloned between the *Bam*HI and *Age*I sites of pRev(1.4)-GFP, sandwiched between the Rev and the green fluorescent protein (GFP) coding sequences.[14] The GFP-Foxo3a fusion protein was kindly provided by T. Finkel (National Institutes of Health, Bethesda, MD).

Cell culture and stable transfections

The human osteosarcoma cell line U2OS was obtained from the American Type Culture Collection (Manassas, VA) and cultured in Dulbecco's modified Eagle's medium, supplemented with 10% fetal bovine serum (Sigma) and antibiotics-antimycotics. Cell cultures were maintained in a humified incubator at 37°C with 5% CO_2 and passaged when confluent using trypsin/EDTA. Transfection of plasmids was performed using jetPEI™ transfection reagent (Polyplus Transfection, Ilkirch, France) according to the manufacturer's instructions. Forty-eight hours after transfection, cells were selected with 800 μl/ml G418 for 10 days. Stable transfectants were fluorescence-activated cell sorting (FACS)-sorted to ensure that they expressed similar levels of fluorescent reporter protein. Clonal U2OS cells expressing pRev$_{\mathrm{MAPKKnes}}$GFP reporter protein and U2OS cells expressing GFP-Foxo3a reporter protein were seeded in six-well plates and incubated at 37°C with 5% CO_2 for 12 h. Then, cells were treated with 4 n*M* leptomycin B or 20 μM LY294002 for 1 h and photographed with a fluorescent microscope.

U2nesRELOC assay

Cells of the clonal U2OS cell line expressing pRev$_{\mathrm{MAPKKnes}}$GFP reporter protein (U2nesRELOC cells) were seeded at a density of 1.0×10^5 cells/ml into black-wall clear-bottom 96-well microplates (BD Biosciences, Franklin Lakes, NJ) using a Multidrop automatic dispenser (Titertek, Huntsville, AL). The final volume of the cell suspension was 200 μl in each well. After incubation at 37°C with 5% CO_2 for 12 h, 2 μl of each test compound was transferred from the mother plates to the assay plates using a robotic workstation (Biomek® FX, Beckman Coulter, Fullerton, CA). Cells were incubated in the presence of the compounds for 1 h. All additional pipetting steps were performed by the robotic workstation. The culture medium was removed by aspiration, and then the plates were washed with 1× phosphate-buffered saline (PBS) twice and fixed in 100 μl of 6% paraformaldehyde for 30 min at room temperature. After aspiration of the paraformaldehyde, fixed cells were washed twice with 1× PBS and, in order visualize the cell nucleus, stained with 4′,6-diamidino-2-phenylindole (DAPI) (Invitrogen, Carlsbad, CA) for 20 min at room temperature. The DAPI solution was removed by aspiration. Finally the plates were washed with 1× PBS twice and stored at 4°C before analysis.

Image acquisition and processing

Assay plates were read on the BD Biosciences Pathway™ 855 Bioimager equipped with a 488/10 nm enhanced GFP (EGFP) excitation filter, a 380/10 nm DAPI excitation filter, a 515LP nm EGFP emission filter, and a 435LP nm DAPI emission filter. Images were acquired in the DAPI and GFP channels of each well using a 10× dry objective. The plates were exposed 0.066 ms (Gain 31) to acquire DAPI images and 0.55 ms (Gain 30) for GFP images.

Data analysis

The BD Pathway Bioimager outputs its data in standard text files. Data were imported into the data analysis software BD Image Data Explorer. The nuclear/cytoplasmic ratios of fluorescence intensity were determined by dividing the fluorescence intensity of the nucleus by the cytoplasmic fluorescence intensity. A threshold ratio of greater than 1.8 was employed to define nuclear accumulation of fluorescent signal for each cell. Based on this procedure we calculated the percentage of cells per well displaying nuclear translocation or inhibition of nuclear export. Compounds that induced a nuclear accumulation of the fluorescent signal greater than 60% of that obtained from wells treated with 4 nM leptomycin B were considered as hits.

In order to estimate the quality of the HCS assay, the Z' factor was calculated by the equation: $Z' = 1 - [(3 \times$ standard deviation of positive controls$) + (3 \times$ standard deviation of negative controls$)/($mean of positive controls$) - ($mean of negative controls$)]$ as previously described by Zhang *et al.*[15]

Results

Generation of the U2nesRELOC reporter cells

In order to generate a system suitable to monitor CRM-1-dependent nuclear export in a HTS format we used a reporter protein previously described as extremely active in an *in vivo* nuclear transport assay. Henderson and

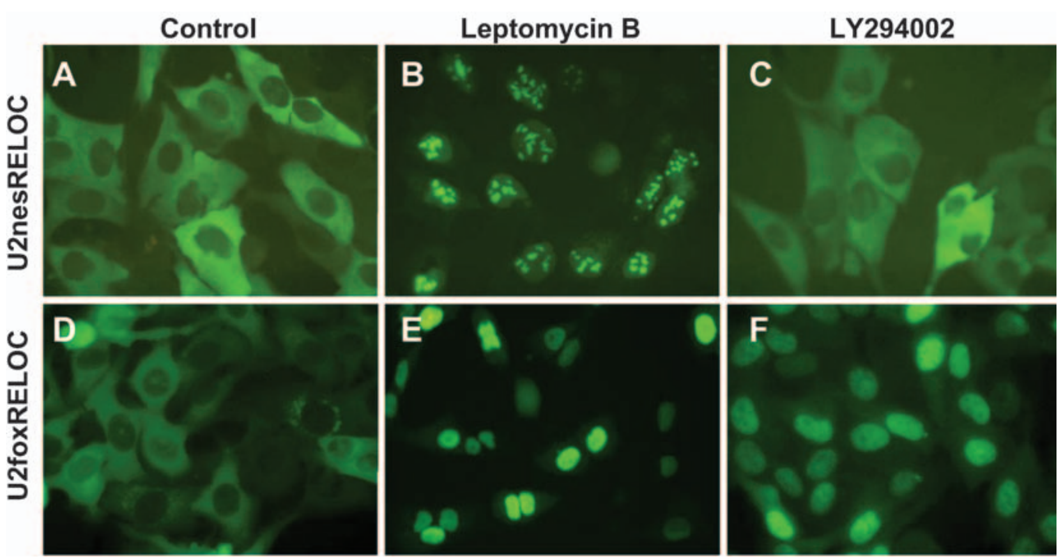

FIG. 1. Different behavior of U2nesRELOC and U2foxRELOC assay cell lines. Cells stably expressing $REV_{MAPKKnes}GFP$ (U2nesRELOC; **A–C**) or a FoxO-GFP fusion protein (U2foxRELOC; **D–F**) were seeded in six-well plates, incubated for 12 h, and treated with DMSO (Control, A and D), 4 nM leptomycin B (B and E), or 20 μM LY294002 (C and F) for 1 h and photographed using a fluorescence microscope.

Eleftheriou[14] restored nuclear export activity in an export-defective mutant of a human immunodeficiency virus type-1 Rev-GFP fusion protein by inserting several different heterologous NES sequences between Rev and the GFP coding sequence. The strongest export signals were mediated by the NES from MAPKK or protein kinase inhibitor-α. We stably transfected a GFP reporter plasmid that carries the NES from MAPKK ($Rev_{MAPKKnes}$GFP) into U2OS cells and prepared cell clones. In order to obtain the homogeneously GFP-expressing assay cell line U2nesRELOC, we performed several rounds of FACS. As a proof of principle we treated U2nesRELOC cells and cells stably expressing a FoxO-GFP fusion protein (U2foxRELOC) with one of the two pathway reference compounds, leptomycin B or LY294002. Leptomycin B is an inhibitor of the CMR-1-dependent nuclear export that covalently binds to a single cysteine residue of the CRM1 protein.[16] LY294002 is a broad-spectrum phosphoinositide 3-kinase (PI3K) inhibitor widely used to suppress activation of PI3K/Akt signaling.[17] In unstimulated U2nesREOC cells, GFP fusion protein was exclusively cytoplasmic. FoxO-GFP was present in both cytoplasm and nucleus, with a significantly higher level in the cytoplasm than in the nucleus of unstimulated U2foxRELOC cells. Leptomycin B inhibited the nuclear export of $Rev_{MAPKKnes}$GFP and FoxO-GFP, leading to localization of the fluorescent signal in the cell nucleus of both cell lines. In contrast, LY294002 only induced nuclear translocation of FoxO-GFP (Fig. 1). PI3K inhibition had no effect on $Rev_{MAPKKnes}$ GFP localization, indicating the capacity of U2nesRELOC to deconvolute signaling pathways. Drug washout experiments, replacing the drug solution with fresh medium, showed that the nuclear accumulation of $REV_{MAPKKnes}$GFP upon leptomycin B treatment was reversible. Removal of the drug restored the cytoplasmic localization of the fluorescent reporter protein almost completely 24 h after washout (data not shown).

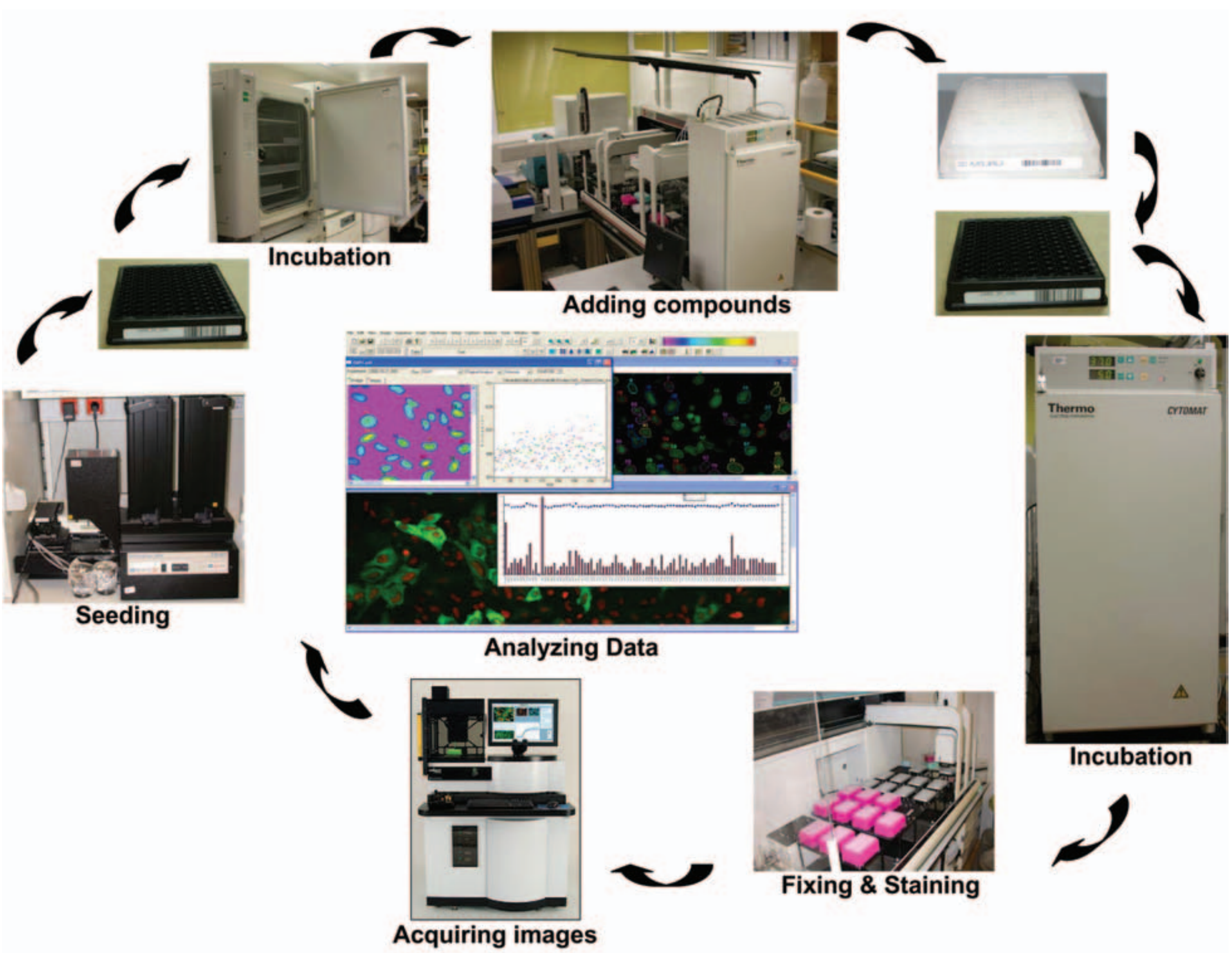

FIG. 2. The automated workflow for the U2nesRELOC assay allows standardization of the process. Cells were seeded automatically and incubated overnight. The test compounds were transferred from mother plates to assay plates using a robotic workstation. After a 1-h incubation at 37°C in medium containing the compounds cells were washed, fixed, and stained in a fully automated manner using a robotic workstation. For automated microscopy we used the BD Biosciences Pathway HT cell imaging platform.

Up-scaling and automation

The U2nesRELOC-based assay was formatted in 96-well plates, and workflow has been automated (Fig. 2). Cells were seeded at a density of 20,000 cells per well using a Multidrop dispenser. All liquid handling for compound treatment, washing, fixing, and staining steps was performed by a robotic workstation. The BD Pathway HT cell imaging platform was used for automated image acquisition. Cells were stained with DAPI to facilitate autofocus of the microscope and to aid the image segmentation. An image algorithm was applied to allow the cell nucleus segmentation based on a local thresholding. Our segmentation strategy assumes that the cell's cytoplasm surrounds the nucleus. Consequently, cytoplasmic fluorescence intensity is calculated from all the pixels within a circumferential ring surrounding the nuclear ring mask. The width of the ring was defined to be small enough to avoid ambiguities due to irregular cell shape. Based on the definition of cell compartments, the nuclear and cytoplasmic levels of GFP fluorescence were quantified. The nuclear/cytoplasmic ratios of fluorescence intensity were determined by dividing the fluorescence intensity of the nucleus by that of the cytoplasm. A threshold ratio of greater than 1.8 was employed to define nuclear accumulation of fluorescent signal for each cell. Based on this procedure we calculated the percentage of cells per well displaying nuclear translocation or inhibition of nuclear export.

Kinetics of leptomycin B-induced nuclear GFP accumulation in U2nesRELOC cells

In order to define the optimal time period of compound treatment for the U2nesRELOC-based end-point assay, we investigated the kinetics of leptomycin B-induced nuclear GFP accumulation using the above-described automated procedure. We performed leptomycin B treatment at 4 n*M*, a concentration widely used to study nuclear export. Nuclear accumulation of $REV_{MAPKKnes}GFP$ reporter protein in U2nesRELOC cells was detectable as early as 10 min after blocking nuclear export by leptomycin B treatment and further increased during a period of 1 h (Fig. 3).

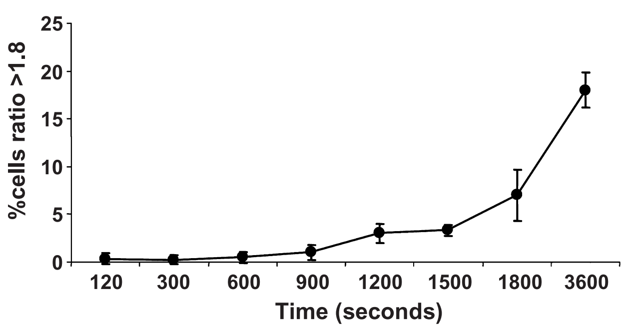

FIG. 3. Kinetics of leptomycin B-induced nuclear GFP accumulation using the U2nesRELOC assay system in HTS format. Cells were seeded automatically at appropriate density in 96-well (200 μl per well) black-wall clear-bottom tissue culture plates and allowed to attach overnight. Cells were then treated with 4 n*M* leptomycin B. All liquid handling for compound treatment, washing, fixing, and staining steps was performed by a robotic workstation. Nuclear accumulation of GFP reporter was assessed after 2 min, 5 min, 10 min, 15 min, 20 min, 25 min, 30 min, and 60 min. Data shown here represent three independent experiments.

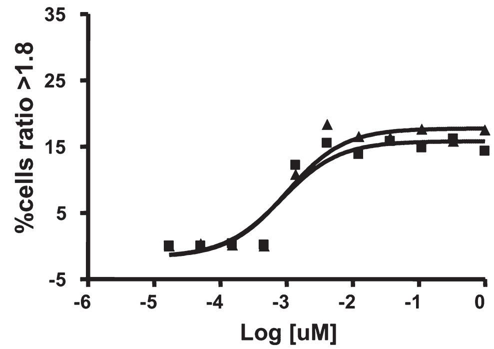

FIG. 4. Dose–response of the leptomycin B inhibition of nuclear export measured using the U2nesRELOC assay system in HTS format. Cells were seeded automatically at appropriate density in 96-well (200 μl per well) black-wall clear-bottom tissue culture plates and allowed to attach overnight. Cells were then treated with different concentrations of leptomycin B for 1 h. All liquid handling for compound treatment, washing, fixing, and staining steps was performed by a robotic workstation. Graphs represent the growth of the cells relative to cells treated only with carrier. Each curve is the average of two independent experiments performed in triplicate samples.

Leptomycin B dose–response analysis using U2nesRELOC cells

We next determined the 50% inhibitory concentration (IC_{50}) value of the reference compound leptomycin B in the U2nesRELOC assay. Cells were cultured as indicated in Materials and Methods and treated with different doses of leptomycin B for 1 h. Figure 4 shows that U2nesRELOC is very sensitive in detecting the presence of leptomycin B at concentrations as low as 50 p*M*. The IC_{50} value was calculated as being the inhibitor concentration that increases nuclear accumulation of the reporter protein by 50%. The IC_{50} of leptomycin B was 0.91 n*M* in the U2nesRELOC assay. IC_{50} values for leptomycin B-mediated inhibition of nuclear export in the low nanomolar range have been reported in several earlier reports for other cell types.[18,19]

Screening a panel of test compounds using the U2nesRELOC-based assay

To assess specificity of the assay we screened a panel of commercially available compounds of known mechanism of action (Table 1), using the U2nesRELOC cell system. The panel of compounds consisted of inhibitors of different kinases, including PI3K, Akt, MAPK, MAPKK, Raf1, MEK-1, MEK-2, mammalian target of rapamycin, Src, protein kinase A, protein kinase C, platelet-derived growth factor β-receptor kinase, inhibitors of phospholipase C, guanylate cyclase, Ras farnesyltransferase, RNA polymerase, p34cdc2, p53, NF-κB, Flk-1, epidermal growth factor, calcineurin, activators of adenylate cyclase, intracellular calcium release,

TABLE 1. PANEL OF COMPOUNDS OF KNOWN MECHANISM OF ACTION TESTED IN THE U2NESRELOC CELL SYSTEM

		Concentration			
Compound	*Source*	*Low*	*Medium*	*High*	*Description*
Akt inhibitor	Calbiochem	1 μM	10 μM	30 μM	Akt inhibitor
Akt inhibitor VIII	Calbiochem	50 nM	500 nM	5 μM	Akt inhibitor
Akt inhibitor X	Calbiochem	50 nM	500 nM	5 μM	Akt inhibitor
Bay11-7082	Calbiochem	1 μM	10 μM	30 μM	NF-κB inhibitor
Brefeldin	LC Laboratories	200 nM	1 μM	20 μM	Membrane transport blocker
Caffeine	Sigma	500 nM	4 nM	10 nM	(Cyclic AMP) phosphodiesterase inhibitor
Calmidazolium chloride	Sigma	1 μM	10 μM	30 μM	Inhibitor of calmodulin-regulated enzymes
Cisplatin	C. Navarro	3 μM	30 μM	300 μM	DNA-damaging antitumor compound
Cyclosporin A	LC Laboratories	40 nM	400 nM	4 μM	Calcineurin inhibitor
D000	Labotest/ICOS	100 nM	500 nM	2 μM	PI3Kδ inhibitor
D609	Alexis	1 μM	10 μM	30 μM	Phospholipase C inhibitor
EGF	ReliaTech	0.5 ng/ml	5 ng/ml	25 ng/ml	Growth factor
Etoposide	Sigma	100 nM	10 μM	100 μM	Topoisomerase II inhibitor
Forskolin	LC Laboratories	200 nM	1 μM	20 μM	Activator of adenylate cyclase
Gencitabine	Eli Lilly	100 nM	500 nM	1 μM	Nucleoside analogue with antitumor activity
Genistein	Sigma	200 nM	20 μM	50 μM	Protein tyrosine kinase inhibitor
H-89	LC Laboratories	50 nM	500 nM	5 μM	Inhibitor of protein kinase A
IGF-I, human	Roche	1 ng/ml	20 ng/ml	50 ng/ml	Growth factor
Insulin, human	Roche	0.5 μg/ml	2 μg/ml	10 μg/ml	Growth factor
Ionomycin	Calbiochem	5 nM	50 nM	200 nM	Inducer of calcium influx
Kenpaullone	Calbiochem	100 nM	500 nM	20 μM	Protein kinase inhibitor
Leptomycin B	LC Laboratories	0.5 nM	1 nM	4 nM	Inhibitor of nuclear export
LY294002	Calbiochem	1 μM	20 μM	50 μM	PI3K inhibitor
LY83583	Alexis	1 μM	10 μM	20 μM	Guanylate cyclase inhibitor
Manumycin A	Alexis	500 nM	5 μM	25 μM	Ras farnesyltransferase inhibitor
Minerval	P. Escriba	25 μM	100 μM	200 μM	Modulator of membrane lipid structure
NL71-101	Calbiochem	200 nM	2 μM	10 μM	Akt inhibitor
PD98059	Calbiochem	1 μM	10 μM	30 μM	Inhibitor of MEK
PDGF	ReliaTech	0.2 ng/ml	1 ng/ml	10 ng/ml	Growth factor
Pifithrin-α cyclic	Alexis	10 nM	200 nM	20 μM	p53 inhibitor
PP1	Calbiochem	10 nM	100 nM	10 μM	Src inhibitor
Raf1 kinase inhibitor	Calbiochem	5 nM	20 nM	200 nM	Raf1 kinase inhibitor
Rapamycin	LC Laboratories	50 pM	0.5 nM	5 nM	mTOR inhibitor
Ratjadone A	Calbiochem	4 pM	4 nM	40 nM	Inhibitor of nuclear export
Roscovitine	LC Laboratories	200 nM	2 μM	30 μM	Inhibitor of $p34^{cdc2}$
Rifampicin	Alexis	3 nM	300 nM	3 μM	RNA polymerase inhibitor
SB203580	Calbiochem	5 nM	40 nM	400 nM	MAP kinase inhibitor
Sataurosporine	Sigma	2 nM	20 nM	10 μM	Protein kinase inhibitor
Thapsigargin	LC Laboratories	5 nM	20 nM	200 nM	Intracellular calcium releaser
Tyrphostin AG 82	Alexis	1 μM	10 μM	20 μM	Protein tyrosine kinase inhibitor
Tyrphostin AG 1433	Alexis	1 μM	10 μM	20 μM	Inhibitor of the PDGF b-receptor kinase
Tyrphostatin AG 1478	LC Laboratories	5 nM	20 nM	200 nM	Inhibitor of the EGF-receptor kinase
Tyrphostatin SU1498	LC Laboratories	700 nM	10 μM	30 μM	Inhibitor of the VEGF-receptor kinase
Tetradecanoyl phorbol acetate	Sigma	10 nM	150 nM	10 μM	Activator of PKC
U0126	LC Laboratories	1 μM	20 μM	50 μM	MEK-1 and MEK-2
UCN01	NCI	200 nM	1 μM	10 μM	
W-7 HCl	Calbiochem	1 μM	20 μM	50 μM	Calmodulin antagonist
W-13 HCl	Calbiochem	400 nM	4 μM	40 μM	Calmodulin antagonist
Wortmannin	Calbiochem	50 nM	150 nM	500 nM	PI3K inhibitor

We exposed U2nesRELOC cells to three different concentrations (low, medium, and high) of test compounds. EGF, epidermal growth factor; IGF-I, insulin-like growth factor-I.

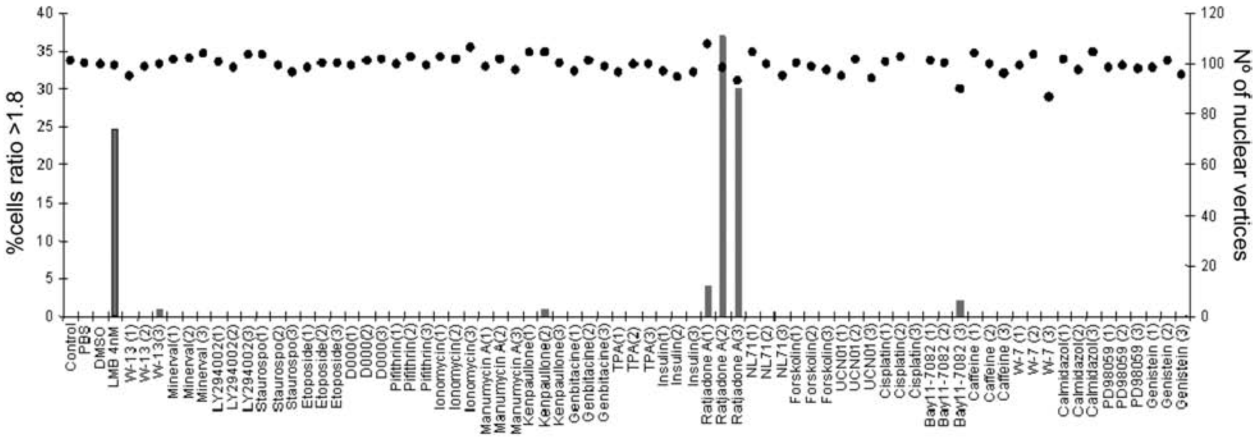

FIG. 5. Nuclear accumulation of $REV_{MAPKKnes}GFP$ reporter protein achieved upon treatment with test compounds. We exposed U2nesRELOC cells to three different concentrations. Low, medium, and high concentrations are indicated by (1), (2), and (3), respectively. Control wells containing phosphate-buffered saline (PBS), DMSO, ethanol, and leptomycin B are indicated by PBS, DMSO, control, and LMB, respectively. TPA, 12-*O*-tetradecanoylphorbol 13-acetate. The bar graph and the corresponding left *y*-axis show the percentage of cells in each well exhibiting nuclear/cytoplasmic ratios of fluorescence intensity greater than 1.8. Black dots represent the average number of nuclear vertices in each well. The right *y*-axis indicates measurement of the average number of nuclear vertices. Data shown here represent three independent experiments.

translocation of proteins from the endoplasmic reticulum, etc. We also included the antifungal metabolite ratjadone A, a well-described, potent inhibitor of CRM1-mediated nuclear export.[20] A robotic workstation was used to prepare mother plates containing three different concentrations of these compounds. We exposed U2nesRELOC cells to equal volumes of test compounds resulting in a range of final concentrations of greater than

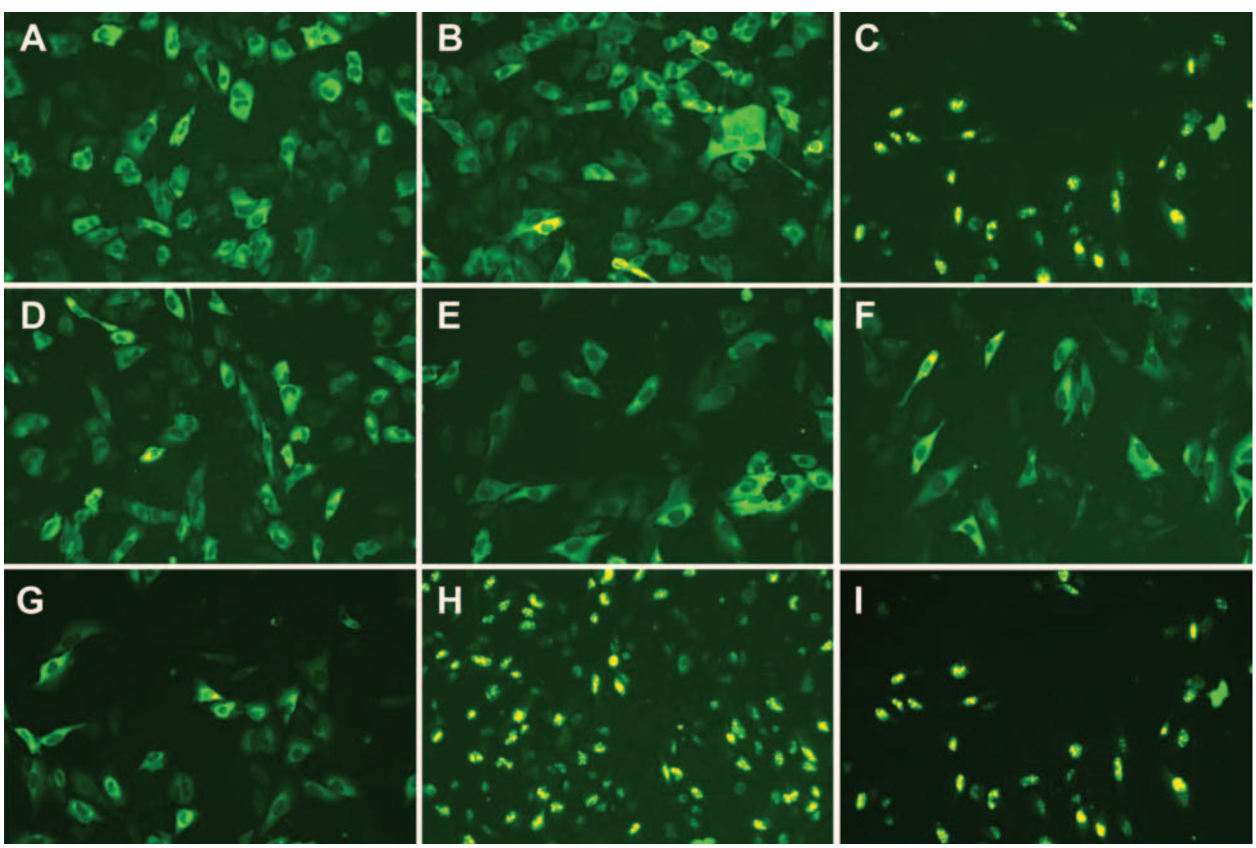

FIG. 6. Representative images of the compound-treated assay cell line using the high throughput format of the U2nesRELOC system: (**A**) vehicle control (1% DMSO); (**B**) vehicle control (1% ethanol); (**C**) positive control (4 n*M* leptomycin B); (**D**) 1 μM forskolin; (**E**) 30 μM Bay11-7082; (**F**) 40 n*M* SB203580; (**G**) 4 p*M* ratjadone A; (**H**) 4 n*M* ratjadone A; and (**I**) 40 n*M* ratjadone A.

two orders of magnitude around the IC_{50} value for each compound. The final concentration of dimethyl sulfoxide (DMSO) was kept at 1% after addition of the compounds. Each plate contained several internal controls, including wells without treatment and wells treated with different concentrations of DMSO or ethanol. As a reference compound we used leptomycin B at 4 n*M* in triplicate. To determine the cutoff threshold for primary hits, the accumulation of fluorescent signal triggered by leptomycin B in the U2nesRELOC-based assay was defined as 100% activity. The primary hits were defined as those samples that had an activity of greater than 60%. Ratjadone A at concentrations of 4 n*M* and 40 n*M* fulfilled these criteria (Fig. 5). In contrast, treatment of U2nesRELOC cells with 4 p*M* ratjadone A did not trigger significant nuclear accumulation of the GFP reporter protein. None of the other compounds tested scored as hits, not even at the highest concentration more likely to produce unspecific effects (Fig. 5 and data not shown). These data indicate that nuclear accumulation of the reporter protein $REV_{MAPKKnes}$GFP is a very specific event and is suitable to monitor inhibition of the general nuclear export machinery.

In addition, we used auxiliary algorithms to monitor information related to cell viability. Analyzing the number of nuclear vertices we could not detect compound-related toxicity probably because of the short incubation period. Furthermore, visual inspection of images generated by the BD Pathway Bioimager was used to qualitatively confirm quantitative data from the data analysis process (Fig. 6). The quality of the U2nesRELOC-based assay has been assessed by calculating the Z' values. The U2nesRELOC-based assay has great performance with an average Z' higher than 0.76.

Discussion

Cell-based screens analyzing multiple intervention points within signaling pathways to identify small molecule inhibitors are increasingly gaining importance in drug discovery. Nucleocytoplasmic translocation of GFP-based reporter molecules has been used as a reliable readout of pathway activity. However, most of the reporter proteins used in translocation assays have been found to be subject to complex regulation, demanding the incorporation of a series of counterscreens to deconvolute the effects of compound treatment.

In the present study we established U2nesRELOC, a highly sensitive and selective cell-based assay for nucleocytoplasmic shuttling suitable for HTS. The assay strategy is based on a fluorescent reporter protein containing a heterologous NES that is efficiently exported from the nucleus into the cytoplasm. The reporter protein used in our screen was preselected with respect to the strength of the export signal based on the systematic comparison of Rev-type NES established by Henderson and Eleftheriou.[14] In fact, in untreated U2nesRELOC cells, the fluorescent signal is exclusively cytoplasmic. Conversely, in U2foxRELOC cells stably expressing a Foxo3a-GFP fusion protein that also carries a functional NES, subcellular localization of the fluorescent reporter was both cytoplasmic and nuclear. Consistently, compounds that interfere with the NES-mediated export lead to the nuclear accumulation of fluorescent reporter proteins in both cell lines. In contrast, inhibition of PI3K/Akt signaling known to induce nuclear translocation of Foxo transcription factors resulted in accumulation of fluorescent signal in U2foxRELOC but not in U2nesRELOC cells. These data demonstrate the utility and potential of the U2nesRELOC system for pathway deconvolution in a whole-cell environment.

We implemented U2nesRELOC as a fixed-cell assay and automated the workflow using a Multidrop dispenser, robotic workstation, and robotic cell imaging platform. We assessed the properties of this HTS translocation assay using leptomycin B as a reference compound. Using the full automated procedure, we monitored the kinetics of nuclear accumulation of the fluorescent reporter protein, confirming earlier studies that revealed leptomycin B-mediated inhibition of nuclear export as a fast event.[18,19] The fast kinetics of the assay allowed us to reduce the incubation time necessary to attain unambiguous responses to compound treatment, which is an important factor to minimize possible toxic effects interfering with data analysis procedures. Dose–response studies underscored the sensitivity of the U2nesRELOC system in HTS format, allowing the detection of leptomycin B at the picomolar level. Taken together, these data demonstrate that U2nesRELOC provides a fast and sensitive method to monitor inhibition of nuclear export in a high throughput manner. However, the usefulness of U2nesRELOC as a counterscreen for pathway deconvolution depends greatly on its ability to provide a tool to deselect hit compounds from other translocation screens that specifically inhibit nuclear export. We assessed the specificity of U2nesRELOC using a panel of test compounds of known mechanism of action aimed to interfere with the major known signaling pathways. In order to mimic characteristics of a real single-point concentration screening scenario where biologically active concentrations can fluctuate widely, we performed the test screening with three different concentrations for each compound. The fact that only the reference compound leptomycin B and the cytotoxic metabolite ratjadone A, known as a potent nuclear export inhibitor,[20] induced the nuclear accumulation of $REV_{MAPKKnes}$GFP reporter suggests that the major known signaling pathways targeted by the panel of test compounds do not significantly interfere with NES-mediated nuclear export and demonstrates the ability of the U2nesRELOC assay in high throughput format to identify specifically inhibitors of nuclear export. Since the U2nesRELOC assay is performed in intact cells in the presence of serum, insoluble, membrane-impermeable, or unstable compounds or compounds with strong serum binding affinities are excluded by default. The single-cell imaging approach of the U2nesRELOC system provides the possibility of automatically deselecting false-positives in the primary screening using auxiliary algorithms like number of nuclear vertices relating to cellular morphology. In addition, visual inspection of the hit wells allows the identification of fluorescent compounds and compounds with toxic effects. In summary, we have developed U2nesRELOC, a cell-based, high throughput, high content assay suitable for primary screening of antagonists of nuclear export or counterscreening aimed at the deselection of nuclear export inhibitors from pathway-specific high content protein translocation assays. U2nesRELOC is fast, robust, and reproducible, providing the intrinsic benefits of image-based HCS and delivering excellent Z' values.

Acknowledgments

This work was supported by Spanish MCyT grant BIO2002-00197 and by the Spanish MEC (project BIO2006-02432). F.Z. is the recipient of a Marie Curie Fellowship. The authors acknowledge B. GarcÌa for expert technical assistance, the staff at BD Biosciences for their contribution to establishing the technology, and C. Blanco, J.F. Martinez, and O. Renner for helpful discussions and critical reading of this manuscript.

References

1. Haney SA, LaPan P, Pan J, Zhang A: High-content screening moves to the front of the line. *Drug Discov Today* 2006;11:889–894.
2. Lang P, Yeow K, Nichols A, Scheer A: Cellular imaging in drug discovery. *Nat Rev Drug Discov* 2006;5:343–356.
3. Harrison BC, Roberts CR, Hood DB, Sweeney M, Gould JM, Bush EW, *et al.*: The CRM1 nuclear export receptor controls pathological cardiac gene expression. *Mol Cell Biol* 2004;24:10636–10649.
4. Ferrigno P, Silver PA: Regulated nuclear localization of stress-responsive factors: how the nuclear trafficking of protein kinases and transcription factors contributes to cell survival. *Oncogene* 1999;18:6129–6134.
5. Ben-Levy R, Hooper S, Wilson R, Paterson HF, Marshall CJ: Nuclear export of the stress-activated protein kinase p38 mediated by its substrate MAPKAP kinase-2. *Curr Biol* 1998;8:1049–1057.
6. Almholt DLC, Loechel F, Nielsen SJ, Krog-Jensen C, Terry R, Bjorn SP, *et al.*: Nuclear export inhibitors and kinase inhibitors identified using a MAPK-activated protein kinase 2 Redistribution® screen. *Assay Drug Dev Technol* 2004;2:7–20.
7. Bertelsen M, Sanfridson A: Inflammatory pathway analysis using a high content screening platform. *Assay Drug Dev Technol* 2005;3:261–271.
8. Granas C, Lundholt BK, Loechel F, Pedersen HC, Bjorn SP, Linde V, *et al.*: Identification of RAS-mitogen-activated protein kinase signaling pathway modulators in an ERF1 redistribution screen. *J Biomol Screen* 2006;11: 423–434.
9. Kau TR, Schroeder F, Ramaswamy S, Wojciechowski CL, Zhao JJ, Roberts TM, *et al.*: A chemical genetic screen identifies inhibitors of regulated nuclear export of a Forkhead transcription factor in PTEN-deficient tumor cells. *Cancer Cell* 2003;4:463–476.
10. Fukuda M, Asano S, Nakamura T, Adachi M, Yoshida M, Yanagida M, *et al.*: CRM1 is responsible for intracellular transport mediated by the nuclear export signal. *Nature* 1997;390:308–311.
11. Fornerod M, Ohno M, Yoshida M, Mattaj IW: CRM1 is an export receptor for leucine-rich nuclear export signals. *Cell* 1997;90:1051–1060.
12. Gorlich D, Kutay U: Transport between the cell nucleus and the cytoplasm. *Annu Rev Cell Dev Biol* 1999;15: 607–660.
13. Kudo N, Wolff B, Sekimoto T, Schreiner EP, Yoneda Y, Yanagida M, *et al.*: Leptomycin B inhibition of signal-mediated nuclear export by direct binding to CRM1. *Exp Cell Res* 1998;242:540–547.
14. Henderson BR, Eleftheriou A: A comparison of the activity, sequence specificity, and CRM1-dependence of different nuclear export signals. *Exp Cell Res* 2000; 256:213–224.
15. Zhang JH, Chung TDY, Oldenburg KR: A simple statistical parameter for use in evaluation and validation of high throughput screening assays. *J Biomol Screen* 1999;4: 67–73.
16. Kudo N, Matsumori N, Taoka H, Fujiwara D, Schreiner EP, Wolff B, *et al.*: Leptomycin B inactivates CRM1/exportin 1 by covalent modification at a cysteine residue in the central conserved region. *Proc Natl Acad Sci U S A* 1999;96:9112–9117.
17. Walker EH, Pacold ME, Perisic O, Stephens L, Hawkins PT, Wymann MP, *et al.*: Structural determinants of phosphoinositide 3-kinase inhibition by wortmannin, LY294002, quercetin, myricetin, and staurosporine. *Mol Cell* 2000;6: 909–919.
18. Yao Z, Flash I, Raviv Z, Yung Y, Asscher YD, Pleban S, *et al.*: Non-regulated and stimulated mechanisms cooperate in the nuclear accumulation of MEK1. *Oncogene* 2001;20:7588–7596.
19. Wolff B, Sanglier JJ, Wang Y: Leptomycin B is an inhibitor of nuclear export: inhibition of nucleo-cytoplasmic translocation of the human immunodeficiency virus type 1 (HIV-1) Rev protein and Rev-dependent mRNA. *Chem Biol* 1997;4:139–147.
20. Koster M, Lykke-Andersen S, Elnakady YA, Gerth K, Washausen P, Hofle G, *et al.*: Ratjadones inhibit nuclear export by blocking CRM1/exportin 1. *Exp Cell Res* 2003;286:321–331.

Address reprint requests to:
Wolfgang Link, Ph.D.
Experimental Therapeutics Program
Centro Nacional de Investigaciones Oncologicas
Melchor Fernandez Almagro, 3
28029 Madrid, Spain

E-mail: wlink@cnio.es

3.1.2 Second Project: The U2transLUC system

Summary

The activity of FOXO transcription factors is mainly regulated via post-translational modifications. Phosphorylation is the best characterized mode of regulation of FOXO and it influences both FOXO subcellular relocalization and transcriptional activity. FOXO transcriptional activity can be further influenced once FOXO proteins are localized in the cell nucleus. It has been reported that other post-translational modifications, namely monoubiquitylation and acetylation also contribute to change FOXO affinity to DNA and may direct FOXO-dependent transcription to different programs, suggesting that nuclear translocation constitutes a starting point for the modulation of FOXO activity. Hence, to fully understand the mechanisms underlying FOXO modulation it is fundamental to distinguish the stimuli that can induce different levels of regulation of nuclear FOXO. Classically, FOXO-GFP translocation has been applied in High Content Assays and FOXO-induced luciferase activity has been used in High Throughput Assays for the readout of either subcellular relocalization or transcriptional activity underlying FOXO activation separately. The combination of both assays constitutes an interesting approach for the further dissection of the impact a given stimuli can have upon FOXO. We developed U2transLUC, an assay system in which luciferase and fluorescent read-outs can be multiplexed to provide a powerful cell-based high content screening method. Nuclear-cytoplasmic FOXO shuttling and FOXO-driven transcription can be measured simultaneously for the analysis of these two key features of FOXO regulation in a single assay, increasing the amount of information obtained from each experiment. The combination of different biological read-outs in a single cell line offers significant advantages over conventional cell-based assays. U2transLUC is suitable for high throughput screening and can identify small molecules that interfere with FOXO signaling at different levels.

Personal contribution

I generated the cell-based system, performed the experiments required for its validation and adaptation to the high-throughput format. I performed the experiments carried with the compounds mentioned with the assistance of Aránzazu Rosado and helped in the data analysis and interpretation.

Publication:

Zanella F, Rosado A, García B, Carnero A and Link W. **Using multiplexed regulation of luciferase activity and GFP translocation to screen for FOXO modulators**. *BMC Cell Biology*, in revision.

Using multiplexed regulation of luciferase activity and GFP translocation to screen for FOXO modulators

Fabian Zanella,[1] Aranzazú Rosado,[1, 2] Beatriz Garcia,[1] Amancio Carnero[1] and Wolfgang Link*[1]

Address: [1]Experimental Therapeutics Programme, Centro Nacional de Investigaciones Oncologicas (CNIO), Melchor Fernandez Almagro 3, 28029 Madrid, Spain.

[2]Current address: NKI-AVL, Plesmanlaan 121, 1066 CX, Amsterdam, The Netherlands.

Email: Fabian Zanella – fazanella@cnio.es; Aranzazú Rosado – a.rosado@nki.nl; Beatriz Garcia - bgserelde@cnio.es; Amancio Carnero - acarnero@cnio.es; Wolfgang Link - wlink@cnio.es

* Corresponding author

Abstract

Background: Independent luciferase reporter assays and fluorescent translocation assays have been successfully used in drug discovery for several molecular targets. We developed U2transLUC, an assay system in which luciferase and fluorescent read-outs can be multiplexed to provide a powerful cell-based high content screening method.

Results: The U2transLUC system is based on a stable cell line expressing a GFP tagged FOXO transcription factor and a luciferase reporter gene under the control of human FOXO-responsive enhancers. The U2transLUC assay measures nuclear-cytoplasmic FOXO shuttling and FOXO-driven transcription, providing a means to analyze these two key features of FOXO regulation in the same experiment. We challenged the U2transLUC system with chemical probes with known biological activities and we were able to identify compounds with translocation and/or transactivation capacity.

Conclusions: Combining different biological read-outs in a single cell line offers significant advantages over conventional cell-based assays. The U2transLUC assay facilitates the maintenance and monitoring of homogeneous FOXO transcription factor expression and allows the reporter gene activity measured to be normalized with respect to cell viability. U2transLUC is suitable for high throughput screening and can identify small molecules that interfere with FOXO signaling at different levels.

Background

Forkhead box O (FOXO) proteins are emerging as transcriptional integrators of pathways that regulate a variety of cellular processes, including differentiation, metabolism, stress response, cell cycle and apoptosis (1-3). FOXO transcription factors have been proposed to act as *bona fide* tumor suppressors due to their inhibitory effects on cell cycle and survival (4), properties mediated by their binding as monomers to consensus DNA binding sites. Their transcriptional activity is governed by a network of signaling events, the best recognized of which is the phosphorylation of FOXO proteins at three highly conserved serine and threonine residues by Akt that provokes its association with 14-3-3 protein and in turn, the nuclear exclusion of phospho-FOXO. However, the relocation of FOXO from the nucleus to the cytoplasm alone cannot account for the inhibitory effect of PI3K/Akt signaling on FOXO activity since a nuclear form of FOXO1 in which the nuclear export sequence is disrupted is still inhibited by the PI3K/Akt pathway (5). Indeed, the introduction of a negative charge in the positively charged DNA binding domain by means of FOXO phosphorylation at the second of the three Akt consensus sites inhibits DNA binding of FOXO (6, 7). The FOXO DNA interaction is also regulated by the transfer of acetyl groups to lysine residues in FOXO proteins by the histone acetyltransferases (HATs) CBP and p300 (2), which alters the DNA binding capacity of FOXO1 and FOXO3a (8). Conversely, Sirt1 deacetylases deacetylate FOXO factors and regulate their DNA binding at specific target genes. Taken together, these observations suggest that translocation and transactivation are different and separate means to regulate FOXO. However, large scale tools are not available to assess the different levels of FOXO regulation. Therefore systematic chemical genetic or loss of function studies to investigate the complex regulation of FOXO factors have been limited only to certain aspects (9).

In anticancer drug discovery, much effort is directed towards identifying small molecule inhibitors of PI3K/Akt signaling using cell based high content screening. In particular, monitoring the intracellular localization of FOXO transcription factors has been used to screen large numbers of small molecules (10, 11). Despite being commonly used as a reporter-gene system in drug discovery, luciferase-based transcriptional assays have not been applied to massive compound screens for PI3K/Akt inhibitors. Inhibiting the PI3K/Akt pathway causes FOXO3a to remain in the cell nucleus and subsequently, it induces the transcription of downstream genes. To take advantage of these regulatory features we generated the stable U2transLUC dual assay cell line that expresses FOXO responsive luciferase activity and GFP labelled FOXO. Thus, U2transLUC can be used to simultaneously monitor the intracellular translocation and the transcriptional activity of FOXO proteins. We have used this cell line in an attempt to identify small molecules that interfere with FOXO signaling.

Results

Generation and testing of luciferase reporter gene constructs

FOXO proteins drive the transcription of downstream genes by binding to the TTGTTTAC FOXO responsive enhancer element, generally referred to as a daf-16 family protein-binding element (DBE) (12). To take advantage of these regulatory features, we engineered several luciferase reporter constructs that contained one to six copies of the DBE consensus cassette in front of a SV40 minimal viral promoter that was linked to a luciferase reporter gene. The resulting reporter gene construct were designated as pGL-1xDBE, pGL-2xDBE, pGL-3xDBE, pGL-4xDBE, pGL-5xDBE and pGL-6xDBE (Fig.1A), and the luciferase activity driven by FOXO from these constructs was evaluated after they were transiently transfected into U2OS osteosarcoma cells. Since endogenous FOXO3a is only weakly expressed in these cells, ectopic FOXO3a also had to be expressed to achieve acceptable basal levels of luciferase activity (data not shown). In transient co-transfection assays, all the luciferase reporter constructs that carried FOXO responsive DBE elements produced a significant increase in luciferase activity when compared to the empty pGL3-Promoter vector. Constructs that contained three or six copies of the DBE element conferred significantly stronger FOXO-dependent transcriptional activity than those with one, two, four or five copies (Fig. 1B). A reporter plasmid that carried three copies of a mutated DBE (pGL-3xDBEmut) element did not promote significant luciferase activity, confirming the specificity of the original constructs for FOXO-mediated transcriptional activity.

In order to evaluate the responsiveness of the reporter constructs to the inhibition of the PI3K/Akt pathway, we transiently co-transfected the pGL-3xDBE or pGL-6xDBE construct with FOXO3a into U2OS cells and then treated them with the PI3K inhibitor, LY294002 (20µM). Inhibition of the PI3K pathway increased FOXO-dependent transcription from both the pGL-3xDBE and pGL-6xDBE constructs approximately 3-fold (Figure 1B). By contrast, activation of the PI3K/Akt signaling pathway following exposure to insulin decreased this luciferase activity. However, the differences between the transcriptional activity of FOXO3a in untreated and insulin treated U2OS cells were small, indicating that steady-state level of PI3K/Akt activity was already quite high. In addition, to confirm the specificity of our system we examined the effect of constitutive FOXO activation by co-expressing the pGL-3xDBE or pGL-6xDBE reporter construct with FOXO3a-A3, a constitutively active form of FOXO3a in which the three PI3K-dependent phosphorylation sites have been mutated to alanine. The expression of FOXO3a-A3 induced a strong increase in pGL-3xDBE or pGL-6xDBE driven luciferase activity. Together, these data indicate that the firefly luciferase-based read-out of FOXO activity is very specific, and that it provides a large window to measure any upregulation in the response (e.g. upon the inhibition of the PI3K/Akt pathway). Since the responsiveness of the triple tandem repeat of DBE (pGL-3xDBE) to PI3K inhibition was slightly higher than that of pGL-6xDBE, the p3xDBE-luc construct was used to generate the stable cell assay line, U2transLUC.

Generation of the assay cell line, U2transLUC

We recently reported the use of a high-throughput cellular imaging assay to monitor the nucleo-cytoplasmic translocation of a GFP-FOXO3a fusion protein in U2OS cells (U2foxRELOC) for a chemical genetic study (9). In order to generate an assay system that combines the benefits of large-scale image-based analysis and luciferase-based end point measurements, we examined the compatibility of transcriptional and translocational reporters expressed in a single cell line. We first explored whether the GFP-tagged FOXO protein is still capable of driving luciferase expression from FOXO responsive reporters. We compared the reporter activity of the pGL-3xDBE construct or the mutated version (pGL-3xDBEmut) co-expressed with either untagged FOXO3a wt protein or EGFP-tagged FOXO3a. Hence, we transiently transfected untagged FOXO3a and EGFP-FOXO3a into U2OS cells and measured the luciferase activities 4 hours after exposure to LY294002 or DMSO. The N-terminal EGFP tag did not significantly affect transcriptional function of FOXO3a in U2OS cells (Fig. 2) indicating the compatibility of luminescent and fluorescent read-outs in a single cell line. In addition, we compared the level of luciferase activity driven by the pGL-3xDBE construct in the context of stable EGFP-FOXO3a expression in U2foxRELOC cells (9) and with the transient co-expression of the fluorescent fusion protein. The luciferase expression in the presence of stable EGFP-FOXO3a expression was only slightly lower than that in U2OS cells transiently overexpressing EGFP-FOXO3a. To stably integrate the pGL-3xDBE construct into the genome of U2foxRELOC cells, we modified the pGL3-promoter construct by inserting a puromycin-resistance cassette to obtain pGLpuro-3xDBE. Puromycin-resistant stable clones were generated (U2transLUC) and one was chosen for further use based on FOXO-induced luciferase activity.

The use of GFP fusion protein for normalization

We examined whether the expression of the GFP fusion protein could be used to normalize the transcriptional reporter gene to the changes in cell viability. U2transLUC cells were seeded and allowed to attach to the wells overnight. Subsequently, they were incubated with increasing doses of sodium azide, a known inhibitor of the respiratory chain that provokes necrosis in many cell types (13, 14). Cell viability was estimated through a crystal violet assay or through the intensity of the fluorescence measured in each well. Both methods take advantage of the fact that when epithelial cells undergo apoptosis or necrosis, they detach from plates and are no longer detectable by these assays. After a 6 hour exposure to 0.05% sodium azide the viability of U2transLUC cells was slightly reduced with no significant differences between crystal violet or fluorescent intensity read-outs. Higher doses of sodium azide dramatically compromised U2transLUC viability, as reflected by both measures of viability. A normalization procedure using crystal violet staining or the GFP-FOXO mediated fluorescent signal resulted in similar indices of viability (Fig. 3), indicating that the fluorescent reporter protein can be used to monitor the viability of U2transLUC cells.

Multiplexed U2transLUC assay

The U2transLUC-based assay was formatted for 96-well plates and the workflow has been automated. To assess the specificity of the transcriptional and the translocational read-out, we challenged the U2transLUC system with small molecule inhibitors under living cell conditions in order to observe the translocation of the fluorescent reporter protein and luciferase activity as the transcriptional end point. We exposed U2transLUC cells to a panel of test compounds with known biological activity. Three different doses were used that resulted in a range of final concentrations greater than two orders of magnitude around the IC_{50} value for each individual compound. The live cells were stained with the fluorescent nuclear dye DRAQ5 and images were obtained on an automatic microscope. The nuclear/cytoplasmic (Nuc/Cyt) fluorescence intensity ratios were determined and the percentage of cells per well displaying nuclear translocation or the inhibition of nuclear export was calculated. Compounds that induced the nuclear accumulation of the fluorescent signal above 60% of that obtained from wells treated with LY294002 were considered as hits. Several compounds known to inhibit PI3K activity or the nuclear export machinery fulfilled these criteria (Fig 4A). As expected from the results of a previous study in U2foxRELOC cells (9, 15), the PI3K inhibitors PI-103 and LY294002 were capable of inducing FOXO translocation into the nucleus of U2transLUC cells. By contrast, known activators of the PI3K/Akt pathway produced little nuclear localization of GFP-FOXO, including EGF, IGF and PDGF. The exposure of U2transLUC cells to the nuclear export inhibitors leptomycin B or ratjadone A provoked the nuclear accumulation of fluorescent signal, as shown previously for U2foxRELOC cells (9, 15). Conversely, through the measurement of the FOXO-dependent production of firefly luciferase, leptomycin B and ratjadone A exerted no significant effect on the transcriptional activity of FOXO (Fig 4B). Finally, exposure to

PI-103 and LY294002 triggered a dramatic increase in FOXO-dependent luciferase activity. Together, these data show that the U2transLUC assay serves as an automated high throughput assay that can identify inhibitors of PI3K/Akt signaling through the high content analysis of protein translocation in conjunction with an independent analysis of the transcriptional activity of FOXO transcriptions factors.

Discussion and conclusion

FOXO transcription factors are tightly regulated at different levels, including their intracellular translocation and transcriptional activity (1, 3). Here we report the generation of a multiplexed assay system that is capable of simultaneously monitoring these signaling events. The assay system is based on U2transLUC cells that stably express two different reporter constructs. The intracellular translocation of FOXO factors is followed using a fluorescent tagged FOXO reporter protein, whereas transcriptional activity is monitored via FOXO-dependent luciferase production. We show here that the fluorescent and luminescent read-outs are compatible in the same cell.

The design of the U2transLUC screen presented here offers some major advantages over more classical cellular assays. Primary and secondary screens of small molecule compounds are usually performed in different cell systems. By contrast, the U2transLUC provides the possibility of using two different read-outs within the same experiment, enabling a direct comparison of the hits from each of these. These hits might be divided into translocation, transactivation and dual hits, and they may in turn be analyzed according to a corresponding hit ranking. The U2transLUC assay does not need the introduction of additional plasmids and hence, it avoids the limitations associated with transfection procedures.

The use of the GFP-FOXO fusion protein provides a multifunctional tool that allows for versatile assay read outs, measurement of cell viability/number and sorting and maintaining a homogeneous cell assay population. We show that the fluorescent signal from the GFP-FOXO fusion protein is suitable to monitor viability and it can be used to normalize the values obtained by measuring firefly luciferase activity. Furthermore, the fluorescent FOXO functions as a reporter protein for FOXO translocation and as an effector protein that drives DBE-dependent luiferase production. On the other hand the GFP-FOXO fusion protein offers the possibility to control the level of expression of the transcriptional effector in the luciferase assay, and at the same time it serves as a sorting tool to maintain a homogenous cell population. Thus, the multifunctional use of GFP-FOXO allows also to reduce the variability of the assay. The U2transLUC is an image based high throughput assay that enables compounds that produce artifacts and cytotoxicity to be identified on a single cell basis. Finally, the U2transLUC assay design might be adaptable to any transcription factor that undergoes nucleo-cytoplasmic shuttling. We challenged the U2transLUC system with chemical agents with known biological activity and were able to identify known PI3K inhibitors as double-hits that score in the translocation and the transactivation read-out. By contrast, chemical probes that inhibit the general nuclear export machinery failed to produce an increase in luciferase activity although GFP–FOXO was trapped in the cell nucleus.

In summary, our data demonstrate that U2transLUC is a sensitive and robust assay to identify small-molecule inhibitors of signaling events that regulate the subcellular localization and/or the transcriptional activity of FOXO proteins. The signaling events identified here include PI3K/Akt signaling and nuclear export. Our data raise the expectation that a more extensive chemical interrogation of the U2transLUC read-outs could lead to the identification of new molecular targets and small molecules that might contribute to the development of more potent therapeutic agents to treat tumors.

Methods

Compound supply and recombinant proteins

All chemicals were purchased from commercial sources except for the PI3K inhibitor PI-103, which was synthesized following published patent specifications. Cisplatin was provided by C. Navarro, Minerval was generously provided by P. Escriba, and all other chemicals were purchased from commercial sources: LY294002, Ratjadone A, were purchased from Calbiochem (San Diego, CA); Forskolin, Leptomycin B and Rapamycin, were purchased from LC Laboratories (Woburn, MA, U.S .A.); DMSO was purchased from Sigma-Aldrich (St. Louis, USA); Epidermal growth factor (EGF), platelet-derived growth factor (PDGF) were purchased from RELIATech A.S. (Braunschweig, Germany); and human Insulin-Like Growth Factor-I (IGF-I) and human insulin were purchased from (Roche Diagnostics, Mannheim, Germany). Stock solutions of the test compounds were deposited in three different concentrations in 96-well master plates, transferred to multiple replica plates and frozen at -80ºC.

Plasmids

The luciferase reporter constructs pGL-1xDBE, pGL-2xDBE, pGL-3xDBE, pGL-4xDBE, pGL-5xDBE and pGL-6xDBE were generated by inserting one to six copies of the DBE consensus sequence (12) in front of a SV40 minimal viral promoter of the pGL3-Promoter vector (Promega). The annealed and phosphorylated oligonucleotides 5´-CTAGAAGTAAACAA-3´ (1xDBE-forward) and 5´-GATCTT-GTTTAC-3´ (1xDBE-reverse) or 5´-CTAGAAGTAAACAACTATGTAAACAA-3´ (2xDBEforward) and 5′-GATCTTGTTTACATAGTTGTTTACTT-3′ (2xDBE-reverse) were ligated as single copy or concatemerized into NheI and BglII digested pGL3 promoter vector. In order to generate the negative control plasmid pGL-3xDBEmut, three copies of a DBE sequence that contains a point mutation that prevents FOXO binding (annealed and phosphorylated oligonucleotides (3xmDBE-forward) 5′-CTAGAAGTA-AGCAACTATGTAAG-CAACTATGTAAGCAA-3′ and (3xmDBE-reverse) 5′-GAT-CTTGCTTACATAGTTGCTTACATAGTTGCT-TACATAG-3′) were inserted into pGL3-Promoter vector. The constitutively active construct FOXO3a-A3, in which three PI3K-dependent phosphorylation sites have been mutated to alanine was kindly provided by Dr. M. Hu (University of Texas M. D. Anderson Cancer Center, Houston). In order to generate stable cell lines for the assay, we inserted a puromycin-resistance cassette into the pGL-3xDBE construct. This was achieved by PCR amplifying the puromycin resistance gene from pBABEpuro vector and cloning it into the SalI and BamHI sites of the pGL3-Promoter vector derived pGL-3xDBE construct, thereby obtaining pGLpuro-3xDBE.

Cell culture

U2-OS cells obtained from the ATCC were cultivated in Dulbecco's modified Eagle's medium (DMEM), supplemented with 10% fetal bovine serum (FBS, Sigma), antibiotics and antimycotics in a humidified incubator at 37°C with 5% CO_2. U2foxRELOC cells have been described previously (9).

Transfection and Luciferase assays

U2OS cells were cultured in a 96-well plate (100 µl final volume per well) and transfected at 70% confluence with the plasmids indicated using the effectene transfection reagent (Qiagen). LY294002 or insulin were added individually to wells 42 hours later, at a final concentration of 20 µM or 5mg/ml, respectively, and the cells were incubated for an additional 6 h. Luciferase assays were carried out using the Dual-Luciferase Reporter Assay System (Promega), according the manufacturer's instructions on a multilabel plate reader (Wallac Victor**,** Perkin-Elmer), and the ratio of *firefly*- to *Renilla*-luciferase activities was calculated. All values were presented as means ± SEM. The unpaired t-test (two-tailed) was performed for statistical analysis using the GraphPad PRISM® Version 4.0 program. Differences with a p value < 0.05 were considered statistically significant.

Generation and maintenance of U2transLUC cells

U2foxRELOC cells were transfected at 75% confluence with pGLpuro-3xDBE using the effectene transfection reagent (Qiagen). Cells were selected with puromycin (Calbiochem) for five days and the resistant colonies that best expressed the reporter constructs were then recovered and cultured, as was the most homogeneous population. Fluorescence-activated cell sorting (FACS) of GFP-FOXO expressing cells was performed on a FACSAria (BD Biosciences, San Jose, CA, USA). U2transLUC cell clones were maintained in DMEM, supplemented with 10% FBS (Sigma), antibiotics and antimycotics, 0.1 mg/ml Neomycin and 1 µg/ml puromycin. Cell cultures were maintained in a humidified incubator at 37°C with 5% CO_2, and they were passaged when confluent using trypsin/EDTA.

Crystal violet assay

Triplicate samples of 10^4 cells were seeded in 2.5 cm dishes and allowed to attach. After 24 hours, the medium was removed and replaced with culture medium with sodium azide at the concentrations indicated, while the controls remained untreated. After the appropriate time period the cells were fixed with 0.5% glutaraldehyde and stained with 1% crystal violet. After extensive washing, crystal violet was resolubilized in 10% acetic acid and quantified at 595 nm as a relative measure of cell number.

Viability assay measuring fluorescent intensity

Samples of 10^4 cells per well were allowed to attach overnight in 96-well Greiner plates and the following day the culture medium was replaced with fresh medium containing the concentrations of sodium azide indicated. After a three hour treatment, the cells were washed with PBS and the fluorescent intensity was measured in a multilabel plate reader (Wallac Victor 2**,** Perkin-Elmer) using UV light as the excitation source, as well as a F485 CW lamp Filter and a F535 CW emission filter for 0.5 seconds per well. The values are the averages obtained from experiments carried out in triplicate.

U2transLUC assay

U2transLUC cells were seeded at a density of 1.0×10^5 cells/ml in black-wall clear-bottom 96-well microplates (BD Biosciences) using a Titan Multidrop 384 automatic dispenser (Titertek Instruments, Inc., Huntsville, AL). The final volume of the cell suspension was 200 µl in each well. After incubation at 37°C in 5% CO_2 for 12 hours, 2µl of each test compound was transferred from the master plate to the assay plate. Cells were incubated in the presence of the compounds for 1 hour and the far-red fluorescent cell-permeable DNA probe, DRAQ5™ (Biostatus Ltd,Leicestershire, UK), was then added to all wells at a final concentration of 5 mM 15 minutes prior to obtaining the images. The images were acquired as described previously (16) using a BD Pathway™ 855 Bioimager equipped with a incubation chamber that provided a constant temperature of 37°C in 5% CO_2. Images were acquired in the GFP and DRAQ5 channels using 488/10 nm EGFP excitation filter, a 515LP nm EGFP emission filter and 635/20 nm/695/55 nm DRAQ5 excitation/emission filter with a 10x dry objective. The plates were exposed for 0.066 ms (Gain 31) to acquire DAPI images and 0.55 ms (Gain 30) for GFP images. Image and data analysis was performed as described previously (15). After image acquisition, the plates were incubated for another 5 hours at 37°C and then the average GFP intensity per well was measured as described above. Finally, U2transLUC cells were processed to measure the firefly luciferase activity using the Luciferase Assay System (Promega) on a multilabel plate reader (Wallac Victor, Perkin-Elmer) according to the manufacturer's instructions. The relative luciferase activity, as a measurement of FOXO3a's transcriptional activity was calculated dividing the value obtained for Firefly luciferase activity for each well by the the average GFP intensity from the same well.

Authors´ contributions

WL designed the research, interpreted the results and wrote the paper; AR and FZ performed the research; BG provided technical support. AC co-developed and co-refined the research. All authors read and approved the final manuscript.

Acknowledgments

This work was supported by a grant from the Spanish MCyT BIO2002-00197 and the Spanish MEC (project BIO2006-02432). F. Z. is recipient of a Marie Curie Fellowship. The authors acknowledge the supply of PI-103 synthesized by R. Álvarez at the Medicinal Chemistry Department (CNIO), the expert technical assistance of E. Gonzalez and F. Blanco, and the assistance of the staff at BD Biosciences for their contribution in establishing the technology.

References

1. **Van Der Heide LP, Hoekman MF Smidt MP (2004) *Biochem J* 380:297-309.**
2. **Huang H Tindall DJ (2007) *J Cell Sci* 120:2479-87.**
3. **Calnan DR Brunet A (2008) *Oncogene* 27:2276-88.**
4. **Paik JH, Kollipara R, Chu G, Ji H, Xiao Y, Ding Z, Miao L, Tothova Z, Horner JW, Carrasco DR, Jiang S, Gilliland DG, Chin L, Wong WH, Castrillon DH DePinho RA (2007) *Cell* 128:309-23.**
5. **Tsai WC, Bhattacharyya N, Han LY, Hanover JA Rechler MM (2003) *Endocrinology* 144:5615-22.**
6. **Nasrin N, Ogg S, Cahill CM, Biggs W, Nui S, Dore J, Calvo D, Shi Y, Ruvkun G Alexander-Bridges MC (2000) *Proc Natl Acad Sci U S A* 97:10412-7.**
7. **Zhang X, Gan L, Pan H, Guo S, He X, Olson ST, Mesecar A, Adam S Unterman TG (2002) *J Biol Chem* 277:45276-84.**
8. **Matsuzaki H, Daitoku H, Hatta M, Aoyama H, Yoshimochi K Fukamizu A (2005) *Proc Natl Acad Sci U S A* 102:11278-83.**
9. **Zanella F, Rosado A, Garcia B, Carnero A Link W (2008) *Chembiochem* 9:2229-37.**
10. **Kau TR, Schroeder F, Ramaswamy S, Wojciechowski CL, Zhao JJ, Roberts TM, Clardy J, Sellers WR Silver PA (2003) *Cancer Cell* 4:463-76.**
11. **Schroeder FC, Kau TR, Silver PA Clardy J (2005) *J Nat Prod* 68:574-6.**
12. **Furuyama T, Nakazawa T, Nakano I Mori N (2000) *Biochem J* 349:629-34.**
13. **Vaux DL, Whitney D Weissman IL (1996) *Microsc Res Tech* 34:259-66.**
14. **Lizard G, Fournel S, Genestier L, Dhedin N, Chaput C, Flacher M, Mutin M, Panaye G Revillard JP (1995) *Cytometry* 21:275-83.**
15. **Zanella F, Rosado A, Blanco F, Henderson BR, Carnero A Link W (2007) *Assay Drug Dev Technol* 5:333-41.**
16. **Rosado A, Zanella F, Garcia B, Carnero A Link W (2008) *PLoS ONE* 3:e1823.**

Figure Legends

Figure 1.

FOXO-driven transcriptional activity measured by Luciferase production from different reporter gene constructs

A. Schematic diagram of the luciferase reporter constructs used in this study. One to six copies of the DBE binding cassettes were cloned upstream of the luciferase reporter gene in the pGL3-Promoter vector to create the plasmids pGL-1xDBE, pGL-2xDBE, pGL-3xDBE, pGL-4xDBE, pGL-5xDBE and pGL-6xDBE. The empty pGL3-Promoter vector and a reporter plasmid that carries three copies of a mutated DBE (mDBE) region were used as control plasmids. B. Each construct was transiently co-transfected with plasmids encoding FOXO3a and Renilla luciferase into U2OS cells, and the luciferase activities were determined as described in the "Methods" section. The data were normalized to the Renilla luciferase (phRG-TK vector) reporter construct and expressed relative to the normalized activity of the pGL3-Promoter vector. The results are given as the mean ± SEM of three independent experiments performed in triplicate. C. Basal and induced FOXO-dependent transcriptional activity conferred by three or six copies of the DBE binding cassette (grey and black bars, respectively). The plasmids pGL-3xDBE or pGL-6xDBE were transiently co-transfected into U2OS cells with plasmids encoding wild type FOXO3a or the constitutively active FOXO3a-A3 and Renilla luciferase. Where indicated cells were treated with 20µM LY294002 or insulin for 6 hours.

Figure 2.

FOXO3a and GFP-FOXO trigger a similar induction of luciferase activities. pGL-3xDBE or pGL-3xDBEmut were transiently co-transfected with plasmids encoding FOXO3a or GFP-FOXO3a into U2OS cells. U2foxRELOC cells that stably express the

GFP-FOXO3a protein (9) were transiently transfected with pGL-3xDBE. LY294002 (20µM, hatched bars) or DMSO (black bars) were added to the transfected cells six hours before processing the cells to assay the luciferase assay. The values are the means ± SEM of relative luciferase activities from three independent experiments performed in triplicates.

Figure 3.

Viability of U2transLUC cells using crystal violet assay or by monitoring the GFP-intensity per well. U2transLUC cells were exposed to 0.05%, 0.10%, 0.25%, 0.50% or 1% sodium azide for three hours and processed as described in the “Methods” section. The values are the means (± SD) of GFP intensity per well or the absorbance at 595nm from three independent experiments.

Figure 4.

Validation of U2transLUC assay using a panel of test compounds. A. The nuclear accumulation of the GFP-FOXO reporter protein and FOXO driven luciferase activity induced by the test compounds. We exposed U2transLUC cells to three different concentrations of the test compounds. The results shown here are the values obtained from the treatment of U2transLUC cells with 4nM Ratjadone A, 20µM LY294002, 1ng/ml PDGF, 100µM Minerval, 1µM Forskolin, 4nM Leptomycin B, 30µM Cisplatin, 100nM PI-103, 0.5nM Rapamycin, 20ng/ml IGF, 5ng/ml EGF and Dimethyl sulfoxide (DMSO) as a negative control. The grey bar graphs and the corresponding left hand y-axis depict the values in relation to the control values normalized to the corresponding measure of viability values. The relative luciferase activity was calculated dividing the value obtained for Firefly luciferase activity for each well by the average GFP intensity from the same well. The right hand y-axis and the hatched bars indicate the percentage of cells in each well exhibiting nuclear/cytoplasmic (Nuc/Cyt) ratios of fluorescence intensity greater than 1.8 normalized to the percentage in DMSO-treated wells.

B. Representative images of treated cells using high throughput format of the U2transLUC system. Images of cells expressing GFP-FOXO and stained with DRAQ5 were obtained by automated microscopy 2 hour after drug exposure. The images correspond to U2transLUC cells exposed to 4nM Ratjadone A, 4nM Leptomycin B, 20µM LY294002, 100nM PI-103 and DMSO. The images are shown from the GFP and DRAQ5 channels, as well as the corresponding merged image in the case of the DMSO treated control cells.

Fig. 1

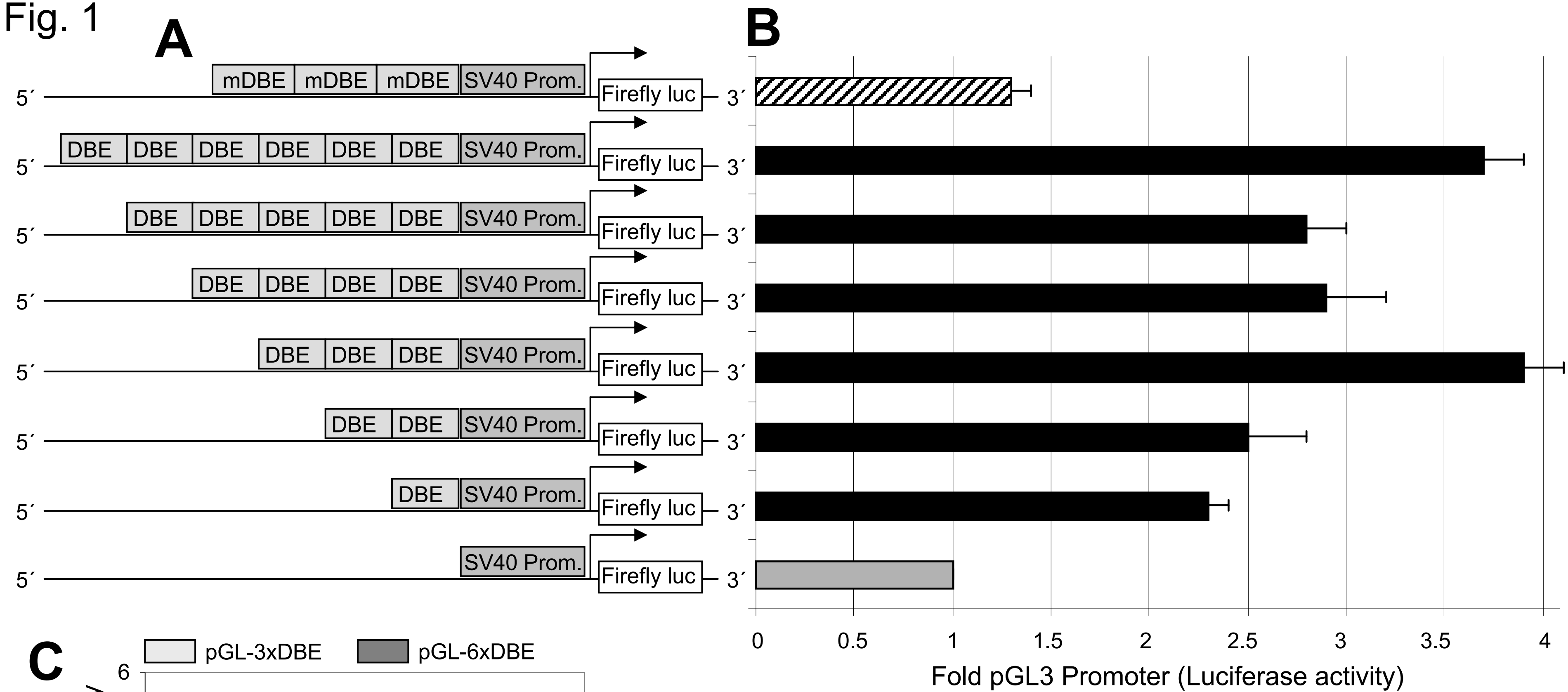

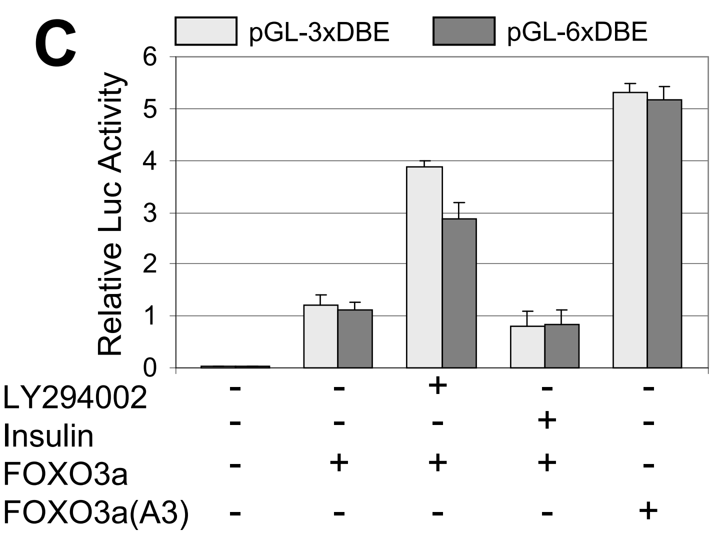

Figure 1. FOXO-driven transcriptional activity measured by Luciferase production from different reporter gene constructs.

A. Schematic diagram of the luciferase reporter constructs used in this study. One to six copies of the DBE binding cassettes were cloned upstream of the luciferase reporter gene in the pGL3-Promoter vector to create the plasmids pGL-1xDBE, pGL-2xDBE, pGL-3xDBE, pGL-4xDBE, pGL-5xDBE and pGL-6xDBE. The empty pGL3-Promoter vector and a reporter plasmid that carries three copies of a mutated DBE (mDBE) region were used as control plasmids. **B**. Each construct was transiently co-transfected with plasmids encoding FOXO3a and Renilla luciferase into U2OS cells, and the luciferase activities were determined as described in the “Methods” section. The data were normalized to the Renilla luciferase (phRG-TK vector) reporter construct and expressed relative to the normalized activity of the pGL3-Promoter vector. The results are given as the mean ± SEM of three independent experiments performed in triplicate. **C**. Basal and induced FOXO-dependent transcriptional activity conferred by three or six copies of the DBE binding cassette (grey and black bars, respectively). The plasmids pGL-3xDBE or pGL-6xDBE were transiently co-transfected into U2OS cells with plasmids encoding wild type FOXO3a or the constitutively active FOXO3a-A3 and Renilla luciferase. Where indicated cells were treated with 20µM LY294002 or insulin for 6 hours.

Fig. 2

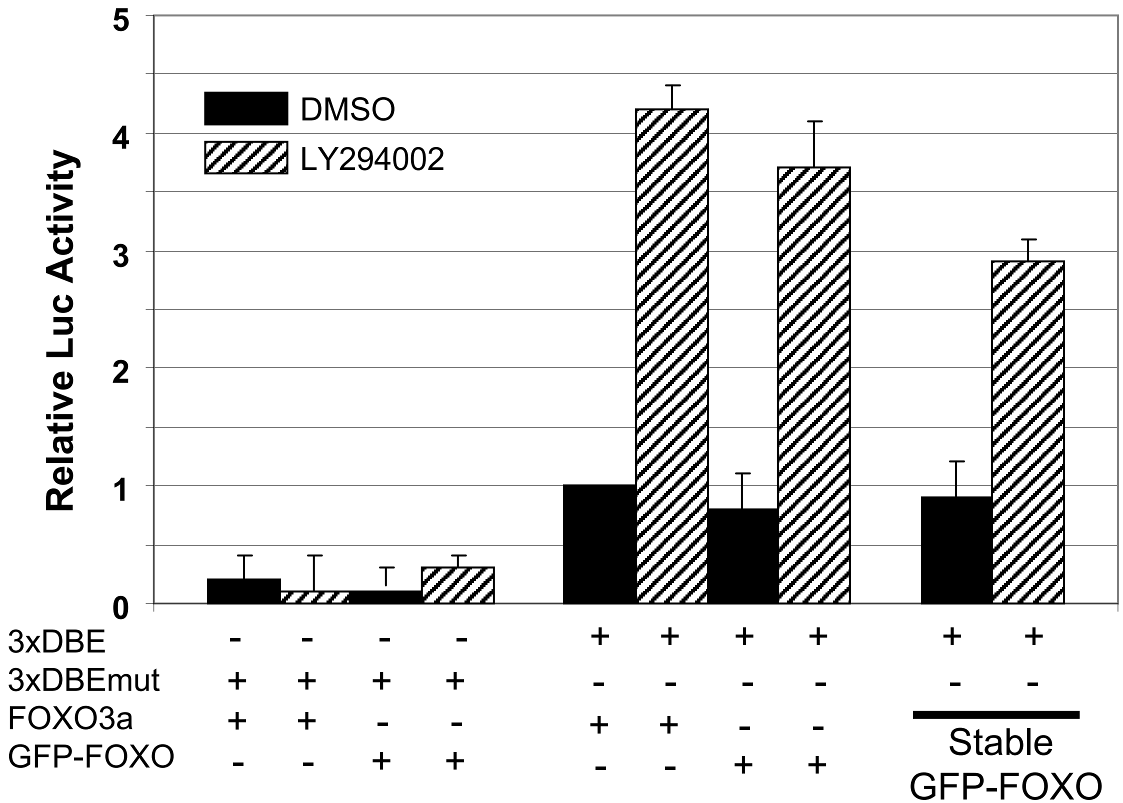

Figure 2. FOXO3a and GFP-FOXO trigger a similar induction of luciferase activities.
pGL-3xDBE or pGL-3xDBEmut were transiently co-transfected with plasmids encoding FOXO3a or GFP-FOXO3a into U2OS cells. U2foxRELOC cells that stably express the GFP-FOXO3a protein (9) were transiently transfected with pGL-3xDBE. LY294002 (20µM, hatched bars) or DMSO (black bars) were added to the transfected cells six *hours before processing the cells* to assay the luciferase assay. The values are the means ± SEM of relative luciferase activities from three independent experiments performed in *triplicates.*

Fig. 3

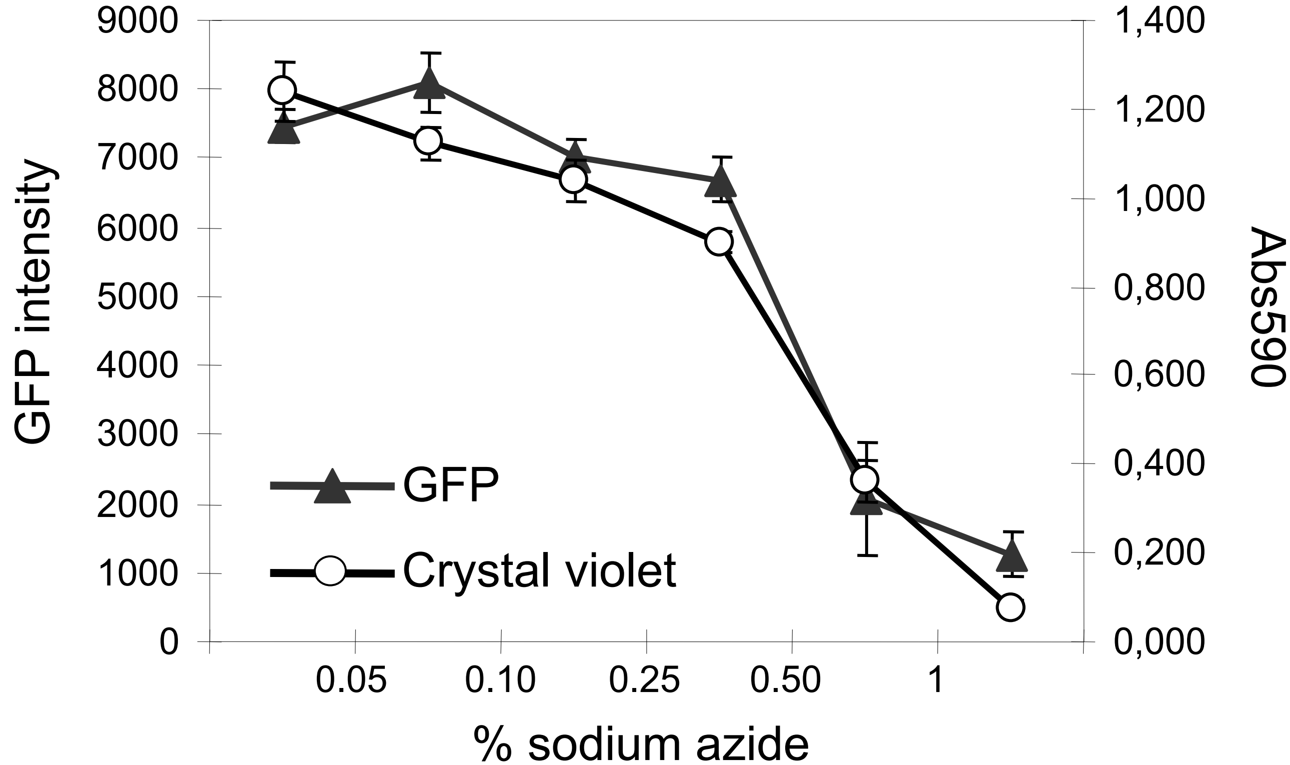

Figure 3. ***Viability of U2transLUC cells using* crystal violet assay or by monitoring the *GFP-intensity per well.*** *U2transLUC cells were exposed to 0.05%, 0.10%, 0.25%, 0.50% or 1%* sodium azide for three hours and processed as described in the "Methods" section. The values are the means (± SD) of GFP intensity per well or the absorbance at 595nm from three independent experiments.

A

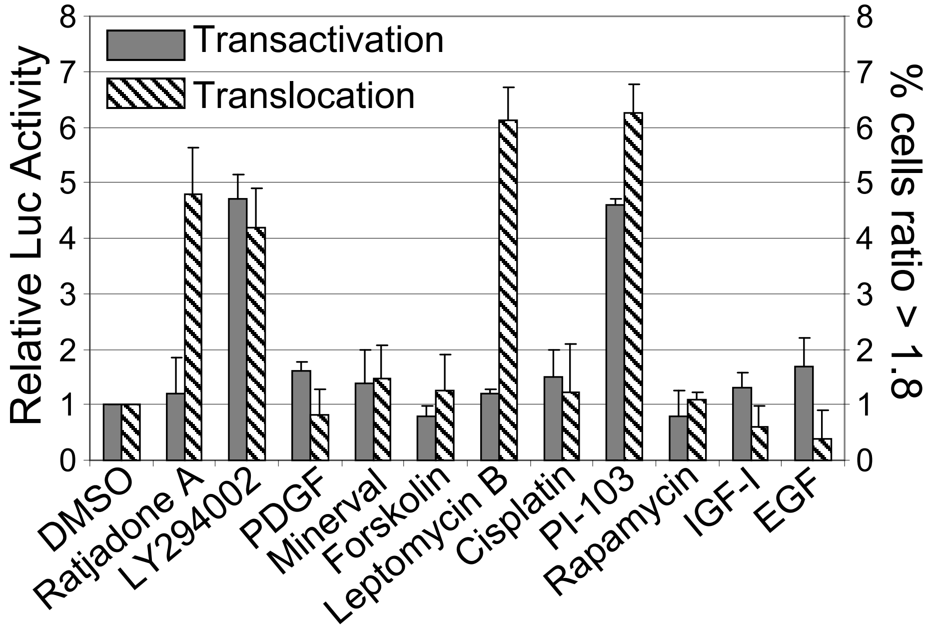

Figure 4. Validation of U2transLUC assay using a panel of test compounds.
A. The nuclear accumulation of the GFP-FOXO reporter protein and FOXO driven luciferase activity induced by the test compounds. We exposed U2transLUC cells to three different concentrations of the test compounds. The results shown here are the values obtained from the treatment of U2transLUC cells with 4nM Ratjadone A, 20µM LY294002, 1ng/ml PDGF, 100µM Minerval, 1µM Forskolin, 4nM Leptomycin B, 30µM Cisplatin, 100nM PI-103, 0.5nM Rapamycin, 20ng/ml IGF, 5ng/ml EGF and Dimethyl sulfoxide (DMSO) as a negative control. The grey bar graphs and the corresponding left hand y-axis depict the values in relation to the control values normalized to the corresponding measure of viability values. The relative luciferase activity was calculated dividing the value obtained for Firefly luciferase activity for each well by the average GFP intensity from the same well. The right hand y-axis and the hatched bars indicate the percentage of cells in each well exhibiting nuclear/cytoplasmic (Nuc/Cyt) ratios of fluorescence intensity greater than 1.8 normalized to the percentage in DMSO-treated wells.

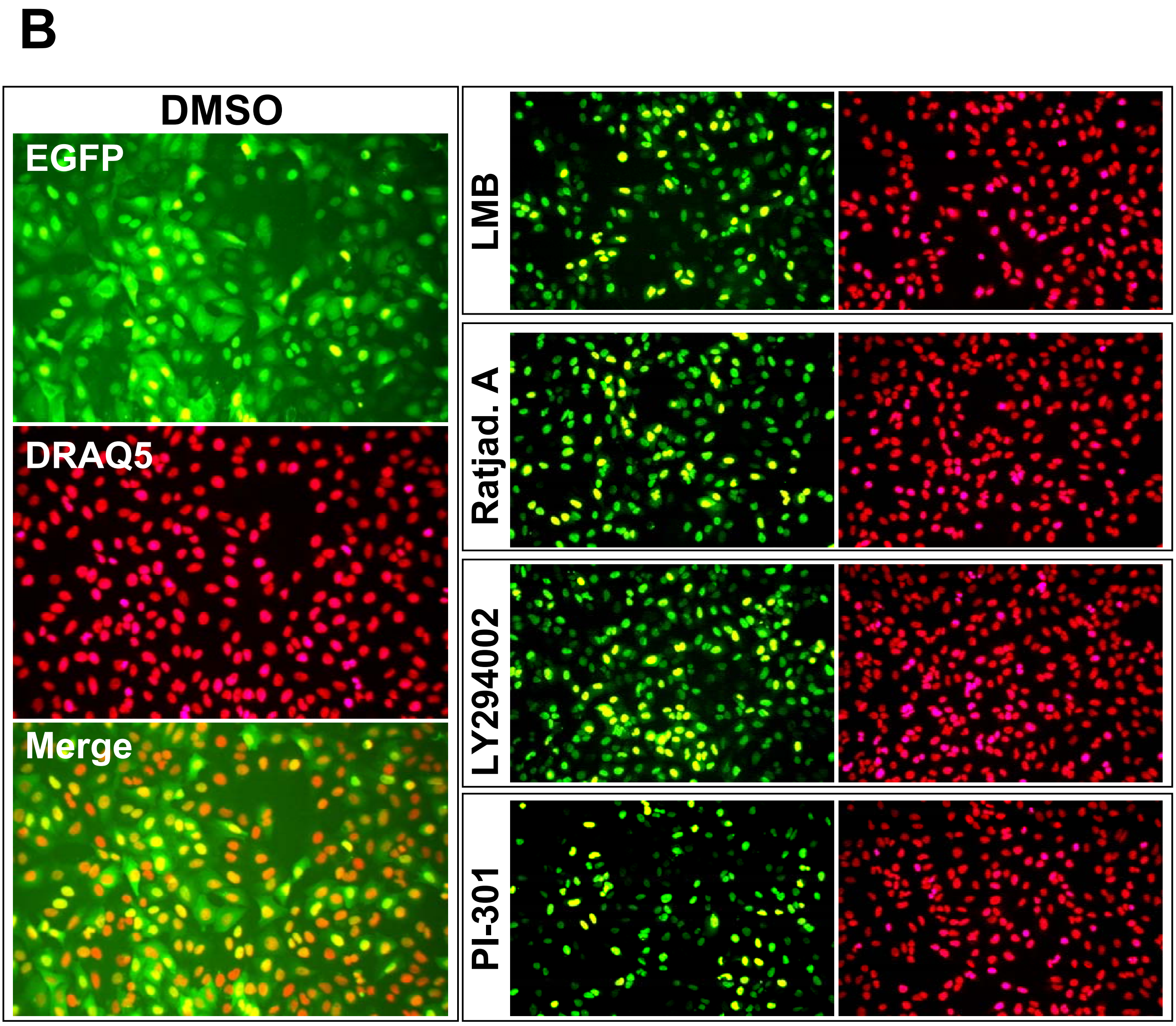

Figure 4. Validation of U2transLUC assay using a panel of test compounds.
B. Representative images of treated cells using high throughput format of the U2transLUC system. Images of cells expressing GFP-FOXO and stained with DRAQ5 were obtained by automated microscopy 2 hour after drug exposure. The images correspond to U2transLUC cells exposed to 4nM Ratjadone A, 4nM Leptomycin B, 20μM LY294002, 100nM PI-103 and DMSO. The images are shown from the GFP and DRAQ5 channels, as well as the corresponding merged image in the case of the DMSO treated control cells.

3.1.3 Third Project: The BaFiso system

Summary

The activation of the PI3K/Akt is an essential feature of virtually all types of cancer and constitutes the primary mechanism by which FOXO is inactivated in human cancers. Therefore, it is important to identify compounds or RNAi that will specifically target this pathway, as inhibition of this pathway induces FOXO activation. In order to determine if the activation of FOXO promoted by a given a stimuli occurs via the inhibition of the Akt we generated a live-cells assay based on Ba/F3 cells that depend on the cytokine IL-3 for their survival and growth. Taking advantage of that specific feature, genetic modifications were carried out in the parental cells in order to express different fluorescent reporters according to the signaling pathway they will rely on for survival. This system has shown to accurately distinguish Akt dependent survival upon treatment with compounds previously described to interfere with this pathway from other interferences. Therefore, this system can be used as a primary screening system for the discovery of new anti- Akt therapies or targets as well as a deconvolution system for FOXO activators.

Personal contribution

The generation of the cell lines described in this work as well as the execution of the experiments required for the adaptation of the system to the high throughput format were done by me in close collaboration with Aránzazu Rosado. We both and analyzed the effects obtained with the panel of compounds used for the publication.

Publication:

Rosado A*, Zanella F*, García B, Carnero A and Link W, **A dual-color fluorescence-based platform to identify selective inhibitors of Akt signaling.** PLoS ONE. 2008; 3(3): e1823. *Both authors contributed equally to this work

A Dual-Color Fluorescence-Based Platform to Identify Selective Inhibitors of Akt Signaling

Aranzazú Rosado[9¤], Fabian Zanella[9], Beatriz Garcia, Amancio Carnero, Wolfgang Link*

Experimental Therapeutics Program, Centro Nacional de Investigaciones Oncologicas (CNIO), Madrid, Spain

Abstract

Background: Inhibition of Akt signaling is considered one of the most promising therapeutic strategies for many cancers. However, rational target-orientated approaches to cell based drug screens for anti-cancer agents have historically been compromised by the notorious absence of suitable control cells.

Methodology/Principal Findings: In order to address this fundamental problem, we have developed BaFiso, a live-cell screening platform to identify specific inhibitors of this pathway. BaFiso relies on the co-culture of isogenic cell lines that have been engineered to sustain interleukin-3 independent survival of the parental Ba/F3 cells, and that are individually tagged with different fluorescent proteins. Whilst in the first of these two lines cell survival in the absence of IL-3 is dependent on the expression of activated Akt, the cells expressing constitutively-activated Stat5 signaling display IL-3 independent growth and survival in an Akt-independent manner. Small molecules can then be screened in these lines to identify inhibitors that rescue IL-3 dependence.

Conclusions/Significance: BaFiso measures differential cell survival using multiparametric live cell imaging and permits selective inhibitors of Akt signaling to be identified. BaFiso is a platform technology suitable for the identification of small molecule inhibitors of IL-3 mediated survival signaling.

Citation: Rosado A, Zanella F, Garcia B, Carnero A, Link W (2008) A Dual-Color Fluorescence-Based Platform to Identify Selective Inhibitors of Akt Signaling. PLoS ONE 3(3): e1823. doi:10.1371/journal.pone.0001823

Editor: Mark R. Cookson, National Institutes of Health, United States of America

Received November 20, 2007; **Accepted** February 4, 2008; **Published** March 19, 2008

Funding: This work was supported by a grant from the Spanish MCyT (BIO2002-00197) and the Spanish MEC (project BIO2006-02432). F.Z. is the recipient of a Marie Curie Fellowship.

Competing Interests: The authors have declared that no competing interests exist.

* E-mail: wlink@cnio.es

¤ Current address: Nederlands Kanker Instituut - Antoni van Leeuwenhoek Ziekenhuis (NKI-AVL), Amsterdam, The Netherlands

9 These authors contributed equally to this work.

Introduction

Cell-based screens have been widely used in drug discovery although historically, these assays are conducted using genetically diverse cell lines derived from human tumors [1,2]. Since the complex intracellular signaling networks that drive cancer cell growth and survival have begun to be elucidated, a more rational approach to drug discovery has become feasible [3]. However, the implementation of target-orientated cell-based screens for anti-cancer drugs remains a challenge, both because of their reliance on defined genetic changes and because of the lack of proper control cells. To overcome this fundamental problem, we have developed a rational strategy for cell-based drug discovery that is based on the convenience and flexibility of the Ba/F3 cell system, an immortalized IL-3-dependent pro-B lymphoblastic cell line [4]. IL-3 supports the growth and survival of Ba/F3 cells through the activation of distinct signaling pathways. Upon binding to its cognate receptor IL-3 activates the Janus kinase signal transduction and transcriptional activation pathways (JAK/STAT) to induce Bcl-x_L [5]. Similarly, IL-3 activation of the PI3K/Akt pathway is involved in inhibiting the intrinsic apoptotic machinery in Ba/F3 cells [6–8].

Overexpression of several constitutively active signaling molecules abrogates the dependence of these cells on IL-3 [9]. Hence, we generated isogenic cell lines derived from Ba/F3 (BaFiso) in which IL-3 independent survival is sustained by independent signaling events. Each of these isogenic lines was genetically labeled with a fluorescent reporter and thus, the ratio of two spectrally distinct cell populations could be used as primary endpoint of the system to monitor pathway-specific cytotoxicity. Accordingly compounds can be screened in co-cultures of these lines and the change in the relative cell number of the two lines readily and rapidly measured to identify those molecules that specifically interact with one of the signaling pathways. In this instance, BaFiso has been designed as a live-cell system suitable to identify specific inhibitors of Akt signaling.

Results

Tagging isogenic Ba/F3 cells individually with two different chromophores

The BaFiso system is a dual fluorescence cell-based screening system in which compounds can be readily monitored thanks to the stable expression of yellow or cyan fluorescent proteins that individually tag each of the isogenic cell lines (Fig. 1). To introduce the genes encoding the different fluorescent proteins into Ba/F3 cells, retroviral supernatants were generated by transfection of

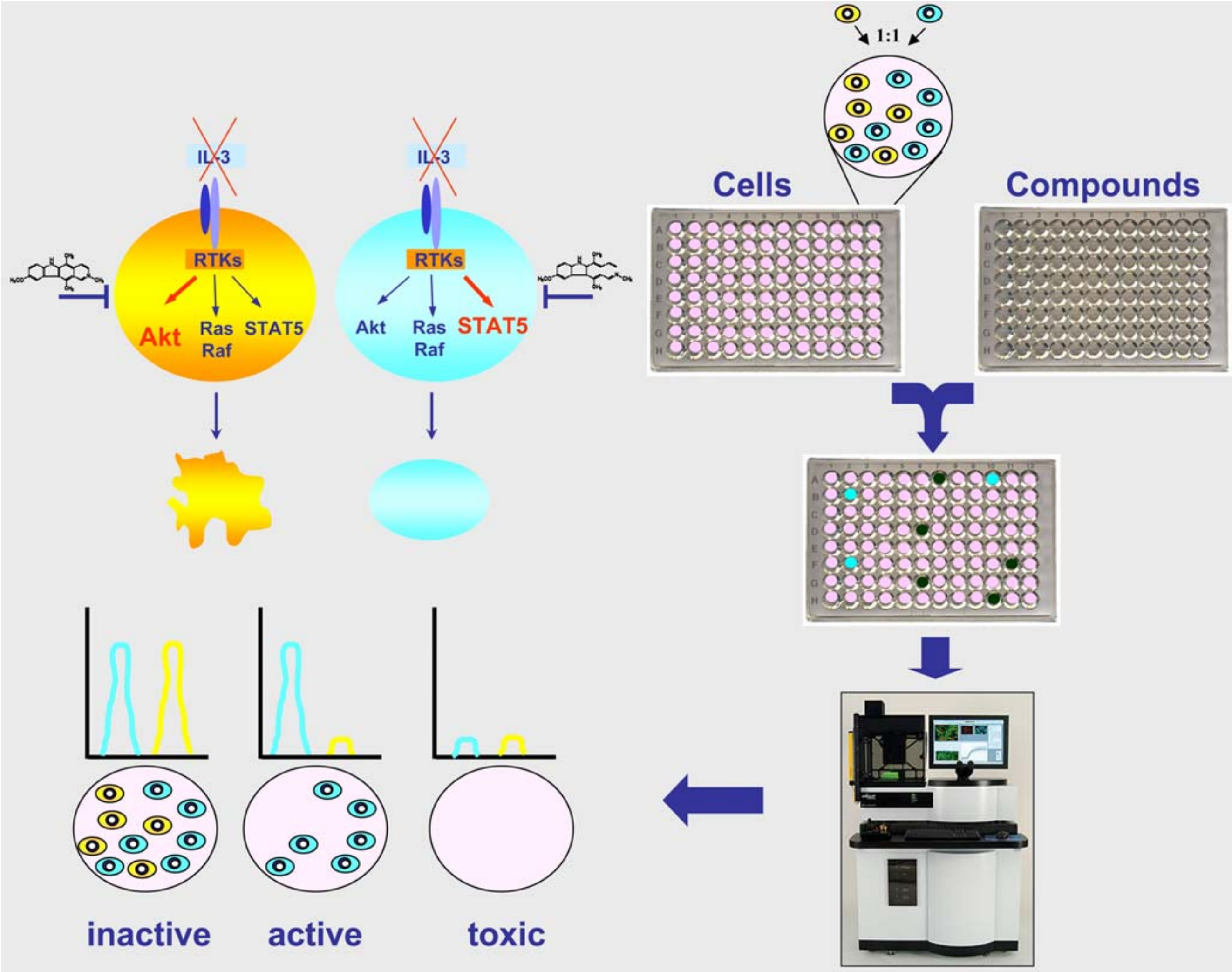

Figure 1. Schematic overview of the BaFiso assay system. BaFiso consists of paired isogenic cell lines that have been engineered to acquire IL-3 autonomous growth through constitutive activation of Akt or Stat5 signaling. The two cell lines to be compared are individually tagged with either yellow or cyan fluorescent proteins. Equal numbers of yellow and cyan cells were co-cultured, treated with compounds and the change in the relative cell number was calculated on the basis of the distinct fluorescent proteins measured. Our strategy aims to identify lead compounds that specifically kill test cells with activated Akt signaling (yellow cells) and that spare the otherwise isogenic control cells (cyan cells).
doi:10.1371/journal.pone.0001823.g001

LinX packaging cells. Through clonal propagation, we were able to establish Ba/F3 cell lines that robustly and homogeneously expressed ECFP (Fig. 2A and B) or EYFP (Fig. 2C and D). Stable transfectants of these proteins were FACS-sorted to ensure that they expressed similar levels of the fluorescent reporter protein.

Generation of double stable Ba/F3 cell lines

The strategy described here is based on paired isogenic cell lines whose survival in the absence of IL-3 is sustained by the activation of independent signaling pathways. Several signaling pathways have been implicated in IL-3-mediated survival, including those involving Akt and Stat5 [10,11]. In order to introduce constitutively active forms of these genes into our dual fluorescence cell-based system, we used retroviral constructs carrying a myristoylated derivate of Akt and STAT5A1*6, which contains two activating amino acid substitutions [11]. The yellow labeled Ba/F3 cells were used to generate Akt-dependent reporter cells whereas the cyan tagged cells were used to establish PI3K/Akt independent reporter cells. The retroviral supernatants of LinX packaging cells were employed to transduce Ba/F3/EYFP cells (BY) with myr-Akt and Ba/F3/ECFP cells (BC) with STAT5A1*6 (Fig. 2E). Stably expressing cell clones were selected and the expression of the transgenes was confirmed by western blot analysis (Fig. 2F). The level of Akt expression was monitored using an antibody that recognizes Akt irrespective of its phosphorylation state. Akt migrates as a single band with an apparent molecular weight of 60 kDa, although a larger protein was also identified in immunoblots of Akt from lysates of BYA cells. This additional form can be explained by the difference in size produced by the myristoylation signal present in the constitutive active form of Akt used to generate the BYA cell line. Despite the Stat5a protein present in the parental BC cells, ectopic expression of the constitutively active form of Stat5a in BCS cells could be unequivocally demonstrated in western blots probed with an antibody directed against the Flag-tag. Indeed, STAT5A1*6 expression also increased the total Stat5a protein level in BCS cells as shown by immunoblotting using an antibody recognizing Stat5.

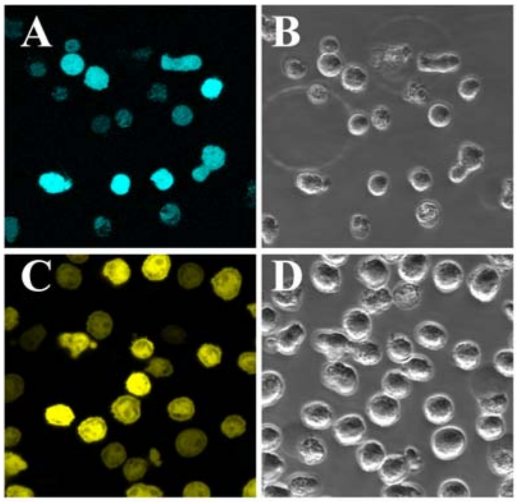

E

Cell line	Parental cells	Activated gene
BY	BAF3/YFP	none
BYA	BAF3/YFP	Akt
BC	BAF3/CFP	none
BCA	BAF3/CFP	Stat5a

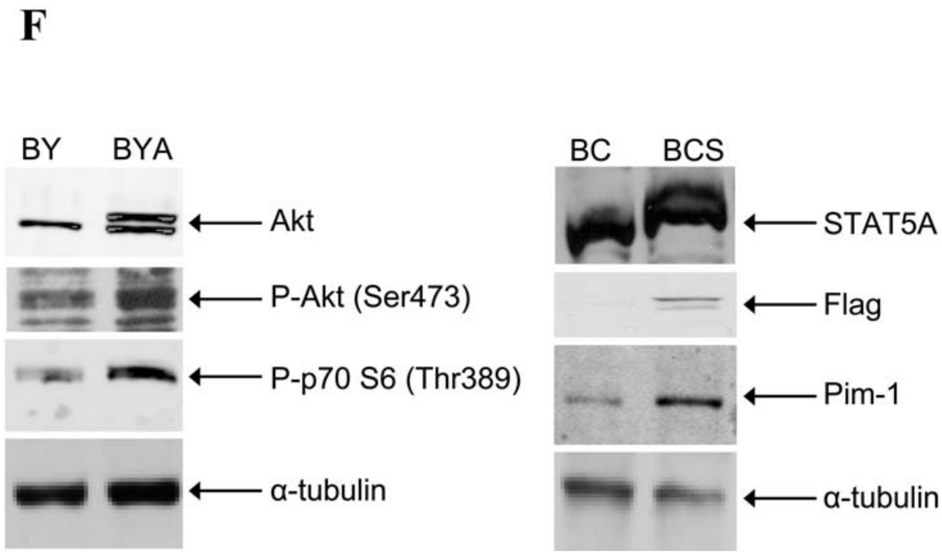

Figure 2. The generation of BaFiso cell lines. Ba/F3 cells were transduced with retroviral supernatant carrying pBabePuro-EYFP or pBabePuro-ECFP. Cell clones were established and sorted in a fluorescence activated cell sorter (FACS) to generate lines homogeneously expressing the corresponding fluorescent tags. (**A**) and (**C**), viable Ba/F3 cells show robust and homogeneous expression of the respective fluorescent protein. (**B**) and (**D**), corresponding light field views. (**E**), Generation of stable BaFiso cell lines. Clonal Ba/F3 cells stably expressing EYFP (BY) or ECFP (BC) were used to generate stable BaFiso cell lines that co-express yellow fluorescence and myr-Akt (BYA), or cyan fluorescence and STAT5A1*6 (BCS). Cell clones were established and analyzed. (**F**), Analysis of transgene expression and downstream activation of the corresponding signaling pathways by western blotting. Antibodies against total Akt, Stat5a, Flag phospho-Akt (Ser473), phospho-p70 S6 (Thr389) and Pim-1 were used and the signals normalized to the respective α-tubulin levels.
doi:10.1371/journal.pone.0001823.g002

To examine whether PI3K/Akt or Stat5 signaling is indeed activated in the stable BYA or BCS cells respectively, we analyzed downstream elements in these two pathways. Phosphorylation of Akt (Ser473) has been widely used as a read out of activation of the PI3K pathway. When we compared the level of Akt phosphorylation in lysates of BY and BYA cells cultured in the presence of IL-3, there was dramatic increase in Ser473 phosphorylation of Akt in BYA cells, reflecting the activity of this pathway. To investigate whether the activation of Akt in BYA cells had an impact on downstream events, we analyzed the Thr389 phosphorylation of the linker domain of the p70 S6 kinase that is constitutively activated upon overexpression of a gag fusion of Akt [12]. There was a significant increase in the intensity of the band corresponding to p70 S6 kinase (Thr389) in BYA cells when compared to BY control cells. On the other hand, the expression of the known STAT5 target gene, pim-1, was upregulated upon expression of constitutive activated Stat5a, consistent with previous studies [13].

Ectopic expression of activated Akt and Stat5a confers IL-3 independence

Consistent with previous reports, expression of constitutively active mutants of Akt and Stat5a provide signals for cytokine-independent survival of Ba/F3 cells [9,11]. The increased resistance to IL-3 withdrawal of the BYA and BCS cell lines when compared to the parental BY and BC cell lines was

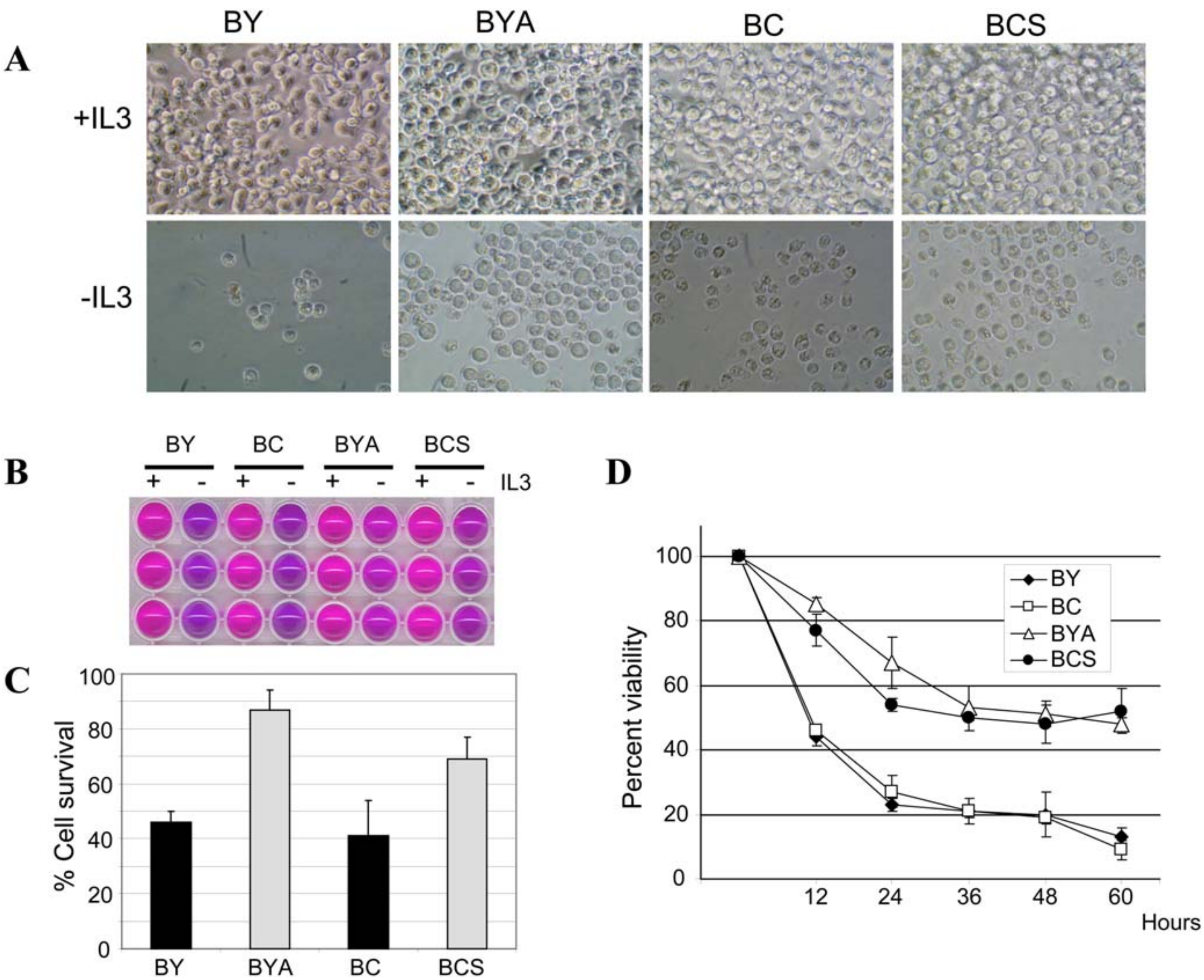

Figure 3. The viability of BaFiso cell lines in the absence of IL-3. (**A**) Parental Ba/F3 derived BY and BC cells, and the BaFiso cell lines BYA and BCS were maintained in the presence or absence of IL-3 (+IL3 and −IL3). Photos were taken 24 h after transferring the cells to medium without IL-3 or in the presence of 3 ng/ml of the recombinant cytokine. (**B**) Measurement of cell viability using the Alamar blue assay. Alamar blue fluoresces and changes color in response to chemical reduction, and the extent of the conversion is a reflection of cell viability. Metabolic conversion of Alamar blue to its reduced, pink derivative upon cytokine-deprivation (−IL-3) or in its presence (+IL-3). (**C**), Bar graph showing the results of Alamar Blue cell viability assay. Maximal absorbance of the reduced and oxidized forms of AlamarBlue^{TM}, 570 and 600 nm was measured using Victor 1420 multilabel counter 24 h after IL-3 withdrawal. The percentage of cell survival was calculated compared with control cells in the presence of 3 ng/ml of IL3. The data represents three independent experiments performed in triplicate samples. (**D**) Time course of cell viability upon IL-3 withdrawal. Cells were washed twice in PBS and seeded in media lacking IL-3. Viability was assessed at 12 hour intervals by trypan blue exclusions followed by cell countings. Black rhombs and open squares represent percentage viability of BY and BC cells, respectively. Open triangles and black circles represent percentage viability of BYA and BCS cells, respectively. Data are presented as mean±SD from three independent experiments.
doi:10.1371/journal.pone.0001823.g003

confirmed by morphological assessment. Parental BY and BC cells were cultured in the presence or absence of IL-3 and the degree of cell death was assessed after 24 hours by microscopic examination (Fig. 3A). The number of cells with an apoptotic phenotype increased significantly after IL-3 withdrawal in the cultures. The effect of the constitutive activation of Akt or Stat5 signaling was examined when IL-3 was withdrawn from representative BYA and BCS cell clones. As such, the capacity of the constitutively active forms of the signaling molecules Akt and Stat5a to impede apoptosis was evident and accordingly, cell death was dramatically reduced in Ba/F3 cells ectopically expressing myr-Akt or STAT5A1*6, even in the absence of IL-3 (Fig. 3A). We also determined the metabolic activity as a measure of cell viability using the alamar blue assay, in which a redox indicator changes color from blue to pink depending on metabolic status of the cells (Fig. 3B). The activity of myr-Akt in BYA cells was significantly higher in the absence of IL-3 than that of the parental cells. Similarly, STAT5A1*6 also maintained the activity of BCS cells albeit to slightly lesser degree (Fig. 3C). We examined the time course of cell viability following IL-3 withdrawal (Fig. 3D) and 24 hours after IL-3 deprivation, approximately 60% of the BYA or BCS cells remained viable compared to approximately 25% of the parental BY and BC cell lines. The viability of BY and BC cells further diminished after 60 hours of IL-3 starvation to 13% and 9%, respectively. In contrast, the viability of BYA and BCS cells remained around 50% after 60 hours in the absence of IL-3.

The protection from IL-3 withdrawal afforded by enhanced Stat5 signaling is independent of Akt activity

The capacity to monitor pathway-specific cytotoxicity in our assay is based on the use of isogenic control cells that confer survival in the absence of IL-3 in an Akt-independent manner. Since Akt is one of the major downstream targets of PI3K signaling, its phosphorylation status is commonly used to monitor the activity of the PI3K/Akt pathway. We analyzed the impact of ectopic expression of myr-Akt and STAT5A1*6 on Akt activation using an antibody that specifically recognizes Ser473 phosphorylated Akt (Fig. 4). The intensity of Akt phosphorylation was compared to the overall expression of Akt and α-tubulin using specific antibodies. Parental BY and BC cells possess relatively low basal levels of Akt phosphorylation which further decreased upon withdrawal of IL-3. Ectopic constitutively active Stat5a expression had no significant impact on the phosphorylation of Akt in the presence or absence of IL-3, indicating that the enhanced survival of BCS cells triggered by STAT5A1*6 upon IL-3 starvation is independent of Akt signaling. Consistent with previous studies, overexpression of myr-Akt dramatically augmented Ser473 phosphorylation [14] and high levels of Akt phosphorylation were still detected in the complete absence of IL-3 (Fig. 4).

In conclusion, these results show that we have generated stable Ba/F3-derived cell lines in which the inhibition of the intrinsic apoptotic machinery is mediated by ectopic expression of constitutively active mutants of Akt or Stat5a. Since the abrogation of IL-3 dependence occurred through the activation of independent signaling pathways, these cell lines can be used together as paired isogenic test and control cells to identify pathway specific inhibitors.

Detection of selective toxicity associated with activated Akt signaling

The BaFiso assay was set up in 96-well plates and with an automated workflow [15]. Equal numbers of BYA and BCS cells were mixed and seeded at a density of 20,000 cells per well using multidrop dispenser. All liquid handling for treatment and staining was carried out by a robotic workstation and the BD Pathway 855 cell imaging platform was used for automated image acquisition. In order to test the sensitivity and the capacity to detect EYFP and ECFP separately using BD Pathway 855 bioimager, the co-cultured cells were photographed for the two fluorochromes sequentially and the images superimposed. In order to avoid ECFP bleeding into the EYFP emission channel, a special filter set was used that clearly separates the two fluorochromes. A third fluorochrome, the far red/infrared fluorescent cell-permeant DNA probe, DRAQ5, was employed to perform automated segmentation of cell nuclei. An image algorithm was applied to segment the cell nucleus based on local thresholds. The ratios of the cyan and yellow fluorescence signals were determined by dividing the number of ECFP positive cells by the number of EYFP positive cells in each well.

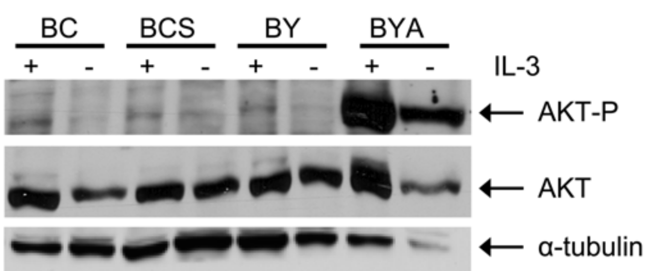

Figure 4. The analysis of Akt phosphorylation in BaFiso cell lines. Immunoblot analysis of total lysates from the Ba/F3 derived cell lines BY, BC, BYA and BCS. Cells were seeded, grown to 80% confluence and starved for 12 h in IL-3 free medium (−IL-3) or maintained in medium containing 3 ng/ml of the recombinant cytokine (+IL-3). Relevant proteins are indicated by arrows in the blot from a representative experiment.
doi:10.1371/journal.pone.0001823.g004

As a proof of principle, we sought to determine how a panel of commercially available agents of known mechanism of action would behave in the BaFiso screen. The test compounds included: the DNA-damaging chemotherapeutic compound cisplatin; the modulator of membrane lipid structure Minerval; the Akt inhibitor 10-(4′-(N-diethylamino)butyl)-2-chlorophenoxazine (Akt Inhibitor X); the protein tyrosine kinase inhibitor Genistein; the inhibitor of nuclear export Leptomycin B; the broad protein kinase inhibitor Staurosporine; the PDK1 inhibitor UCN-01; the Raf1 Kinase Inhibitor; the PI3K inhibitor LY294002; the topoisomerase II inhibitor Etoposide; and Lithium chloride, a GSK-3 inhibitor.

A robotic workstation was used to prepare mother plates containing three different concentrations of these compounds. Co-cultured BaFiso BYA/BCS cells were exposed to equal volumes of the test compounds, resulting in a final concentration range greater than two orders of magnitude around the IC_{50} value for each compound. The final concentration of dimethyl sulfoxide was kept at 1% after addition of the compounds. Each plate contained several internal controls, including untreated wells and wells treated with different concentrations of DMSO or ethanol alone. The performance of the BaFiso system upon exposure to the panel of test compounds was measured in terms of the ECFP/EYFP ratio. The majority of the test compounds reduced the number of DRAQ5 positive cells (Fig. 5A) without affecting the ratio of cyan and yellow fluorescent signals (Fig. 5B), suggesting a non-selective cytotoxic effect on both BaFiso cell lines independent of the gene that has been engineered to sustain interleukin-3 independent survival of the cells. In contrast exposure to Minerval or LiCl did not affect the viability of the BaFiso cell lines (Fig. 5A) nor did it alter the ratio of the fluorescent signals (Fig. 5B). Most importantly, two compounds that are known to inhibit the kinase activity of Akt, UCN-01 and Akt Inhibitor X, [16,17] selectively compromised the viability of the yellow tagged BYA cells thereby increasing the ratio of cyan to yellow fluorescent cells (Fig. 5B, C and D). In contrast, the broad spectrum PI3K isoform inhibitor LY294002 failed to affect the proportion of the fluorescent signals, indicating that the myristoylated form of Akt bypasses the requirement of PIP3-mediated membrane recruitment for its activity. Taken together, these data demonstrate that we have developed an image-based screening system that is capable of identifying specific inhibitors of the Akt pathway.

Discussion

The most frequently used anti-cancer therapies were discovered on the basis of their anti-proliferative activity in functional cell assays but with no pre-existing knowledge of the mechanism of action. As a result none of the current drugs directly targets the molecular lesions responsible for malignant transformation and they are not selective. Indeed this lack of selectivity between cancer cells and normal cells is currently one of the main reasons for the failure of conventional chemotherapy. In recent years, our understanding of the genetics of human cancer has increased rapidly, enabling more rational approaches to drug discovery for anti-cancer therapies to be adopted. Accordingly, the present study set out to develop a rational cell-based drug discovery strategy, an approach that has historically been compromised by the lack of appropriate control cells [18].

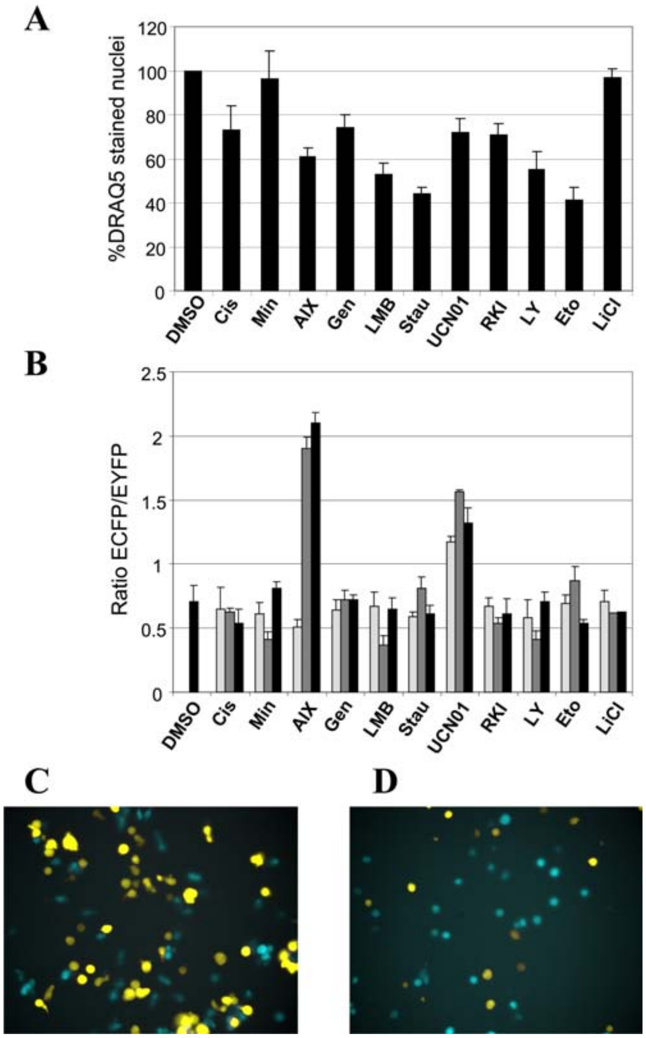

Figure 5. Validation of BaFiso assay using a panel of test compounds. (**A**) Analysis of the general toxicity of compound treatment. The total cell numbers in each well were determined by nuclear counterstain with the far-red fluorescent DNA probe DRAQ5. The number of DRAQ5-stained nuclei was determined after exposure to 30 μM Cisplatin (Cis), 100 μM Minerval (Min), 500 nM Akt Inhibitor X (AIX), 20 μM Genistein (Gen), 1 nM Leptomycin B (LMB), 20 nM Staurosporine (Stau), 1 μM UCN-01, 20 nM Raf1 Kinase Inhibitor (RKI), 20 μM LY294002 (LY), 10 μM Etoposide (Eto) and 1 mM lithium chloride (LiCl) for 12 hours and compared to vehicle treatment. (**B**) Equal numbers of BCS and BYA cells were co-cultured in IL-3-free medium. We exposed the paired BaFiso cell lines to 3 μM, 30 μM and 300 μM Cisplatin (Cis), 25 μM, 100 μM, 200 μM Minerval (Min), 50 nM, 500 nM, 5 μM Akt Inhibitor X (AIX), 200 nM, 20 μM, 50 μM Genistein (Gen), 0.5 nM, 1 nM, 4 nM Leptomycin B (LMB), 2 nM, 20 nM, 10 μM Staurosporine (Stau), 200 nM, 1 μM, 10 μM UCN-01; 5 nM, 20 nM, 200 nM Raf1 Kinase Inhibitor (RKI), 1 μM, 20 μM, 50 μM LY294002 (LY), 100 nM, 10 μM, 100 μM Etoposide (Eto) and 100 μM, 1 mM, 10 mM lithium chloride (LiCl), and Dimethyl sulfoxide (DMSO) as a negative control (striped bar). Three images specific for ECFP, EYFP or DRAQ5 from each well were acquired using BD Pathway Bioimager. The ECFP/EYFP ratio was determined by dividing the number of ECFP positive cells by the number of EYFP positive cells. Light, dark grey and black bars represent low, medium and high concentrations of the corresponding compounds, respectively. The data shown here represents three independent experiments. The average Z′ value for BaFiso was 0.53. (**C**) Untreated, co-cultured BaFiso cells imaged before exposure to Akt Inhibitor X and (**D**) 12 h after treatment with 5 μM AIX.
doi:10.1371/journal.pone.0001823.g005

With the objective of identifying lead compounds that specifically kill cells with activated Akt signaling and that spare control cells, we have combined the use of co-cultured isogenic cell lines with fluorescent technology. We introduced a myristoylated form of Akt which constitutively localizes to the plasma membrane, bypassing the requirement for PIP3 in Akt activation. This myr-Akt has been shown to constitutively inactivate pro-apoptotic downstream targets [14]. In order to generate Ba/F3 cells that survive in the absence of IL-3 independent of activated PI3K/Akt signaling, we transduced Ba/F3 cells with a retrovirus encoding STAT5A1*6, an activated mutant of STAT5. STAT5A1*6 has two amino acid substitutions and it is constitutively phosphorylated, localized in the cell nucleus and transcriptionally active in the absence of IL-3 [11]. In the BaFiso system presented here, the protective potential of myr-Akt is slightly greater than that provided by STAT5A1*6, which may be explained by the greater expression of myr-Akt. The design of the screen relies on the lack of relevant crosstalk between the pathways engineered to support IL-3 independent survival. Previous work has shown that the induced expression of bcl-xL and pim-1 promotes the IL-3-independent survival of Ba/F3 cells upon activation of STAT5 [13]. In contrast, studies in multiple cell lines suggest that Akt phosphorylates and inactivates proapoptotic proteins such as GSK-3β, Foxo3a and Bad in response to IL-3 [8,19,20]. We confirmed that the activation of Stat5 signaling in BCS cells did not increase Akt activity either in the presence or absence of IL-3.

Another common source of interference to be mitigated in multiplexed screening procedures is the bleed-through of fluorescence from one channel to the other. BaFiso allows simultaneous viewing of three different fluorescent signals and sharp separation of the emission signals from the cyan and yellow protein is achieved using a special filter set. We implemented BaFiso as an automated live-cell assay using a multidrop dispenser, a robotic workstation and a robotic cell imaging platform. We assessed the properties of this HTS co-culture assay using a panel of test compounds of known activity. The cytotoxicity of the test compounds was monitored by quantifying the DRAQ5 labelled cells and all compounds tested except LiCl and Minerval reduced the viability of Ba/F3 cells. The fact that only two compounds known to selectively interfere with Akt signaling, Akt inhibitor X and UCN-01, reduced the number of yellow tagged BYA cells demonstrates the specificity of the BaFiso system. The Akt inhibitor X is a N-substituted phenoxazine that inhibits the activity of Akt even in the absence of its pleckstrin homology domain and it has been suggested that it may bind in the ATP binding site [17]. In contrast, UCN-01 has been reported to inhibit several kinases including PDK1, a key regulator of Akt activity [16]. Interestingly, staurosporine that differs from UCN-01 only by the absence of a hydroxy group on the lactam ring failed to change the ratio of the BaFiso cell lines. A specificity analysis against a kinase panel revealed different patterns of inhibition for UCN-01 with respect to staurosporine [16]. It remains to be determined if these differences in specificity could account for the different behaviour observed for these two compounds in the BaFiso assay.

The BaFiso screening design presented here offers some major advantages over traditional *in vitro* biochemical assays or more classical cellular assays. Co-culture and simultaneous testing of the paired isogenic cell lines in this assay provides an internal control and eliminates errors resulting from separate assessments. BaFiso is an image based high throughput assay that enables compound that produce artefacts and cytotoxicity to be identified on a single cell basis. Live cell imaging of the BaFiso cell lines permits the repeated monitoring of the same cells over the timecourse of an experiment, leading to a more accurate assessment that minimizes the variability in cell numbers between wells. Finally, the dual fluorescence co-culture system used in BaFiso is adaptable to any gene or pathway that can support IL-3 independent survival of Ba/F3 cells.

Methods

Expression Vectors and Reagents

The enhanced fluorescent protein vectors (pECFP-C1 and pEYFP-C1) were purchased from Clontech. The cDNAs encoding ECFP and EYFP were subcloned into the SnaBI sites of the pBABE-puro retroviral vector. The myr-Akt was kindly provided by Dr. Philip Tsichlis and we PCR amplified myr-Akt-HA using forward 5′–CGCGGATCCATGGGGAGCAGCAAGAGCAAGC–3′ and reverse 5′–ACGCGTCGACTCATCTAGAAGCGTAATCTGGAACC–3′ primers, before subcloning the BamHI and SalI digested PCR product into the corresponding restriction site of the retroviral vector pWZL-Blast. The Stat5A1*6-Flag construct was a kind gift from T. Nosaka (University of Tokyo). The nature of all constructs was confirmed by DNA sequencing.

All chemicals were purchased from commercial sources except UCN-01 which was kindly provided by NCI, Cisplatin which was provided by C. Navarro (Universidad Autónoma de Madrid, Spain), and Minerval which was generously provided by P. Escriba (University of the Balearic Islands, Palma de Mallorca, Spain). The Akt Inhibitor X, LY294002 and Raf1 Kinase Inhibitor were purchased from Calbiochem (San Diego, CA), Leptomycin B and Genistein were purchased from LC Laboratories (Woburn, MA, USA), Lithium chloride (LiCl), Etoposide and Staurosporine ware all purchased from Sigma-Aldrich (St. Louis, USA).

Cell Culture

Murine pro-B Ba/F3 cells were obtained from the American Type Culture Collection (ATCC) and maintained in RPMI 1640 containing: 10% fetal calf serum; 2 mM L-glutamine; 50 μM 2-mercaptoethanol (Sigma); antibiotics and antimycotics (Gibco); and 3 ng/ml of recombinant murine IL-3 (R&D Systems, Minneapolis, MN, USA). LinXE ecotropic retrovirus producing cells [21] were grown in Dulbecco's modified Eagle's medium with glutamax supplemented with 10% fetal bovine serum (FBS), penicillin, streptomycin and fungizone (Gibco). Cell cultures were maintained in a humified incubator at 37°C with 5% CO_2. To remove IL-3, the cells were washed twice in PBS at room temperature. Retroviral constructs were introduced into packaging cells by standard calcium phosphate transfection and retroviral-mediated gene transfer was performed as described previously [22]. After infection of Ba/F3 cells with retroviral supernatants containing either EYFP or ECFP, stable cell lines were selected in medium containing 2 μg/ml of puromycin for one week. In order to establish Ba/F3 cell lines homogeneously expressing EYFP or ECFP, we performed clonal propagation in Clona-cell TCS semi-solid culture medium (Stem Cell Technologies, Vancouver, Canada) containing 2 μg/ml puromycin according to the manufacturer's protocol. Ba/F3 cell clones stably expressing EYFP (BY cells) or ECFP (BC cells) were used as parental cells for the secondary stable infection with retroviral supernatants containing either myr-Akt or Stat5A1*6-Flag, respectively. Stable Ba/F3 cells co-expressing EYFP and myr-Akt (BYA cells) were selected with 0.8 mg/ml Neomycin and 1 μg/ml puromycin for 2 weeks. Stable Ba/F3 cells co-expressing ECFP and Stat5A1*6-Flag (BCS cells) were selected with 15 μg/ml Blasticidine and 1 μg/ml puromycin for 2 weeks. The generation of cell clones was performed as described above. Fluorescence-activated cell sorting (FACS) of EYFP or ECFP expressing cells was performed on a FACSAria (BD Biosciences, San Jose, CA, USA).

Western Blot Analysis

Cells incubated under different conditions were washed twice with TBS prior to lysis in buffer containing: 50 mM Tris HCl, 150 mM NaCl, 1% NP-40, 2 mM Na_3VO_4, 100 mM NaF, 20 mM $Na_4P_2O_7$, and protease inhibitor cocktail (Roche Molecular Biochemicals, Indianapolis, IN). Proteins were resolved on 10% SDS-PAGE, and transferred to PVDF membranes (Immobilon-P, Millipore). The membranes were incubated with the first antibody overnight at 4°C, washed and incubated with anti-mouse (1:10000) or anti-rabbit (1:5000) horseradish peroxidase conjugated antibodies. Immunoreactive proteins were visualized using the enhanced chemiluminescence (ECL) Western blotting detection system (Amersham Pharmacia Biotech) and Kodak-X-Omat LS film (Kodak). Antibodies against phospho-AKT (Ser473) and AKT were purchased from Cell Signaling (Beverly, MA), those against STAT-5 from (R&D Systems, Minneapolis, MN, USA), and the antibodies against α-tubulin and Flag were obtained from Sigma (St Louis, MO).

Survival assay

Each cell line was individually seeded at 10^4 cells per well in a 96 well plate, in the presence or absence of IL-3. AlamarBlue™ (Serotec, Oxford, UK) was added to the culture medium at a final concentration of 10% (v-v) and after 24 hours, absorbance was measured at the two different wavelengths of maximal absorbance of the reduced and oxidized forms of AlamarBlue™, 570 and 600 nm using Victor 1420 Multilabel Counter (Perkin-Elmer, Wellesley, USA). The percentage cell survival was calculated according to the manufacturers' instructions. Time course experiments of cell viability post IL-3 withdrawal were performed using trypan blue exclusion.

BaFiso assay

Equal numbers of parental BC/BY cells or activated test cells BCS/BYA were mixed in culture medium deprived of IL-3 and seeded in 96-well black clear bottom microplates coated with Poly-D-Lysine (Becton Dickinson Biosciences, San Jose, California, USA) at a density of 20,000 cells per well using Titan Multidrop 384 automatic dispenser (Titertek Instruments, Inc., Huntsville, AL). The final volume of the cell suspension was 200 μl in each well. After incubation at 37°C with 5% CO_2 for 1 hour the far-red fluorescent cell-permeable DNA probe, DRAQ5™ (Biostatus Ltd, Leicestershire, UK) was added at a final concentration of 5 μM to all wells 15 minutes prior to obtaining the first images. Then, 2 μl of each test compound or vehicle was transferred from the mother plates to the assay plates using a robotic workstation (Biomek® FX Beckman). Cells were incubated in the presence of the test compounds for 12 hours.

Image acquisition and processing

Assay plates were read on the BD Pathway™ 855 Bioimager (Becton Dickinson Biosciences, San Jose, California, USA) equipped with a 430/25 nm/470/30 nm ECFP excitation/emission filter, 500/20 nm/535/30 nm EYFP excitation/emission filter and 635/20 nm/695/55 nm DRAQ5 excitation/emission filter. Images for each well were acquired in the three different channels for ECFP, EYFP and DRAQ5 using a 20× dry objective. The plates were exposed for 0.55 ms (Gain 14) to acquire ECFP images, 0.68 ms (Gain 32) for EYFP images and

0.47 ms (Gain 5) to acquire DRAQ5 images. The far red fluorescence intensity of DRAQ5 was used to perform automated segmentation of the cell nuclei and in turn to quantify the total cell number.

Data analysis

The data output of the BD Pathway Bioimager is as standard text files. These files contained the raw fluorescence data for each cells population. Data were imported into the data analysis software, BD Image Data Explorer, and the ratios of the ECFP positive cells to EYFP positive cells were determined by dividing the number of cyan fluorescence-emitting single cells by the number of yellow fluorescence-emitting single cells in each well. This procedure was repeated for each well. By measuring changes in the ratio between the cyan and yellow signal, the possible pathway-specific cytotoxicity of each compound could be determined. In order to estimate the quality of the HCS assay, the Z' factor was calculated by the equation: Z' = 1 – [(3×std. dev. of positive controls)+(3×std. dev. of negative controls)/(mean of positive controls) - (mean of negative controls)] as described previously [23].

Acknowledgments

The authors acknowledge F. Blanco for his expert technical assistance, the staff at BD Biosciences for their contribution in establishing the technology, S. Tenbaum for his help in preparing the figures and C. Blanco, J.F. Martinez and O. Renner for helpful discussions and critical reading of this manuscript.

Author Contributions

Conceived and designed the experiments: WL. Performed the experiments: AR FZ BG. Analyzed the data: AR FZ. Wrote the paper: WL. Other: Co-directed research: AC.

References

1. Drews J (2000) Drug discovery: a historical perspective. Science 287: 1960–1964.
2. Balis FM (2002) Evolution of anticancer drug discovery and the role of cell-based screening. J Natl Cancer Inst 94: 78–79.
3. Gibbs JB (2000) Mechanism-based target identification and drug discovery in cancer research. Science 287: 1969–1973.
4. Palacios R, Steinmetz M (1985) Il-3-dependent mouse clones that express B-220 surface antigen, contain Ig genes in germ-line configuration, and generate B lymphocytes in vivo. Cell 41: 727–734.
5. Socolovsky M, Fallon AE, Wang S, Brugnara C, Lodish HF (1999) Fetal anemia and apoptosis of red cell progenitors in Stat5a-/-5b-/- mice: a direct role for Stat5 in Bcl-X(L) induction. Cell 98: 181–191.
6. Sato N, Sakamaki K, Terada N, Arai K, Miyajima A (1993) Signal transduction by the high-affinity GM-CSF receptor: two distinct cytoplasmic regions of the common beta subunit responsible for different signaling. Embo J 12: 4181–4189.
7. Songyang Z, Baltimore D, Cantley LC, Kaplan DR, Franke TF (1997) Interleukin 3-dependent survival by the Akt protein kinase. Proc Natl Acad Sci U S A 94: 11345–11350.
8. Maurer U, Charvet C, Wagman AS, Dejardin E, Green DR (2006) Glycogen synthase kinase-3 regulates mitochondrial outer membrane permeabilization and apoptosis by destabilization of MCL-1. Mol Cell 21: 749–760.
9. Hoover RR, Gerlach MJ, Koh EY, Daley GQ (2001) Cooperative and redundant effects of STAT5 and Ras signaling in BCR/ABL transformed hematopoietic cells. Oncogene 20: 5826–5835.
10. Leverrier Y, Thomas J, Mathieu AL, Low W, Blanquier B, et al. (1999) Role of PI3-kinase in Bcl-X induction and apoptosis inhibition mediated by IL-3 or IGF-1 in Baf-3 cells. Cell Death Differ 6: 290–296.
11. Onishi M, Nosaka T, Misawa K, Mui ALF, Gorman D, et al. (1998) Identification and characterization of a constitutively active STAT5 mutant that promotes cell proliferation. Molecular and Cellular Biology 18: 3871–3879.
12. Burgering BM, Coffer PJ (1995) Protein kinase B (c-Akt) in phosphatidylinositol-3-OH kinase signal transduction. Nature 376: 599–602.
13. Nosaka T, Kawashima T, Misawa K, Ikuta K, Mui AL, et al. (1999) STAT5 as a molecular regulator of proliferation, differentiation and apoptosis in hematopoietic cells. Embo J 18: 4754–4765.
14. Chan TO, Rittenhouse SE, Tsichlis PN (1999) AKT/PKB and other D3 phosphoinositide-regulated kinases: kinase activation by phosphoinositide-dependent phosphorylation. Annu Rev Biochem 68: 965–1014.
15. Zanella F, Rosado A, Blanco F, Henderson BR, Carnero A, et al. (2007) An HTS approach to screen for antagonists of the nuclear export machinery using high content cell-based assays. Assay Drug Dev Technol 5: 333–341.
16. Komander D, Kular GS, Bain J, Elliott M, Alessi DR, et al. (2003) Structural basis for UCN-01 (7-hydroxystaurosporine) specificity and PDK1 (3-phosphoinositide-dependent protein kinase-1) inhibition. Biochem J 375: 255–262.
17. Thimmaiah KN, Easton JB, Germain GS, Morton CL, Kamath S, et al. (2005) Identification of N10-substituted phenoxazines as potent and specific inhibitors of Akt signaling. J Biol Chem 280: 31924–31935.
18. Torrance CJ, Agrawal V, Vogelstein B, Kinzler KW (2001) Use of isogenic human cancer cells for high-throughput screening and drug discovery. Nat Biotechnol 19: 940–945.
19. del Peso L, Gonzalez-Garcia M, Page C, Herrera R, Nunez G (1997) Interleukin-3-induced phosphorylation of BAD through the protein kinase Akt. Science 278: 687–689.
20. Plas DR, Thompson CB (2003) Akt activation promotes degradation of tuberin and FOXO3a via the proteasome. J Biol Chem 278: 12361–12366.
21. Carnero A, Hudson JD, Hannon GJ, Beach DH (2000) Loss-of-function genetics in mammalian cells: the p53 tumor suppressor model. Nucleic Acids Res 28: 2234–2241.
22. Link W, Rosado A, Fominaya J, Thomas JE, Carnero A (2005) Membrane localization of all class I PI 3-kinase isoforms suppresses c-Myc-induced apoptosis in Rat1 fibroblasts via Akt. J Cell Biochem 95: 979–989.
23. Zhang JH, Chung TDY, Oldenburg KR (1999) A simple statistical parameter for use in evaluation and validation of high throughput screening assays. Journal of Biomolecular Screening 4: 67–73.

3.2 Identification of Novel Targets implicated in FOXO regulation by High Content-High Throughput screenings

3.2.1 Fourth Project: A chemical genetics screening for compounds able to induce FOXO nuclear translocation

Summary

In this project a HCS system generated with U2-OS human osteosarcoma cells stably transfected with a GFP-FOXO3A fusion protein was used. Automated image analysis allows for the quantification of nuclear/cytoplasmic ratios of the reporter signal as a readout for FOXO activation. This system allowed us to perform a chemical genetic analysis of 73 compounds. Some of them, previously related to PI3K/Akt inhibition scored positive in our study, as well as the small tubuline-binding molecule Vimblastine, previously reported to activate the JNK pathway. Moreover, the effect of Calmodulin inhibition on FOXO translocation was detected and further analyzed. This system was also used for the validation of the hits obtained in our RNAi screening.

Personal contribution

I generated the cell-based system and performed the experiments required for its validation and adaptation to the high-throughput format. Once established, together with Aránzazu Rosado and Beatríz García, I performed the experiments carried with the compounds mentioned and processed the data analysis and interpretation.

Publication:

Zanella F, Rosado A, García B, Carnero A and Link W, **Chemical genetic analysis of FOXO nuclear-cytoplasmic shuttling using Image-Based Cell Screening.** ChemBiochem. 2008. Sep 22;9(14):2229-37.

DOI: 10.1002/cbic.200800255

Chemical Genetic Analysis of FOXO Nuclear–Cytoplasmic Shuttling by Using Image-Based Cell Screening

Fabian Zanella,[a] Aranzazú Rosado,[a, b] Beatriz García,[a] Amancio Carnero,[a] and Wolfgang Link*[a]

FOXO proteins are direct targets of PI3K/Akt signaling and they integrate the signals of several other transduction pathways at the transcriptional level. FOXO transcription factors are involved in normal cell homeostasis and neoplasia, and they are regulated by multiple post-transcriptional modifications. In cancer research, the regulation of the FOXO factors is receiving increasing attention as their activation has been linked to cell-cycle arrest and apoptosis. Hence, FOXO proteins have been proposed to act as tumor suppressors. Here, we applied a chemical biology approach to study the mechanisms that influence the intracellular localization of the FOXO family member FOXO3a. We established a high-throughput cellular-imaging assay that monitors the nuclear–cytoplasmic translocation of a GFP–FOXO3a fusion protein in tumor cells. Nuclear accumulation of fluorescent signals upon treatment with the known PI3K inhibitors LY294002, wortmannin, PIK-75, and PI-103 was dose dependent and agreed well with the IC_{50} values reported for PI3Kα inhibition in vitro. Additionally, we identified 17 compounds from a panel of 73 low-molecular-weight compounds capable of inducing the nuclear accumulation of GFP–FOXO. These compounds include chemicals known to interfere with components of the PI3K/Akt signaling pathway, as well as with nuclear export and Ca^{2+}/calmodulin (CaM)-dependent signaling events. Interestingly, the therapeutic agent vinblastine induced efficient nuclear translocation of the FOXO reporter protein. Our data illustrate the potential of chemical genetics when combined with robust and sensitive high-content-screening technology.

Introduction

Mammalian FOXO proteins are the orthologues of *Candida elegans* DAF16, and they pertain to the O class of forkhead transcription factors that have a characteristic forkhead box DNA binding domain. FOXO proteins function as transcriptional regulators in the cell nucleus and they bind as monomers to their consensus DNA binding sites. They are components of highly conserved signal-transduction pathways that link growth and stress signals to the control of gene expression. The ever-growing list of target genes for these factors contains many elements that function in metabolism, apoptosis, resistance to oxidative stress, and cell-cycle inhibition, and includes glucose-6-phosphatase, phosphoenolpyruvate carboxykinase,[1] FasL, Bim,[2,3] MnSOD, catalase, $p27^{KIP1}$, p130, and cyclin G_2.[4–6] FOXO factors are inactivated in a variety of cancers and indeed, FOXO3a was found mainly in the cytoplasm in human primary breast cancer where nuclear exclusion was closely correlated with poor survival.[7] Moreover, the expression of a constitutively active form of FOXO1 diminished tumorigenesis in cells with aberrant PI3K/Akt activity in nude mice.[8] In fact, the simultaneous disruption of the three principal FOXO genes leads to thymic lymphoma and haemangiomas, indicative that FOXO factors are bona fide tumor suppressors.[9]

Despite these consequences of their inactivation and somewhat surprisingly, no inactivating mutations in the FOXO genes have yet been reported. Hence, inactivation of FOXO proteins in human cancer seems to be mainly due to aberrant upstream signaling. Subcellular localization of FOXO proteins plays a major role in the regulation of their activity. Nuclear–cytoplasmic shuttling of FOXO factors is controlled by a sophisticated signaling network that integrates information from PI3K/Akt and stress-induced signaling pathways via the Jun N-terminal kinase (JNK), the mammalian sterile 20-like kinase MSTI, and the NAD-dependent deacetylase SIRT1.[10] In the absence of growth factor signaling, FOXO factors are localized in the nucleus and are transcriptionally active. By contrast, FOXO transcription factors are phosphorylated by several kinases in response to growth and survival factors, including AKT, SGK, and CK1,[11] and phosphorylation by DYRK1A and IKKβ has been shown to drive FOXO factors out of the nucleus.[7,11] Akt negatively regulates FOXO proteins through the phosphorylation of residues at three highly conserved RXRXXS/T consensus sites; this leads to conformational changes that facilitate 14-3-3 binding and that activate CRM-1-mediated nuclear export. Stress signals have been shown to antagonize Akt signaling by preventing the binding of FOXO to 14-3-3 by phosphorylation of FOXO at S207 by MST1 and the phosphorylation of 14-3-3

[a] *F. Zanella, A. Rosado, B. García, Dr. A. Carnero, Dr. W. Link*
Experimental Therapeutics Program
Centro Nacional de Investigaciones Oncologicas (CNIO)
Melchor Fernandez Almagro 3, 28029 Madrid (Spain)
E-mail: wlink@cnio.es

[b] *A. Rosado*
Current address: NKI-AVL
Plesmanlaan 121, 1066 CX, Amsterdam (The Netherlands)

Supporting information for this article is available on the WWW under http://www.chembiochem.org or from the author.

by JNK.[12,13] Furthermore, oxidative stress promotes Ral-mediated, JNK-dependent phosphorylation of FOXO4.[14] Additionally, monoubiqutination and SIRT-dependent deacetylation of FOXO proteins in response to increased cellular oxidative stress is thought to induce their nuclear translocation.[15,16] Despite considerable efforts, our understanding of how non-Akt-mediated regulation of FOXO factors affects their subcellular localization is very limited. To define the circuit that regulates the subcellular transport of FOXO proteins, we performed chemical genetic studies to interrogate the FOXO shuttling system.

Results

U2foxRELOC cells respond to inhibition of the PI3K/Akt pathway

To generate a system suitable to monitor nuclear–cytoplasmic shuttling of FOXO protein in a high-throughput-screening (HTS) format, we stably transfected a GFP–FOXO3a reporter plasmid into U2OS cells and prepared cell clones. As a proof of principle, we treated U2foxRELOC cells with LY294002, a broad spectrum PI3K inhibitor widely used to suppress the activation of PI3K/Akt signaling. Whereas the GFP fusion protein was present in both the cytoplasm and nucleus in U2foxRELOC cells, with significantly more GFP in the cytoplasm than in the nucleus, when exposed to LY294002 for 1 h almost all the GFP–FOXO3a translocated to the nucleus of these cells (Figure 1). To analyze whether treatment with LY294002 compromised the integrity of the cell cytoplasm, we used cell-tracker orange as a vital cytoplasmic counterstain. The overall morphology of U2foxRELOC cells remained unaffected by exposure to LY294002 (Figure 1 F), indicating that the kinetics of the assay allowed us to reduce the incubation time necessary to attain unambiguous responses when cells were exposed to different compounds. This is an important factor to minimize the possible toxic effects that might interfere with the analysis, as well as other indirect effects.

Dose-response analysis of PI3K inhibitors with different IC_{50} values by using automated U2foxRELOC

We next explored the feasibility of extracting quantitative data from the U2foxRELOC system by analyzing the effects of PI3K

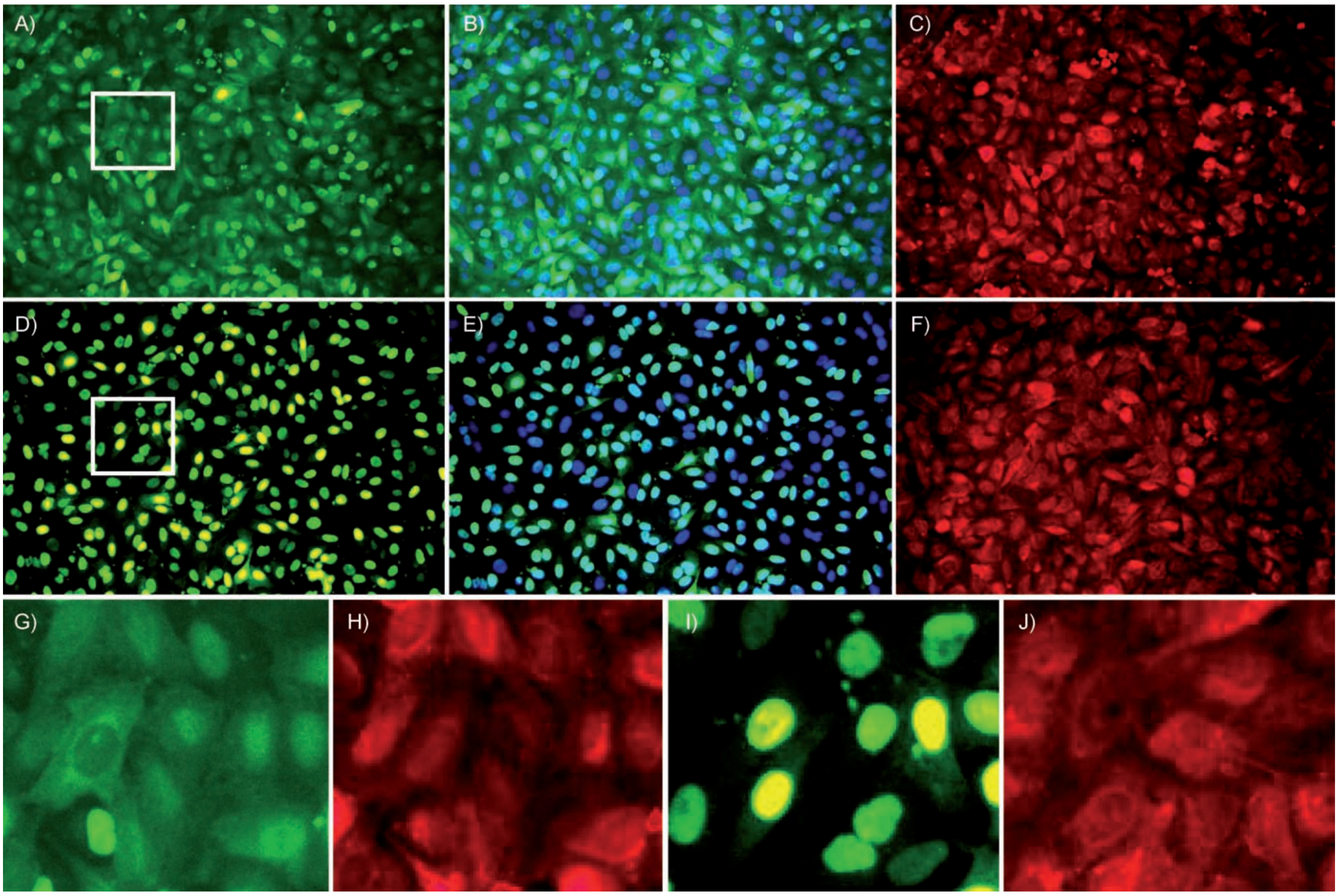

Figure 1. Translocation of GFP–FOXO following PI3K inhibition. U2foxRELOC cells stably expressing GFP–FOXO fusion protein were seeded in 96-well plates, incubated for 12 h, preincubated with cell-tracker orange dye, and treated with DMSO (A–C) or 20 μM LY294002 (D–F). After 1 h at 37 °C, the cells were washed, fixed, and stained with DAPI in a fully automated manner by using a robotic workstation. The cells were photographed by using a BD Pathway HT cell-imaging platform. A) and D) GFP; B) and E) GFP and DAPI merged images; C) and F) cell-tracker orange. G) a close-up view of the region in (A) outlined by the square. I) Close-up view of the region in (D) outlined by the square. H) and J) Corresponding cell-tracker orange images.

inhibitors that act on the recombinant p110α protein with different IC_{50} values. The IC_{50} in vitro value of the competitive, pan-PI3K inhibitor LY294002 is 500 nM and hence, it is about 60-fold less potent than the imidazopyridine inhibitor PIK-75 (7.8 nM), about 135-fold less potent than the synthetic selective class I PI3K inhibitor PI-103 (IC_{50} = 3.7 nM) and about 900-fold less potent than the fungal metabolite wortmannin (IC_{50} = 0.57 nM).[17] U2foxRELOC cells were exposed to eleven different concentrations of the PI3K inhibitors for 1 h in culture, the final concentrations of the inhibitors ranging from 50 μM to 1.6 nM. The morphological integrity of the assayed cells was confirmed by cell-tracker orange fluorescence of cytoplasm of viable cells (data not shown). The data obtained from these experiments agree well with the IC_{50} values for the corresponding compounds in biochemical assays (Figure 2). Thus, LY294002 induced nuclear translocation of the FOXO reporter protein at 50 μM, and 33.3 μM, and was slightly less efficient at 11.1 μM. However, exposure of U2foxRELOC cells to 3.7 μM LY294002 failed to affect the intracellular localization of the fluorescent signal. By contrast, wortmannin triggered nuclear shuttling of GFP–FOXO even at low nanomolar concentrations. PI-103 produced fluorescent precipitates at 50 μM and 33.3 μM, visible in both the DAPI and the GFP channel, although nuclear accumulation of GFP–FOXO was also evident under these conditions. Importantly, exposure of U2foxRELOC cells to concentrations as low as 46 nM of PI-103 or 15 nM of wortmannin was sufficient to induce the nuclear translocation of the FOXO reporter protein. The slightly greater potency of PI-103 in comparison with PIK-75 on the recombinant p110α protein was reflected by the small difference in the minimal effective concentration at which accumulation of the fluorescent signal could be detected in the U2foxRELOC system. In contrast to PI-103, PIK-75 was unable to induce significant translocation of the reporter protein at 46 nM. Hence, the U2foxRELOC appeared to be a very sensitive system to detect inhibitors of the PI3K/Akt pathway with different potencies.

Chemical interrogation of nuclear–cytoplasmic shuttling of FOXO by using the U2foxRELOC-based assay

We applied a chemical biology approach to study the signaling network that regulates the intracellular localization of FOXO transcription factors. Accordingly, we screened a panel of compounds with known biological activity in the U2foxRELOC cell system (see Table S1 in the Supporting Information for the complete list of compounds studied). The initial test panel consisted of 73 compounds known to interfere with the major signal transduction pathways. A major concern when using small molecules for pathway analysis is their specificity for their corresponding target. To draw useful conclusions, it is recommended to use two structurally unrelated compounds for each target[18] and therefore, we included several independent small-molecule inhibitors for the same molecular target wherever possible. Likewise, to distinguish on target and off target effects, different concentrations of the compounds were assessed in the primary screen. We exposed U2foxRELOC cells to equal volumes of test compounds at final concentrations in a range of two orders of magnitude around their IC_{50} value. As reference compounds we used LY294002 and the nuclear export inhibitor leptomycin B. To determine the cutoff threshold for primary hits, the nuclear accumulation of fluorescence triggered by LY294002 in the U2foxRELOC assay was defined as 100% activity. Primary hits were defined as those samples that have an activity above 60% and several test compounds fulfilled these criteria (Figure 3 A).

Ras farnesyltransferase inhibitor, manumycin A was shown to be capable of inducing FOXO translocation into the nucleus. Several small molecule compounds known to interfere with the PI3K/Akt pathway, one of the major signaling branches downstream of Ras, also induced nuclear FOXO translocation. Namely, the Akt inhibitors, Akt inhibitor VIII, Akt inhibitor X, PI-103, wortmannin, D000, and UCN01, were active in this assay at concentrations previously reported to affect targets related to PI3K/Akt signaling, demonstrating the capacity of the U2foxRELOC system to identify inhibitors of the PI3K/Akt pathway. In contrast, known activators of the PI3K/Akt pathway including EGFP, IGF, PDGF, and insulin produced little nuclear localization of GFP–FOXO. However, insulin was the only factor that decreased the number of cells with nuclear fluorescent signal below the level of vehicle-treated cells. Rapamycin, is a widely used inhibitor of mTOR that has no effect on GFP–FOXO localization; this indicates that the rapamycin-sensitive mTOR complex acts downstream of the PI3K/Akt-associated signaling events relevant for the regulation of FOXO activity.

To analyze the involvement of alternative downstream Ras signaling pathways in FOXO translocation, we tested several compounds previously shown to interfere with different elements in the MAPK cascade. Inhibition of Raf1, Mek1/2, JNK, or p38α MAP kinase upon treatment with GW5074, arctigenin, U0126, PD98059, SP600125, JNK inhibitor VIII, or SB202190, did not induce nuclear translocation of GFP–FOXO. Conversely, the p38 MAP kinase inhibitor SB203580 triggered the accumulation of nuclear fluorescence, although at a concentration that has been shown to decrease Akt activity in several cell lines.[19,20] As anticipated, staurosporine, a relatively nonselective protein kinase inhibitor that blocks many kinases to a differing extent was capable of inducing the nuclear accumulation of the FOXO reporter protein. We analyzed the effect of six different tyrosine kinase inhibitors on translocation in the U2foxRELOC assay, including tyrphostatin SU1498, tyrphostin AG 82, tyrphostin AG 1478, tyrphostin AG 1433, tyrphostatin SU 1498, genistein, and PP1 analogue. Only the broad tyrosine kinase specific inhibitor genistein induced GFP–FOXO nuclear translocation.

From a subgroup of drugs currently used in anticancer chemotherapy and known to act through different molecular mechanisms, including etoposide, camptothecin, cisplatin, oxaliplatin, flavopiridol, gemcitabine, paclitaxel, and vinblastine, only the latter drug displayed activity in the U2foxRELOC assay. Vinblastine has been shown to activate the JNK pathway.[21] Whether FOXO translocation mediated by these drugs is due to the activation of JNK and in turn, the phosphorylation of 14-3-3 protein, or the direct inactivating phosphorylation of FOXO3a remains to be determined. Roscovitine is a

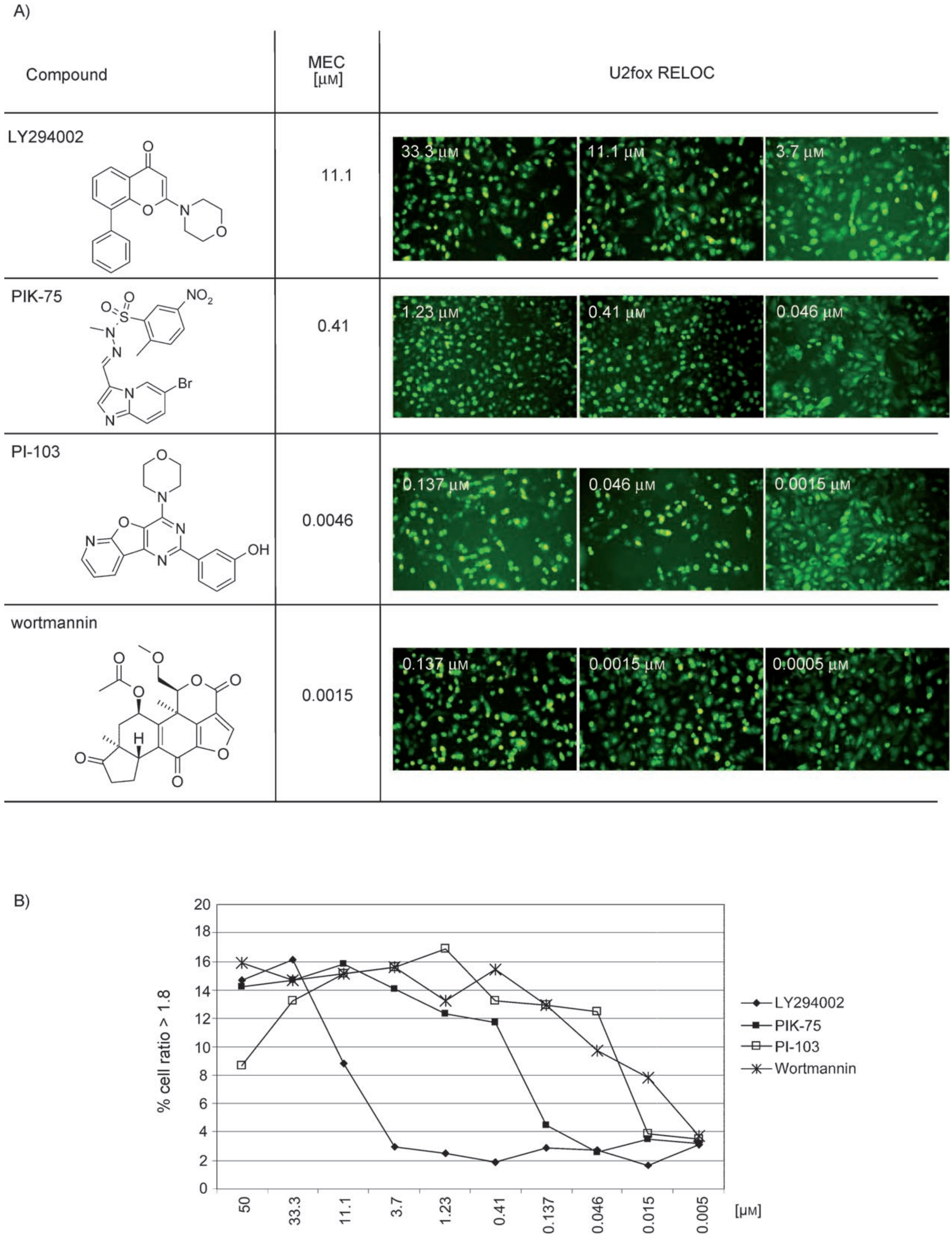

Figure 2. Dose-response relationship of the nuclear–cytoplasmic shuttling of FOXO following PI3K inhibition. A) We used LY294002, wortmannin, PIK-75, and PI-103, four structurally unrelated PI3K inhibitors that inhibit the recombinant p110α protein with IC_{50} values of 500, 7.8, 3.7, and 0.57 nM, respectively.[17] U2foxRELOC cells were seeded in 96-well plates, incubated for 12 h, and treated with eleven different concentrations of LY294002, PIK-75, PI-103, or wortmannin ranging from 50 μM to 1.6 nM. After 1 h at 37 °C in medium containing one of each of the compounds, the cells were washed, fixed, and stained with DAPI and photographed by using automated microscopy. The minimal effective concentration (MEC) is the lowest dose of each corresponding compound that induced GFP–FOXO translocation, as determined by assessing 11 different concentrations. B) The graph shows the proportion of cells exhibiting nuclear/cytoplasmic (Nuc/Cyt) ratios of fluorescence intensity greater than 1.8 for each treatment.

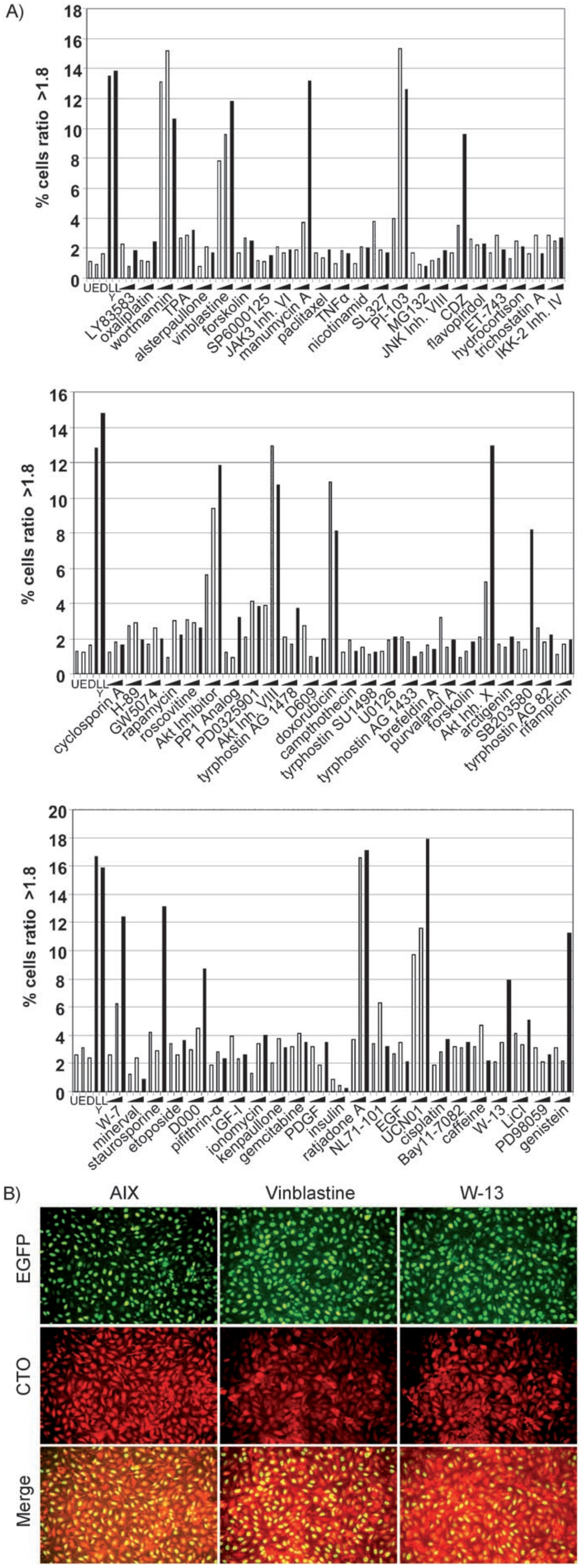

potent pan-CDK inhibitor currently undergoing phase II clinical testing that failed to induce FOXO protein translocation into the nucleus. Hence, despite promoting a cytoplasmic localization of FOXO1,[22] CDK-mediated phosphorylation is not involved in the nuclear–cytoplasmic shuttling of the FOXO3a-reporter protein. Likewise, other CDK inhibitors, such as kenpaullone, alsterpaullone, and purvalanol A, had no effect in this assay.

As expected, exposure of U2foxRELOC cells to the nuclear export inhibitor ratjadone A resulted in the nuclear accumulation of fluorescent signal. In agreement with previous data,[23] the calmodulin antagonists W-7, W-13, and calmidazolium chloride (CDZ) also produced a positive result in the U2foxRELOC assay. The nuclear accumulation of fluorescent signal was not attributable to shrinkage of the cell cytoplasm, as witnessed by vital staining when using cell-tracker orange fluorescent dye (Figure 3 B and data not shown).

Further analysis of the compounds that produce FOXO relocation

After screening the initial panel of compounds, we validated the compounds of interest to identify those whose activity was not specific for FOXO3a nuclear translocation using independent image-based translocation assays. To rule out general perturbations affecting the fluorophore, we tested the hit compounds using a U2gfpRELOC assay based on U2OS cells stably expressing GFP alone. GFP localization was unaffected upon exposure to the compounds identified in the U2foxRELOC assay (data not shown). Likewise, when analyzed in the U2nesRELOC assay, a cell-based system to detect inhibition of the general export machinery, only the two known nuclear export inhibitors, ratjadone A and leptomycin B, were shown to induce nuclear trapping of the reporter protein (ref. [24] and data not shown).

As specificity is closely correlated with the concentrations used, we determined the minimal dose necessary to induce the nuclear accumulation of GFP–FOXO for each hit compound (Table 1). We performed dose-response experiments at eleven different concentrations and ratjadone A, leptomycin B, PI-103, wortmannin, and vinblastine were identified as the most potent activators of GFP–FOXO nuclear translocation, acting in the low nanomolar range. Submicromolar concentrations of D000 were sufficient to induce nuclear shuttling of the report-

Figure 3. Nuclear accumulation of the GFP–FOXO reporter protein induced by the test compounds. A) We exposed U2foxRELOC cells to three different concentrations of the 73 compounds for 1 h. Bar graphs show the percentage of the cells in each well exhibiting nuclear/cytoplasmic (Nuc/Cyt) ratios of fluorescence intensity greater than 1.8. Low, medium, and high concentrations are indicated by light gray, gray, and dark gray bars, respectively. Untreated wells are indicated by U, control wells containing dimethyl sulfoxide, ethanol, LY294002, or leptomycin B are indicated by D, E, Ly, and L, respectively. The data shown represent three independent experiments. B) The morphology of U2foxRELOC cells remained unaffected by exposure to Akt inhibitor X (AIX), vinblastine, or W13. U2foxRELOC cells were preincubated with cell-tracker orange dye and exposed to the Akt inhibitor X (AIX, 5 μM), vinblastine (100 nM), or W13 (20 μM). After 1 h at 37 °C, the cells were processed as described in Figure 1.

Table 1. The compounds capable of inducing the nuclear accumulation of GFP–FOXO and their main molecular targets.

COMPOUND	TARGET	MEC [μM][a]
manumycin A	Ras-farnesyltransferase	11.1
LY294002	PI3K	11.1
wortmannin	PI3K	0.015
PI-103	PI3K	0.046
PIK-75	PI3K	0.41
D000	PI3Kδ	11.1
Akt inhibitor	Akt	11.1
Akt inhibitor VIII	Akt	3.7
Akt inhibitor X	Akt	3.7
UCN01	PDK1, other protein kinases	0.045
staurosporine	protein kinases	11.1
leptomycin B	CRM1	0.045
ratjadone A	CRM1	0.045
genistein	tyrosine protein kinases	11.1
vinblastine	tubulin	0.045
W7	CaM	11.1
W13	CaM	11.1
calmidazolium chloride	CaM	11.1

[a] The minimal effective concentration (MEC) is the lowest dose of each corresponding compound that induced GFP–FOXO translocation, as determined by assessing 11 different concentrations.

er protein whereas micromolar concentrations of manumycin A, LY294002, Akt inhibitor, Akt inhibitor VIII, Akt inhibitor X, staurosporine, genistein, CDZ, W-7, and W-13 were required to obtain the same result.

Analysis of calcium signaling

We investigated whether the nuclear accumulation of the FOXO-reporter protein upon exposure to the calmodulin (CaM) inhibitors W-7, W-13, and CDZ was mediated by specific inhibition of CaM. We took advantage of a closely related naphthalene-sulfonamide analogue that displays a very different inhibitory profile on CaM. W-7 and W-13 inhibit the CaM regulated activity of Ca^{2+}-modulin-dependent phosphodiesterase at IC_{50} values of 28 μM and 68 μM, respectively.[25] The related W-12, a compound that lacks chlorine, is a much less effective CaM inhibitor[25] than W-7 or W-13, and it was used to distinguish CaM-specific inhibitory effects from nonspecific drug effects. Indeed, W-12 failed to produce nuclear translocation of the FOXO reporter protein even at 50 μM (Figure 4B). Conversely, the minimal effective concentrations of W-7 or W-13 necessary to induce nuclear localization of GFP–FOXO were in good agreement with the IC_{50} values reported previously for CaM inhibition by these two naphthalene-sulfonamide analogues. Taken together these data indicate that CaM is involved in regulating FOXO translocation.

To further study the implication of Ca^{2+} signaling in FOXO shuttling, we used different chemical probes capable of altering the cellular Ca^{2+} homeostasis. When the reporter cells were loaded with the intracellular Ca^{2+}-chelator, BAPTA-AM, we confirmed the nuclear accumulation of the fluorescent signal, in agreement with a role for Ca^{2+} signaling in mediating the nuclear translocation of FOXO3a. In addition, the extracellular Ca^{2+}-chelator EGTA also produced the nuclear accumulation of the FOXO reporter protein, providing further evidence that intracellular and extracellular Ca^{2+} regulates the subcellular localization of FOXO proteins. In contrast, the increase in cytosolic Ca^{2+} induced by caffeine, thapsigargin, or ionomycin did not promote the nuclear retention of GFP–FOXO, nor did they restore its cytoplasmic localization when applied together with W-7, W-13, and CDZ (Figure 4 and data not shown).

The molecular mechanisms by which the CaM antagonists exert their effect on FOXO translocation were further explored by examining the impact of inhibiting of multifunctional calcium/CaM-dependent protein kinases. KN-62 and K-93 inhibit CaMKI, CaMKII, and CaMKIV, yet they had no effect on the subcellular localization of FOXO. Likewise, when using ML-7 to inhibit the calcium/CaM-dependent protein kinase, myosin light-chain kinase (MLCK), failed to induce nuclear accumulation of the fluorescent reporter. Furthermore, inhibiting the CaM-kinase-kinases (CaMKK), upstream activators of the calcium/CaM-dependent protein kinases, CaMKI and CaMKIV, did not reproduce the effect of CaM inhibition on FOXO translocation. To explore the effect on Akt/PI3K signaling of the chemical probes that interfere with Ca^{2+} signaling and that induce nuclear FOXO localization, we monitored the phosphorylation of Akt. In Western blots probed with a specific antibody against Akt Ser473, a dramatic decrease in Akt phosphoylation on Ser473 was evident upon treatment with W-7, W-13, Bapta AM, or EGTA. These data indicate a direct relationship between blocking CaM activity and decreased Akt phosphorylation.

Discussion

Chemical genetics has emerged as an exciting new research field that explores the interface between chemistry and biology. In this study, we demonstrate the potential of chemical genetics combined with high-content screening to dissect out the complex regulation of the subcellular localization of FOXO transcription factors. We established U2foxRELOC, a quantitative cell-based high-content screening assay that monitors the nuclear–cytoplasmic translocation of a GFP–FOXO3a fusion protein. Herein, U2foxRELOC was used to obtain quantitative information about the impact of different PI3K inhibitors on downstream signaling, to perform a large-scale chemical genetic study with a panel of test compounds. We also used this system to analyze the effect of chemical probes that modulate Ca^{2+} signaling on the nuclear–cytoplasmic shuttling of a FOXO reporter protein. High-throughput cellular imaging has enabled us to measure the minimal effective concentration of different PI3K inhibitors necessary to induce nuclear shuttling of a FOXO reporter protein. Using this approach we screened a panel of 73 compounds with a known mechanism of action and we identified 17 compounds that induced the nuclear accumulation of the fluorescent reporter. The majority of these small molecules are known inhibitors of the PI3K/Akt pathway confirming the essential role of signaling through PI3K, PDK1, and Akt in regulating the subcellular localization of FOXO proteins. Interestingly, D000 a compound claimed to specifically

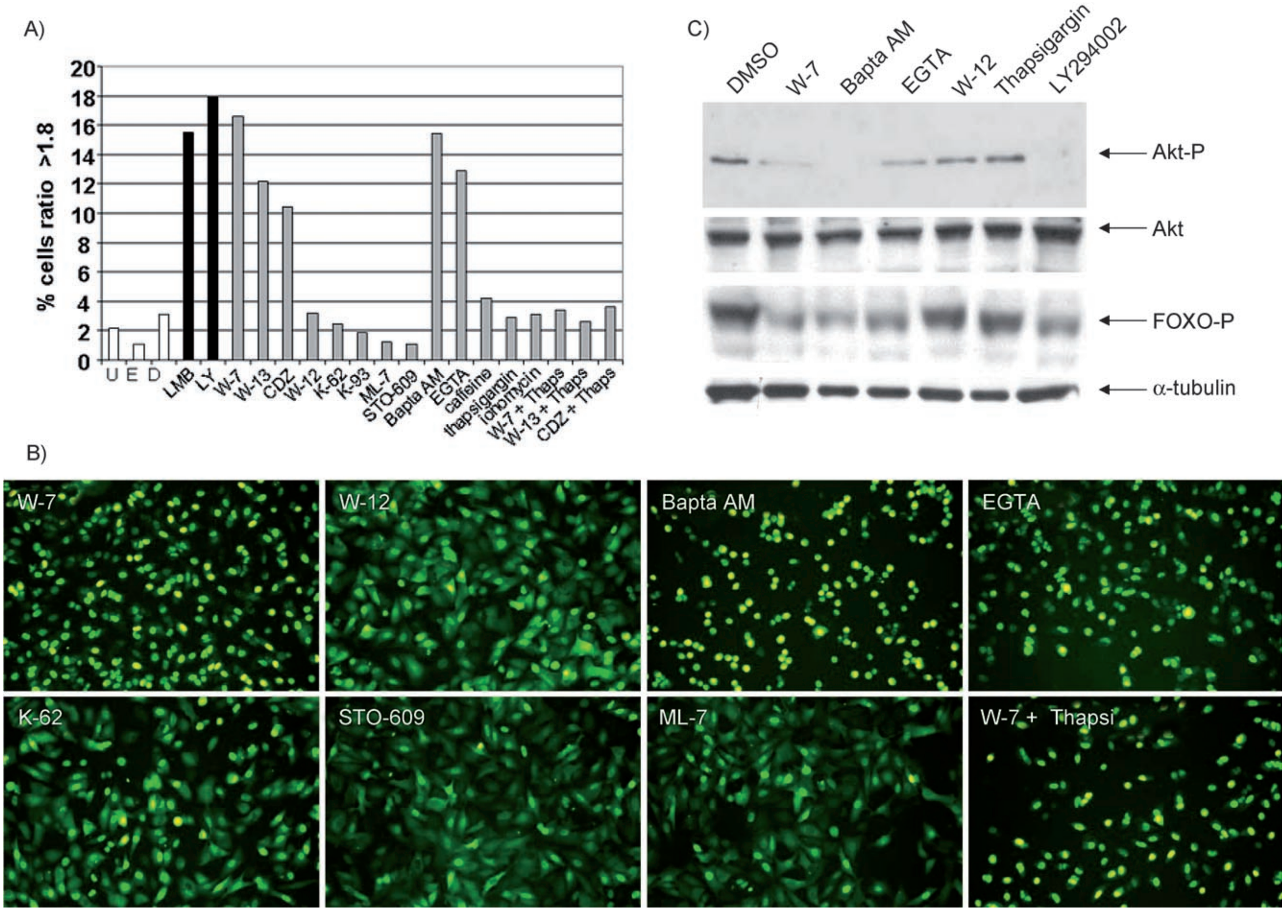

Figure 4. A) Nuclear accumulation of the GFP–FOXO reporter protein following treatment with chemical probes that interfere with Ca^{2+} signaling. Bar graphs show the percentage of cells in each well exhibiting nuclear/cytoplasmic (Nuc/Cyt) ratios of fluorescence intensity greater than 1.8. Untreated wells are indicated by U, control wells containing dimethyl sulfoxide, ethanol, LY294002, or leptomycin B are indicated by D, E, LY, and LMB, respectively. We exposed U2-foxRELOC cells to W7 (20 μM), W13 (20 μM), calmidazolium chloride (CDZ, 20 μM), W12 (50 μM), KN62 (30 μM), KN93 (30 μM), ML-7 (30 μM), STO-609 (1 $\mu g\,mL^{-1}$), Bapta AM (100 μM), EGTA (5 mM), caffeine (4 mM), thapsigargin (200 nM), ionomycin (200 nM), and to thapsigargin (200 nM) in the presence of W7 (20 μM), W13 (20 μM), or CDZ (20 μM). The data shown represent three independent experiments. B) Representative images of treated cells by using the high-throughput format of the U2foxRELOC system. Images of fixed and DAPI-stained cells were taken by automated microscopy 1 h after drug exposure. Images corresponding to U2foxRELOC cells exposed to W7 (20 μM), W12 (200 μM), Bapta AM (100 μM), EGTA (5 mM), KN62 (30 μM), STO-609 (1 $\mu g\,mL^{-1}$), ML-7 (30 μM), or W7 (20 μM) in the presence of thapsigargin (200 nM) are shown. C) Immunoblot analysis of total lysates from U2foxRELOC cells exposed to DMSO (1 %), W7 (20 μM), Bapta AM (100 μM), EGTA (5 mM), W12 (50 μM), thapsigargin (200 nM), or LY294002 (20 μM) for 1 h. A representative experiment is shown and the relevant proteins are indicated by arrows.

inhibit p110δ,[26] was capable of inducing the translocation of the GFP–FOXO reporter. These data are in agreement with our previous observation that a constitutively active form of p110δ efficiently induced the activation of Akt in Rat1 fibroblasts.[27] However, whether the nuclear shuttling of the FOXO reporter protein on exposure to D000 is due to the specific inhibition of the delta isoform of PI3K remains to be determined.

We tested an extensive panel of chemotherapeutic agents reported to target a variety of cellular macromolecules including topoisomerase I, topoisomerase II, thymidylate synthetase, DNA, tubulin, and cyclin-dependent kinases. However, the majority of these drugs failed to produce nuclear trapping of GFP–FOXO. Although the tubulin-targeting agent paclitaxel has been shown to induce nuclear translocation in MCF7 cells,[28] it had no impact on the subcellular translocation of GFP–FOXO in the U2foxRELOC assay. These differences might be due to the experimental setting or the different cell lines used in these experiments. Indeed, FOXO translocation in MCF7 cells was identified after 16 h in the presence of paclitaxel, whereas U2foxRELOC were exposed to paclitaxel for only 1 h.[28] Conversely, we identified the vinca alkaloid vinblastine as a very potent FOXO translocating agent, active in the low-nanomolar range. Vinblastine is a microtubule-depolymerizing drug whose mode of action has been characterized.[29] Our data suggest that the molecular mechanisms employed for the nuclear translocation of FOXO factors following exposure to the small tubulin-binding molecules paclitaxel and vinblastine differ. Paclitaxel and vinblastine bind to different sites in tubulin and they promote microtubule bundling or microtubule disassembly in vitro, respectively. Whether these contrasting effects on microtubule dynamics account for the different behavior observed in the U2foxRELOC assay remains to be determined.

The inhibition of the Ca^{2+}-binding protein CaM produces the nuclear accumulation of FOXO proteins in cell assays based on the immunodetection of transiently expressed reporter protein.[23] We confirmed this observation using U2foxRELOC, a technology based on the stable expression of a genetically tagged FOXO reporter protein. Importantly, we extended previous data regarding the implication of Ca^{2+}-signaling in the regulation of FOXO transcription factors by analyzing the effect of several chemical probes in the U2foxRELOC assay and on Akt phosphorylation.

Chemical genetic analysis of the Ca^{2+}-dependent regulation of FOXO localization revealed the important role of intra- and extracellular calcium concentrations. Calcium/calmodulin-regulated FOXO-translocation is not directly mediated either by multifunctional or dedicated calcium/CaM-dependent protein kinases, or by upstream CaM-kinase-kinases. This is consistent with a model in which low calcium concentrations decrease the activity of CaM, in turn inhibiting Akt and the translocation of FOXO proteins into the cell nucleus. Akt associates with CaM in mouse mammary carcinoma cells and has been proposed as a CaM-binding protein.[30] However, whether a decrease in CaM-binding induces the nuclear translocation of FOXO proteins by directly affecting Akt activity remains to be explored. CaM expression is altered in several cancers and its inhibition might be a strategy to restore the tumor suppressor activity of the FOXO factors.

In summary, our data demonstrate that U2foxRELOC is a sensitive and robust assay system suitable for identifying small-molecule inhibitors of signaling events that regulate the subcellular localization of FOXO proteins. The signaling events identified here include PI3K/Akt signaling, nuclear export, and calcium/CaM-dependent signaling. This work illustrates the power of chemical genetics combined with image-based cellular screening to analyze signaling pathways. Moreover, our data raise expectations that a more extensive chemical interrogation of the nuclear–cytoplasmic shuttling of FOXO could lead to the identification of new molecular targets and small molecules that might aid the development of more potent therapeutic agents to treat tumors.

Experimental Section

Compound supply and recombinant proteins: A complete list of compounds used in the present study is given in Table 1 of the Supporting Information. The PI3K inhibitors PIK-75 and PI-103 were synthesized according to published patent specifications. UCN01 and flavopiridol were kindly provided by the NCI, National Institutes of Health, cisplatin was provided by C. Navarro, minerval was generously provided by P. Escriba, and gemcitabine was a gift from Eli Lilly Pharmaceuticals (Indianapolis, IN). All other chemicals were purchased from commercial sources. Akt inhibitor, Akt inhibitor VIII, Akt inhibitor X, alsterpaullone, Bapta-AM, Bay11–7082, ionomycin, JAK3 inhibitor VI, JNK inhibitor VIII, kenpaullone, KN62, KN93, LY294002, MG132, ML-7, NL71–101, PD98059, PP1, purvalanol A, ratjadone A, SB202190, SB203580, W-13 HCl, W-7 HCL, W-12 HCL, and wortmannin were purchased from Calbiochem (San Diego, CA, USA). Brefeldin, cyclosporin A, forskolin, genistein, H89, leptomycin B, rapamycin, roscovitine, thapsigargin, tyrphostin AG 1478, tyrphostatin SU1498, and U0126 were purchased from LC Laboratories. (Woburn, MA, USA); D-609, LY83583, manumycin A, pifithrin-α cyclic, rifampicin, tyrphostin AG 82, and tyrphostin AG 1433 were purchased from Alexis Biochemicals (San Diego, CA, USA); Caffeine, calmidazolium chloride, EGTA, etoposide, GW5074, hydrocortisone, nicotinamid, oxaliplatin, paclitaxel, staurosporine, STO-609, 12-O-tetradecanoylphorbol-13-acetate (TPA), trichostatin A, and vinblastine were purchased from Sigma–Aldrich.

Arctigenin, SL327 and SP6000125 were purchased from Biaffin (Kassel, Germany); lithium chloride (LiCl) was purchased from Merck; D000 was purchased from Labotest (Niederschoena, Germany); epidermal growth factor (EGF), and platelet-derived growth factor (PDGF) were purchased from RELIATech A.S. (Braunschweig, Germany) and human insulin-like growth factor-I (IGF-I) and human insulin were purchased from Roche Diagnostics. Stock solutions of the test compounds were deposited in three different concentrations onto 96-well mother plates, transferred to multiple replica plates, and frozen at $-80\,^{\circ}C$.

Generation and maintenance of U2foxRELOC and U2gfpRELOC cells: U2-OS cells obtained from the ATCC were cultivated as indicated. These cells were transfected at confluence with the plasmid containing the GFP–FOXO3a fusion protein (a gift from T. Finkel) as described by Zanella et al,[24] or that containing EGFP alone, by using the effectene transfection reagent (Qiagen). Selection was performed with G418 ($1\,mg\,mL^{-1}$, Calbiochem) for one week and the resistant colonies were then cultured selecting those that best expressed the reporter by FACS, as well as the most homogeneous population. The selected clones, designated as U2foxRELOC or U2gfpRELOC, were then cultured in Dulbecco's modified Eagle's medium (DMEM; Sigma) supplemented with 10% FBS (Sigma), antibiotics (penicillin, streptomycin), antimycoplasm (plasmocin), and G418 at $100\,\mu g\,mL^{-1}$.

Compound administration and relocalization assay: The U2foxRELOC-based assay was formatted in 96-well plates and workflow has been automated. All liquid handling for compound treatment, washing, fixing, and staining steps was performed by a robotic workstation.[31] Clonal U2foxRELOC cells were seeded at a density of 1.0×10^5 cells$\,mL^{-1}$, in black-walled clear-bottomed 96-well microplates (BD Biosciences), in a final volume of $200\,\mu L$ per well distributed by using a multidrop automatic dispenser. Cells were allowed to attach for 12 h at $37\,^{\circ}C$ in an atmosphere of 5% CO_2, and each test compound was then automatically administered to the assay plates in $2\,\mu L$ by using a robotic workstation (Biomek 1000, Beckman). Treated cells were then incubated for 1 h before the culture medium was aspired, the cells were washed with PBS twice, and they were fixed in paraformaldehyde ($100\,\mu L$, 6%) for 30 min at RT. The fixed cells were then washed twice with PBS and stained with DAPI (Invitrogen) for 20 min at RT to define the nucleus. The DAPI solution was removed by aspiration and finally, the plates were washed with PBS twice and stored in the dark at $4\,^{\circ}C$ before analysis. Vital staining with the cell-tracker orange (CMTMR) fluorescent dye (Invitrogen) was performed following the manufacturer's guidelines. As such, cell-tracker orange working solution ($5\,\mu M$) was added to the assay plates and incubated at $37\,^{\circ}C$. After 30 min the dye solution was replaced with fresh medium, and the cells were incubated for another 30 min. Cells were then fixed and processed as described above.

Assay readout: Assay plates were read on the BD Pathway™ 415 Bioimager equipped with a 488/10 nm EGFP excitation filter, a 380/10 nm DAPI excitation filter, a 515 LP nm EGFP emission filter, and a 435 LP nm DAPI emission filter. Images were acquired in the

DAPI and GFP channels of each well by using 20× dry objective. The plates were exposed for 0.066 ms (Gain 31) to acquire DAPI images and 0.55 ms (Gain 30) for GFP images.

Data analysis: Data was exported from the BD Pathway Bioimager as text files and imported into the data analysis software BD Image Data Explorer for processing. The nuclear/cytoplasmic (Nuc/Cyt) ratios of fluorescence intensity were determined by dividing the intensity of the GFP fluorescence from the nucleus by that in the cytoplasm. We applied a threshold ratio of greater than 1.8 to define nuclear accumulation of fluorescent signal for each cell. Based on this procedure we calculated the percentage of cells per well exhibiting nuclear translocation. Compounds that induced nuclear accumulation of the fluorescent reporter above 60% of the signal obtained from wells treated with 20 μM LY294002 were considered as hits.

Western blot analysis: Subconfluent cells were incubated under different conditions and washed twice with TBS prior to lysis. Lysis buffer was added containing 50 mM Tris HCl, 150 mM NaCl, 1% NP40, 2 mM Na_3VO_4, 100 mM NaF, 20 mM $Na_4P_2O_7$, and protease inhibitor cocktail (Roche Molecular Biochemicals). The proteins were resolved on 10% SDS-PAGE and transferred to nitrocellulose membrane (Schleicher & Schuell, Dassel, Germany). The membranes were incubated overnight at 4 °C with antibodies specific for Akt, phospho-Ser-473-Akt (Cell Signaling Technology), phospho-Thr32-FOXO3a (Upstate), and α-tubulin (Sigma), they were washed and then incubated with IRDye800 conjugated anti-mouse and Alexa Fluor 680 goat anti-rabbit IgG secondary antibodies. The bands were visualized by using an Odyssey infrared imaging system (Li-Cor Biosciences).

Acknowledgements

This work was supported by a grant from the Spanish MCyT BIO2002-00197 and the Spanish MEC (project BIO2006-02432). F.Z. is recipient of a Marie Curie Fellowship. The authors acknowledge the supply of PIK-75 and PI-103 synthesized by D. Soilán and R. Álvarez at the Medicinal Chemistry Department, CNIO, the expert technical assistance of E. Gonzalez and F. Blanco, the assistance of the staff at BD Biosciences for their contribution in establishing the technology, and C. Blanco, J. F. Martinez, and O. Renner for helpful discussions and critical reading of this manuscript.

Keywords: antitumor agents · chemical genetics · FOXO · high-throughput screening

[1] A. Barthel, D. Schmoll, K. D. Kruger, G. Bahrenberg, R. Walther, R. A. Roth, H. G. Joost, *Biochem. Biophys. Res. Commun.* **2001**, *285*, 897.
[2] A. Brunet, A. Bonni, M. J. Zigmond, M. Z. Lin, P. Juo, L. S. Hu, M. J. Anderson, K. C. Arden, J. Blenis, M. E. Greenberg, *Cell* **1999**, *96*, 857.
[3] M. Stahl, P. F. Dijkers, G. J. P. L. Kops, S. M. A. Lens, P. J. Coffer, B. M. T. Burgering, R. H. Medema, *J. Immunol.* **2002**, *168*, 5024.
[4] G. J. Kops, R. H. Medema, J. Glassford, M. A. Essers, P. F. Dijkers, P. J. Coffer, E. W. Lam, B. M. Burgering, *Mol. Cell. Biol.* **2002**, *22*, 2025.
[5] N. Nakamura, S. Ramaswamy, F. Vazquez, S. Signoretti, M. Loda, W. R. Sellers, *Mol. Cell. Biol.* **2000**, *20*, 8969.
[6] L. Martinez-Gac, M. Marques, Z. Garcia, M. R. Campanero, A. C. Carrera, *Mol. Cell. Biol.* **2004**, *24*, 2181.
[7] M. C. Hu, D. F. Lee, W. Xia, L. S. Golfman, F. Ou-Yang, J. Y. Yang, Y. Zou, S. Bao, N. Hanada, H. Saso, R. Kobayashi, M. C. Hung, *Cell* **2004**, *117*, 225.
[8] S. Ramaswamy, N. Nakamura, I. Sansal, L. Bergeron, W. R. Sellers, *Cancer Cell* **2002**, *2*, 81.
[9] J. H. Paik, R. Kollipara, G. Chu, H. Ji, Y. Xiao, Z. Ding, L. Miao, Z. Tothova, J. W. Horner, D. R. Carrasco, S. Jiang, D. G. Gilliland, L. Chin, W. H. Wong, D. H. Castrillon, R. A. DePinho, *Cell* **2007**, *128*, 309.
[10] A. van der Horst, B. M. Burgering, *Nat. Rev. Mol. Cell Biol.* **2007**, *8*, 440.
[11] L. P. van der Heide, M. F. Hoekman, M. P. Smidt, *Biochem. J.* **2004**, *380*, 297.
[12] M. K. Lehtinen, Z. Yuan, P. R. Boag, Y. Yang, J. Villen, E. B. Becker, S. DiBacco, N. de La Iglesia, S. Gygi, T. K. Blackwell, A. Bonni, *Cell* **2006**, *125*, 987.
[13] J. Sunayama, F. Tsuruta, N. Masuyama, Y. Gotoh, *J. Cell Biol.* **2005**, *170*, 295.
[14] M. A. Essers, S. Weijzen, A. M. de Vries-Smits, I. Saarloos, N. D. de Ruiter, J. L. Bos, B. M. Burgering, *Embo J.* **2004**, *23*, 4802.
[15] A. van der Horst, A. M. de Vries-Smits, A. B. Brenkman, M. H. van Triest, N. van den Broek, F. Colland, M. M. Maurice, B. M. Burgering, *Nat. Cell Biol.* **2006**, *8*, 1064.
[16] D. Frescas, L. Valenti, D. Accili, *J. Biol. Chem.* **2005**, *280*, 20589.
[17] C. Chaussade, G. W. Rewcastle, J. D. Kendall, W. A. Denny, K. Cho, L. M. Gronning, M. L. Chong, S. H. Anagnostou, S. P. Jackson, N. Daniele, P. R. Shepherd, *Biochem. J.* **2007**, *404*, 449.
[18] J. Bain, L. Plater, M. Elliott, N. Shpiro, C. J. Hastie, H. McLauchlan, I. Klevernic, J. S. Arthur, D. R. Alessi, P. Cohen, *Biochem. J.* **2007**, *408*, 297.
[19] J. W. Mockridge, M. S. Marber, R. J. Heads, *Biochem. Biophys. Res. Commun.* **2000**, *270*, 947.
[20] Y. Taniyama, M. Ushio-Fukai, H. Hitomi, P. Rocic, M. J. Kingsley, C. Pfahnl, D. S. Weber, R. W. Alexander, K. K. Griendling, *Am. J. Physiol. Cell Physiol.* **2004**, *287*, C494.
[21] C. Brantley-Finley, C. S. Lyle, L. Du, M. E. Goodwin, T. Hall, D. Szwedo, G. P. Kaushal, T. C. Chambers, *Biochem. Pharmacol.* **2003**, *66*, 459.
[22] H. Huang, K. M. Regan, Z. Lou, J. Chen, D. J. Tindall, *Science* **2006**, *314*, 294.
[23] T. R. Kau, F. Schroeder, S. Ramaswamy, C. L. Wojciechowski, J. J. Zhao, T. M. Roberts, J. Clardy, W. R. Sellers, P. A. Silver, *Cancer Cell* **2003**, *4*, 463.
[24] F. Zanella, A. Rosado, F. Blanco, B. R. Henderson, A. Carnero, W. Link, *Assay Drug Dev. Technol.* **2007**, *5*, 333.
[25] T. Tanaka, T. Ohmura, H. Hidaka, *Pharmacology* **1983**, *26*, 249.
[26] C. Sawyer, J. Sturge, D. C. Bennett, M. J. O'Hare, W. E. Allen, J. Bain, G. E. Jones, B. Vanhaesebroeck, *Cancer Res.* **2003**, *63*, 1667.
[27] W. Link, A. Rosado, J. Fominaya, J. E. Thomas, A. Carnero, *J. Cell. Biochem.* **2005**, *95*, 979.
[28] A. Sunters, P. A. Madureira, K. M. Pomeranz, M. Aubert, J. J. Brosens, S. J. Cook, B. M. Burgering, R. C. Coombes, E. W. Lam, *Cancer Res.* **2006**, *66*, 212.
[29] B. Gigant, C. Wang, R. B. Ravelli, F. Roussi, M. O. Steinmetz, P. A. Curmi, A. Sobel, M. Knossow, *Nature* **2005**, *435*, 519.
[30] T. B. Deb, C. M. Coticchia, R. B. Dickson, *J. Biol. Chem.* **2004**, *279*, 38903.
[31] A. Rosado, F. Zanella, B. Garcia, A. Carnero, W. Link, *PLoS ONE* **2008**, *3*, e1823.

Received: April 15, 2008
Published online on August 29, 2008

3.2.2 Fifth Project: A large scale RNAi screening for novel genes implicated in FOXO regulation.

Summary

Luciferase-based reporter assays have been widely used for a transcriptional readout of interference with pathways that culminate in the activation or repression of transcription factors. Taking advantage of that technology we generated the 293foxREP system, in which firefly luciferase transcription occurs upon FOXO activation and binding to its recognition sequence, DBE. The assay was adapted to a high throughput fashion to perform a large scale RNAi screening in which genes previously implicated in PI3K/Akt signaling events known to be important for FOXO function appeared as positive hits. This screening also confirmed our chemical genetics results, as calmodulin was obtained as a positive hit. shRNA targeting calmodulin also triggered FOXO3A transcriptional activity, strengthening the notion that inhibition of Calmodulin plays an important role in FOXO activation. Most importantly, we revealed a previously unrecognized FOXO-repressor function of the pseudokinase TRIB2, the mammalian homolog of the drosophila gene *tribbles*. TRIB2 expression was found to be elevated in malignant melanoma and our functional studies suggested that TRIB2 plays a fundamental role in those skin neoplasias by maintaining the tumorigenic potential of those cells.

Personal contribution

I generated the 293foxREP cell-based system and performed the experiments required for its validation and adaptation to the high-throughput format. Once established, I performed the complete screening of the NKI shRNA library, confirmed and validated the hits obtained. The further experiments referring to TRIB2 characterization in the melanoma system were carried out by me with punctual assistance of Beatriz García and Sergio Callejas. All the data analysis and interpretation were carried by me.

Publication:

Zanella F, Renner O, García B, Callejas S, Dopazo A, Carnero A and Link W. **Human TRIB2 is a repressor of FOXO-function required for the maintenance of the malignant phenotype of melanoma cells.** Manuscript currently in preparation.

Human TRIB2 is a repressor of FOXO-function that contributes to the malignant phenotype of melanoma cells

Fábian Zanella[†], Oliver Renner[†], Beatriz García[†], Sergio Callejas[‡], Ana Dopazo[‡], Sandra Peregrina[†], Amancio Carnero[†] and Wolfgang Link[†§]

[†] Experimental Therapeutics Program, Centro Nacional de Investigaciones Oncologicas (CNIO), Melchor Fernandez Almagro 3, 28029 Madrid, Spain.

[‡] Genomics Unit, Centro Nacional de Investigaciones Cardiovasculares (CNIC), Melchor Fernandez Almagro 3, 28029 Madrid, Spain.

[§] To whom correspondence should be addressed. E-mail: wlink@cnio.es

FOXO transcription factors are evolutionarily conserved proteins that orchestrate programs of gene expression known to control a variety of cellular processes such as cell cycle, apoptosis, DNA repair and protection from oxidative stress. Since the abrogation of FOXO function is a key feature of many tumor cells, regulation of the FOXO factors is receiving increasing attention in cancer research. In order to discover genes involved in the regulation of FOXO activity, we performed a large-scale RNAi screen using cell based reporter systems that monitor transcriptional activity and subcellular localization of FOXO. We identified genes previously implicated in PI3K/Akt signaling events which are known to be important for FOXO function. In addition, we discovered a previously unrecognized FOXO-repressor function of TRIB2, the mammalian homolog of the drosophila gene tribbles. A cancer profiling array revealed specific overexpression of TRIB2 in malignant melanoma, but not in other types of skin cancer. We provide experimental evidence that the TRIB2 transcript levels correlate with the degree of the cytoplasmic localization of FOXO3a. Moreover we show that TRIB2 is important in the maintenance of the oncogenic properties of melanoma cells since its silencing reduces cell proliferation, colony formation and wound healing. Tumor growth was also substantially reduced upon RNAi-mediated TRIB2 knockdown in an *in vivo* melanoma xenograft model. Our studies suggest that TRIB2 provides the melanoma cells with growth and survival advantages through the abrogation of FOXO function. Altogether, our results demonstrate the potential of large scale cell-based RNAi screens to identify promising diagnostic markers and therapeutic targets.

Introduction

FOXO transcription factors are *bona fide* tumor suppressors that are inactivated in the majority of human cancers, due to the overactivation of the PI3K/Akt pathway (1). The four members of mammalian FOXO proteins - FOXO1, FOXO3a, FOXO4 and FOXO6 - belong to the class O of the forkhead/winged helix transcription factors (Fox). FOXO proteins can regulate a variety of genes that influence cell proliferation, survival, metabolism and responses to stress (2). The FOXOs are regulated via synthesis, phosphorylation, acetylation and ubiquitination at three different levels: subcellular localization, stability and transcriptional activity (3). Upon the activation of PI3K/Akt, signaling FOXOs undergo Akt-mediated phosphorylation, which promotes binding to 14-3-3, nuclear export via CRM1 and cytoplasmic sequestration. In stress conditions or in the absence of growth or survival factors when the PI3K/Akt pathway is inhibited, FOXO proteins translocate to the cell nucleus, where their transcriptional functions can be executed (4).

Triple knockout mouse models proved the tumor suppressor properties of FOXOs, as mice lacking the principal members of the mammalian FoxO subfamily FoxO1, FoxO3a and FoxO4 simultaneously are prone to develop hemangiomas and lymphoproliferative diseases (5). Conversely, the individual or paired inactivation of FoxO1, FoxO3a or FoxO4 resulted in a less severe phonotype supporting the idea of functional redundancy of these FOXO factors (5). Furthermore, forced expression of FOXO has been shown to curb tumorigenesis in xenograft experiments using human tumor-cell-lines grown in nude mice (6, 7). Therefore, reactivation of FOXO based on its tumor suppressor properties is considered as a very attractive anti-cancer strategy.

Contrary to other tumor suppressors like p53 or PTEN whose functions are abrogated via genetic or epigenetic changes, inactivation of FOXO occurs mostly due to the overactivation of their inhibitory inputs (1). That offers a wide range of possibilities for restoring FOXO activity with small molecule inhibitors targeting up-regulated FOXO repressors. Nevertheless, since FOXO also induces genes involved in resistance to cellular stress, including the multidrug resistance gene ABCB1 (8, 9) such a strategy has to be carefully evaluated and the most suitable points of intervention must be identified. The transcriptional program finally executed by FOXO is thought to be dependent on the pattern of its post-transcriptional modifications (10). Hence, the characterization of the components that participate in the signaling network that controls the activity of FOXO is essential to reveal possible therapeutic targets for future anticancer therapies. In order to identify endogenous suppressors of FOXO which could be exploited pharmacologically to restore FOXO function in human tumors we conducted a systematic large-scale loss-of-function screening. Among the genes identified and validated as negative FOXO regulators we found the pseudokinase TRIB2. *In vitro* and *in vivo* results reported here indicate that TRIB2 can facilitate the growth and survival of melanomas by downregulating FOXO activity

Results

Generation of the assay cell line 293foxREP

FOXO proteins bind to TTGTTTAC FOXO responsive enhancer element, generally referred to as daf-16 family protein-binding element, DBE (11) and drive transcription of downstream genes. In order to establish a cell line capable of measuring the transcriptional activity of FOXO and suitable for a transfection-based RNAi screening we introduced the reporter construct pGLpuro-3xDBE (Zanella et al, in press) into HEK293T cells. pGLpuro-3xDBE contains three copies of the DBE consensus cassette in front of a SV40 minimal viral promoter linked to a luciferase reporter gene and a puromycin-resistance cassette (Fig S1A). Stable 293foxREP cells displayed a strong responsiveness to the inhibition of the PI3K/Akt pathway (Fig. S1B) and hence proved to be suitable tools to screen for the interference with FOXO regulation.

Screening of a RNAi library against 7914 human genes

The identification of components implicated in the regulatory network that determines the activity of FOXO proteins is an essential step to develop targeted therapies that reactivate specific FOXO functions in human tumors. Hence we performed a large scale loss of function screen aimed at the identification of genes that suppress transcriptional activity and the nuclear localization of FOXO transcription factors (Fig. S2). We employed a vector-based RNAi library with 23742 shRNAs against 7914 genes that has been widely used for target discovery efforts (12, 13). We introduced these shRNA constructs in pools of three RNAi per gene into 293foxREP cells and monitored the activation of firefly luciferase, normalizing these values against the luminescence that resulted from *Renilla* luciferase. Those pools of shRNAs that caused activation of normalized luciferase activity greater than three fold when compared with the control shRNA vector were analyzed for its capacity to induce nuclear translocation of FOXO in the U2foxRELOC system that has been described previously (14). Briefly, U2foxRELOC cells stably express a GFP-tagged version of FOXO3a to monitor the subcellular localization of FOXO proteins. We prioritized those hits scoring positive in both 293foxREP and U2foxRELOC cells (Table 1). Among these dual hits were several genes known to be part of the PI3K/Akt signalling cascade, including PIK3CA and Akt-3, indicating the specificity of our screening strategy. Importantly, several genes previously not associated with the regulation of FOXO activity were identified.

Validation of TRIB2 silencing

The RNAi mediated silencing of TRIB2, the human homolog of the *Drosophila* gene tribbles, resulted in the induction of FOXO-dependent transcription in 293foxREP cells and the nuclear translocation of GFP-FOXO in U2foxRELOC cells. We isolated and verified the sequences of the corresponding shRNA pool. qPCR analysis revealed that two of the three shRNAs of the silencing pool were capable of reducing TRIB2 transcript levels. In order to validate our findings with independent RNAi agents against TRIB2, we analyzed different siRNA oligonucleotides as well as vector based shRNA constructs for their efficiency to silence the expression of TRIB2. These shRNAs and siRNAs were chosen to contain different sequences 5´-portion of the guide strand which has been implicated in unintended transcript silencing (15) Several RNAi-based agents effectively reduced the expression of TRIB2 (Table S1). Two different vector based shRNA constructs - TRIB2^{NKI} shRNA and TRIB2^{ORI} shRNA - proved to be the most efficient tools to silence TRIB2 and were used for further analysis. Figure 1A shows the reduction of TRIB2 mRNA upon the transfection of HEK293T cells with TRIB2^{NKI} shRNA as compared with cells transfected with the corresponding control vector. Importantly, the transient expression of TRIB2^{NKI} shRNA resulted in increased FOXO-driven luciferase activity (Fig. 1B). and the nuclear localization of GFP-FOXO (Fig.1C and D). In contrast, unrelated shRNA sequences failed to produce similar effects on FOXO (data not shown). On the other hand, the overexpression of a V5-tagged versions of TRIB2 which was detected by western blot analysis using a V5-specific antibody (Fig 2A) markedly decreased FOXO-driven luciferase activity in 293foxREP cells (Fig. 2B). These results suggest that TRIB2 act as a repressor of FOXO promoting its cytoplasmatic sequestration and impairing its transcriptional functions.

TRIB2 transcript levels are elevated in malignant melanoma

The implication of TRIB2 in the regulation of the tumor suppressor FOXO prompted us to analyze its expression levels in human tumors. To that end, we used a cancer profiling array containing samples from 154 patients with different tumors including breast, ovary, colon, stomach, lung, kidney, bladder, vulva, prostate, uterus, cervix, rectum, thyroid, testis, skin, small intestine and pancreas. For this array, cDNAs generated from matched normal and tumor tissue samples from individual patients had been spotted side by side on a nylon membrane. In addition cDNAs from nine different cancer cell lines have been included (Figure S3). Interestingly, elevated levels of TRIB2 mRNA were observed in seven out of ten skin cancer samples (Fig. 3A and B). Moreover, the seven samples that showed high TRIB2 expression correspond to malignant melanoma lesions (Fig. 3A: P1-P5, P9; P10) while the remaining three samples (Fig. 3A: P5, P6 and P7) that did not display a significant increase of TRIB2 transcripts refer to squamous-cell carcinomas (Table S2). Consistently, we detected the highest levels of TRIB2 transcripts in G-361 melanoma cells when compared to eight other non-melanoma cells represented on the same membrane (Fig. 3C and D). In order to confirm this observation we analyzed an independent arrayed panel of 43 prenormalized cDNAs selected from normal and melanoma tissues and from mixed ages and genders (Table S3). qRT-PCR analysis of these samples revealed a significantly increased level of TRIB2 expression in malignant melanoma diagnosed at stage III or IV when compared with normal skin tissues (Figure S2C). The same pattern was reproduced when the mRNA level of TRIB2 was analyzed in a panel of melanoma cell lines versus non-melanoma cell lines by qRT-PCR. We detected an abundance of TRIB2 transcripts between three and 23 times greater in cell lines derived from melanoma biopsies than in non-melanoma cells including keratinocytes and fibroblasts (Fig. 4A). Interestingly, human epidermal melanocytes also displayed high levels of TRIB2 transcripts. The levels of Bim, a pro-apoptotic molecule transcriptionally regulated by FOXO were also assessed. We observed a direct inverse correlation between the transcript levels of TRIB2 and Bim (Fig. 4B). In human epidermal melanocytes and melanoma cells high expression of TRIB2 coincides with very low levels of Bim transcripts. In contrast, non-melanoma cell lines with low level of TRIB2 transcription displayed increased abundance of Bim transcripts. Taken together these data suggest that the overexpression of TRIB2 leads to the reduction of FOXO-dependent transcriptional activity in melanocyte- derived cells.

TRIB2 is regulated by calcium signalling in melanoma

TRIB2 has been previously reported to be a highly inducible gene under specific cellular conditions (16, 17). To investigate the mechanisms and signalling events that are implicated in TRIB2 activation in melanoma we treated G-361 cells with a panel of inhibitors or activators of known signalling cascades for 6 hours and total mRNA has been extracted for qRT-PCR analysis. Interestingly, the treatment of G-361 melanoma cells with thapsigargin and caffeine, two agents that have been shown to initiate a rise in intracellular Ca^{2+} significantly increased in the levels of TRIB2 transcripts (Fig 5). The results obtained here suggest that calcium signalling might be responsible for the elevated level of TRIB2 transcripts in melanocyte-derived cells.

TRIB2 knockdown increases the activity of FOXO in melanoma

To assess the influence of TRIB2 on FOXO functions in melanoma, G-361 human melanoma cells were adopted as a model, as they display increased levels of TRIB2 mRNA (see above). G-361 cells stably expressing a GFP-FOXO3a fusion protein and the FOXO-driven luciferase reporter construct pGL3puro-3xDBE, hereafter designated as G-361FireFox, were transiently transfected with shRNA agents against TRIB2, PIK3CA, Akt or their respective empty control plasmids. A significant increase in luciferase-produced luminescense was detected upon silencing of TRIB2, coincident with the nuclear relocalization of the GFP-FOXO fusion protein. The effect obtained was comparable to FOXO stimulation via the knockdown of PI3K or Akt (Fig 6). These data support the hypothesis that TRIB2 may function as a FOXO repressor and proves this model to be suitable to analyze the role of TRIB2 in malignant melanoma.

TRIB2 facilitates the growth and survival of melanoma cells

In order to investigate the importance of TRIB2 for melanoma cells, we developed a stable knockdown system for TRIB2. G-361 melanoma cells were transfected either with a control vector or with a shRNA against TRIB2. Stable cells were isolated via puromycin selection resulting in the cell lines 361C and 361shTRIB, respectively. TRIB2 mRNA levels in these cell lines were monitored by qRT-PCR. Figure 7A shows that continuous silencing of TRIB2 in 361shTRIB cells led to a tenfold decrease of TRIB2 mRNA compared to the transcript level in 361C cells.

In order to explore the role of TRIB2-mediated FOXO inactivation in melanoma we assessed the tumorigenic properties of the generated melanoma knockdown system. 361C and 361shTRIB cells were seeded in triplicates in 6-well plates, maintained in standard growth factor conditions and cell growth was monitored every other day by crystal violet staining. At day 10 cells were lyzed and the measured absorbance of the lysis products was taken as an indirect measurement of the cell growth at each day. 361shTRIB cells showed a significantly decreased proliferation rate when compared to 361C cells (Fig. 7B), indicating that TRIB2 expression confers growth advantage to those melanoma cells. To determine whether TRIB2 influences the ability of melanoma cells to overcome apoptosis in the absence of cell contact, 10^4 361C or 361shTRIB cells were seeded at low density in 10 cm plates in triplicates and allowed to grow over a period of 10 days when cells were fixed, stained and the number of colonies was quantified. 361C cells were considerably more efficient in bypassing the barriers of low density seeding than 361shTRIB cells, as the latter generated a significantly reduced number of colonies in this assay (Fig. 7C).

The ability of these cells to grow in anchorage-independent conditions was analyzed by seeding 10^5 cells from both cell lines in soft agar and allowing them to grow for one month. Importantly, 361C cells produced a significantly greater number of foci than 361shTRIB cells (Fig. 7D). Furthermore, the foci formed by 361shTRIB cells displayed increased size and pigmentation (Fig 7E).

To investigate the influence of TRIB2 in the migration properties of melanoma cells, both cell lines were seeded in 24 well plates and allowed to reach confluence. At that point, a wound was produced in the central vertical axis of each well, the growth medium was replaced and a fixed point of reference for microscopic photography was set. Pictures taken every 24 hours indicated a greater efficiency of 361C cells in refilling the wounded area, closing of the wound over a period of 72 hours, while 361shTRIB cells were unable to refill the wounded area even 96 hours after the wound had been created. (Fig. 7F). Furthermore, 361shTRIB cells showed contact inhibition upon reaching confluence, while 361C cells piled up and formed colonies beyond the cell monolayer, a feature of transformed cells. Taken together, these results support the hypothesis that TRIB2 is necessary for the maintenance of the tumorigenic properties of melanoma cells.

TRIB2 knockdown impairs melanoma growth *in vivo*

To investigate the possible effects of TRIB2 knockdown in a tumorigenic process *in vivo*, 7 x 10^5 361C or 361shTRIB cells respectively were xenografted subcutaneously in ZSCID mice, and their respective tumor growth was followed over a period of 10 weeks. Once a week, tumors were measured and their volumes calculated as described in Material & Methods. Tumor development occurred significantly faster in those mice injected with control cells (361C) when compared with animals in which TRIB2 knockdown cells (361shTRIB) have been implanted (Fig 8A). Except for time point day 34, the comparison of the tumor volumes of the two mouse cohorts was statistical significant. The p-values for the time points day 41 to day 69 were 0.0075, 0.0024, 0.0082, 0.0149, and 0.0080, respectively. On day 69 pictures taken from the animals before sacrifice and after tumor resection show a clear difference in the *in vivo* growth potential of the cell populations implanted (Fig 8B). While 361C cells produced larger, spherical tumors 361shTRIB cells could rarely grew beyond a few mm^3.

Discussion

The advent of RNA-mediated interference (RNAi)-based functional genomics in mammals paved the way for unbiased screens in human cell systems. In the present work we report a large scale loss of function screen aimed at the identification and validation of gene targets involved in the framework of signalling events that control the activity of FOXO transcription factors.

Based on two independent cell-based systems which were shown to effectively report FOXO-dependent transcriptional activity and the subcellular localization of GFP-FOXO fusion protein, we screened a vector-based RNAi expression library that direct the synthesis of short hairpin RNAs targeting 7,914 different human genes for suppression. Those genes whose silencing produced positive hits in both screening systems were included in the high confident list of FOXO suppressors. PIK3CA and Akt-3, both components of the canonical PI3K/Akt pathway were among these selected genes. Interestingly, silencing of the Ca^{2+}-binding protein Calmodulin 2 increased FOXO driven luciferase activity and induced nuclear translocation of FOXO reporter protein. These data are in agreement with the previous observation that inhibition of Calmodulin by its specific small molecule inhibitors W7, W13 and Calmidazol led to the nuclear accumulation of FOXO (14) and strengthens the notion that calcium signaling is an important factor influencing the subcellular localization of FOXO. The presence of genes within our priority list that are known to be involved in the regulation of FOXO validated the specificity of our screening systems. Among the genes that have not been associated previously with FOXO functions we identified TRIB2, the human homolog of the Drosophila gene tribbles. Tribbles has been reported to regulate ventral furrow formation in Drosophila through binding to String/CDC25 (2). The three human orthologs of tribbles, namely TRIB1, TRIB2 and TRIB3 share a strong similarity in their peptide sequence, consisting essentially of their pseudokinase domain (16, 18).

We found TRIB2 highly expressed specifically in melanoma malignancies, melanocyte-derived cells and melanoma cell lines. Interestingly, overexpression was not observed in samples from other tumor sources, including non-basal skin carcinoma. Our data suggest a potential use of TRIB2 as a diagnostic marker for detection of malignant melanoma, although more studies are needed to confirm its utility as a tool in a diagnostic setting. Further experiments including a larger patient cohort with survival information also must elucidate its clinical significance.

The regulatory mechanisms that maintain high TRIB2 expression in melanocyte-derived cells remain unknown at present. TRIB2 expression might be regulated by lineage-specific signaling events such as the signal transduction cascade initiated by c-kit shown to modulate the activity and stability of the tissue-restricted dimeric transcription factor MITF (19).

We identified several features within the TRIB2 gene including an ATTTA potential mRNA destabilizing element in the 3'-untranslated region (20) and several conserved binding sites for inducible transcription factors in the promoter region that suggest its regulation at the transcript level .

The fact that the TRIB2 mRNA expression is increased upon the treatment with compounds which increase the intracellular concentration of calcium, namely thapsigargin and caffeine suggests that calcium signaling might be involved in the molecular events that lead to the high expression level of TRIB2 in melanocyte-derived cells. Interestingly, recent studies reported the overexpression of Ca^{2+} channels and elevated intracellular Ca^{2+} influx in human melanoma cell lines (21, 22). Our data presented here, together with our previous findings on the implication of calcium in the regulation of FOXO (14) support the hypothesis that high level of intracellular calcium leads to the inactivation of FOXO proteins through the activation of the FOXO repressors calmodulin and TRIB2.

Malignant melanoma is one of the most aggressive human tumors that arise from the malignant transformation of melanocytes, the pigment-producing cells that reside in the basal epidermal layer in human skin. Several signaling pathways are thought to exert key functions in melanoma development and progression, including Ras-Raf-MEK-ERK (MAPK) and the PI3K/Akt signaling pathways (23). A recent study reported the upregulation miR-182 in melanoma cell lines and tissue samples promoting the repression of FOXO3a (24). Interestingly, ectopic expression of a non-phosphorylable, constitutively nuclear form of FOXO has been shown to induce apoptosis in A375 melanoma cells (25).

In the present study we provide strong evidence for an alternative mode of FOXO inactivation in melanocyte-derived and melanoma cells through overexpression of TRIB2. One appealing possibility is that downregulation of FOXO activity through TRIB2 is one of the elusive intrinsic survival features of paternal melanocytes that determines the aggressive and highly resistant behavior of melanocyte-derived malignancies nourished by additional alterations acquired during tumor progression (26).

In functional assays we could show that suppression of TRIB2 protein in melanoma cells resulted in a significant decrease in cell proliferation, cell migration and anchorage-independent growth. Thus, high TRIB2 expression could contribute to the formation and progression of melanoma lesions. Consistently, retroviral expression of TRIB2 has been shown to immortalize hematopoietic progenitors and TRIB2-reconstituted mice uniformly developed fatal transplantable acute myelogenous leukemia (27). Our study further reveals that *in vivo* tumor formation of G361 cells in immunocompromised mice was impaired upon silencing of TRIB2. Taken together, our data lead to the conclusion that TRIB2 can promote the growth of melanoma cells and support *in vivo* tumorigenesis of those cells. Future experiments should determine whether TRIB2 is part of the differentiation program of normal melanocytes which predisposes their transformed derivatives to forming aggressive tumors (28).

In summary, sophisticated cell based screening systems allowed us to systematically interrogate the signaling network that controls the activity of FOXO proteins and to identify possible targets for the restoration of FOXO functions independent of preconceived notions of mechanistic relationships. Our work identifies TRIB2 as a suppressor of FOXO activity overexpressed in malignant melanoma and provides evidence that TRIB2 contributes to the maintenance of the malignant phenotype of melanoma cells. Thus, further investigation on the role of TRIB2 in the pathogenesis of melanoma lesions may provide new therapeutic insights into this most aggressive form of skin cancer resistant to all standard anticancer therapies.

Materials and Methods

Reagents and plasmids

The PI3K inhibitor PI-103 was synthesized following published patent specifications. All other chemicals were purchased from commercial sources. Akt Inhibitor X, Bapta-AM, JNK Inhibitor V, LY294002, PD98059, SB203580, were purchased from Calbiochem (San Diego, CA). Forskolin, Thapsigargin and U0126 were purchased from LC Laboratories. (Woburn, MA, U.S .A.); Caffeine, and GW5074 were purchased from Sigma-Aldrich (St. Louis, USA). SP6000125 were purchased from Biaffin (Kassel, Germany); human insulin was purchased from (Roche Diagnostics, Mannheim, Germany). The NKI shRNA libray was provided by R. Bernards. The RNAi agents to validate TRIB2 silencing were purchased from Applied Biosystems, Thermo Fisher Scientific and OriGene. The sequences of the shRNAs and siRNAs are shown in table S1. The RNAi constructs targeting PIK3CA or Akt carried the small hairpin RNAs 5´-AAAAA GACCATCATCAGGTGAACTTCTCTTGAAAGTTCACCTGATGATGGTCGG-3´ or 5´-AAAAAGGAGATCATGCAGCATCGCTCTCTTGAAGCGATGCTGCATGA TCTCCGGG-3´ respectively, in the pRS vector backbone (Berns et al)

The wild type form of FOXO3a cloned into a pCL-neo vector as well as a constitutively active construct FOXO3a-A3, in which three PI3K-dependent phosphorylation sites have been mutated to alanine was kindly provided by Dr. M. Hu (University of Texas M. D. Anderson Cancer Center, Houston).

TRIB2 cDNA was amplified from HEK293T cells by PCR with primers 5’-CACCATGAACATACACAGGTCTACCCCCATC-3’ and 5’- GTTAAAGAAAGG GTCCAAGTTCTCTTCC-3’ to be cloned into a pCDNA/V5/GW/D-TOPO vector. Subsequently, PCR was used to amplify TRIB2-V5 with primers 5’-AGCGGCTAGCACCATGAACATACACAGGTCTACCCCCATC-3’ and 5’-ACG CGGATCCCTAACCGGTACGCGTAGAATCGAGACC-3’, and the resulting fragment was cloned into a pIRESpuro2 vector.

Cell culture

U2-OS, HEK293T, A375, Hs895T, Sk-Mel-94, Sk-Mel-19, UACC-257, Hs 895 T, Sk-Mel-147, VA-13 and HACAT cells were obtained from the American Type Culture Collection (ATCC) and cultivated in Dulbecco’s Modified Eagle’s medium (DMEM) (Sigma), supplied with 10% Fetal Bovine Serum (FBS). Sk-mel-5, Sk-mel-28, UACC62 and M14 cells were obtained from ATCC and cultivated in RPMI supplemented with 10%FBS (Sigma). G-361 cells obtained from the ATCC were maintained in Mc Coy's 5A medium complemented with 10% FBS. Previously described U2foxRELOC cells (29) stably expressing a plasmid containing a FOXO3a-GFP fusion protein were cultivated in 10% FBS DMEM with 100ug/ml G-418 (Gibco). Human epidermal melanocytes were obtained from Cascade Biologics and maintained in medium 254 (Cascade Biologics) supplemented with HMGS (Cascade Biologics). Cell cultures were maintained in a humified incubator at 37ºC with 5% CO_2.

Generation of 293lucRep Cells

HEK293T (human embryonic kidney) cells were cultivated to appropriate confluence and transfected with a plasmid containing 3 copies of the DBE sequence cloned upstream of firefly luciferase cDNA, as well as puromycin resistance cassette (pGL3-DBE3X-Luc-Puro) (Zanella et al,,in press). After selection with puromycin, resistant clones were sub-cultivated in order to be assayed for luciferase expression. The cell clones were assayed for luciferase activity and responsiveness to the inhibition of PI3K/Akt signaling. The most suitable clone was selected as the assay cell line and designated 293foxREP.

Preparation of the shRNA library

Prior to its transfection the bacteria cultures of the arrayed shRNA library were replicated and purified. The replication was carried out using a Biomek FX liquid handler (Beckman-Coulther). The plasmids contained in the bacterial cultures were purified using the Montage plasmid extraction kit of Millipore adapted to a vacuum manifold preceded by a preclearing with the Wizard SV96 lysate clearing plates of Promega.

Western Blot analysis

Cells were grown in a 10 cm plate until confluence and washed twice with cold TBS and lysed with 1 ml of a solution containing 50mM Tris-Cl, 150mM NaCl, 1% Igpal, 10 ug of Aprotinin and 10 ug of Leupeptin. A pan proteases inhibitor (Roche) and a pan phosphatase inhibitor (Roche) were also used, according to manufacturers instructions. Protein amounts were quantified using the Bio Rad Protein Assay, absorbance at 590 nm was measured in a Victor3a (Perkin Elmer) plate reader. 100ug of total protein were loaded in a 7,5% SDS-PAGE and ran for 1 h at 150 V, in a Bio Rad system. Transference to a nitrocellulose membrane was carried in a Bio Rad System, at 200 mA, for 2 hours. After transference, nitrocellulose membranes were blocked in a infra-red specific solution (Li-Cor) for a minimum of 4 hours, at 4ºC. Incubation with the primary antibodies was carried for 4-12 hours, at 4ºC with constant shaking.

TRIB2 levels were probed using an anti-V5 antibody (Invitrogen) and α-tubulin levels were probed as a loading control with a commercially available antibody (Sigma). All the dilutions used were indicated in the manufacturers instructions.

Luciferase Assays

2 X 10^5 293foxREP cells were seeded per well in transparent round-bottom 96-well plates (Nunc), and allowed to attach for at least 6 hours at 37°C with 5% CO2, before transfection. Once attached, cells were co-transfected with 25ng of

the pCDNA3 vector containing cDNA for FOXO3a, 50 ng of the commercially available pRG-TK vector (Promega), containing *Renilla* Luciferase cDNA for normalization of results, and 25 ng of the empty pSuperRetro vector (in the case of controls and wells to be treated with LY294002), or pSuperRetro containing shRNAs against PI3K and Akt, or each shRNA pool contained in the library plate. All transfection experiments were performed in triplicates, with Effectene transfection reagent (Qiagen) following the manufacturers' instructions. All liquid handlings were performed automatically in a Biomek 2000 station (Beckman & Coulter). After transfection cells were incubated for 48 hours prior to LY294002 administration, when mentioned. Following incubation automated luciferase assays were carried out using the Dual-Luciferase Reporter Assay System (Promega), according the manufacturer's instructions on a multilabel plate reader (Wallac Victor**,** Perkin-Elmer), and the ratio of *firefly*-to *Renilla*-luciferase activities was calculated. For triplicate experiments the average value has been calculated to be presented as the final result.

HCS Assays

U2foxReloc cells were seeded at a density of 10^5 cells/ml into black-wall clear-bottom 96-well microplates (BD Biosciences) with a multidrop automatic dispenser, to a final volume of 200µl per well. Cells were then allowed to attach for 12 h at 37°C with 5% CO_2, and transfected as mentioned above. The cells were then incubated for 48 hours prior to aspiration of culture medium, washing with 1X PBS twice and fixation in 100µl of 6% paraformaldehyde for 30 min at room temperature (RT). After aspiration of the paraformaldehyde, fixed cells were washed twice with 1X PBS and stained with DAPI (Invitrogen) for 20 min at RT for cell nucleus definition. DAPI solution was removed by aspiration, and finally the plates were washed with 1X PBS twice and stored at 4ºC before analysis.

Assay plates were read on the BD Pathway™ 855 Bioimager as previously reported (29, 30). Images were acquired in the DAPI and GFP channels of each well using 10X dry objective. The nuclear/cytoplasmic (Nuc/Cyt) ratios of fluorescence intensity were determined by dividing the intenstity of the GFP fluorescence of the nucleus by the cytoplasmic. We applied a threshold ratio of greater than 1.8 to define nuclear accumulation of fluorescent signal for each cell. Based on this procedure we calculated the percentage of cells per well displaying nuclear translocation.

Cancer profiling Array

TRIB2 cDNA was PCR-amplified with primers 5´-AGCGAAGCTTACCATGAAC-ATACACAGGTCTACCCCCATC-3´ and 5'-ACGCGGATCCCTGTTAAAGAAA-GGGTCCAAGTTCTCTTCC-3', resulting in a 950 bp fragment which was purified with Phenol/Chloroform. 25 ng of this probe were radioactively labeled in a mix of 10ul of labeling buffer (Promega), 2 ul of 10mg/ul BSA, 2ul of a solution containing 5mM of dATP, dGTP and dTTP nucleotides, 5ul of ^{32}P-labelled dCTP-Nucleotides (Amersham), and 30 units of the Klenow polymerase (Promega) for 2 hours at 37ºC. After purification of the radiolabeled probe in a NICK column (Amersham) following the manufacturers' instructions, the probe was boiled for 3 min at 100ºC, transferred to ice and hybridized overnight to the Cancer Profiling Array II membrane (BD biosciences) previously incubated with 10 ml of a solution containing 5X SSPE, 2,5X Denhardts solution, 0,25% SDS and 0,15 mg/ml salmon sperm DNA. The membrane was then washed for 20 min 2 times with 2XSSPE, 0,1% SDS, once with 1XSSPE, 0,1% SDS and finally with 0,1XSSPE, 0,1% SDS, at 65ºC. Following the washing steps the membrane was exposed to an Amersham Phosohor Screen overnight and scanned in a Typhoon 9400 Variable Mode Imager (Amersham). After stripping off the probe specific for TRIB2, the membrane was re-hybridized with a probe specific for the housekeeping gene Ubiquitin. Quantification of TRIB2 levels was carried in the Quantity One software version 4.5.2 (BioRad), using the signal obtained for ubiquitin for normalization. For each patient, samples were normalized against their respective ubiquitin signal and the tumoral samples were normalized against their corresponding normal tissue samples.

Quantitative RT-PCR

Total RNA was extracted using TRI-Reagent (Sigma), according to the manufacturers' indications. After RNA isolation DNAse I (Roche) treatment was performed using 40 units of enzyme in the presence of 40 units of RNAse inhibitor (Roche) per sample, at 37ºC, for 1h. Following Phenol-Chloroform purification RNAs were quantified in a NanoDrop® 1000 spectophotometer quality-checked in a MOPS-1,2% Agarose gel and cDNA synthesis was carried out using the High Capacity cDNA Reverse Transcription Kit (Applied Biosystems) using 1 ug of total RNA as starting material for each sample. PCR reactions were set up in 96-well optical plates (Applied Biosystems) and run in a ABI PRISM® 7900HT sequence detection system (Applied Biosystems). Reaction mix was prepared as using 1x SYBRGreen Master Mix (Applied Biosystems), 50nM of each primer [TRIB2: 5'-GCCAGACTGTTCTACCAGATT-

GC-3' (forward) and 5'- GCTTGACCCGAGT-CCTCTCTT-3' (reverse). GAPDH: 5'-ATCACCATCTTCCAGGAGCG-3' (forward) and 5'- CCTGCAAATGAGCC-CCAG-3' (reverse) Bim: 5'-CACAAAA-CCCCAAGTCCTCCTT-3' (forward) and (5'-TTCAGCCTGCCTCATGGAA-3' reverse)] and 100ng of cDNA in a final volume of 50ul. Cycling conditions were set to 10 min at 95ºC followed by 40 cycles of 15 sec at 95ºC and 1min at 60ºC. Identical PCR conditions were used with the human melanoma TissueScan™ Tissue qPCR Array (OriGene). Finally, a dissociation curve was carried out to check specificity of amplification. Results were analyzed and the relative mRNA quantity calculated using the qBasePlus software (31). TRIB2 levels were quantified using GAPDH or 18S RNA expression levels for normalization.

Generation of 361C and 361shTRIB cells

G-361 cells were transfected at 70-80% confluency using the Effectene (QIAGEN) reagent, according to the manufacturers indications either with an empty pSuperRetro vector (361C) or with the validated TRIB2^{NKI} shRNA (361shTRIB). After selection with Puromycin, both cell populations were maintained in Mc Coy's 5A Medium supplemented with 10% FBS and 0,5 ug/ml puromycin.

Proliferation and Doubling time Assay

361C and 361shTRIB cells were seeded in triplicates at a density of 10^4 cell/well in 6-well plates. After 24 hours growth medium was changed (day 0) and a point of the curve was taken every second day. For each point of the curve, cells were fixed with 0,5% glutaraldehyde for 30 min and stained with 1%

crystal violet. After washing for removal of excess of dye cells were lysed with 15% acetic acid and the lysis products were transferred to clear bottom 96-well plates, (Nunc) and the absorbance at 590 nm wavelength was measured in a Victor3 (Perkin Elmer) plate reader. The relative number of cells was determined as a direct measurement of the absorbance obtained in each well. Doubling time has been calculated at exponential growth.

Clonogenic Assay

361C and 361shTRIB cells were seeded in triplicates at a density of 10^4 cells/well in 10 cm plates. Growth medium was changed every second day and cells were allowed to grow for a period of 10 days. At day 10 cells were fixed with 0,5% glutaraldehyde for 30 min and stained with 1% crystal violet. After washing for removal of excess of dye, colonies were counted.

Growth in Soft Agar

The anchorage-independent growth of 361C and 361shTRIB cells was analyzed by seeding triplicates of 4 x 10^5 cells/well of each population in 1.4% agarose D-1 Low EEO (Pronadisa) growth medium containing 10% FBS, disposed onto previously solidified base of growth medium containing 2.8% agar (agarose D-1 Low EEO, Pronadisa) in a 6-well plate. Once the soft agar had been solidified 1 ml of growth medium was added. After 24 hours, media containing 10% FBS was added to each well and renewed twice weekly. Colonies were scored after one month of growth. Photographs were taken in a Olympus CK40 microscope equipped with a Olympus DP12 camera at 40X magnification.

Wound Healing Assays

361C and 361shTRIB cells were seeded in triplicates at a density of 5 x 10^5 cells/well in 24-well plates and allowed to attach overnight. Following attachment a wound was produced in the cell monolayer with a 10ul pipette tip, growth medium was replaced and a picture was taken (Day 0) in a Olympus CK40 microscope equipped with a Olympus DP12 camera at 40X magnification. Pictures were taken every 24 hours in the same fields, until the time point in which the wound from a given group was totally closed.

Xenografts

ZSCID mice were injected with 7 x 10^5 361C and 361shTRIB cells and the growth of the resulting tumours was followed by direct measurement of tumour volume every 7 days over a total period of 69 days. The smallest and the largest diameter of tumors were mearsured with a digital caliper, and tumor volumes were calculated using the following formula: volume (mm3) = [(smallest diameter) 2 x (lagest diameter)] / 2. All values were presented as means ± SE. The unpaired t-test (two-tailed) was performed for statistical analysis using the GraphPad PRISM® Version 4.0 program. The photos of the animals and their respective tumors were taken at day 69, before animal sacrifice and after tumor dissesection. All animal procedures were conducted according to the experimental protocol approved by the Institutional Committee for Care and Use of Animals of the Spanish National Cancer Research Centre which complies with European legislation on the care and use of animals, NIH guidelines for the use of laboratory animals, and related codes of ethic practice.

Acknowledgments

This work was supported by a grant from the Spanish MEC (project BIO2006-02432). F. Z. is recipient of a Marie Curie Fellowship. The authors acknowledge the expert technical assistance of D. Megias, J. C. Cigudosa, J. Monsech and O. Dominguez. We are indebted to R. Bernards for advice and for providing us with the NKI shRNA library.

References

1. Dansen, T. B. & Burgering, B. M. (2008) *Trends Cell Biol* **18,** 421-9.
2. Huang, H. & Tindall, D. J. (2007) *J Cell Sci* **120,** 2479-87.
3. Myatt, S. S. & Lam, E. W. (2007) *Nat Rev Cancer* **7,** 847-59.
4. Brunet, A., Bonni, A., Zigmond, M. J., Lin, M. Z., Juo, P., Hu, L. S., Anderson, M. J., Arden, K. C., Blenis, J. & Greenberg, M. E. (1999) *Cell* **96,** 857-68.
5. Paik, J. H., Kollipara, R., Chu, G., Ji, H., Xiao, Y., Ding, Z., Miao, L., Tothova, Z., Horner, J. W., Carrasco, D. R., Jiang, S., Gilliland, D. G., Chin, L., Wong, W. H., Castrillon, D. H. & DePinho, R. A. (2007) *Cell* **128,** 309-23.
6. Hu, M. C., Lee, D. F., Xia, W., Golfman, L. S., Ou-Yang, F., Yang, J. Y., Zou, Y., Bao, S., Hanada, N., Saso, H., Kobayashi, R. & Hung, M. C. (2004) *Cell* **117,** 225-37.
7. Cheng, J. Q., Lindsley, C. W., Cheng, G. Z., Yang, H. & Nicosia, S. V. (2005) *Oncogene* **24,** 7482-92.
8. Vlahos, C. J., Matter, W. F., Hui, K. Y. & Brown, R. F. (1994) *J Biol Chem* **269,** 5241-8.
9. Gomes, A. R., Brosens, J. J. & Lam, E. W. (2008) *Cell Cycle* **7,** 3133-6.
10. Calnan, D. R. & Brunet, A. (2008) *Oncogene* **27,** 2276-88.
11. Furuyama, T., Nakazawa, T., Nakano, I. & Mori, N. (2000) *Biochem J* **349,** 629-34.

12. Berns, K., Hijmans, E. M., Mullenders, J., Brummelkamp, T. R., Velds, A., Heimerikx, M., Kerkhoven, R. M., Madiredjo, M., Nijkamp, W., Weigelt, B., Agami, R., Ge, W., Cavet, G., Linsley, P. S., Beijersbergen, R. L. & Bernards, R. (2004) *Nature* **428,** 431-7.
13. Bernards, R., Brummelkamp, T. R. & Beijersbergen, R. L. (2006) *Nat Methods* **3,** 701-6.
14. Zanella, F. & Carnero, A. (2008) *EMBO Rep* **9,** 853-8.
15. Birmingham, A., Anderson, E. M., Reynolds, A., Ilsley-Tyree, D., Leake, D., Fedorov, Y., Baskerville, S., Maksimova, E., Robinson, K., Karpilow, J., Marshall, W. S. & Khvorova, A. (2006) *Nat Methods* **3,** 199-204.
16. Hegedus, Z., Czibula, A. & Kiss-Toth, E. (2007) *Cell Signal* **19,** 238-50.
17. Lin, K. R., Lee, S. F., Hung, C. M., Li, C. L., Yang-Yen, H. F. & Yen, J. J. (2007) *J Biol Chem* **282,** 21962-72.
18. Hegedus, Z., Czibula, A. & Kiss-Toth, E. (2006) *Cell Mol Life Sci* **63,** 1632-41.
19. Hou, L., Panthier, J. J. & Arnheiter, H. (2000) *Development* **127,** 5379-89.
20. Shaw, G. & Kamen, R. (1986) *Cell* **46,** 659-67.
21. Deli, T., Varga, N., Adam, A., Kenessey, I., Raso, E., Puskas, L. G., Tovari, J., Fodor, J., Feher, M., Szigeti, G. P., Csernoch, L. & Timar, J. (2007) *Int J Cancer* **121,** 55-65.
22. Fedida-Metula, S., Elhyany, S., Tsory, S., Segal, S., Hershfinkel, M., Sekler, I. & Fishman, D. (2008) *Carcinogenesis* **29,** 1546-54.
23. Andjelkovic, M., Alessi, D. R., Meier, R., Fernandez, A., Lamb, N. J., Frech, M., Cron, P., Cohen, P., Lucocq, J. M. & Hemmings, B. A. (1997) *J Biol Chem* **272,** 31515-24.
24. Segura, M. F., Hanniford, D., Menendez, S., Reavie, L., Zou, X., Alvarez-Diaz, S., Zakrzewski, J., Blochin, E., Rose, A., Bogunovic, D., Polsky, D., Wei, J., Lee, P., Belitskaya-Levy, I., Bhardwaj, N., Osman, I. & Hernando, E. (2009) *Proc Natl Acad Sci U S A* **106,** 1814-9.
25. Hilmi, C., Larribere, L., Deckert, M., Rocchi, S., Giuliano, S., Bille, K., Ortonne, J. P., Ballotti, R. & Bertolotto, C. (2008) *Pigment Cell Melanoma Res* **21,** 139-46.
26. Soengas, M. S. & Lowe, S. W. (2003) *Oncogene* **22,** 3138-51.

27. Keeshan, K., He, Y., Wouters, B. J., Shestova, O., Xu, L., Sai, H., Rodriguez, C. G., Maillard, I., Tobias, J. W., Valk, P., Carroll, M., Aster, J. C., Delwel, R. & Pear, W. S. (2006) *Cancer Cell* **10,** 401-11.

28. Gupta, P. B., Kuperwasser, C., Brunet, J. P., Ramaswamy, S., Kuo, W. L., Gray, J. W., Naber, S. P. & Weinberg, R. A. (2005) *Nat Genet* **37,** 1047-54.

29. Zanella, F., Rosado, A., Garcia, B., Carnero, A. & Link, W. (2008) *Chembiochem* **9,** 2229-37.

30. Zanella, F., Rosado, A., Blanco, F., Henderson, B. R., Carnero, A. & Link, W. (2007) *Assay Drug Dev Technol* **5,** 333-41.

31. Hellemans, J., Mortier, G., De Paepe, A., Speleman, F. & Vandesompele, J. (2007) *Genome Biol* **8,** R19.

Figure Legends

Table 1

List of gene targets of sequence-verified shRNAs identified in two independent cell-based systems. For candidate validation, multiple RNAi agents directed against independent sequences within a gene target were tested for modification of luciferase activity. Gene targeting region for the silencing pools are shown. ORF, open reading frame; 5'UTR and 3'UTR, five-prime and three-prime untranslated regions, respectively.

Fig. 1. Silencing of TRIB2 induces FOXO driven luciferase activity and nuclear translocation of GFP-FOXO. A. Relative TRIB2/GAPDH mRNA levels after transfection of HEK293T cells with the shRNA construct TRIB2_NKI. Cells were harvested 48 hours after transfection and processed for qPCR using methods described above. B. Transcriptional activity of FOXO upon silencing of TRIB2 with shRNA construct TRIB2_NKI as measured by FOXO-driven expression of

luciferase in co-transfection experiments. Each construct was transiently co-transfected with plasmids encoding FOXO3a and Renilla luciferase into 293foxREP cells, and the luciferase activities were determined as described in the "Materials and Methods" section. The data were normalized to the Renilla luciferase (phRG-TK vector) reporter construct. The results are given as the mean ± SEM of three independent experiments performed in triplicate. C and D. Subcellular localization of fluorescent FOXO reporter protein after transfection of U2foxRELOC cells with control vector (C) or shRNA construct TRIB2_NKI (D).

Fig. 2. Ectopic expression of TRIB2 increased FOXO-driven luciferase expression. A. TRIB2 cDNA was tagged with a V5 epitope and expressed in HEK293T cells. Overexpression was detected by western blot analysis using a specific antibody against the V5 tag. Equal loading was confirmed by the specific detection of α-tubulin expression. Relevant proteins are indicated by arrows in the blot from a representative experiment. B. Luciferase expression from a FOXO driven promoter was monitored upon expression of control plasmid or V5 tagged TRIB2 cDNA. Each construct was transiently co-transfected with plasmids encoding FOXO3a and Renilla luciferase into 293foxREP cells, and the luciferase activities were determined as described above. The data were normalized to the Renilla luciferase (phRG-TK vector) reporter construct. The results are given as the mean ± SEM of three independent experiments performed in triplicate.

Fig. 3. TRIB2 is overexpressed in malignant melanoma. A cancer profiling array was hybridized separately with a radiolabeled probe for the housekeeping gene ubiquitin and a radiolabeled probe for TRIB2. Hybridization signals were detected by phosphoimaging. A. Samples from ten patients (P1 – P10) with skin cancer and matched normal tissue are shown. N = normal; T = tumor. B. Quantification of TRIB2 levels was performed using Quantity One software. The hybridization signals for TRIB2 were normalized against signals obtained for ubiquitin. Then, the ratio between normalized values from normal tissue to those from tumors was calculated for each patient (P1 – P10). Black bars represent malignant melanoma, white bars indicate non-melanoma skin cancer. C. Hybridization signals from nine different cancer cell lines were shown. D. Quantification of TRIB2 levels was performed as described above. Black bars represent melanoma cells, dashed bars indicate non-melanoma cancer cell lines.

Fig. 4. TRIB2 expression negatively correlates with Bim expression. qRT-PCR analysis of TRIB2 (A) and BIM (B) mRNA levels in a panel of cell lines. Black bars refer to melanocyte-derived cells while white bars correspond to non-melanocyte derived cells. Error bars refer to standard error. Normalization of the results was performed taking 18S mRNA levels as reference.

Fig. 5. Calcium signalling regulates the abundance of TRIB2 mRNA. G361 cells were treated with several compounds for a period of 6 hours, followed by RNA extraction for qRT-PCR quantification of TRIB2 mRNA levels. Error bars refer

to standard error. Normalization of the results was performed taking 18S mRNA levels as reference.

Fig. 6. Silencing of TRIB2 in melanoma cells activates FOXO dependent transcription. G-361FireFOX cells were transiently transfected with 2 different shRNAs against TRIB2 respectively or with shRNAs against PI3K or Akt, using *Renilla* luciferase as a transfection control. After 48 hours, firefly luciferase activity was measured and normalized against *Renilla* luciferase activity. The results refer to the average obtained in triplicate experiments and the error bars are representative of the standard deviation obtained in each triplicate.

Fig. 7. Silencing of TRIB2 decreases the malignant phenotype of melanoma cells. A. qRT-PCR analysis of TRIB2 mRNA levels in 361C and 361shTRIB cells. Error bars refer to standard error. Normalization of the results was performed taking 18S mRNA levels as reference. B. 361C and 361shTRIB cells were grown in standard culture conditions over a period of 10 days and cell density was measured every second day. The relative number of cells was estimated by crystal violet staining.as described above. C. In order to investigate their clonagenic potential 361C and 361shTRIB cells were seeded at low density and allowed to grow for 10 days prior to fixation, crystal violet staining and quantification of the number of colonies formed. D. 361C and 361shTRIB cells were seeded in soft agar and maintained for one month for anchorage-independent growth analysis. Bars refer to the average number of colonies obtained from triplicates of each cell line with their respective standard deviation. E- Microscopic detail of the colonies formed by 361C and 361shTRIB

cells in soft agar after one month of culture. F- 361C and 361shTRIB cells were grown until confluence and their migratory capabilities were analyzed in a wound healing assay.

Fig. 8. Silencing of TRIB2 reduces tumor growth *in vivo.* $7x10^5$ 361shTRIB or 361C cells were xenografted in ZSCID mice and the growth of the tumors formed by each cell population was followed. The statistical significance for each time point was determined by unpaired t-test. Except for the first depicted time point, the differences of all time points were significant. B and C, At day 69, both groups of animals were photographed, euthanized, and tumors were dissected and photographed. Mice (B) and dissected tumors (C) representative for the both groups are depicted. The rulers at the bottoms of the photographs (C) are scaled in mm.

Table S1

RNAi agents used for the validation of TRIB2 silencing. In order to rule out off-target effects several independent TRIB2 interfering agents from different sources were tested and their respective induced knockdown over TRIB2 mRNA was analyzed by qRT-PCR. 1- Both shRNAs obtained from the NKI library initially included in the same pool. For further characterization both oligos were isolated and characterized independently. 2- This pool contains four different siRNAs. ORF, open reading frame; 5'UTR, five-prime untranslated regions.

Table S2

Description of samples included in the cancer profiling array. Information about the cDNAs and controls immobilized on the cancer profiling array and the corresponding hybridization signals specific for TRIB2. Normalization was performed against signals obtained using the ubiquitin control probe.

Table S3

Description of samples included in the Tissue qPCR Arrays. qRT-PCR was performed using TissueScan Melanoma Tissue qPCR Array I containing 43 tissues (OriGene Technologies, Rockville, MD). Quantification of TRIB2 mRNA levels was performed using qPCR. qRT-PCR amplification signals specific for TRIB2 were normalized against *GAPDH* expression.

Fig. S1.

A. General structure of the construct used to generate the 293foxREP cells. B. Validation of the 293foxREP system. FOXO-driven expression of luciferase was determined upon activation or inhibition of the PI3K/Akt pathway. Each construct was transiently co-transfected with plasmids encoding FOXO3a or constitutively active A3 FOXO3a mutant and Renilla luciferase into 293foxREP cells, and the luciferase activities were measured as described above. The data were normalized to the Renilla luciferase (phRG-TK vector) reporter construct. The results are given as the mean ± SEM of three independent experiments performed in triplicate.

Fig. S2.

Schematics of the strategy used to screen the NKI library of shRNAs for novel modulators of FOXO activity. The shRNA library was introduced in pools of three RNAi per gene into 293foxREP cells. Those pools of shRNAs that caused activation of FOXO driven luciferase activity were analyzed for its capacity to induce nuclear translocation of FOXO in the U2foxRELOC system.

Fig. S3.

A and B. The Cancer Profiling Array II membrane after hybridization with the TRIB2 and ubiquitin probes. Tissue sources are listed above each sample group. C. Relative abundance of TRIB2 as compared with *GAPDH* expression as determined by comparison of TRIB2 and *GAPDH* qRT-PCR amplification signals. cDNAs studied were normal skin tissues (n=3), malignant melanoma diagnosed at stage III (n = 21) or IV (*n* = 19). The P-values were calculated using unpaired t test with Welch's correction for comparisons of normal skin versus melanoma stage III (P = 0.0421) and for normal skin versus melanoma stage IV (P = 0.0288)

Table 1. Suppressors of FOXO Function

Gene	Full Name	Previously Known Function	Targeting region
Akt-3	v-Akt murine thyoma viral oncogene homolog 3	Protein Kinase	ORF
PIK3CA	Phosphatidylinositol 3- kinase catalytic, alpha polypeptide	Lipid kinase	ORF
TRIB2	Tribbles homolog 2	Kinase-like protein	5´UTR / ORF
CALM2	Calmodulin 2	Ca^{2+}-binding protein	5´UTR / ORF
DCLK1	Doublecortin-like 1 kinase	Protein Kinase	ORF / 3´UTR
ZNF281	Zink finger protein 281	Transcription factor	5´UTR / ORF

Table 1. List of gene targets of sequence-verified shRNAs identified in two independent cell-based systems. For candidate validation, multiple RNAi agents directed against independent sequences within a gene target were tested for modification of luciferase activity. Gene targeting region for the silencing pools are shown. ORF, open reading frame; 5'UTR and 3'UTR, five-prime and three-prime untranslated regions, respectively.

Fig. 1

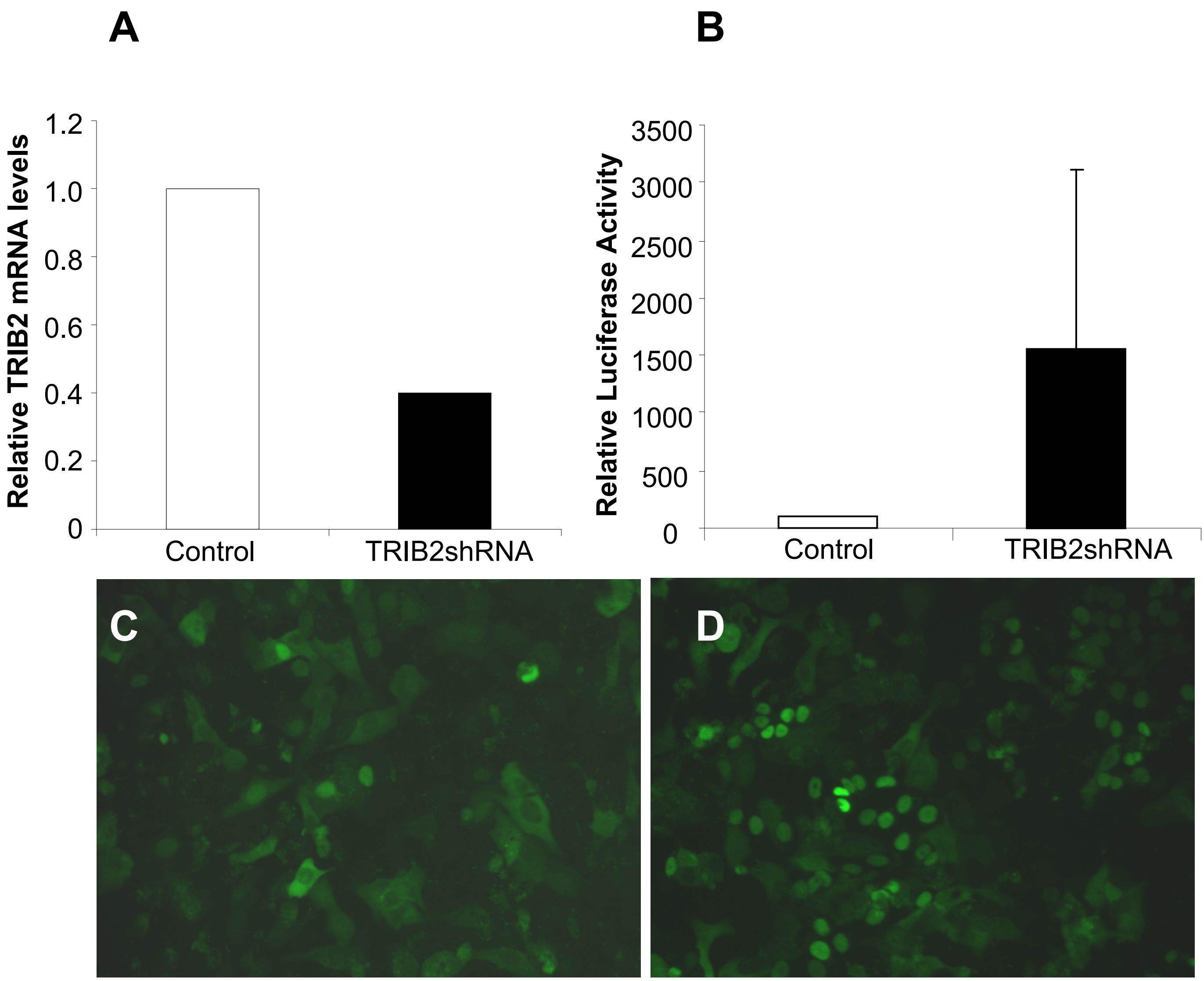

Fig. 1. Silencing of TRIB2 induces FOXO driven luciferase activity and nuclear translocation of GFP-FOXO. A. Relative TRIB2/GAPDH mRNA levels after transfection of HEK293T cells with the shRNA construct TRIB2_NKI. Cells were harvested 48 hours after transfection and *processed for qPCR* using methods described above. **B**. Transcriptional activity of FOXO upon silencing of TRIB2 with shRNA construct TRIB2_NKI as measured by FOXO-driven expression of luciferase in co-transfection experiments. Each construct was transiently co-transfected with plasmids encoding FOXO3a and *Renilla* luciferase into 293foxREP cells, *and the luciferase activities* were determined as described in the "Materials and Methods" section. The *data were normalized to the Renilla* luciferase (phRG-TK vector) reporter construct. The results are given as the mean ± SEM of three independent experiments performed in triplicate. **C** and **D**. Subcellular localization of fluorescent FOXO reporter protein after transfection of U2foxRELOC cells with control vector (C) or shRNA construct TRIB2_NKI (D).

Fig. 2

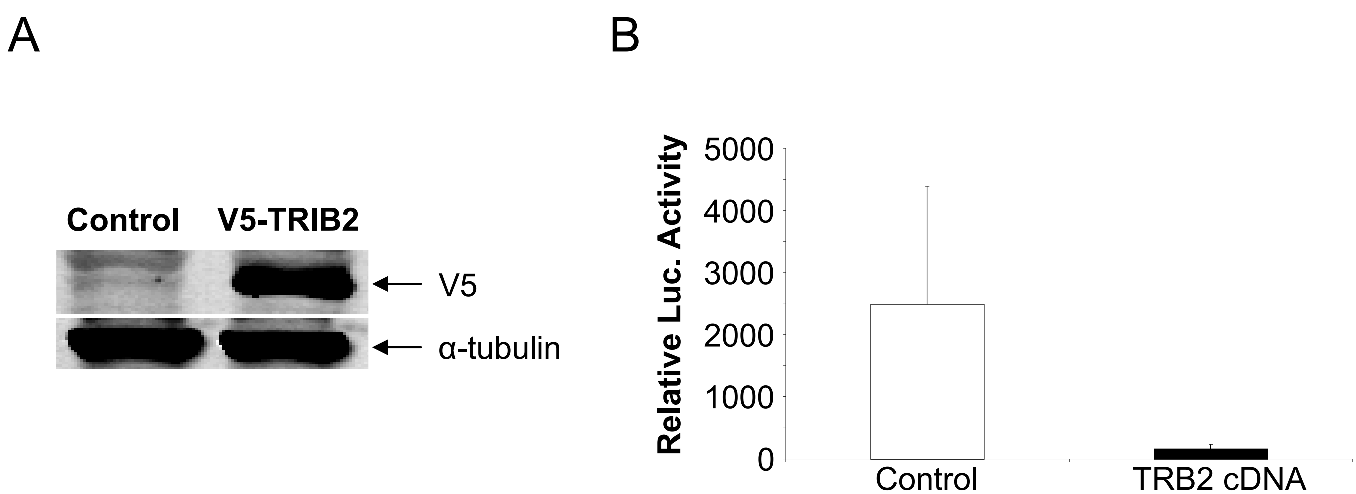

Fig. 2. Ectopic expression of TRIB2 increased FOXO-driven luciferase expression. A. TRIB2 cDNA was tagged with a V5 epitope and expressed in HEK293T cells. Overexpression was detected by western blot analysis using a specific antibody against the V5 tag. Equal loading was confirmed by the specific detection of α-tubulin expression. Relevant proteins are indicated by arrows in the blot from a representative experiment. **B**. Luciferase expression from a FOXO driven promoter was monitored upon expression of control plasmid or V5 tagged TRIB2 cDNA. Each construct was transiently co-transfected with plasmids encoding FOXO3a and *Renilla* luciferase into 293foxREP cells, *and the luciferase activities* were determined as described above. The *data were normalized to the Renilla* luciferase (phRG-TK vector) reporter construct. The results are given as the mean ± SEM of three independent experiments performed in triplicate.

Fig. 3

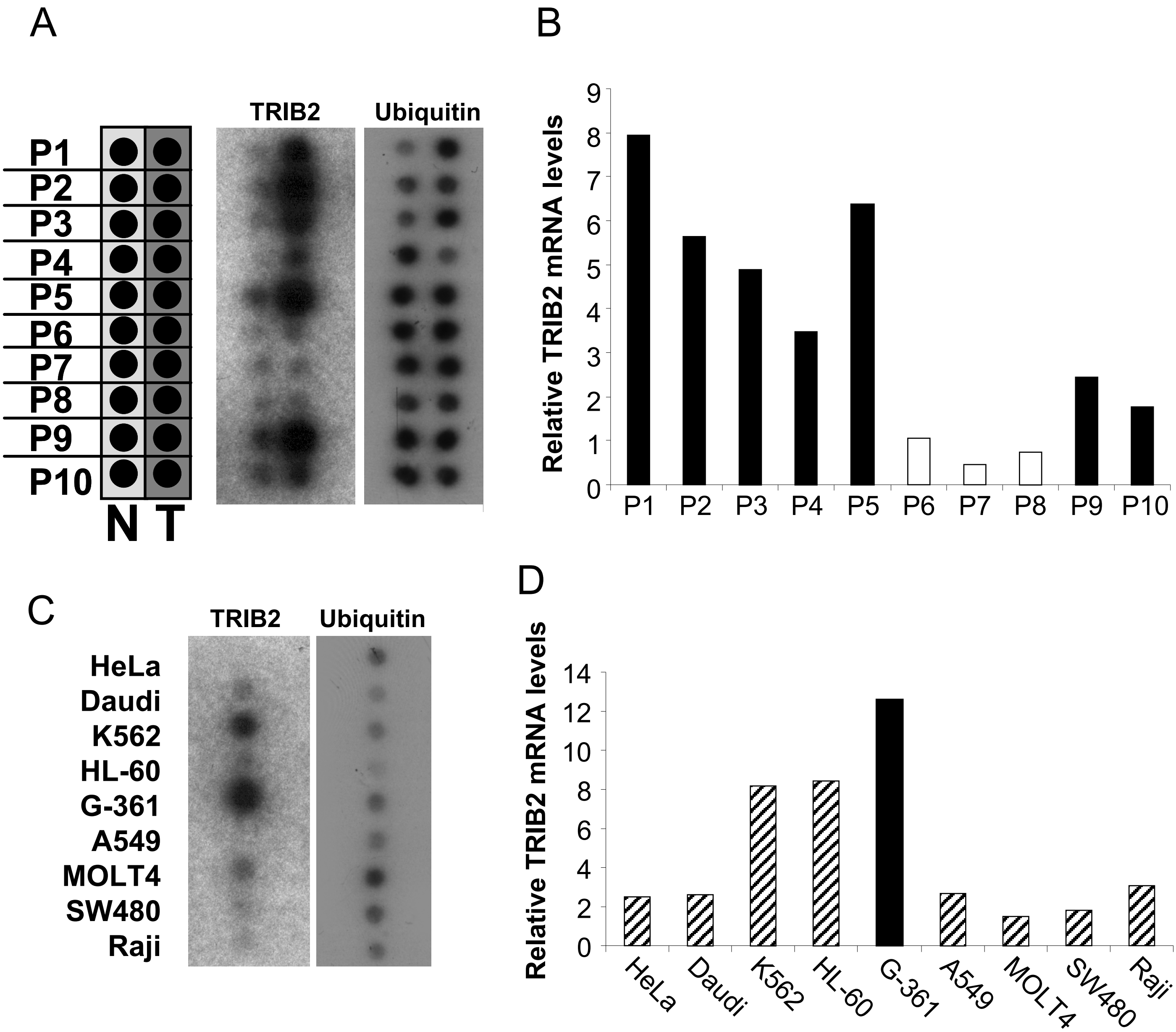

Fig. 3. TRIB2 is overexpressed in malignant melanoma. A cancer profiling array was hybridized separately with a radiolabeled probe for the housekeeping gene ubiquitin and a radiolabeled probe for TRIB2. Hybridization signals were detected by phosphoimaging. A. Samples from ten patients (P1 – P10) with skin cancer and matched normal tissue are shown. N = normal; T = tumor. **B.** Quantification of TRIB2 levels was performed using Quantity One software. The hybridization signals for TRIB2 were normalized against signals obtained for ubiquitin. Then, the ratio between normalized values from normal tissue to those from tumors was calculated for each patient (P1 – P10). Black bars represent malignant melanoma, white bars indicate non-melanoma skin cancer. **C**. Hybridization signals from nine different cancer cell lines were shown. **D**. Quantification of TRIB2 levels was performed as described above. Black bars represent melanoma cells, dashed bars indicate non-melanoma cancer cell lines.

Fig. 4

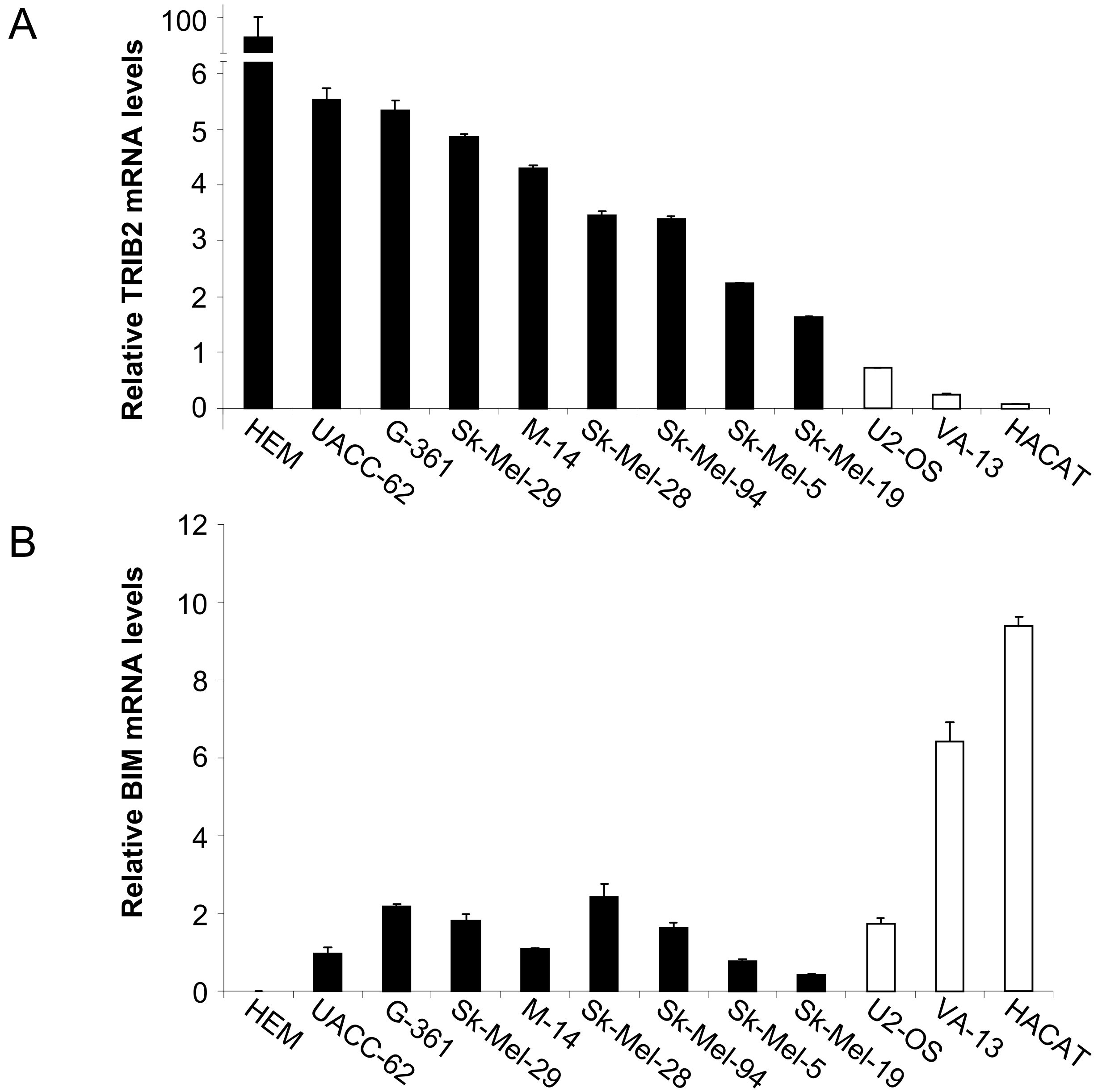

Fig. 4. TRIB2 expression negatively correlates with Bim expression. qRT-PCR analysis of TRIB2 **(A)** and BIM **(B)** mRNA levels in a panel of cell lines. Black bars refer to melanocyte-derived cells while white bars correspond to non-melanocyte derived cells. Error bars refer to standard error. Normalization of the results was performed taking 18S mRNA levels as reference.

Fig. 5

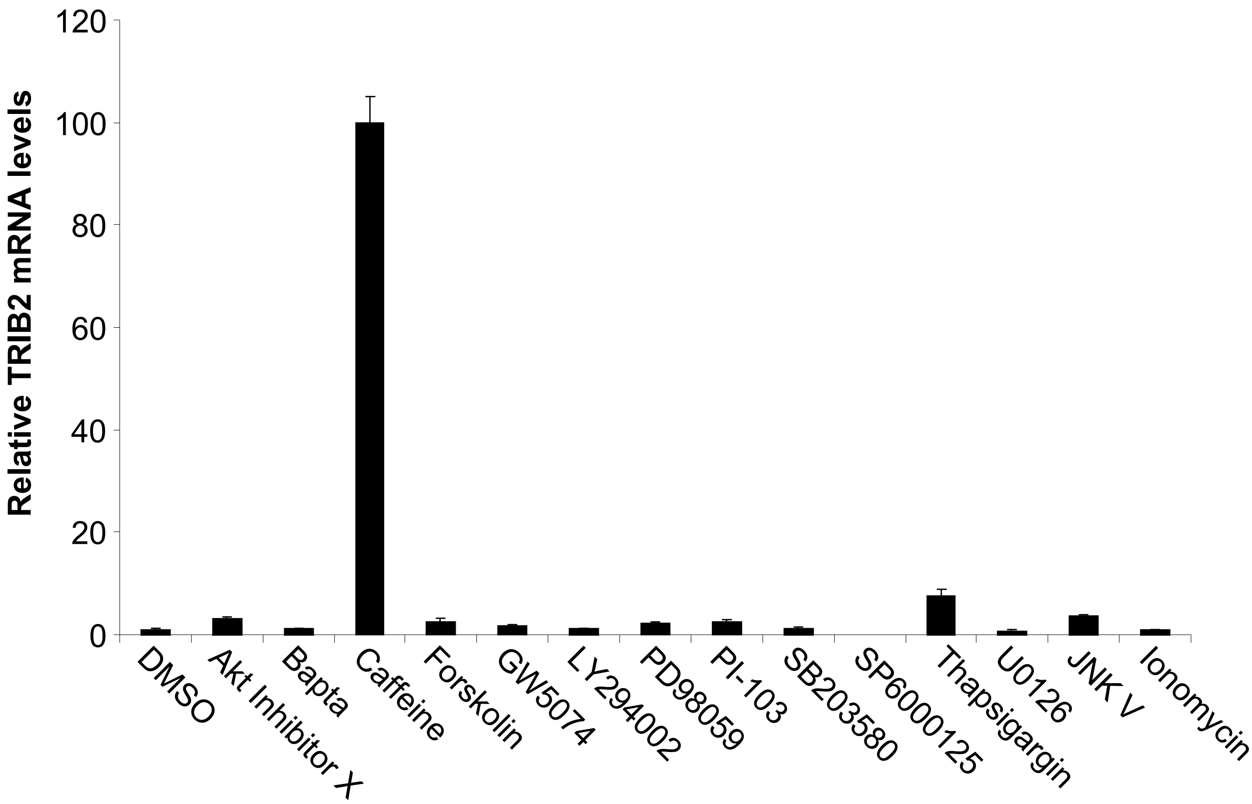

Fig. 5. Calcium signalling regulates the abundance of TRIB2 mRNA. G361 cells were treated with several compounds for a period of 6 hours, followed by RNA extraction for qRT-PCR quantification of TRIB2 mRNA levels. Error bars refer to standard error. Normalization of the results was performed taking 18S mRNA levels as reference.

Fig. 6

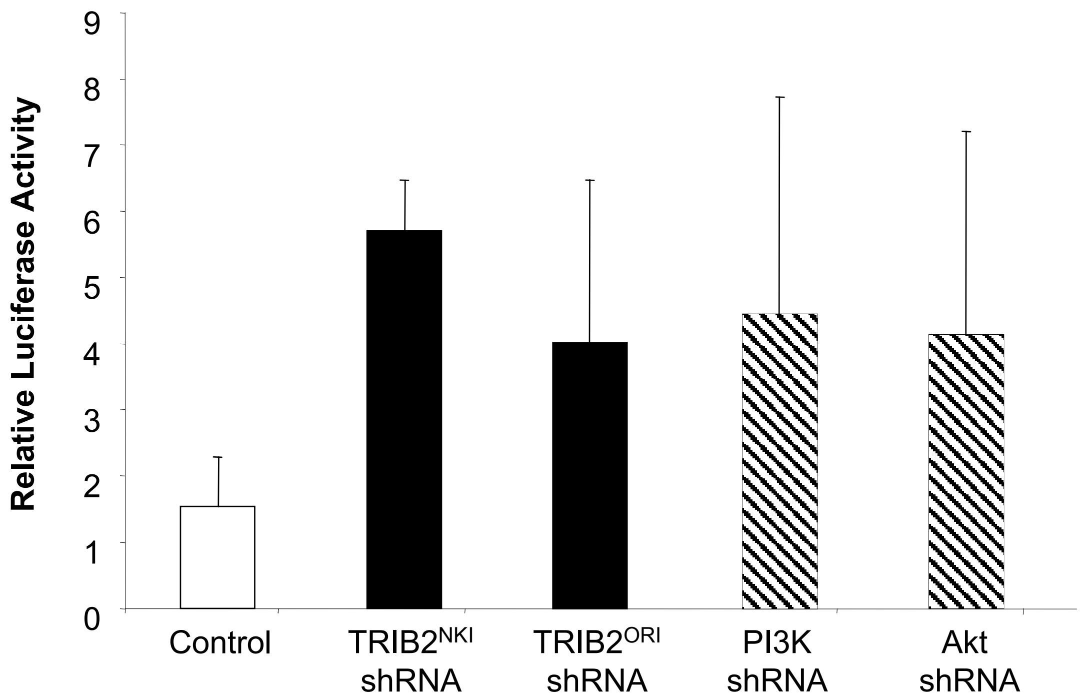

Fig. 6. Silencing of TRIB2 in melanoma cells activates FOXO dependent transcription. G-361FireFOX cells were transiently transfected with 2 different shRNAs against TRIB2 respectively or with shRNAs against PI3K or Akt, using *Renilla* luciferase as a transfection control. After 48 hours, firefly luciferase activity was measured and normalized against *Renilla* luciferase activity. The results refer to the average obtained in triplicate experiments and the error bars are representative of the standard deviation obtained in each triplicate.

Fig. 7

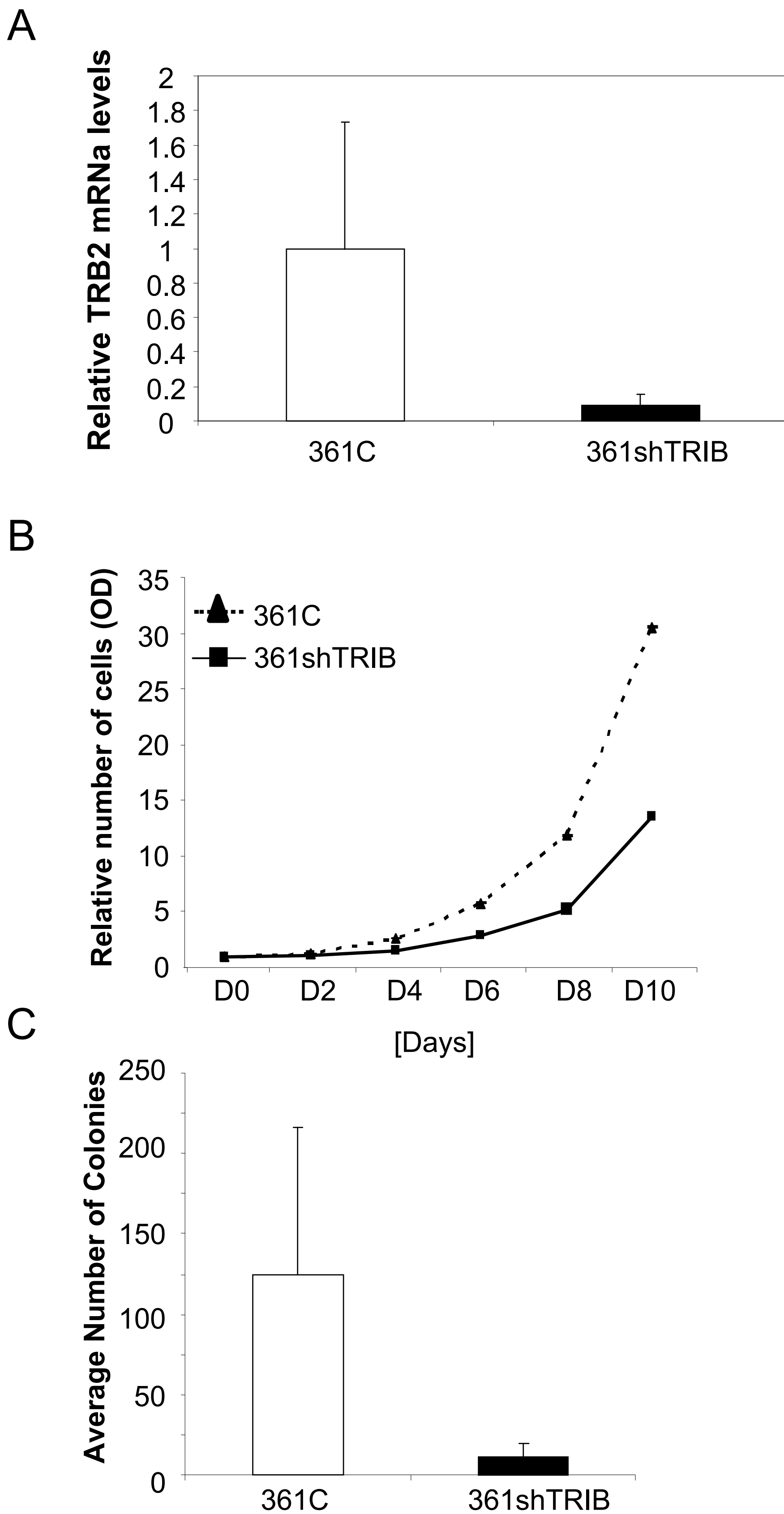

Fig. 7. Silencing of TRIB2 decreases the malignant phenotype of melanoma cells. **A**. qRT-PCR analysis of TRIB2 mRNA levels in 361C and 361shTRIB cells. Error bars refer to standard error. Normalization of the results was performed taking 18S mRNA levels as reference. **B**. 361C and 361shTRIB cells were grown in standard culture conditions over a period of 10 days and cell density was measured every second day. *The relative number of cells was* estimated by *crystal violet* staining.as described above. **C**. In order to investigate their clonagenic potential 361C and 361shTRIB cells were seeded at low density and allowed to grow for 10 days prior to fixation, *crystal violet* staining and quantification of the number of colonies formed.

Fig. 7

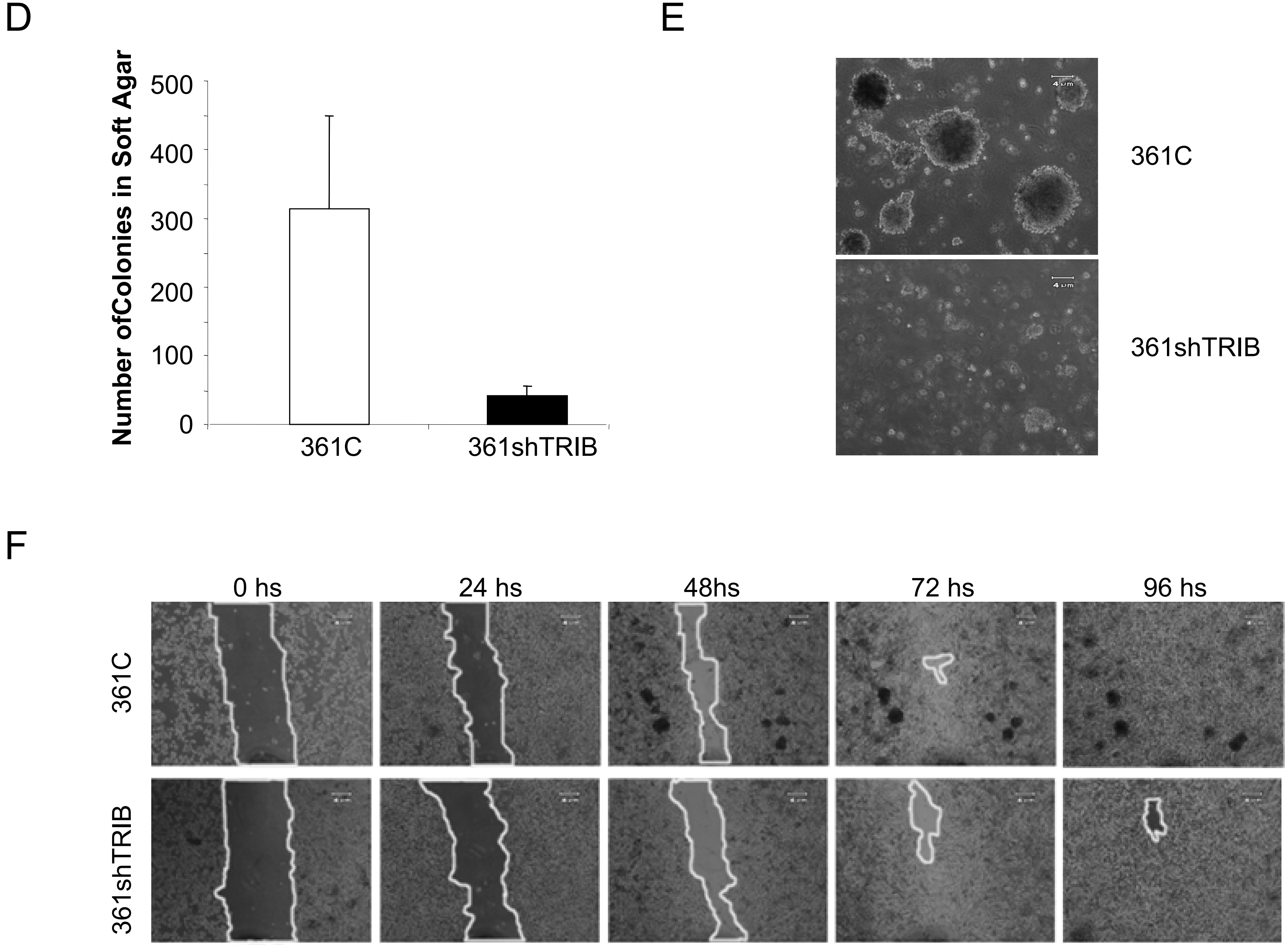

Fig. 7. Silencing of TRIB2 decreases the malignant phenotype of melanoma cells. D. 361C and 361shTRIB cells were seeded in soft agar and maintained for one month for anchorage-independent growth analysis. Bars refer to the average number of colonies obtained from triplicates of each cell line with their respective standard deviation. **E**- Microscopic detail of the colonies formed by 361C and 361shTRIB cells in soft agar after one month of culture. **F**- 361C and 361shTRIB cells were grown until confluence and their migratory capabilities were analyzed in a wound healing assay.

A

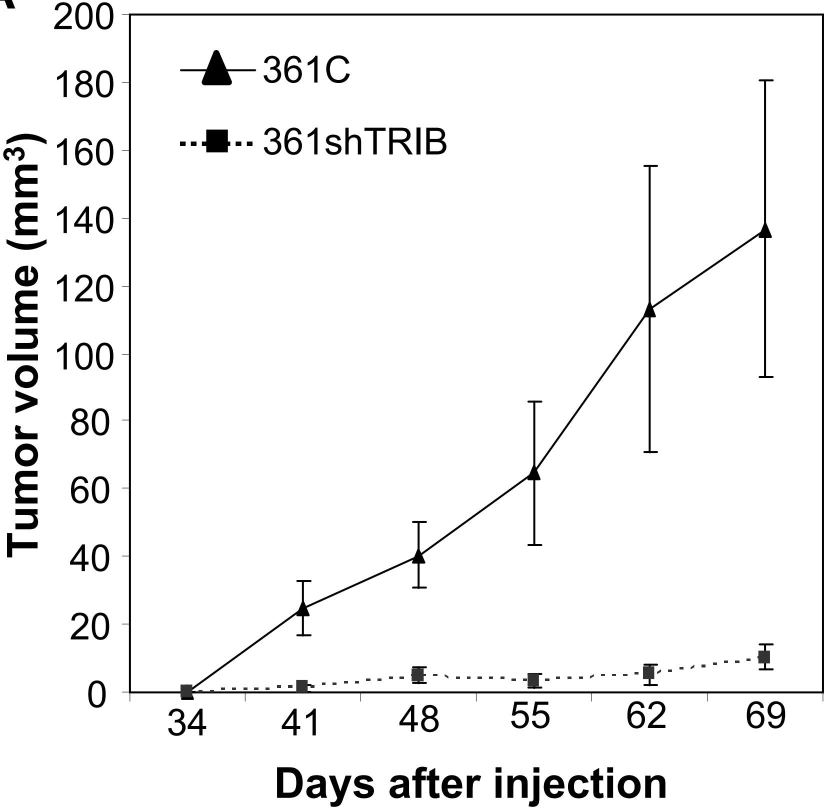

Fig. 8. Silencing of TRIB2 reduces tumor growth *in vivo*. A. $7x10^5$ 361shTRIB or 361C cells were xenografted in ZSCID mice and the growth of the tumors formed by each cell population was followed. The statistical significance for each time point was determined by unpaired t-test. Except for the first depicted time point, the differences of all time points were significant. **B** and **C**, At day 69, both groups of animals were photographed, euthanized, and tumors were dissected and photographed. Mice (**B**) and dissected tumors (**C**) representative for the both groups are depicted. The rulers at the bottoms of the photographs (**C**) are scaled in mm.

B C

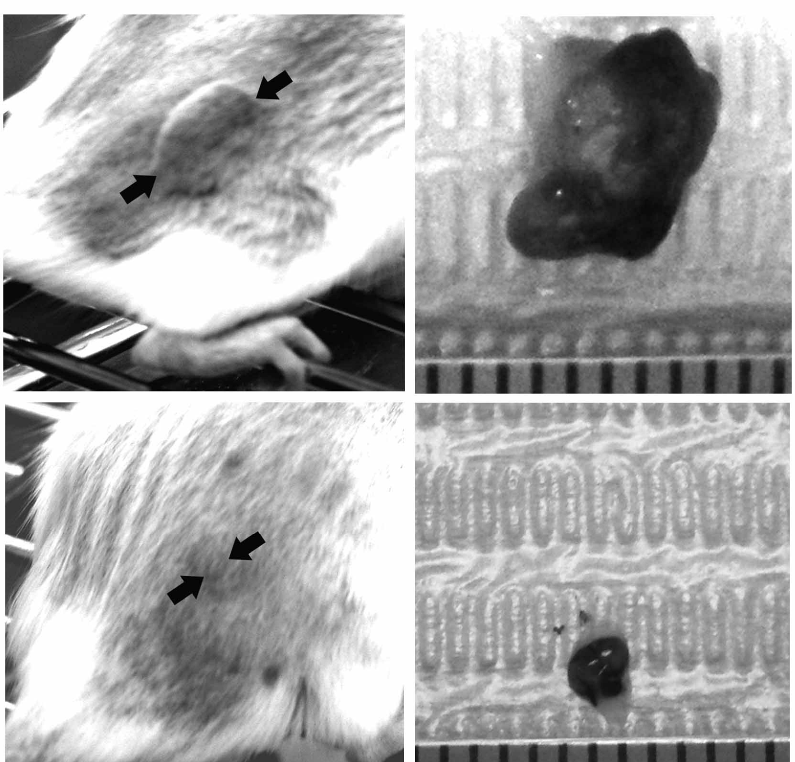

361C

361shTRIB

Fig. S1

A

B

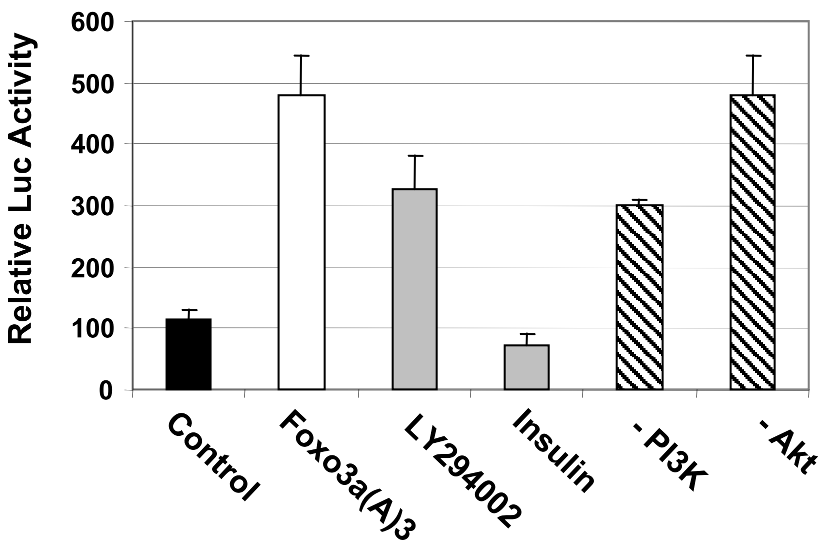

Fig. S1. **A**. General structure of the construct used to generate the 293foxREP cells. **B**. Validation of the 293foxREP system. FOXO-driven expression of luciferase was *determined* upon activation or inhibition of the PI3K/Akt pathway. Each construct was transiently co-transfected with plasmids encoding FOXO3a or *constitutively* active *A3 FOXO3a* mutant and *Renilla* luciferase into 293foxREP cells, *and the luciferase activities* were measured as described above. The *data were normalized to the Renilla* luciferase (phRG-TK vector) reporter construct. The results are given as the mean ± SEM of three independent experiments performed in triplicate.

Fig. S2

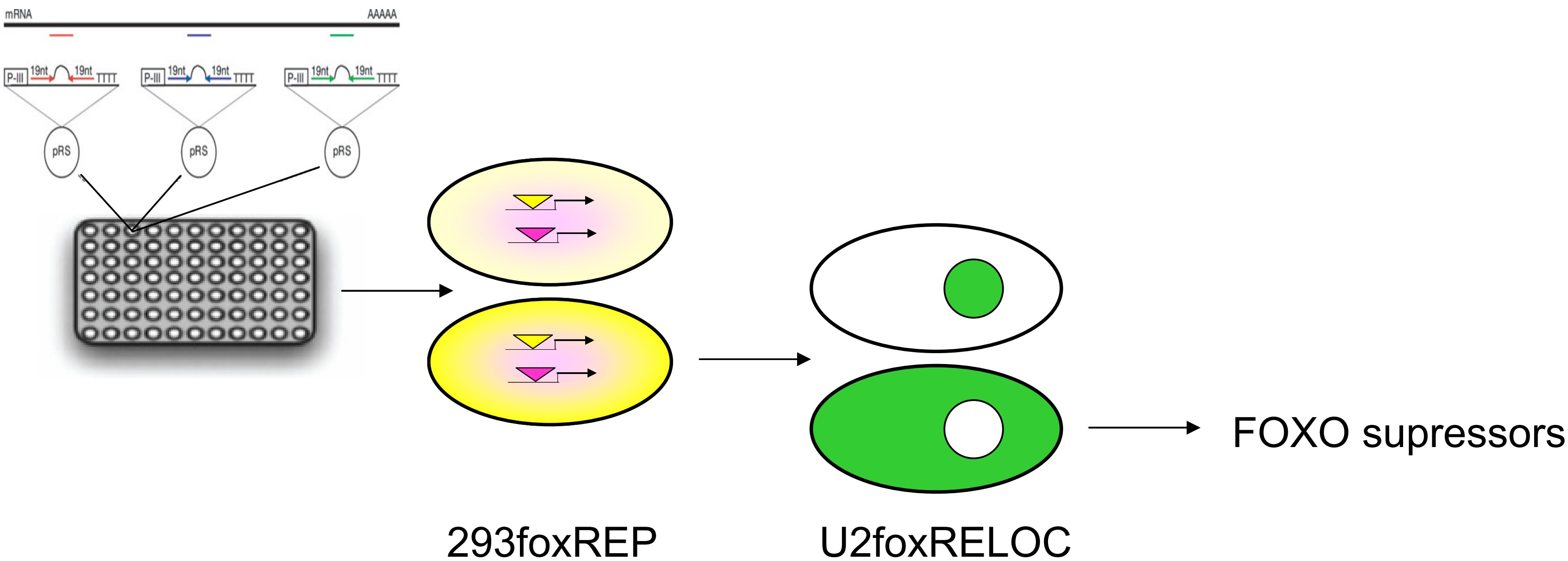

Fig. S2. **Schematics of the strategy used to screen the NKI library of shRNAs for novel modulators of FOXO activity**. The shRNA library was introduced in pools of three RNAi per gene into 293foxREP cells. Those pools of shRNAs that caused activation of FOXO driven luciferase activity were analyzed for its capacity to induce nuclear translocation of FOXO in the U2foxRELOC system.

Fig. S3

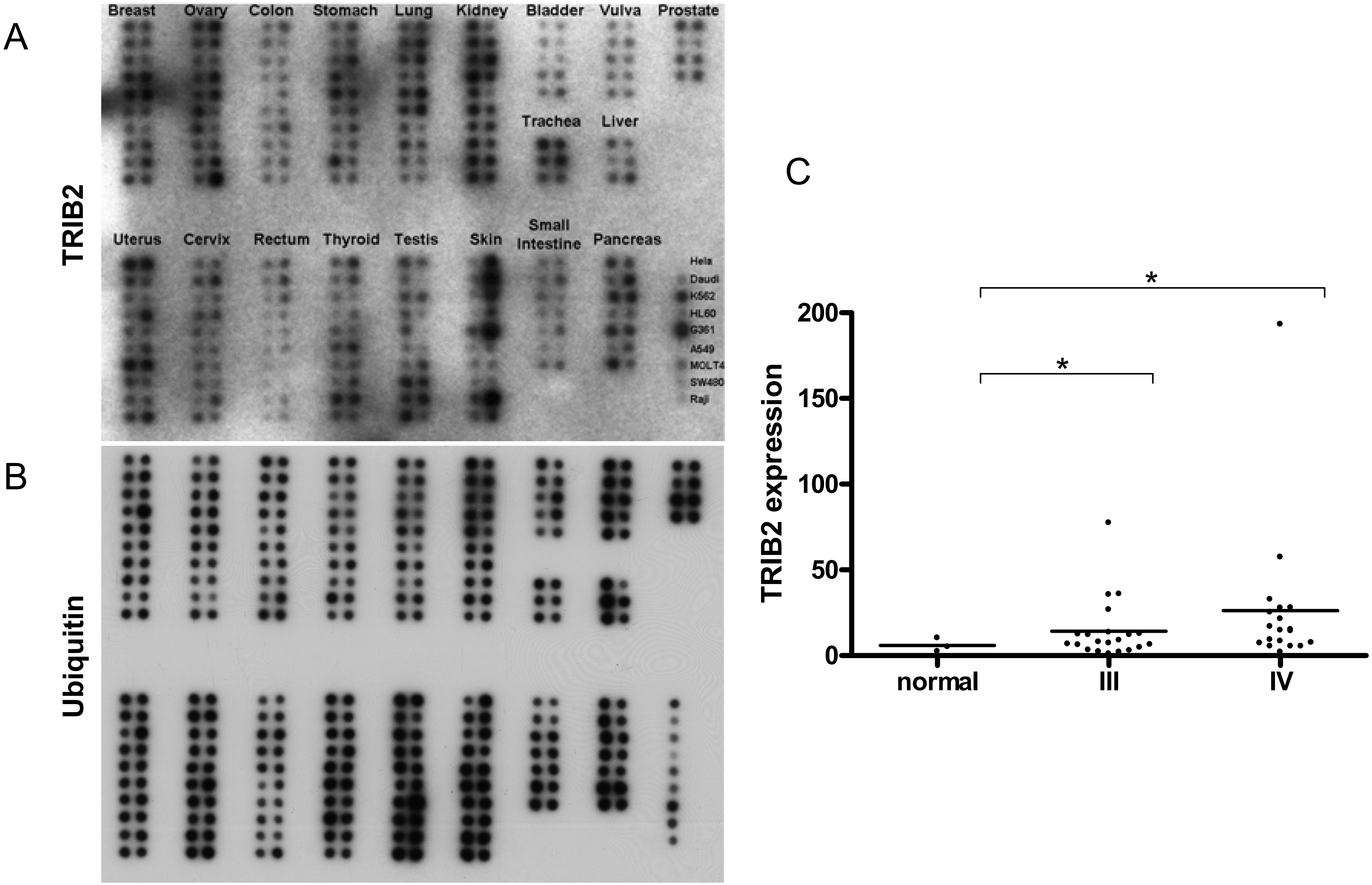

Fig. S3. A and **B**. The Cancer Profiling Array II membrane after hybridization with the TRIB2 and ubiquitin probes. Tissue sources are listed above each sample group. **C**. Relative abundance of TRIB2 as compared with *GAPDH* expression as determined by comparison of TRIB2 and *GAPDH* qRT-PCR amplification signals. cDNAs studied were normal skin tissues (n=3), malignant melanoma diagnosed at stage III (n = 21) or IV (*n* = 19). The P-values were *calculated using unpaired t test* with Welch's correction *for comparisons of normal skin versus* melanoma stage III (P = 0.0421) and for *normal skin versus* melanoma stage IV (P = 0.0288)

Table S1. RNAi agents used to validate TRIB2 silencing

Provider	Presentation	Reference	Sequence	Targeting region	Knockdown effciency
NKI	shRNA Pool[1]	102911	5’-GCTATTAGGAAGTCAAACG-3’	5’UTR	30%
NKI	shRNA Pool[1]	102911	5’-GAAAGACACACTCTTAAGT-3’	ORF	80%
Origene	shRNA Single	TI200873	5’-CCAGGACGAGATCCAGTTCTC-3	5’UTR	30%
Origene	shRNA Single	TI200874	5’-CCTGCCGACCGAGGACCCCCG-3	5’UTR	10%
Origene	shRNA Single	TI200875	5’-TAAAATCAGTGGCACCGAGGC-3’	5’UTR	20%
Origene	shRNA Single	TI200876	5’-CTCCCTCTTCAGCAAGATCCG-3’	ORF	90%
Origene	shRNA Single	TI200877	5’-CCCAGGAGTGAGCGAGGGCAG-3’	ORF	0%
Origene	shRNA Single	TI200878	5’-AGCGAGATATGGGAGATCGCG-3’	ORF	40%
Dharmacon	siRNA Pool[2]	D-005391-01	5’-GAAGAGUUGUCGUCUAUAA-3’	5’UTR	
		D-005391-02	5’-GAGAGGAGCUGGUGUGCAA-3’	ORF	80%
		D-005391-03	5’-CCAAAUCACUGAAAUUAUC-3’	ORF	
		D-005391-05	5’-UCGAAGAGUUGUCGUCUAU-3’	5’UTR	

Table S1. RNAi agents used for the validation of TRIB2 silencing. In order to rule out off-target effects several independent TRIB2 interfering agents from different sources were tested and their respective induced knockdown over TRIB2 mRNA was analyzed by qRT-PCR. 1- Both shRNAs obtained from the NKI library initially included in the same pool. For further characterization both oligos were isolated and characterized independently. 2- This pool contains four different siRNAs. ORF, open reading frame; 5'UTR, five-prime untranslated regions.

Table S2A Description of samples from skin cancer patients included in the cancer profiling array

Patient	Tissue Source	Stage	Normalized TRIB2 levels	Gender	Age
P1	Malignant melanoma NOS	I; T2N0M0	7.94	Female	49
P2	Malignant melanoma NOS	III;T4N0M0	5.64	Female	45
P3	Malignant melanoma NOS	III;T4N0M0	4.89	Male	73
P4	Malignant melanoma NOS	IV; N/A	3.49	Male	58
P5	Malignant melanoma NOS	III;T4N0M0	6.37	Female	74
P6	Unknown	N/A; N/A	1.06	Male	64
P7	Squamous cell carcinoma	II; T2N0M0	0.46	Female	70
P8	Squamous cell carcinoma, keratinizing type NOS	II; T2N0M0	0.74	Male	68
P9	Malignant melanoma NOS	III;T4N0M0	2.45	Female	40
P10	Malignant melanoma NOS	I; T2N0M0	1.77	Female	43

Table S2B Description of samples from cancer cell lines included in the cancer profiling array

Cell line	Organ / Cell type	Disease	Normalized TRIB2 levels	Gender	Age
HeLa	Cervix	Adenocarcinoma	2.48	Female	31
Daudi	Peripheral blood	Burkitt's lymphoma	2.60	Male	16
K562	Bone marrow	Chronic myelogenous leukemia	8.18	Female	53
HL60	Peripheral blood	Acute promyelocytic leukemia	8.43	Female	36
G361	Skin	Malignant melanoma	12.61	Male	31
A549	Lung	Carcinoma	2.70	Male	58
MOLT4	T lymphoblast	Acute lymphoblastic leukemia	1.52	Male	19
SW480	Colon	Colorectal adenocarcinoma	1.81	Male	50
Raji	B lymphocyte	Burkitt's lymphoma	3.06	N/A	N/A

Table S2. Description of samples included in the cancer profiling array. Information about the cDNAs and controls immobilized on the cancer profiling array and the corresponding hybridization signals specific for TRIB2. Normalization was performed against signals obtained using the ubiquitin control probe.

Table S3 Description of samples included in the Tissue qPCR Array

Patient	Tissue Source	Diagnosis	Stage	Normalized TRIB2 levels	Gender	Age
1	Normal skin	Normal	0	2.44	Male	36
2	Normal skin	Normal, Merkel cell carcinoma	0	10.30	Not Sp	69
3	Normal skin	Normal	0	5.04	Male	51
4	Skin / Lymph node	Malignant melanoma, metastatic	III	8.84	Female	42
5	Skin / Lymph node	Malignant melanoma, metastatic	III	2.90	Female	59
6	Skin / Lymph node: sentinel	Malignant melanoma, metastatic	III	35.62	Female	66
7	Skin / Lymph node	Malignant melanoma, metastatic	III	7.18	Male	56
8	Skin / Lymph node	Malignant melanoma, metastatic	III	3.26	Male	46
9	Skin / Lymph node	Malignant melanoma, metastatic	III	2.01	Female	66
10	Skin / Lymph node	Malignant melanoma, metastatic	III	13.50	Female	34
11	Skin / Lymph node	Malignant melanoma, metastatic	III	6.70	Female	56
12	Skin / Lymph node	Malignant melanoma, metastatic	III	2.17	Male	59
13	Skin / Lymph node	Malignant melanoma, metastatic	III	4.81	Female	49
14	Skin / Lymph node	Malignant melanoma, metastatic	IIIA	77.42	Female	67
15	Skin / Lymph node	Malignant melanoma, metastatic	IIIB	1.02	Male	61
16	Skin / Lymph node	Malignant melanoma, metastatic	IIIB	12.00	Male	43
17	Skin / Lymph node	Malignant melanoma, metastatic	IIIB	6.17	Male	42
18	Skin / Lymph node	Malignant melanoma, metastatic	IIIB	12.42	Female	49
19	Skin / Lymph node	Malignant melanoma, metastatic	IIIB	35.87	Female	72
20	Skin / Groin	Malignant melanoma, metastatic	IIIB	12.77	Male	50
21	Skin / Lymph node	Malignant melanoma, metastatic	IIIC	12.08	Male	56
22	Skin / Lymph node	Malignant melanoma, metastatic	IIIC	26.81	Male	81
23	Skin / Lymph node	Malignant melanoma, metastatic	IIIC	7.97	Male	66
24	Skin / Lymph node	Malignant melanoma, metastatic	IIIC	6.38	Female	52
25	Skin / Lymph node	Malignant melanoma, metastatic	IV	15.29	Male	66
26	Skin / Lung	Malignant melanoma, metastatic	IV	8.42	Female	42
27	Skin / Lymph node	Malignant melanoma, metastatic	IV	5.44	Female	45

Table S3. Description of samples included in the Tissue qPCR Arrays. qRT-PCR was performed using TissueScan Melanoma Tissue qPCR Array I containing 43 tissues (OriGene Technologies, Rockville, MD). Quantification of TRIB2 mRNA levels was performed using qPCR. qRT-PCR amplification signals specific for TRIB2 were normalized against *GAPDH* expression.

Table S3 Description of samples included in the Tissue qPCR Array

Patient	Tissue Source	Diagnosis	Stage	Normalized TRIB2 levels	Gender	Age
28	Skin / Lung	Malignant melanoma, metastatic	IV	5.41	Female	74
29	Skin / Lymph node	Malignant melanoma, metastatic	IV	5.37	Male	54
30	Skin / Mesentery	Malignant melanoma, metastatic	IV	27.95	Male	48
31	Skin / Jejunum	Malignant melanoma, metastatic	IV	25.19	Male	60
32	Skin / Lung	Malignant melanoma, metastatic	IV	21.48	Male	58
33	Skin / Lung	Malignant melanoma, metastatic	IV	193.29	Male	45
34	Skin / Small intestine	Malignant melanoma, metastatic	IV	27.75	Male	75
35	Skin / Liver	Malignant melanoma, metastatic	IV	14.77	Male	56
36	Skin / Jejunum	Malignant melanoma, metastatic	IV	32.78	Male	46
37	Skin / Lung	Malignant melanoma, metastatic	IV	16.85	Male	56
38	Skin / Omentum	Malignant melanoma, metastatic	IV	57.47	Female	66
39	Skin / Small intestine	Malignant melanoma, metastatic	IV	7.33	Male	56
40	Skin / Lymph node	Malignant melanoma, metastatic	IV	9.22	Male	81
41	Skin / Lung	Malignant melanoma, metastatic	IV	14.37	Male	56
42	Skin / Lung	Malignant melanoma, metastatic	IV	7.54	Male	73
43	Skin / Skin	Malignant melanoma, metastatic	IV	2.06	Female	42

Table S3. Description of samples included in the Tissue qPCR Arrays. qRT-PCR was performed using TissueScan Melanoma Tissue qPCR Array I containing 43 tissues (OriGene Technologies, Rockville, MD). Quantification of TRIB2 mRNA levels was performed using qPCR. qRT-PCR amplification signals specific for TRIB2 were normalized against *GAPDH* expression.

4 Discussion

4.1 High Content Screening: Applications and limitations.

In the present work we presented novel cell–based platforms that enable the identification of molecules that influence FOXO activity. We established previously undescribed molecular factors that repress the activity of FOXO, including Calmodulin and TRIB2.

The core technology used, high content screening (HCS), has emerged as a powerful technology which as been increasingly and successfully implemented both in the academic research and pharmaceutical industry for the discovery of novel targets and potential interfering small molecules. The concept of HCS *per se* consists in obtaining the most information possible in a single cell-based assay and it is well suited to monitor the phenotype of cells in systematic loss-of-function studies.

The sequencing of the human genome provided many potential therapeutic targets for developing new drugs. However, the lack of knowledge concerning the function of the gene products has limited the success of target-based drug discovery (132).

HCS has filled an important technological gap in the post-genomic era with a breakthrough: The possibility to analyze gene function through genetic-like studies.

In this post-genomic era, the perceived pitfalls of target-based drug discovery has recently led to the renaissance of a more holistic approach that involves the screening of test compounds to determine whether they elicit any phenotypic changes in organism model systems, such as worm, fly, and zebrafish but at present it is mainly mammalian cells in culture that are compatible with high-throughput screening (HTS) with a phenotypic read-out. Hence, our choice to use high content cell basaed assays to search for novel molecules implicated the modulation of FOXO activity.

Our strategy consisted in the combination of phenotypic and target-based approaches to monitor a specific molecular event, taking the benefits of both methodologies. This approach, which goes beyond individual genes and proteins as it involves the investigation of signaling pathways in a systems-based manner, constitutes an unbiased approach for the identification of novel targets implicated in a given event (17). A wide range of different technologies can be used to identify molecular targets that underlie the phenotypic effects elicited by small organic molecules or RNAi in complex biological assay systems (145). For our FOXO-related assays the phenotypical changes to be monitored were cytoplasmic/nuclear shuttling and transcriptional activity. As for the BaFiso system, cell viability and integrity are the main parameters evaluated. In addition, taking advantage of our image-based readouts morphological changes associated with toxicity, namely cell shrinkage, can be further detected and analyzed.

We designed our assays aiming for a restricted target space. However, it is not always possible to isolate the particular molecular target responsible for the phenotypes observed, and hence the need for target deconvolution.

Target deconvolution is the retrospective identification of the molecular targets that underlie the observed phenotypic responses. Deconvolution is not only important for elucidating the biological mechanisms of disease, aspects that are related to target-specific toxicity and side effects can be addressed. Hence, target deconvolution is an important aspect of current target discovery. The final aim of all strategies and methods for target deconvolution is not only the identification of biological targets that are directly affected by a given agent, but also the confirmation that modulation of the identified target is associated with functional effects that are detectable in the phenotypic assay that was originally used for the identification of the interfering agent. Our strategy consisted in developing independent cell-based assays in which the hits could be re-screened for deconvolution, so that the information obtained in each system can complement the previous data, allowing us to cut-off less interesting candidates early in the screening process, prior to a deeper analysis with small-scale molecular biology techniques.

All cell-based platforms presented here can function as primary screening systems, but particularly the U2nesRELOC and the BaFiso systems have been proven extremely useful for deconvolution. With the U2nesRELOC system, it was possible to specifically detect inhibitors of the nuclear export machinery from a panel of compounds (165). Hence, this system constitutes a valuable tool for dissecting the mode of action of a agents scored as FOXO activators in the U2foxRELOC or in U2transLuc system, but which inhibit the general nuclear export machinery.

All screening procedures have to account for the risk of obtaining “off-target effects” and hence the need for appropriate validation steps. RNAi off target effects are mainly a consequence of a shared similarity between the sequence designed to target the transcripts of a given gene and similarity to other gene transcripts. It has been shown that a perfect complementarity between the 5’ end of the siRNA sequence and the seed region of the 3’ UTR of a transcript is enough to trigger the knockdown of its respective gene, by the same mechanism of action reported for miRNAs (9). Conversely, small molecules can elicit off target effects due to high structural similarity between the target and another protein, resulting in unspecific binding and unspecific activity. Off target effects can induce phenotypical changes that resemble the effects of the silencing of the initial target, masking the undesired and unspecific inhibition of another protein (57). The hits obtained in our chemical genetic analysis and in our RNAi screening were subjected to a thorough validation process in which off-target effects could be successfully detected and discarded. For both screens we tried redundancy strategies which involved the use of several independent inhibitors of the same target (small molecules with different chemical structures) and several independent siRNA agents (vector-based shRNAs and siRNAs with different 3' sequence ends).

The principles applied in the generation of the assays described here can be extrapolated to other signaling pathways, maintaining the general characteristics of the assays. In fact, over the last years other assays have been published based on the translocation properties of molecules like NF-kB, p38 and c-JUN (7).

In order to establish robust and reproducible reporter systems we engineered stable and clonal cell lines. Those characteristics are fundamental since the generation of quantitative data requires homogeneous cell populations that provide consistent readouts.

In the U2foxRELOC cells, a reduction on the intensity of the GFP signal can be observed after long periods of culture. This issue can be overcome by re-sorting the cultured cells, discarding the population with lower signal intensity or simply by replacing the assay cells with a freshly thawed vial from a backup stock, highlighting another fundamental step of assay development: the generation of a large stock of frozen vials shortly after the assay cell line has been established and purified.

The final parameter we used in the U2foxRELOC system to determine the impact of the interfering agents over FOXO translocation was the percentage of cells displaying a nuclear/cytoplasmic ratio of the intensity of the GFP signal superior to 1,8. This was shown to accurately link the phenotypical changes observed in the assays with their respective quantitative data. The establishment of this parameter was based on several observations and optimization experiments. In control conditions we could still observe some nuclear localization of the GFP signal, suggesting that FOXO translocation does not occur as an “all-or-nothing” event, but as a shift in the cytoplasmatic/nuclear ratio instead. Interestingly, the kinetics of FOXO translocation is still to be determined. To clarify how the spatial distribution of FOXO is altered upon stimulation it would be interesting to analyze the patterns of migration of florescent-labeled FOXO proteins through live-video high resolution microscopy. Of note, the basal levels of the nuclear localization of our reporter protein did not interfere with the quantitative data obtained using our defined parameters.

The definition of our measurement parameter allowed us to tackle another challenge of high content analysis: The generation of an assay robust enough to provide quantitative data. Using the U2foxRELOC system we demonstrated that the IC50 values of the well characterized PI3K inhibitors LY294002, PIK-75, PI-103 and

Wortmannin were in agreement with previously established data obtained from classical *in vitro* biochemical assays. The U2foxRELOC is, therefore, a very sensitive system capable of providing quantitative data upon inhibition of the PI3K/Akt pathway.

Due to the intrinsic characteristics of the parental cell line (U2-OS osteosarcoma cells), we observed that the U2foxRELOC cells and the U2transLuc cells display a lower transfection efficiency than the HEK293T-derived 293foxREP cells. Thus, although both cells are appropriate for high throughput experiments, we decided to use the 293foxREP system for our transfection-based screening, to assure that the results were not limited by transfection issues. Conversely, compound screenings were shown more feasible with the U2foxRELOC and U2transLuc cells. We determined that one hour of incubation is sufficient for a robust readout of FOXO translocation in those cells. This short incubation time constitutes an advantage, as it minimizes the risk of unspecific toxicity. On the other hand, either FOXO, our luciferase reporter or both are already stably expressed in those cells, while 293foxREP cells need to be transfected with FOXO and a transfection control (e .g. *Renilla* luciferase) 48hs before treatment with the compounds. Furthermore, U2-OS are bigger, attach strongly to the plates and tend to grow stretched and exclusively in monolayer, all features very desirable for image analysis. Contrarily, HEK293T cells detach easily, complicating the washing steps which are required for automated fixing and staining. Also, they have a reduced size, making it harder to define the nuclei/cytoplasm transition and they may grow irregularly and eventually form foci, generating different focal planes which complicate image analysis.

For the U2foxRELOC, U2transLUC and U2nesRELOC systems we took advantage of the benefits of fixation to establish our screening workflows. The use of fixed cells avoids the need to use live stains which lead to cytotoxicity after extended periods of exposure. Furthermore, fixation allowed us to perform DAPI staining for nuclei definition. DAPI was shown to be a robust nuclear stain with minimal signal loss for periods of up to one month which enables a flexible scheduling of the analysis and also permits the re-analysis of the plates.

On the other hand, the use of live cells enables a kinetic analysis and toxicology studies in a ‘real-time’ manner (87).

The live cell assay BaFiso was shown to accurately discriminate dependency on activated Akt or STAT5 for survival. The versatility of this system allows for its adaptation to any signaling pathways or genes which confer IL3-independent survival to BaF/3 cells. Therefore, this system possesses an immense potential for target and drug discovery, offering a wide array of options for dissecting the signaling pathways downstream of the engineered gene activations.

We challenged this system with a panel of test compounds of known activity and the only two compounds known to selectively interfere with Akt signaling, Akt inhibitor X and UCN-01, reduced the number of yellow tagged BYA cells demonstrating the specificity of the BaFiso system. The Akt inhibitor X is a N-substituted compound reported to inhibit Akt activity even in the absence of its pleckstrin homology domain and it has been suggested that it may bind in the ATP binding site (147). In contrast, UCN-01 has been reported to inhibit several kinases including PDK1, an upstream activator of Akt (82). Interestingly, staurosporine which shares a high structural similarity with UCN-01, differing only by the absence of a hydroxy group on the lactam ring, failed to change the ratio of the BaFiso cell lines. A specificity analysis against a kinase panel revealed different patterns of inhibition for UCN-01 with respect to staurosporine (82). It remains to be determined if these differences in specificity could account for the different behavior observed for these two compounds in the BaFiso assay.

The BaFiso screening design offers some major advantages over traditional in vitro biochemical assays or more classical cellular assays. Co-culture and simultaneous testing of the paired isogenic cell lines in this assay provides an internal control and eliminates errors resulting from separate assessments. BaFiso is an image based high throughput assay that enables the identification of compounds that produce artifacts and cytotoxicity on a single cell basis. Live cell imaging of the BaFiso cell lines permits the constant monitoring of the same cells over the time course of an experiment, leading to a more accurate analysis that minimizes the variability in cell numbers between wells.

One of the major challenges of BaFiso and live cell assays in general is the cytotoxicity of the nuclear stain required for image segmentation. At the moment, there is no availability of non-toxic nuclear dyes although the staining finally adopted for this system – DRAQ5 – was shown to be less toxic, but only if a long exposure is avoided. An alternative approach would involve the stable expression of an exclusively nuclear RFP-tagged construction that would allow object definition needless of other reagents.

The assay design of BaFiso also has to cope with the fact that the cells are not adherent, which requires special attention for automatic image capture.

4.2 Multiplexed Assays: Adding more content to screening

Several studies have been carried out over the last years, aiming for the identification of new genes and molecules implicated in FOXO regulation in a mono-parametric fashion, measuring either FOXO translocation or FOXO transcriptional activity separately as readouts (73, 98).

With the U2transLuc system, both translocation and transactivation can be resolved in a single assay, while cell viability can be monitored needless of additional reagents. The multiplexing of fluorescent and luciferase-based readouts is a new concept and constitutes a breakthrough in the screening field, as the amount of information gathered in a single assay is importantly increased. The same cell plate is initially used for an *in vivo* translocation assay and the scores on nuclear trapping are re-checked for transcriptional activity immediately afterwards in a luciferase assay.

Importantly, different effects of a given agent in FOXO translocation, transcriptional activity and proliferation can be analyzed side by side in the same experiment allowing for the construction of the activity profiles.

This system allows the investigation of one of the most intriguing issues of FOXO regulation, which is the interdependency between translocation and transactivation.

There is some evidence pointing that transcription and subcellular localization are events that can be regulated independently. It has been documented that a mutation within the NES of FOXO1 that lead to its permanent nuclear localization did not override the influence of Akt signaling over FOXO transcriptional activity (149), showing that nuclear sequestration *per se*, at least in the experimental setting used, does not implicate transactivation.

This system adds to the above mentioned technological platforms developed in the course of this work. The integration of these systems allows for the realization of multiplexed screens which, opposite to classical candidate gene approaches, provide unbiased data for novel interactions that translate to target discovery.

4.3 Chemical Genetics: New Insights on FOXO

Chemical genetics is gaining relevance as a promising research field that explores the interface between chemistry and biology. In the course of this work we demonstrated the potential of chemical genetics combined with high-content screening to dissect the complex regulation of the subcellular localization of FOXO transcription factors.

In our chemical genetics analysis of a panel of 73 compounds with known mechanism of action, the majority of the drugs tested failed to produce nuclear trapping of GFP–FOXO. However, we identified 17 compounds that induced the nuclear accumulation of the fluorescent reporter. Most of these small molecules were described as inhibitors of the PI3K/Akt pathway, in agreement with the essential role of signaling through PI3K, PDK1, and Akt in the regulation of the subcellular localization of FOXO proteins.

The vinca alkaloid vinblastine scored as a very potent FOXO translocating agent, active in the low nanomolar range. Vinblastine is a microtubule-depolymerizing drug whose mode of action has been characterized (45). Currently vinblastine is a component of a number of chemotherapy regimens, including ABVD (adriamycin, bleomycin, vimblastine and dacarbazine), which was shown specially effective in Hodgkin Lymphoma (156). Recent data suggest that many classical chemotherapeutic agents are able to activate FOXO (47). However, it remains to be determined if the functions of FOXO are required for the therapeutic effect of vinblastine.

It has been reported that the inhibition of the Ca^{2+}-binding protein CaM produces the nuclear accumulation of FOXO proteins in cell assays based on the immunodetection of transiently expressed reporter protein (73). With the U2foxRELOC system we were able to reproduce this observation and we extended previous data regarding the implication of Ca^{2+}-signaling in the regulation of FOXO transcription factors by analyzing the effect of several chemical probes in the U2foxRELOC assay and on Akt phosphorylation. Chemical genetic analysis of the Ca^{2+}-dependent regulation of FOXO localization revealed the important role of intra- and extracellular calcium. Calcium/calmodulin-regulated FOXO translocation is not directly mediated either by multifunctional or dedicated calcium/CaM-dependent protein kinases, or by upstream CaM-kinase-kinases. This is consistent with a model in which low calcium concentrations decrease the activity of CaM, in turn inhibiting Akt and facilitating the translocation of FOXO proteins to the cell nucleus. Akt associates with CaM in mouse mammary carcinoma cells and has been proposed as a CaM-binding protein (28). However, whether a decrease in CaM-binding induces the nuclear translocation of FOXO proteins by directly affecting Akt activity remains to be explored. CaM expression is altered in several cancers and its inhibition might be a strategy to restore the tumor suppressor activity of the FOXO factors.

4.4 The novel association of TRIB2 with FOXO repression in melanoma

The technological platforms which have been generated in the scope of this work allowed us to perform a large-scale RNAi screening leading to the identification of several FOXO repressors including TRIB2, a homolog of *Drosophila* tribbles. Our findings suggest that TRIB2 is an essential gene in melanoma malignancies, correlated with low levels of pro-apoptotic transcripts via the inhibition of FOXO.

Melanoma commonly arises within the epidermis from melanocytes, which are cells of neuroectodermal origin that provide pigmentation to the skin in the form of melanin (24). Of the three most common skin cancers, malignant melanoma is the rarest but by far the most deadly because metastatic malignant melanoma is highly resistant to treatment (77, 131).

Our findings that TRIB2 are elevated in malignant melanomas and in melanocytes are in accordance with the melanocytic origin of melanoma.

Since Akt activity is one of the principal mechanisms of FOXO inactivation, a possible influence of TRIB2 on Akt signaling could explain its effects seen on FOXO translocation and transcriptional activity. However, western blot analysis did not reveal any changes in Akt or FOXO phosphorylation upon TRIB2 overexpression or knockdown, suggesting that the effect on FOXO subcellular localization and transcriptional activity mediated by TRIB2 occurs independently of Akt signaling.

TRIB2 has been reported to bind to C/EBPα and C/EBPβ and to promote their degradation in a proteasome-dependent manner, causing acute myelogenous leukemia (74) and suppressing adipocyte differentiation (106), respectively. Those observations prompted us to analyze whether TRIB2 could exert the same effect over FOXO, however a direct binding association between the two proteins could not be demonstrated in co-immunoprecipitation assays.

TRIB2 has been reported to be a highly inducible gene (60, 80, 94) and our investigations support this idea. Sequence analysis of the promoter of the TRIB2 gene revealed several binding sites for inducible transcription factors and a conserved mRNA instability motif in the 3'UTR of the transcribed sequence. TRIB2 protein has also been reported to be highly unstable (61), suggesting that TRIB2 is rapidly induced upon designated stimuli and its expression is shut down shortly after the cessation of the triggering stimuli and the protein levels are brought to basal levels.

Our findings suggest that TRIB2 is highly inducible upon intracellular Calcium release, as seen by the increase in TRIB2 transcript levels upon stimulation of G-361 cells with Caffeine and Thapsighargin, both agents shown to trigger the release of intracellular Ca^{2+} (37, 146). Interestingly, some reports associate high levels of intracellular Ca^{2+} in melanoma cells with resistance to apoptosis (40). As TRIB2 was seen to be induced by intracellular Ca^{2+}, the elevated levels of intracellular Ca^{2+} observed in some melanoma cells could constitute the a mechanism by which TRIB2 is elevated in those cells.

Previous reports from our lab showed that FOXO translocates to the cell nucleus when intracellular calcium is chelated. In agreement with this observation, CaM was obtained in our RNAi screening as a FOXO repressor. Thus, enhanced CaM activity and increased TRIB2 expression might constitute parallel means to repress FOXO function in response to Ca^{2+} signaling events. In summary, through a large-scale RNAi screen we identified two novel molecular associations that were shown to influence FOXO subcellular localization and transcriptional activity: Calmodulin and TRIB2. Interestingly, both associations are linked to the intracellular calcium homeostasis, reinforcing the importance of calcium signaling in the modulation of FOXO activity.

5 Conclusions

1. We developed, characterized, and validated an image-based system suitable for monitoring of FOXO cytoplasmic/nuclear translocation in a high throughput manner.

2. We developed, characterized, and validated a transcription-based assay suitable to monitor the recovery of FOXO transcriptional activity in a high throughput manner.

3. We developed, characterized and validated a multiplexed system that combines luminescent and fluorescent readouts to monitor simultaneously subcellular localization of FOXO and FOXO-driven transcription in a single cell line and in a in a single high throughput assay.

4. We developed, characterized, and validated a cell-based system suitable for high throuput detection of nuclear export inhibitors. This system can be used either as a primary screening or as a deconvolution system to further investigate the candidates obtained in our FOXO-based systems.

5. We developed, characterized, and validated a live cell-based system suitable for high throuput analysis of signaling events downstream of engineerd genetic modifications. This system was shown accurate for the detection of Akt inhibitors and can also be used as a deconvolution system to further investigate the dependency on different signaling pathways for BaF/3 cells survival.

6. Through a large-scale RNAi screening we identified an undescribed FOXO repressor function of TRIB2.

7. TRIB2 is highly expressed in melanocyte-derived cells, which correlates with diminished FOXO-driven transcription of the pro-apoptotic gene Bim. In functional studies, TRIB2 knockdown diminished the tumorigenicity of melanoma cells *in vitro* and in a *in vivo* xenograft model, suggesting that the maintenance of high levels of TRIB2 is a pre-requisite for melanomas to keep their malignancy.

8. Through Chemical Genetics and RNAi studies we came to the conclusion that intracellular calcium regulation is crucial in the modulation of FOXO activity.

5 Conclusiones

1. Hemos desarrollado, caracterizado, y validado un sistema basado en imágenes adecuado al análisis de la translocación de FOXO entre el citoplasma y el núcleo adaptado para HTS.

2. Hemos desarrollado, caracterizado y validado un sistema basado en transcripción adecuado para avaliar la recuperación de la actividad transcripcional de FOXO adaptado para HTS.

3. Hemos desarrollado, caracterizado, validado y adaptado para HTS un sistema multiparamétrico que combina datos de fluorescencia y de luminiscencia, proprcionando informaciones a cerca de la translocación y de la actividad transcripcional de FOXO en un único ensayo.

4. Hemos desarrollado, caracterizado, validado y adaptado para HTS un sistema adecuado a la detección de inibidores del exporte nuclear, que puede funcionar bien como un sistema de rastreo primário o como unb sistema de deconvolución para una investigación más detallada de las dianas obtenidas a través de los sistemas basados en FOXO.

5. Hemos desarrollado, caracterizado, y validado un sistema adecuado al análisis de la señalización dependente de modificaciones genéticas previamente diseñadas, adaptado para HTS. Este sistema se ha mostrado fiable para detectar inhibidores de Akt y puede tambien ser usado para una investigación más detallada de la dependencia de células BaF/3 a diferentes vías de señalización para supervivencia.

6. A través de nuestro rastreo por RNA de interferencia hemos identificado TRIB2 como un nuevo represor de FOXO.

7. TRIB2 tiene un alto nivel de expresión en melanocitos normales y en melanomas malignos, lo que se correlaciona con una baja expresión de la transcripción mediada por FOXO del gen pro-apoptótico Bim. A través de estudios funcionales hemos verificado que la reducción de los niveles de TRIB2 disminuye las capacidades tumorigénicas de células de melanoma en cultivo y en un modelo de xenograft, lo que sugiere que la manutención de altos niveles de TRIB2 es un pre-requisito de los melanomas para que puedan mantener su malignidad.

8. A través de estudios de genética química e RNA de interferencia hemos podido concluir que la regulación del calcio intracelular tiene un papel fundamental en la modulación de la actividad de FOXO.

9. References

1. **Ahn, S. H., W. L. Cheung, J. Y. Hsu, R. L. Diaz, M. M. Smith, and C. D. Allis.** 2005. Sterile 20 kinase phosphorylates histone H2B at serine 10 during hydrogen peroxide-induced apoptosis in S. cerevisiae. Cell **120:**25-36.
2. **Alessi, D. R., S. R. James, C. P. Downes, A. B. Holmes, P. R. Gaffney, C. B. Reese, and P. Cohen.** 1997. Characterization of a 3-phosphoinositide-dependent protein kinase which phosphorylates and activates protein kinase Balpha. Curr Biol **7:**261-9.
3. **Aoki, M., H. Jiang, and P. K. Vogt.** 2004. Proteasomal degradation of the FoxO1 transcriptional regulator in cells transformed by the P3k and Akt oncoproteins. Proc Natl Acad Sci U S A **101:**13613-7.
4. **Asano, T., Y. Yao, J. Zhu, D. Li, J. L. Abbruzzese, and S. A. Reddy.** 2004. The PI 3-kinase/Akt signaling pathway is activated due to aberrant Pten expression and targets transcription factors NF-kappaB and c-Myc in pancreatic cancer cells. Oncogene **23:**8571-80.
5. **Bachman, K. E., P. Argani, Y. Samuels, N. Silliman, J. Ptak, S. Szabo, H. Konishi, B. Karakas, B. G. Blair, C. Lin, B. A. Peters, V. E. Velculescu, and B. H. Park.** 2004. The PIK3CA gene is mutated with high frequency in human breast cancers. Cancer Biol Ther **3:**772-5.
6. **Bader, A. G., S. Kang, and P. K. Vogt.** 2006. Cancer-specific mutations in PIK3CA are oncogenic in vivo. Proc Natl Acad Sci U S A **103:**1475-9.
7. **Bertelsen, M., and A. Sanfridson.** 2005. Inflammatory pathway analysis using a high content screening platform. Assay Drug Dev Technol **3:**261-71.
8. **Biggs, W. H., 3rd, J. Meisenhelder, T. Hunter, W. K. Cavenee, and K. C. Arden.** 1999. Protein kinase B/Akt-mediated phosphorylation promotes nuclear exclusion of the winged helix transcription factor FKHR1. Proc Natl Acad Sci U S A **96:**7421-6.
9. **Birmingham, A., E. M. Anderson, A. Reynolds, D. Ilsley-Tyree, D. Leake, Y. Fedorov, S. Baskerville, E. Maksimova, K. Robinson, J. Karpilow, W. S. Marshall, and A. Khvorova.** 2006. 3' UTR seed matches, but not overall identity, are associated with RNAi off-targets. Nat Methods **3:**199-204.
10. **Bluher, M., B. B. Kahn, and C. R. Kahn.** 2003. Extended longevity in mice lacking the insulin receptor in adipose tissue. Science **299:**572-4.
11. **Broderick, D. K., C. Di, T. J. Parrett, Y. R. Samuels, J. M. Cummins, R. E. McLendon, D. W. Fults, V. E. Velculescu, D. D. Bigner, and H. Yan.** 2004. Mutations of PIK3CA in anaplastic oligodendrogliomas, high-grade astrocytomas, and medulloblastomas. Cancer Res **64:**5048-50.
12. **Brownawell, A. M., G. J. Kops, I. G. Macara, and B. M. Burgering.** 2001. Inhibition of nuclear import by protein kinase B (Akt) regulates the subcellular distribution and activity of the forkhead transcription factor AFX. Mol Cell Biol **21:**3534-46.
13. **Brunet, A., A. Bonni, M. J. Zigmond, M. Z. Lin, P. Juo, L. S. Hu, M. J. Anderson, K. C. Arden, J. Blenis, and M. E. Greenberg.** 1999. Akt promotes cell survival by phosphorylating and inhibiting a Forkhead transcription factor. Cell **96:**857-68.
14. **Brunet, A., F. Kanai, J. Stehn, J. Xu, D. Sarbassova, J. V. Frangioni, S. N. Dalal, J. A. DeCaprio, M. E. Greenberg, and M. B. Yaffe.** 2002. 14-3-3 transits to the nucleus and participates in dynamic nucleocytoplasmic transport. J Cell Biol **156:**817-28.
15. **Brunet, A., J. Park, H. Tran, L. S. Hu, B. A. Hemmings, and M. E. Greenberg.** 2001. Protein kinase SGK mediates survival signals by phosphorylating the forkhead transcription factor FKHRL1 (FOXO3a). Mol Cell Biol **21:**952-65.
16. **Brunet, A., L. B. Sweeney, J. F. Sturgill, K. F. Chua, P. L. Greer, Y. Lin, H. Tran, S. E. Ross, R. Mostoslavsky, H. Y. Cohen, L. S. Hu, H. L. Cheng, M.**

P. Jedrychowski, S. P. Gygi, D. A. Sinclair, F. W. Alt, and M. E. Greenberg. 2004. Stress-dependent regulation of FOXO transcription factors by the SIRT1 deacetylase. Science **303:**2011-5.

17. **Butcher, E. C.** 2005. Can cell systems biology rescue drug discovery? Nat Rev Drug Discov **4:**461-7.
18. **Calnan, D. R., and A. Brunet.** 2008. The FoxO code. Oncogene **27:**2276-88.
19. **Campbell, I. G., S. E. Russell, D. Y. Choong, K. G. Montgomery, M. L. Ciavarella, C. S. Hooi, B. E. Cristiano, R. B. Pearson, and W. A. Phillips.** 2004. Mutation of the PIK3CA gene in ovarian and breast cancer. Cancer Res **64:**7678-81.
20. **Carnero, A., C. Blanco-Aparicio, O. Renner, W. Link, and J. F. Leal.** 2008. The PTEN/PI3K/AKT signalling pathway in cancer, therapeutic implications. Curr Cancer Drug Targets **8:**187-98.
21. **Carpten, J. D., A. L. Faber, C. Horn, G. P. Donoho, S. L. Briggs, C. M. Robbins, G. Hostetter, S. Boguslawski, T. Y. Moses, S. Savage, M. Uhlik, A. Lin, J. Du, Y. W. Qian, D. J. Zeckner, G. Tucker-Kellogg, J. Touchman, K. Patel, S. Mousses, M. Bittner, R. Schevitz, M. H. Lai, K. L. Blanchard, and J. E. Thomas.** 2007. A transforming mutation in the pleckstrin homology domain of AKT1 in cancer. Nature **448:**439-44.
22. **Chang, K., S. J. Elledge, and G. J. Hannon.** 2006. Lessons from Nature: microRNA-based shRNA libraries. Nat Methods **3:**707-14.
23. **Cheung, W. L., K. Ajiro, K. Samejima, M. Kloc, P. Cheung, C. A. Mizzen, A. Beeser, L. D. Etkin, J. Chernoff, W. C. Earnshaw, and C. D. Allis.** 2003. Apoptotic phosphorylation of histone H2B is mediated by mammalian sterile twenty kinase. Cell **113:**507-17.
24. **Chudnovsky, Y., P. A. Khavari, and A. E. Adams.** 2005. Melanoma genetics and the development of rational therapeutics. J Clin Invest **115:**813-24.
25. **Dahia, P. L.** 2000. PTEN, a unique tumor suppressor gene. Endocr Relat Cancer **7:**115-29.
26. **Daitoku, H., M. Hatta, H. Matsuzaki, S. Aratani, T. Ohshima, M. Miyagishi, T. Nakajima, and A. Fukamizu.** 2004. Silent information regulator 2 potentiates Foxo1-mediated transcription through its deacetylase activity. Proc Natl Acad Sci U S A **101:**10042-7.
27. **Dansen, T. B., and B. M. Burgering.** 2008. Unravelling the tumor-suppressive functions of FOXO proteins. Trends Cell Biol **18:**421-9.
28. **Deb, T. B., C. M. Coticchia, and R. B. Dickson.** 2004. Calmodulin-mediated activation of Akt regulates survival of c-Myc-overexpressing mouse mammary carcinoma cells. J Biol Chem **279:**38903-11.
29. **Delpuech, O., B. Griffiths, P. East, A. Essafi, E. W. Lam, B. Burgering, J. Downward, and A. Schulze.** 2007. Induction of Mxi1-SR alpha by FOXO3a contributes to repression of Myc-dependent gene expression. Mol Cell Biol **27:**4917-30.
30. **Devi, G. R.** 2006. siRNA-based approaches in cancer therapy. Cancer Gene Ther **13:**819-29.
31. **Dijkers, P. F., K. U. Birkenkamp, E. W. Lam, N. S. Thomas, J. W. Lammers, L. Koenderman, and P. J. Coffer.** 2002. FKHR-L1 can act as a critical effector of cell death induced by cytokine withdrawal: protein kinase B-enhanced cell survival through maintenance of mitochondrial integrity. J Cell Biol **156:**531-42.
32. **Dijkers, P. F., R. H. Medema, J. W. Lammers, L. Koenderman, and P. J. Coffer.** 2000. Expression of the pro-apoptotic Bcl-2 family member Bim is regulated by the forkhead transcription factor FKHR-L1. Curr Biol **10:**1201-4.
33. **Dijkers, P. F., R. H. Medema, C. Pals, L. Banerji, N. S. Thomas, E. W. Lam, B. M. Burgering, J. A. Raaijmakers, J. W. Lammers, L. Koenderman, and P. J. Coffer.** 2000. Forkhead transcription factor FKHR-L1 modulates cytokine-dependent transcriptional regulation of p27(KIP1). Mol Cell Biol **20:**9138-48.

34. **Dillon, R. L., D. E. White, and W. J. Muller.** 2007. The phosphatidyl inositol 3-kinase signaling network: implications for human breast cancer. Oncogene **26:**1338-45.
35. **Downward, J.** 2004. PI 3-kinase, Akt and cell survival. Semin Cell Dev Biol **15:**177-82.
36. **Dykxhoorn, D. M., C. D. Novina, and P. A. Sharp.** 2003. Killing the messenger: short RNAs that silence gene expression. Nat Rev Mol Cell Biol **4:**457-67.
37. **Elmqvist, D., and D. S. Feldman.** 1965. Calcium dependence of spontaneous acetylcholine release at mammalian motor nerve terminals. J Physiol **181:**487-97.
38. **Essafi, A., S. Fernandez de Mattos, Y. A. Hassen, I. Soeiro, G. J. Mufti, N. S. Thomas, R. H. Medema, and E. W. Lam.** 2005. Direct transcriptional regulation of Bim by FoxO3a mediates STI571-induced apoptosis in Bcr-Abl-expressing cells. Oncogene **24:**2317-29.
39. **Essers, M. A., L. M. de Vries-Smits, N. Barker, P. E. Polderman, B. M. Burgering, and H. C. Korswagen.** 2005. Functional interaction between beta-catenin and FOXO in oxidative stress signaling. Science **308:**1181-4.
40. **Fedida-Metula, S., S. Elhyany, S. Tsory, S. Segal, M. Hershfinkel, I. Sekler, and D. Fishman.** 2008. Targeting lipid rafts inhibits protein kinase B by disrupting calcium homeostasis and attenuates malignant properties of melanoma cells. Carcinogenesis **29:**1546-54.
41. **Frescas, D., L. Valenti, and D. Accili.** 2005. Nuclear trapping of the forkhead transcription factor FoxO1 via Sirt-dependent deacetylation promotes expression of glucogenetic genes. J Biol Chem **280:**20589-95.
42. **Furukawa-Hibi, Y., K. Yoshida-Araki, T. Ohta, K. Ikeda, and N. Motoyama.** 2002. FOXO forkhead transcription factors induce G(2)-M checkpoint in response to oxidative stress. J Biol Chem **277:**26729-32.
43. **Furuyama, T., T. Nakazawa, I. Nakano, and N. Mori.** 2000. Identification of the differential distribution patterns of mRNAs and consensus binding sequences for mouse DAF-16 homologues. Biochem J **349:**629-34.
44. **Garcia-Rostan, G., A. M. Costa, I. Pereira-Castro, G. Salvatore, R. Hernandez, M. J. Hermsem, A. Herrero, A. Fusco, J. Cameselle-Teijeiro, and M. Santoro.** 2005. Mutation of the PIK3CA gene in anaplastic thyroid cancer. Cancer Res **65:**10199-207.
45. **Gigant, B., C. Wang, R. B. Ravelli, F. Roussi, M. O. Steinmetz, P. A. Curmi, A. Sobel, and M. Knossow.** 2005. Structural basis for the regulation of tubulin by vinblastine. Nature **435:**519-22.
46. **Gilley, J., P. J. Coffer, and J. Ham.** 2003. FOXO transcription factors directly activate bim gene expression and promote apoptosis in sympathetic neurons. J Cell Biol **162:**613-22.
47. **Gomes, A. R., J. J. Brosens, and E. W. Lam.** 2008. Resist or die: FOXO transcription factors determine the cellular response to chemotherapy. Cell Cycle **7:**3133-6.
48. **Gomez-Gutierrez, J. G., V. Souza, H. Y. Hao, R. Montes de Oca-Luna, Y. B. Dong, H. S. Zhou, and K. M. McMasters.** 2006. Adenovirus-mediated gene transfer of FKHRL1 triple mutant efficiently induces apoptosis in melanoma cells. Cancer Biol Ther **5:**875-83.
49. **Graves, J. D., Y. Gotoh, K. E. Draves, D. Ambrose, D. K. Han, M. Wright, J. Chernoff, E. A. Clark, and E. G. Krebs.** 1998. Caspase-mediated activation and induction of apoptosis by the mammalian Ste20-like kinase Mst1. Embo J **17:**2224-34.
50. **Greer, E. L., and A. Brunet.** 2005. FOXO transcription factors at the interface between longevity and tumor suppression. Oncogene **24:**7410-25.

51. **Hamilton, A. J., and D. C. Baulcombe.** 1999. A species of small antisense RNA in posttranscriptional gene silencing in plants. Science **286:**950-2.
52. **Hammond, S. M., E. Bernstein, D. Beach, and G. J. Hannon.** 2000. An RNA-directed nuclease mediates post-transcriptional gene silencing in Drosophila cells. Nature **404:**293-6.
53. **Hammond, S. M., S. Boettcher, A. A. Caudy, R. Kobayashi, and G. J. Hannon.** 2001. Argonaute2, a link between genetic and biochemical analyses of RNAi. Science **293:**1146-50.
54. **Han, C. Y., K. B. Cho, H. S. Choi, H. K. Han, and K. W. Kang.** 2008. Role of FoxO1 activation in MDR1 expression in adriamycin-resistant breast cancer cells. Carcinogenesis **29:**1837-44.
55. **Hanahan, D., and R. A. Weinberg.** 2000. The hallmarks of cancer. Cell **100:**57-70.
56. **Haney, S. A., P. LaPan, J. Pan, and J. Zhang.** 2006. High-content screening moves to the front of the line. Drug Discov Today **11:**889-94.
57. **Hart, C. P.** 2005. Finding the target after screening the phenotype. Drug Discov Today **10:**513-9.
58. **Hartwell, L. H.** 1991. Twenty-five years of cell cycle genetics. Genetics **129:**975-80.
59. **Harvey, K. F., C. M. Pfleger, and I. K. Hariharan.** 2003. The Drosophila Mst ortholog, hippo, restricts growth and cell proliferation and promotes apoptosis. Cell **114:**457-67.
60. **Hegedus, Z., A. Czibula, and E. Kiss-Toth.** 2007. Tribbles: a family of kinase-like proteins with potent signalling regulatory function. Cell Signal **19:**238-50.
61. **Hegedus, Z., A. Czibula, and E. Kiss-Toth.** 2006. Tribbles: novel regulators of cell function; evolutionary aspects. Cell Mol Life Sci **63:**1632-41.
62. **Henderson, S. T., and T. E. Johnson.** 2001. daf-16 integrates developmental and environmental inputs to mediate aging in the nematode Caenorhabditis elegans. Curr Biol **11:**1975-80.
63. **Hennessy, B. T., D. L. Smith, P. T. Ram, Y. Lu, and G. B. Mills.** 2005. Exploiting the PI3K/AKT pathway for cancer drug discovery. Nat Rev Drug Discov **4:**988-1004.
64. **Holzenberger, M., J. Dupont, B. Ducos, P. Leneuve, A. Geloen, P. C. Even, P. Cervera, and Y. Le Bouc.** 2003. IGF-1 receptor regulates lifespan and resistance to oxidative stress in mice. Nature **421:**182-7.
65. **Honda, Y., and S. Honda.** 1999. The daf-2 gene network for longevity regulates oxidative stress resistance and Mn-superoxide dismutase gene expression in Caenorhabditis elegans. Faseb J **13:**1385-93.
66. **Hu, M. C., D. F. Lee, W. Xia, L. S. Golfman, F. Ou-Yang, J. Y. Yang, Y. Zou, S. Bao, N. Hanada, H. Saso, R. Kobayashi, and M. C. Hung.** 2004. IkappaB kinase promotes tumorigenesis through inhibition of forkhead FOXO3a. Cell **117:**225-37.
67. **Huang, H., K. M. Regan, F. Wang, D. Wang, D. I. Smith, J. M. van Deursen, and D. J. Tindall.** 2005. Skp2 inhibits FOXO1 in tumor suppression through ubiquitin-mediated degradation. Proc Natl Acad Sci U S A **102:**1649-54.
68. **Jackson, J. G., J. I. Kreisberg, A. P. Koterba, D. Yee, and M. G. Brattain.** 2000. Phosphorylation and nuclear exclusion of the forkhead transcription factor FKHR after epidermal growth factor treatment in human breast cancer cells. Oncogene **19:**4574-81.
69. **Johnson, T. E.** 1990. Increased life-span of age-1 mutants in Caenorhabditis elegans and lower Gompertz rate of aging. Science **249:**908-12.
70. **Justice, M. J., J. K. Noveroske, J. S. Weber, B. Zheng, and A. Bradley.** 1999. Mouse ENU mutagenesis. Hum Mol Genet **8:**1955-63.
71. **Kandel, E. S., and N. Hay.** 1999. The regulation and activities of the multifunctional serine/threonine kinase Akt/PKB. Exp Cell Res **253:**210-29.

72. **Kashii, Y., M. Uchida, K. Kirito, M. Tanaka, K. Nishijima, M. Toshima, T. Ando, K. Koizumi, T. Endoh, K. Sawada, M. Momoi, Y. Miura, K. Ozawa, and N. Komatsu.** 2000. A member of Forkhead family transcription factor, FKHRL1, is one of the downstream molecules of phosphatidylinositol 3-kinase-Akt activation pathway in erythropoietin signal transduction. Blood **96:**941-9.
73. **Kau, T. R., F. Schroeder, S. Ramaswamy, C. L. Wojciechowski, J. J. Zhao, T. M. Roberts, J. Clardy, W. R. Sellers, and P. A. Silver.** 2003. A chemical genetic screen identifies inhibitors of regulated nuclear export of a Forkhead transcription factor in PTEN-deficient tumor cells. Cancer Cell **4:**463-76.
74. **Keeshan, K., Y. He, B. J. Wouters, O. Shestova, L. Xu, H. Sai, C. G. Rodriguez, I. Maillard, J. W. Tobias, P. Valk, M. Carroll, J. C. Aster, R. Delwel, and W. S. Pear.** 2006. Tribbles homolog 2 inactivates C/EBPalpha and causes acute myelogenous leukemia. Cancer Cell **10:**401-11.
75. **Kenyon, C.** 2005. The plasticity of aging: insights from long-lived mutants. Cell **120:**449-60.
76. **Kenyon, C., J. Chang, E. Gensch, A. Rudner, and R. Tabtiang.** 1993. A C. elegans mutant that lives twice as long as wild type. Nature **366:**461-4.
77. **Khavari, P. A.** 2006. Modelling cancer in human skin tissue. Nat Rev Cancer **6:**270-80.
78. **Kimura, K. D., H. A. Tissenbaum, Y. Liu, and G. Ruvkun.** 1997. daf-2, an insulin receptor-like gene that regulates longevity and diapause in Caenorhabditis elegans. Science **277:**942-6.
79. **Kirkegaard, T., C. J. Witton, L. M. McGlynn, S. M. Tovey, B. Dunne, A. Lyon, and J. M. Bartlett.** 2005. AKT activation predicts outcome in breast cancer patients treated with tamoxifen. J Pathol **207:**139-46.
80. **Kiss-Toth, E., S. M. Bagstaff, H. Y. Sung, V. Jozsa, C. Dempsey, J. C. Caunt, K. M. Oxley, D. H. Wyllie, T. Polgar, M. Harte, A. O'Neill L, E. E. Qwarnstrom, and S. K. Dower.** 2004. Human tribbles, a protein family controlling mitogen-activated protein kinase cascades. J Biol Chem **279:**42703-8.
81. **Kitamura, Y. I., T. Kitamura, J. P. Kruse, J. C. Raum, R. Stein, W. Gu, and D. Accili.** 2005. FoxO1 protects against pancreatic beta cell failure through NeuroD and MafA induction. Cell Metab **2:**153-63.
82. **Komander, D., G. S. Kular, J. Bain, M. Elliott, D. R. Alessi, and D. M. Van Aalten.** 2003. Structural basis for UCN-01 (7-hydroxystaurosporine) specificity and PDK1 (3-phosphoinositide-dependent protein kinase-1) inhibition. Biochem J **375:**255-62.
83. **Kops, G. J., and B. M. Burgering.** 1999. Forkhead transcription factors: new insights into protein kinase B (c-akt) signaling. J Mol Med **77:**656-65.
84. **Kops, G. J., T. B. Dansen, P. E. Polderman, I. Saarloos, K. W. Wirtz, P. J. Coffer, T. T. Huang, J. L. Bos, R. H. Medema, and B. M. Burgering.** 2002. Forkhead transcription factor FOXO3a protects quiescent cells from oxidative stress. Nature **419:**316-21.
85. **Kops, G. J., R. H. Medema, J. Glassford, M. A. Essers, P. F. Dijkers, P. J. Coffer, E. W. Lam, and B. M. Burgering.** 2002. Control of cell cycle exit and entry by protein kinase B-regulated forkhead transcription factors. Mol Cell Biol **22:**2025-36.
86. **Lam, E. W., R. E. Francis, and M. Petkovic.** 2006. FOXO transcription factors: key regulators of cell fate. Biochem Soc Trans **34:**722-6.
87. **Lang, P., K. Yeow, A. Nichols, and A. Scheer.** 2006. Cellular imaging in drug discovery. Nat Rev Drug Discov **5:**343-56.
88. **Langley, E., M. Pearson, M. Faretta, U. M. Bauer, R. A. Frye, S. Minucci, P. G. Pelicci, and T. Kouzarides.** 2002. Human SIR2 deacetylates p53 and antagonizes PML/p53-induced cellular senescence. Embo J **21:**2383-96.

89. **Lee, S. S., S. Kennedy, A. C. Tolonen, and G. Ruvkun.** 2003. DAF-16 target genes that control C. elegans life-span and metabolism. Science **300:**644-7.

90. **Lehtinen, M. K., Z. Yuan, P. R. Boag, Y. Yang, J. Villen, E. B. Becker, S. DiBacco, N. de la Iglesia, S. Gygi, T. K. Blackwell, and A. Bonni.** 2006. A conserved MST-FOXO signaling pathway mediates oxidative-stress responses and extends life span. Cell **125:**987-1001.

91. **Li, Q., H. Xiao, and K. Isobe.** 2002. Histone acetyltransferase activities of cAMP-regulated enhancer-binding protein and p300 in tissues of fetal, young, and old mice. J Gerontol A Biol Sci Med Sci **57:**B93-8.

92. **Liaw, D., D. J. Marsh, J. Li, P. L. Dahia, S. I. Wang, Z. Zheng, S. Bose, K. M. Call, H. C. Tsou, M. Peacocke, C. Eng, and R. Parsons.** 1997. Germline mutations of the PTEN gene in Cowden disease, an inherited breast and thyroid cancer syndrome. Nat Genet **16:**64-7.

93. **Lin, K., J. B. Dorman, A. Rodan, and C. Kenyon.** 1997. daf-16: An HNF-3/forkhead family member that can function to double the life-span of Caenorhabditis elegans. Science **278:**1319-22.

94. **Lin, K. R., S. F. Lee, C. M. Hung, C. L. Li, H. F. Yang-Yen, and J. J. Yen.** 2007. Survival factor withdrawal-induced apoptosis of TF-1 cells involves a TRB2-Mcl-1 axis-dependent pathway. J Biol Chem **282:**21962-72.

95. **Marsh, D. J., J. B. Kum, K. L. Lunetta, M. J. Bennett, R. J. Gorlin, S. F. Ahmed, J. Bodurtha, C. Crowe, M. A. Curtis, M. Dasouki, T. Dunn, H. Feit, M. T. Geraghty, J. M. Graham, Jr., S. V. Hodgson, A. Hunter, B. R. Korf, D. Manchester, S. Miesfeldt, V. A. Murday, K. L. Nathanson, M. Parisi, B. Pober, C. Romano, C. Eng, and et al.** 1999. PTEN mutation spectrum and genotype-phenotype correlations in Bannayan-Riley-Ruvalcaba syndrome suggest a single entity with Cowden syndrome. Hum Mol Genet **8:**1461-72.

96. **Martineau, H. M., and I. T. Pyrah.** 2007. Review of the application of RNA interference technology in the pharmaceutical industry. Toxicol Pathol **35:**327-36.

97. **Matsuzaki, H., H. Daitoku, M. Hatta, K. Tanaka, and A. Fukamizu.** 2003. Insulin-induced phosphorylation of FKHR (Foxo1) targets to proteasomal degradation. Proc Natl Acad Sci U S A **100:**11285-90.

98. **Mattila, J., J. Kallijarvi, and O. Puig.** 2008. RNAi screening for kinases and phosphatases identifies FoxO regulators. Proc Natl Acad Sci U S A **105:**14873-8.

99. **McElwee, J. J., E. Schuster, E. Blanc, J. H. Thomas, and D. Gems.** 2004. Shared transcriptional signature in Caenorhabditis elegans Dauer larvae and long-lived daf-2 mutants implicates detoxification system in longevity assurance. J Biol Chem **279:**44533-43.

100. **Medema, R. H., G. J. Kops, J. L. Bos, and B. M. Burgering.** 2000. AFX-like Forkhead transcription factors mediate cell-cycle regulation by Ras and PKB through p27kip1. Nature **404:**782-7.

101. **Metzstein, M. M., G. M. Stanfield, and H. R. Horvitz.** 1998. Genetics of programmed cell death in C. elegans: past, present and future. Trends Genet **14:**410-6.

102. **Modur, V., R. Nagarajan, B. M. Evers, and J. Milbrandt.** 2002. FOXO proteins regulate tumor necrosis factor-related apoptosis inducing ligand expression. Implications for PTEN mutation in prostate cancer. J Biol Chem **277:**47928-37.

103. **Morris, J. Z., H. A. Tissenbaum, and G. Ruvkun.** 1996. A phosphatidylinositol-3-OH kinase family member regulating longevity and diapause in Caenorhabditis elegans. Nature **382:**536-9.

104. **Motta, M. C., N. Divecha, M. Lemieux, C. Kamel, D. Chen, W. Gu, Y. Bultsma, M. McBurney, and L. Guarente.** 2004. Mammalian SIRT1 represses forkhead transcription factors. Cell **116:**551-63.

105. **Myatt, S. S., and E. W. Lam.** 2007. The emerging roles of forkhead box (Fox) proteins in cancer. Nat Rev Cancer **7:**847-59.
106. **Naiki, T., E. Saijou, Y. Miyaoka, K. Sekine, and A. Miyajima.** 2007. TRB2, a mouse Tribbles ortholog, suppresses adipocyte differentiation by inhibiting AKT and C/EBPbeta. J Biol Chem **282:**24075-82.
107. **Nakae, J., V. Barr, and D. Accili.** 2000. Differential regulation of gene expression by insulin and IGF-1 receptors correlates with phosphorylation of a single amino acid residue in the forkhead transcription factor FKHR. Embo J **19:**989-96.
108. **Nakae, J., T. Kitamura, D. L. Silver, and D. Accili.** 2001. The forkhead transcription factor Foxo1 (Fkhr) confers insulin sensitivity onto glucose-6-phosphatase expression. J Clin Invest **108:**1359-67.
109. **Nakae, J., B. C. Park, and D. Accili.** 1999. Insulin stimulates phosphorylation of the forkhead transcription factor FKHR on serine 253 through a Wortmannin-sensitive pathway. J Biol Chem **274:**15982-5.
110. **Nakayama, K., N. Nakayama, R. J. Kurman, L. Cope, G. Pohl, Y. Samuels, V. E. Velculescu, T. L. Wang, and M. Shih Ie.** 2006. Sequence mutations and amplification of PIK3CA and AKT2 genes in purified ovarian serous neoplasms. Cancer Biol Ther **5:**779-85.
111. **Nelen, M. R., W. C. van Staveren, E. A. Peeters, M. B. Hassel, R. J. Gorlin, H. Hamm, C. F. Lindboe, J. P. Fryns, R. H. Sijmons, D. G. Woods, E. C. Mariman, G. W. Padberg, and H. Kremer.** 1997. Germline mutations in the PTEN/MMAC1 gene in patients with Cowden disease. Hum Mol Genet **6:**1383-7.
112. **Nemoto, S., M. M. Fergusson, and T. Finkel.** 2004. Nutrient availability regulates SIRT1 through a forkhead-dependent pathway. Science **306:**2105-8.
113. **Nemoto, S., and T. Finkel.** 2002. Redox regulation of forkhead proteins through a p66shc-dependent signaling pathway. Science **295:**2450-2.
114. **Nusslein-Volhard, C., and E. Wieschaus.** 1980. Mutations affecting segment number and polarity in Drosophila. Nature **287:**795-801.
115. **O'Neill, E., L. Rushworth, M. Baccarini, and W. Kolch.** 2004. Role of the kinase MST2 in suppression of apoptosis by the proto-oncogene product Raf-1. Science **306:**2267-70.
116. **Ogg, S., S. Paradis, S. Gottlieb, G. I. Patterson, L. Lee, H. A. Tissenbaum, and G. Ruvkun.** 1997. The Fork head transcription factor DAF-16 transduces insulin-like metabolic and longevity signals in C. elegans. Nature **389:**994-9.
117. **Okano, J., L. Snyder, and A. K. Rustgi.** 2003. Genetic alterations in esophageal cancer. Methods Mol Biol **222:**131-45.
118. **Paik, J. H., R. Kollipara, G. Chu, H. Ji, Y. Xiao, Z. Ding, L. Miao, Z. Tothova, J. W. Horner, D. R. Carrasco, S. Jiang, D. G. Gilliland, L. Chin, W. H. Wong, D. H. Castrillon, and R. A. DePinho.** 2007. FoxOs are lineage-restricted redundant tumor suppressors and regulate endothelial cell homeostasis. Cell **128:**309-23.
119. **Parsons, D. W., T. L. Wang, Y. Samuels, A. Bardelli, J. M. Cummins, L. DeLong, N. Silliman, J. Ptak, S. Szabo, J. K. Willson, S. Markowitz, K. W. Kinzler, B. Vogelstein, C. Lengauer, and V. E. Velculescu.** 2005. Colorectal cancer: mutations in a signalling pathway. Nature **436:**792.
120. **Plas, D. R., and C. B. Thompson.** 2005. Akt-dependent transformation: there is more to growth than just surviving. Oncogene **24:**7435-42.
121. **Plas, D. R., and C. B. Thompson.** 2003. Akt activation promotes degradation of tuberin and FOXO3a via the proteasome. J Biol Chem **278:**12361-6.
122. **Puigserver, P., J. Rhee, J. Donovan, C. J. Walkey, J. C. Yoon, F. Oriente, Y. Kitamura, J. Altomonte, H. Dong, D. Accili, and B. M. Spiegelman.** 2003. Insulin-regulated hepatic gluconeogenesis through FOXO1-PGC-1alpha interaction. Nature **423:**550-5.

123. **Ramaswamy, S., N. Nakamura, I. Sansal, L. Bergeron, and W. R. Sellers.** 2002. A novel mechanism of gene regulation and tumor suppression by the transcription factor FKHR. Cancer Cell **2:**81-91.
124. **Real, P. J., A. Benito, J. Cuevas, M. T. Berciano, A. de Juan, P. Coffer, J. Gomez-Roman, M. Lafarga, J. M. Lopez-Vega, and J. L. Fernandez-Luna.** 2005. Blockade of epidermal growth factor receptors chemosensitizes breast cancer cells through up-regulation of Bnip3L. Cancer Res **65:**8151-7.
125. **Reed, S. I.** 2002. Cell cycling? Check your brakes. Nat Cell Biol **4:**E199-201.
126. **Reid, A., L. Vidal, H. Shaw, and J. de Bono.** 2007. Dual inhibition of ErbB1 (EGFR/HER1) and ErbB2 (HER2/neu). Eur J Cancer **43:**481-9.
127. **Rena, G., S. Guo, S. C. Cichy, T. G. Unterman, and P. Cohen.** 1999. Phosphorylation of the transcription factor forkhead family member FKHR by protein kinase B. J Biol Chem **274:**17179-83.
128. **Rena, G., A. R. Prescott, S. Guo, P. Cohen, and T. G. Unterman.** 2001. Roles of the forkhead in rhabdomyosarcoma (FKHR) phosphorylation sites in regulating 14-3-3 binding, transactivation and nuclear targetting. Biochem J **354:**605-12.
129. **Rena, G., Y. L. Woods, A. R. Prescott, M. Peggie, T. G. Unterman, M. R. Williams, and P. Cohen.** 2002. Two novel phosphorylation sites on FKHR that are critical for its nuclear exclusion. Embo J **21:**2263-71.
130. **Rinner, O., L. N. Mueller, M. Hubalek, M. Muller, M. Gstaiger, and R. Aebersold.** 2007. An integrated mass spectrometric and computational framework for the analysis of protein interaction networks. Nat Biotechnol **25:**345-52.
131. **Rodolfo, M., M. Daniotti, and V. Vallacchi.** 2004. Genetic progression of metastatic melanoma. Cancer Lett **214:**133-47.
132. **Sams-Dodd, F.** 2005. Target-based drug discovery: is something wrong? Drug Discov Today **10:**139-47.
133. **Samuels, Y., Z. Wang, A. Bardelli, N. Silliman, J. Ptak, S. Szabo, H. Yan, A. Gazdar, S. M. Powell, G. J. Riggins, J. K. Willson, S. Markowitz, K. W. Kinzler, B. Vogelstein, and V. E. Velculescu.** 2004. High frequency of mutations of the PIK3CA gene in human cancers. Science **304:**554.
134. **Schmidt, M., S. Fernandez de Mattos, A. van der Horst, R. Klompmaker, G. J. Kops, E. W. Lam, B. M. Burgering, and R. H. Medema.** 2002. Cell cycle inhibition by FoxO forkhead transcription factors involves downregulation of cyclin D. Mol Cell Biol **22:**7842-52.
135. **Schmoll, D., K. S. Walker, D. R. Alessi, R. Grempler, A. Burchell, S. Guo, R. Walther, and T. G. Unterman.** 2000. Regulation of glucose-6-phosphatase gene expression by protein kinase Balpha and the forkhead transcription factor FKHR. Evidence for insulin response unit-dependent and -independent effects of insulin on promoter activity. J Biol Chem **275:**36324-33.
136. **Schrager, C. A., D. Schneider, A. C. Gruener, H. C. Tsou, and M. Peacocke.** 1998. Clinical and pathological features of breast disease in Cowden's syndrome: an underrecognized syndrome with an increased risk of breast cancer. Hum Pathol **29:**47-53.
137. **Seoane, J., H. V. Le, L. Shen, S. A. Anderson, and J. Massague.** 2004. Integration of Smad and forkhead pathways in the control of neuroepithelial and glioblastoma cell proliferation. Cell **117:**211-23.
138. **Stockwell, B. R.** 2000. Chemical genetics: ligand-based discovery of gene function. Nat Rev Genet **1:**116-25.
139. **Stokoe, D.** 2001. Pten. Curr Biol **11:**R502.
140. **Sunters, A., S. Fernandez de Mattos, M. Stahl, J. J. Brosens, G. Zoumpoulidou, C. A. Saunders, P. J. Coffer, R. H. Medema, R. C. Coombes, and E. W. Lam.** 2003. FoxO3a transcriptional regulation of Bim

controls apoptosis in paclitaxel-treated breast cancer cell lines. J Biol Chem **278:**49795-805.

141. **Sunters, A., P. A. Madureira, K. M. Pomeranz, M. Aubert, J. J. Brosens, S. J. Cook, B. M. Burgering, R. C. Coombes, and E. W. Lam.** 2006. Paclitaxel-induced nuclear translocation of FOXO3a in breast cancer cells is mediated by c-Jun NH2-terminal kinase and Akt. Cancer Res **66:**212-20.
142. **Takaishi, H., H. Konishi, H. Matsuzaki, Y. Ono, Y. Shirai, N. Saito, T. Kitamura, W. Ogawa, M. Kasuga, U. Kikkawa, and Y. Nishizuka.** 1999. Regulation of nuclear translocation of forkhead transcription factor AFX by protein kinase B. Proc Natl Acad Sci U S A **96:**11836-41.
143. **Tang, E. D., G. Nunez, F. G. Barr, and K. L. Guan.** 1999. Negative regulation of the forkhead transcription factor FKHR by Akt. J Biol Chem **274:**16741-6.
144. **Teleman, A. A., V. Hietakangas, A. C. Sayadian, and S. M. Cohen.** 2008. Nutritional control of protein biosynthetic capacity by insulin via Myc in Drosophila. Cell Metab **7:**21-32.
145. **Terstappen, G. C., C. Schlupen, R. Raggiaschi, and G. Gaviraghi.** 2007. Target deconvolution strategies in drug discovery. Nat Rev Drug Discov **6:**891-903.
146. **Thastrup, O., H. Linnebjerg, P. J. Bjerrum, J. B. Knudsen, and S. B. Christensen.** 1987. The inflammatory and tumor-promoting sesquiterpene lactone, thapsigargin, activates platelets by selective mobilization of calcium as shown by protein phosphorylations. Biochim Biophys Acta **927:**65-73.
147. **Thimmaiah, K. N., J. B. Easton, G. S. Germain, C. L. Morton, S. Kamath, J. K. Buolamwini, and P. J. Houghton.** 2005. Identification of N10-substituted phenoxazines as potent and specific inhibitors of Akt signaling. J Biol Chem **280:**31924-35.
148. **Tran, H., A. Brunet, J. M. Grenier, S. R. Datta, A. J. Fornace, Jr., P. S. DiStefano, L. W. Chiang, and M. E. Greenberg.** 2002. DNA repair pathway stimulated by the forkhead transcription factor FOXO3a through the Gadd45 protein. Science **296:**530-4.
149. **Tsai, W. C., N. Bhattacharyya, L. Y. Han, J. A. Hanover, and M. M. Rechler.** 2003. Insulin inhibition of transcription stimulated by the forkhead protein Foxo1 is not solely due to nuclear exclusion. Endocrinology **144:**5615-22.
150. **Tsuruta, F., J. Sunayama, Y. Mori, S. Hattori, S. Shimizu, Y. Tsujimoto, K. Yoshioka, N. Masuyama, and Y. Gotoh.** 2004. JNK promotes Bax translocation to mitochondria through phosphorylation of 14-3-3 proteins. Embo J **23:**1889-99.
151. **Tuschl, T., P. D. Zamore, R. Lehmann, D. P. Bartel, and P. A. Sharp.** 1999. Targeted mRNA degradation by double-stranded RNA in vitro. Genes Dev **13:**3191-7.
152. **van der Horst, A., A. M. de Vries-Smits, A. B. Brenkman, M. H. van Triest, N. van den Broek, F. Colland, M. M. Maurice, and B. M. Burgering.** 2006. FOXO4 transcriptional activity is regulated by monoubiquitination and USP7/HAUSP. Nat Cell Biol **8:**1064-73.
153. **Vanhaesebroeck, B., S. J. Leevers, K. Ahmadi, J. Timms, R. Katso, P. C. Driscoll, R. Woscholski, P. J. Parker, and M. D. Waterfield.** 2001. Synthesis and function of 3-phosphorylated inositol lipids. Annu Rev Biochem **70:**535-602.
154. **Vaziri, H., S. K. Dessain, E. Ng Eaton, S. I. Imai, R. A. Frye, T. K. Pandita, L. Guarente, and R. A. Weinberg.** 2001. hSIR2(SIRT1) functions as an NAD-dependent p53 deacetylase. Cell **107:**149-59.
155. **Vivanco, I., and C. L. Sawyers.** 2002. The phosphatidylinositol 3-Kinase AKT pathway in human cancer. Nat Rev Cancer **2:**489-501.
156. **Wedgwood, A., and A. Younes.** 2007. Prophylactic use of filgrastim with ABVD and BEACOPP chemotherapy regimens for Hodgkin lymphoma. Clin Lymphoma Myeloma **8 Suppl 2:**S63-6.

157. **Weigelt, J., I. Climent, K. Dahlman-Wright, and M. Wikstrom.** 2001. Solution structure of the DNA binding domain of the human forkhead transcription factor AFX (FOXO4). Biochemistry **40:**5861-9.
158. **Wu, S., J. Huang, J. Dong, and D. Pan.** 2003. hippo encodes a Ste-20 family protein kinase that restricts cell proliferation and promotes apoptosis in conjunction with salvador and warts. Cell **114:**445-56.
159. **Xing, D., and S. Orsulic.** 2005. A genetically defined mouse ovarian carcinoma model for the molecular characterization of pathway-targeted therapy and tumor resistance. Proc Natl Acad Sci U S A **102:**6936-41.
160. **Xuan, Z., and M. Q. Zhang.** 2005. From worm to human: bioinformatics approaches to identify FOXO target genes. Mech Ageing Dev **126:**209-15.
161. **Yang, J. Y., W. Xia, and M. C. Hu.** 2006. Ionizing radiation activates expression of FOXO3a, Fas ligand, and Bim, and induces cell apoptosis. Int J Oncol **29:**643-8.
162. **Yang, J. Y., C. S. Zong, W. Xia, H. Yamaguchi, Q. Ding, X. Xie, J. Y. Lang, C. C. Lai, C. J. Chang, W. C. Huang, H. Huang, H. P. Kuo, D. F. Lee, L. Y. Li, H. C. Lien, X. Cheng, K. J. Chang, C. D. Hsiao, F. J. Tsai, C. H. Tsai, A. A. Sahin, W. J. Muller, G. B. Mills, D. Yu, G. N. Hortobagyi, and M. C. Hung.** 2008. ERK promotes tumorigenesis by inhibiting FOXO3a via MDM2-mediated degradation. Nat Cell Biol **10:**138-48.
163. **Yeagley, D., S. Guo, T. Unterman, and P. G. Quinn.** 2001. Gene- and activation-specific mechanisms for insulin inhibition of basal and glucocorticoid-induced insulin-like growth factor binding protein-1 and phosphoenolpyruvate carboxykinase transcription. Roles of forkhead and insulin response sequences. J Biol Chem **276:**33705-10.
164. **Zamore, P. D., T. Tuschl, P. A. Sharp, and D. P. Bartel.** 2000. RNAi: double-stranded RNA directs the ATP-dependent cleavage of mRNA at 21 to 23 nucleotide intervals. Cell **101:**25-33.
165. **Zanella, F., A. Rosado, F. Blanco, B. R. Henderson, A. Carnero, and W. Link.** 2007. An HTS approach to screen for antagonists of the nuclear export machinery using high content cell-based assays. Assay Drug Dev Technol **5:**333-41.
166. **Zeng, Z., I. J. Samudio, W. Zhang, Z. Estrov, H. Pelicano, D. Harris, O. Frolova, N. Hail, Jr., W. Chen, S. M. Kornblau, P. Huang, Y. Lu, G. B. Mills, M. Andreeff, and M. Konopleva.** 2006. Simultaneous inhibition of PDK1/AKT and Fms-like tyrosine kinase 3 signaling by a small-molecule KP372-1 induces mitochondrial dysfunction and apoptosis in acute myelogenous leukemia. Cancer Res **66:**3737-46.
167. **Zhao, J. J., Z. Liu, L. Wang, E. Shin, M. F. Loda, and T. M. Roberts.** 2005. The oncogenic properties of mutant p110alpha and p110beta phosphatidylinositol 3-kinases in human mammary epithelial cells. Proc Natl Acad Sci U S A **102:**18443-8.
168. **Zheng, W. H., S. Kar, and R. Quirion.** 2002. FKHRL1 and its homologs are new targets of nerve growth factor Trk receptor signaling. J Neurochem **80:**1049-61.
169. **Zheng, W. H., S. Kar, and R. Quirion.** 2000. Insulin-like growth factor-1-induced phosphorylation of the forkhead family transcription factor FKHRL1 is mediated by Akt kinase in PC12 cells. J Biol Chem **275:**39152-8.

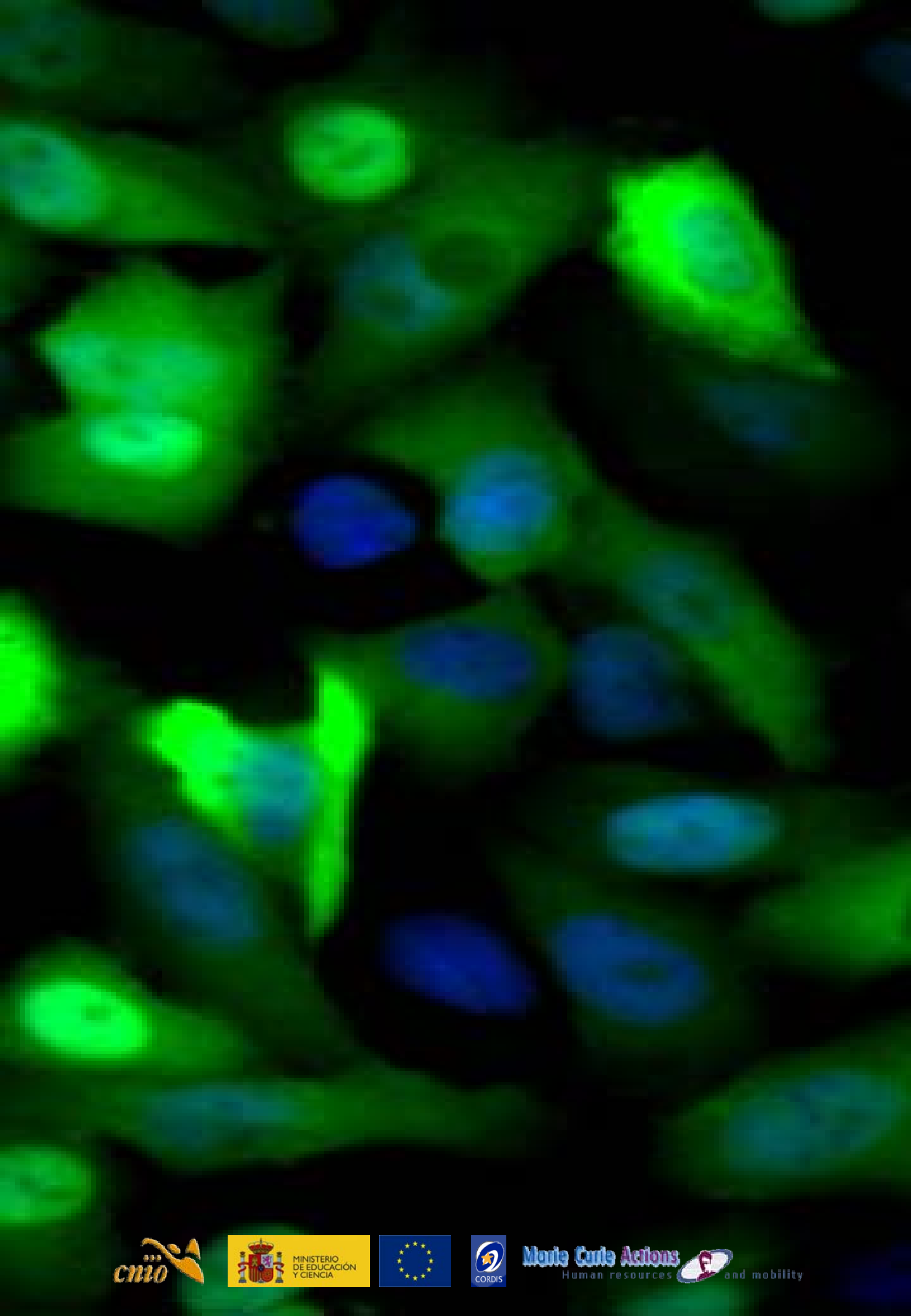
cnio
MINISTERIO DE EDUCACIÓN Y CIENCIA
CORDIS
Marie Curie Actions
Human resources and mobility